Distribution Agreement

In presenting this thesis or dissertation as a partial fulfillment of the requirements for an advanced degree from Emory University, I hereby grant to Emory University and its agents the non-exclusive license to archive, make accessible, and display my thesis or dissertation in whole or in part in all forms of media, now or hereafter known, including display on the world wide web. I understand that I may select some access restrictions as part of the online submission of this thesis or dissertation. I retain all ownership rights to the copyright of the thesis or dissertation. I also retain the right to use in future works (such as articles or books) all or part of this thesis or dissertation.

Signature:

_____ _____

Carly Laurel Lancaster Date

The RNA conserved binding protein Nab2 regulates RNA targets critical for proper neurodevelopment

By

Carly Laurel Lancaster
Doctor of Philosophy

Graduate Division of Biological and Biomedical Sciences
Biochemistry, Cell, and Developmental Biology

_____
Anita H. Corbett, Ph.D.
Advisor

_____
Kenneth H. Moberg, Ph.D.
Advisor

_____
Leila Reider, Ph.D.
Committee Member

_____
David Gorkin, Ph.D.
Committee Member

_____
Gary Bassell, Ph.D.
Committee Member

_____
James Zheng, Ph.D.
Committee Member

Accepted:

_____
Kimberly J. Arriola, Ph.D.
Dean of the James T. Laney School of Graduate Studies

_____
Date

The RNA conserved binding protein Nab2 regulates RNA targets critical for proper neurodevelopment

By

Carly Laurel Lancaster
B.S., University of South Carolina at Columbia, 2019

Advisor: Anita H. Corbett, Ph.D., and Kenneth H. Moberg, Ph.D.

An abstract of
a dissertation submitted to the faculty of the
James T. Laney School of Graduate Studies of Emory University
in partial fulfillment of the requirements for the degree of
Doctor of Philosophy
in Graduate Division of Biological and Biomedical Science (GDBBS)
Biochemistry, Cell and Developmental Biology (BCDB)
2024

ABSTRACT

The RNA conserved binding protein Nab2 regulates RNA targets critical for proper neurodevelopment

By Carly Laurel Lancaster

RNA binding proteins (RBPs) are critical for nearly every aspect of RNA processing and regulation. These regulatory roles for RBPs are particularly important within highly specialized cells such as neurons, which require enhanced fine-tuned spatiotemporal regulation of gene expression to properly pattern complex neuronal networks within the developing nervous system. One such RBP with critical roles in neurons and is required for proper brain development and function is known as ZC3H14 (Zinc finger Cystine-Cystine-Cystine-Histidine containing protein 14). *ZC3H14* encodes a ubiquitously expressed polyadenosine RBP with broad roles in post-transcriptional regulation of gene expression. Moreover, loss of function mutations in human *ZC3H14* cause a form of non-syndromic autosomal recessive intellectual disability (NS-ARID), however, our understanding of ZC3H14-regulated RNAs as well as elevated roles for ZC3H14 in the nervous system remain elusive. To investigate neurological functions of ZC3H14, we employ *Drosophila melanogaster* as a model to explore the role of this conserved RBP in neurodevelopment and neurodevelopmental disease. The *Drosophila* orthologue of ZC3H14, known as Nab2 (Nuclear polyadenosine RNA-binding protein 2), is critical in neurons and is required for proper brain development and function. Here, we present RNA-sequencing analysis of $Nab2^{null}$ heads to define the effect of Nab2 loss on the *Drosophila* head transcriptome. We further define a novel role for Nab2 in the regulation of sex-specific splicing and m^6A methylation status of the *Drosophila Sxl* transcript. We then present evidence that Nab2 regulates splicing and abundance of Trio, a neuronally-enriched Rho guanine nucleotide exchange factor (RhoGEF), to govern, in-part, *Drosophila* brain morphology and neuronal architecture. In aggregate, these data suggest that *Nab2/ZC3H14* may function in neurodevelopment by regulation of m^6A methylation levels and splicing of select neuronally-enriched transcripts to regulate downstream neurodevelopmental events such as regulation of m^6A methylation, brain development, and axon development. Taken together, these studies provide insight into human ZC3H14 function as well as ZC3H14-linked neurodevelopmental disease etiology.

The RNA conserved binding protein Nab2 regulates RNA targets critical for proper neurodevelopment

By

Carly Laurel Lancaster

B.S., University of South Carolina at Columbia, 2019

Advisors: Anita H. Corbett, Ph.D. and Kenneth H. Moberg, Ph.D.

A dissertation submitted to the faculty of the
James T. Laney School of Graduate Studies of Emory University
in partial fulfillment of the requirements for the degree of
Doctor of Philosophy
in Graduate Division of Biological and Biomedical Science (GDBBS)
Biochemistry, Cell and Developmental Biology (BCDB)
2024

ACKNOWLEDGEMENTS

I would like to express my upmost gratitude to everyone who has supported me in the pursuit of my Ph.D. They say it takes a village to raise a kid, and I believe it also takes a village to train a Ph.D. student. I have had the unique fortune of having not one lab, but two- which means I had twice the number of mentors, colleagues and friends which I believe made all the difference in my training and experience. Not only have I had the most wonderful support system at Emory, but I am also lucky to have the worlds' most supportive family who has encouraged me every step of the way. My family always supported me in my endeavors and made sure that I had everything I needed to succeed, and for that I am forever grateful.

First, I would like to acknowledge the many mentors I have during my scientific career:

I would like to start by thanking my PI and mentor Dr. Anita Corbett. I can honestly say that without Anita I would not be writing this thesis. The beginning of graduate school was very tough for me. I struggled deeply with my overall mental health and was riddled with feelings of doubt and imposter syndrome. I had even considered quitting my Ph.D. on several occasions. Despite my own feelings of self-doubt, Anita always believed in me. She continually went out of her way to support me and mentor me even before she was my official PI/mentor. In my time of need she - without hesitation - took me under her wing and provided me with a safe laboratory environment where I could grow and flourish as a scientist and human being. It was in her lab that I fell back in love with science, developed confidence in myself and my abilities, and made friendships that will last forever. She always supported me in and out of the lab and cared not only about my scientific development, but about my personal and professional development as well. Befriending Anita was the best decision I have ever made because now I have a lifelong mentor and supporter, and I truly cannot express in words how her mentorship has impacted my life. Anita- thank you for everything you have done for me and everything you continue to do to help support me and others. Mentors like you are very rare, and I am forever grateful to have had the opportunity to be one of your mentees.

I also want to thank my other truly amazing mentor, Dr. Ken Moberg. Ken's excitement and passion for science is truly what helped keep me going when the going got tough. He sees the best in every piece of data (even the truly garbage data) and the punchline in every complicated scientific story. His positivity and excitement kept my head above water when it felt like the science was trying to drown me. On innumerable occasions I would walk into Ken's office and "anxiety dump", describing to him all my woes and concerns about my experiments and the progress (or lack thereof) of my projects. Inevitably, I would always walk out of his office feeling like a weight had been lifted off my shoulders. He has a way of spinning every piece of negative data, every frustration, every moment of desperation on its head. He recognized my self-doubts and anxieties and always made a point to tell me that I was a worthy, skilled, and competent scientist. Even when I didn't believe him, I always knew that he believed in me, and that really kept my hopes and spirits high. Moreover, Ken always observed the data with an ultra-wide lens. He picked up on things nobody else noticed and many times, his observations drove the project in exciting, new directions. I am thankful to have had Ken as a present and thoughtful mentor who was truly excited about the science. Finally, Ken (with the help of Dr. Colby Schweibenz-Muller) created a lab environment that was incredibly fun and welcoming, promoting students to talk, share ideas, and collaborate- even on non-science activities. Students from other labs would often come by just to hang out with our lab and be a part of the exciting atmosphere. I have had so much fun

in the Moberg lab, and I am so lucky to have had such a positive environment to perform my research. Ken- I want to thank you for supporting me, believing in me, and for believing in the science. Mentors like you are also extremely rare, and I don't know what I did to deserve mentorship by two PIs who are not only wonderful scientists, but wonderful people.

Next, I want to thank my committee members Dr. Gary Bassell, Dr. Leila Rieder, Dr. James Zheng, and Dr. David Gorkin for all their insight and support along the way. I want to thank each of them for their valuable contributions to the project and for encouraging me during each of my committee meetings. They were always kind and welcoming, and I always walked out of my committee meetings feeling good about my progress and my project. I want to give a special thanks to Dr. Leila Rieder for being an angel on earth. She was always extremely attentive and engaged during our meetings and she always made incredibly thoughtful comments and suggestions that helped shape the project. Despite having her hands full with her own awesome lab and two adorable children, she regularly checked in on me and would often take time out of her day to get coffee with me to catch up and provide emotional and scientific support. She has been such a great supporter and mentor, and I couldn't have imagined a committee without her!

I would next like to thank two of my unofficial mentors, Dr. Milo Fasken and Dr. Sara Leung. In my humble opinion, Milo and Sara are two of the world's greatest scientific minds. Milo and Sara taught me how to think like a scientist, they encouraged me to observe data without implicit bias, and always supported my experimental endeavors. Anytime I was in the depths of troubleshooting, Milo and Sara would offer extremely insightful ideas for how to get an assay to work. On several occasions, Milo would take hours out of his day to research my technical problems and later surprise me with ideas to help solve my experimental issues. Their combined experience and guidance probably shaved years off my graduation timeline. I am grateful to have had the opportunity to work with such amazing scientists, and wonderful people. Milo and Sara- Thank you for all you have done for me. I am truly grateful for your encouragement and mentorship throughout these last few years. I hope to one day be as great a scientist as the two of you are.

Finally, I would like to thank my very first mentor, Dr. Laura Jenkins-Lane who served as my mentor when I was a young and under-experienced undergraduate student at the University of South Carolina-Columbia. She was an incredible mentor that provided me with an amazing environment and genuine friendship to grow in my scientific capabilities. She was incredibly patient and taught things as simple as me how to use a pipette and as complicated as how to transfect cells. She encouraged me to pursue a PhD and gave me my first opportunity to think like a scientist, and I am forever grateful for the mentorship she provided me.

Next, I would like to acknowledge each of the life-long friends that I have made during my graduate career:

I would like to start by thanking my best friend Dr. Izabela Suster who not only taught me most of my basic laboratory skills, but also taught me how to stand up for myself in tough situations. Izabela supported me in many ways during my thesis. She often fed me (and introduced me to some amazing vegan recipes), brought me amazing coffee, helped me write sassy emails, and always made sure I was taken care of. She was there for me during the hardest parts of my graduate career, and I am forever grateful for her continued love and friendship along this journey.

I also want to thank my best friend and lab-mate Dr. Celina Jones. Celina is an angel and beauty inside and out. I probably would have graduated several months ago, but Celina and I are like the two naughty kids who can't stop chatting in the back of the class. Some of my favorite memories of grad school will be of Celina and I gossiping in our quiet little corner of the lab. Days

spent with Celina are never boring, and I don't think we could ever run out of things to talk about. I wish that I could take her with me wherever I go next, and I am going to miss rolling my chair over to her desk and saying "OMG, guess what!" and seeing her eyes light up in reply "OMG what??". Celina-thank you for your friendship and for your support. I am so lucky to have had the opportunity to work with and befriend such a lovely human being.

Next, I want to thank my amazing friend, Ms. Judy Baldwin. Ms. Judy is truly one of the most wonderful, genuine, and hilarious human beings I have ever had the pleasure of meeting. I met Ms. Judy early in my graduate career when I was struggling significantly with my mental health. I would pass her in the hallway on my way out in the evening, and she would always say hello and make a point to tell me that she liked my hair, or my outfit, and go out of her way to wish me a wonderful evening. She would always tell me to get home safely and remind me not to be out late, alone at night. Eventually Ms. Judy became one of the best parts of my day, I would look forward to our evening conversations and even roam the halls of Rollins to try and find her before I left for the day. She oozes positivity, and hope, and love. Moreover, she is easily one of the funniest people I have ever known. No matter what kind of day I was having, she always found a way to make me laugh. She has the most wonderful outlook on life, and I hope to implement her positivity, gratitude, and love in my everyday life. Long story short, if you don't know Ms. Judy, you are missing out on one of the world's greatest human beings. I genuinely believe that if everyone was a little bit more like Ms. Judy, this world would be a much better place to live. Ms. Judy- Thank you for your friendship, your love, and your support. You are a one-of-a-kind human being, and I am so lucky to have a true friend like you!

Next, I would like to thank Dr. Maria Sterrett. Maria was another unofficial mentor of mine. When I joined the Corbett and Moberg labs, Maria was the one that happily showed me the ropes and taught me how to do most of the experiments in the Corbett lab. She was always there with words of encouragement and advice when I needed it. My favorite thing about Maria is that she always left me science-themed cartoon doodles on sticky notes at the end of the day. Every evening when I came by my desk to pack up and go home, there was a funny note that always allowed me to end the day on a positive note. Maria reminded me that my experimental success didn't define me as a person, and I am grateful to have had such a wonderful friend and mentor to support me throughout the thick of my thesis work.

I would like to thank Dr. Joanna Wardwell-Ozgo and Dr. Shilpi Verghese, two more of my unofficial mentors for their support throughout my thesis. They were always there to help me troubleshoot my experiments and help support me as I learned to "fly". They often had bits of scientific wisdom that they would sprinkle in our conversations, and they each regularly took time out of their day to support me in any way that I needed. Shilpi was always thinking of other people and regularly went out of her way to support the graduate students in the lab. On several occasions she would take the crying grad students out for walks and would shower us with words of encouragement and love. I am so grateful to have shared a lab with Shilpi and I am thankful for all of the support she has provided me. On the other hand, as the resident mother in the Moberg lab, Joanna in many ways had that mothering presence I adored, especially when living 100s of miles away from my own mother. I am so grateful to have had Joanna as a part of my graduate experience and I appreciate everything she has done to help me along the way.

I would like to thank my friend Jordan Goldy. Jordan is possibly one of the most sarcastic human beings I have ever met. If it weren't for Jordan, I wouldn't understand sarcasm… but now I think I am getting the hang of it. Jordan and I have one of the most sibling-like relationships in the lab, constantly bickering about irrelevant things and laughing about it minutes later. Moreover,

Jordan is the only reason I ever knew what was going on in the program, or where I was supposed to be at any given time. She was not only on top of her schedule, but basically on top of my schedule too. She also regularly guilted me into going to BCDB-sponsored events, and I will admit, I didn't totally hate them. Jordan- thank you for humbling me every day, and for being someone I can jokingly banter with all day long, you keep lab interesting, and I am grateful to have you in my life.

I would also like to thank Tori Placentra and their undergrad Chloe Wells for being two of the most genuine human beings I have ever met. Tori and Chloe have made such positive impacts on the Moberg lab, not only have they made major intellectual contributions, but they have also cleaned and organized the entire lab, making the science easier for all of us. Moreover, Tori was always there to discuss our shared love of trashy reality dating shows where we would pour over the character flaws in each of the stars. Tori's insightful questions and meaningful contributions to lab discussions inspire me to be a better scientist and person. Tori- thank you for your friendship, and I know you are going to be an amazing PI and mentor to very lucky students one day.

Finally, and most importantly, I would like to thank my best friend Dr. Colby Schweibenz-Muller. To be friends with Colby is to have the most genuine and loving friendship that someone can ever hope to have. She truly brings the sunshine into every room she enters and has the most infectiously positive personality. Colby has been one of my favorite things about graduate school, and without her my experience wouldn't have been nearly as wonderful. Weeks after joining the Corbett and Moberg Labs, Colby planned a surprise party for me and went out of her way to get me a vegan cake and vegan wine (which I didn't even know was a thing) and wrote me a heart-felt note that let me know that I was welcome and at home in the lab. I am convinced that Colby spends 99.99% of her time thinking about other people and she was always there with a hug or thoughtful words of encouragement. I am going to miss the days sitting at our adjacent fly benches laughing and listening to Colby's crazy stories. Colby- I do not have enough time or space to adequately articulate the love and appreciation I have for you but knowing you and becoming your friend has made me a better person, and I value every moment that we get to spend together. I love you with all my heart, and although I am sad that our lives might take us to separate cities, I am excited for your next chapter, and I hope to have the opportunity to be a part of it.

Finally, I would like to acknowledge my amazing family:

While I have had an amazing support system at Emory, it goes without saying that my family has been a major source of encouragement and support for me, not only throughout my Ph.D., but throughout my life. I would like to start by acknowledging my parents, Debra and Eric Lancaster, who sacrifice so much to ensure that my sisters and I have everything we need to succeed and have happy, fulfilling lives. I cannot adequately express in words how grateful I am to have parents that love and care for our family unconditionally. I owe a lot of my progress in life to them, and I have innumerable things to thank them for. Specifically, I would like to thank my amazing super-human mother for always being my biggest cheerleader along the way. Her love and encouragement is unwavering. She has been a shoulder to cry on, a hand to hold, and my best friend. I would also like to thank my incredible father for his strength and support throughout the years. Not only has he supported us financially, but he always made sure we each had everything we ever needed, and never once complained. I want to thank my dad for all of his sacrifices, for always reminding me that he was there for me, and for being such amazing, self-less father to his four daughters. We are lucky to have parents that love us so much, and being far away from them for many years has not been easy. Mom and Dad- Thank you for giving me the world and for

supporting me in ways that I cannot even begin to list here. Thank you for the foundation that you provided me in this life and for ensuring that I was set up for success. I am incredibly lucky to have been born to such wonderful parents, and I am grateful for everything you have done to support me as I pursued my dreams. I love you.

Of course, I must also thank my sister, Tori Lancaster, who makes me smile every time I think about her. Lucky doesn't even begin to describe how I feel, because I am certain that I have the world's best (and coolest) sister. She has a charming way of making every situation funny and provides advice that often leads me to forget that she's my younger sibling. She has been such an amazing friend and supporter throughout my life, and I am genuinely not sure what I would do without her. Tori- I know this paragraph is shorter than the others, but that's mostly because there is only one way to say that you're the best sister and friend I could have ever asked for, and I love you. Thank you for supporting me, mentoring me, and loving me.

I would also like to thank my amazing grandparents, Tina (Lola) and Larry (Papou) Agee who have always, always supported me in my personal and academic endeavors. My grandparents have been an incredible source of encouragement and support throughout my life. They have been there for every holiday, school-event, recital, sports competition, and graduation. They have always been engaged, proud, and excited for every next step my life (sometimes more excited than I am). Not only have they supported me every step of the way, but they have also shared their incredible knowledge and wisdom along the way. Papou and Lola have reminded me that the world may be big, but it is still my oyster, and that opportunity always lies ahead. I genuinely hope that I grow to have a life as wonderful and full as the two of you have created for yourselves. I am extremely proud to be your granddaughter, and there are not enough words in the world to emphasize how lucky and grateful I am to have the two by my side.

I was also very fortunate to go to grad school in Atlanta, GA which happens to be where my wonderful Aunt Karen, Uncle Ken, my cousins Peyton and Ansley, and my fabulously witty grandmother, Margret live. I want to thank you guys for providing me with my home away from home. Thank you for inviting Cooper and I to all the family functions and get-togethers. Having you all here was integral to my sanity throughout the years. Thank you for supporting us along the way and I love you all so much.

Most importantly, I want to thank my best friend and incredible partner Cooper Voigt. Cooper- you have been right by my side since the very beginning of this academic journey. I am truly thankful beyond description for the love, support, and security that you have provided me with throughout our time together. These past few years have been incredibly challenging, and I could not have gotten through this without you. You have been my biggest support system providing me with emotional, financial, and at times even scientific security. You have been there to celebrate every success and milestone, and you have been there to help me pick up the pieces and move forward when it felt like my world was falling apart. I cannot thank you enough for everything you have done to see me through to this stage, and I am so beyond excited for the next chapter of our lives together. Thank you for being the best thing in my life- I love you.

LIST OF FIGURES

Chapter 1

Figure 1-1 The Central Dogma
Figure 1-2 Regulation of Gene Expression
Figure 1-3 Transcription
Figure 1-4 N6-methyladenosine and the m^6A mRNA pathway
Figure 1-5 RNA splicing
Figure 1-6 The Nuclear Pore
Figure 1-7 Untranslated Regions
Figure 1-8 Anatomy of a Neuron
Figure 1-9 Translation
Figure 1-10 The *Drosophila melanogaster* Life Cycle
Figure 1-11 The *Gal4/UAS* System
Figure 1-12 The Drosophila brain and mushroom body
Figure 1-13 Class IV ddaC neurons
Figure 1-14 Orthologues of ZC3H14
Figure 1-15 Sex determination cascade in *Drosophila*
Figure 1-16 The GTPase cycle
Figure 1-17 Schematic of human and *Drosophila* Trio proteins

Chapter 2

Figure 2-1 RNA sequencing detects effects of Nab2 loss on the head transcriptome.
Figure 2-2 Significantly up/down-regulated RNAs in *Nab2^{ex3}* heads are enriched for predicated splicing factors
Figure 2-3 *Sxl* alternative splicing and protein levels are disrupted in *Nab2^{ex3}* female heads.
Figure 2-4 Alleles of *Sxl^{M8}* or the DCC component *male-specific lethal-2* (*msl-2*) rescues *Nab2* phenotypes
Figure 2-5 Reduction of the Mettl3 m^6A transferase suppresses viability and behavioral defects in *Nab2* mutant females
Figure 2-6 Nab2 associates with the *Sxl* mRNA and inhibits its m^6A methylation
Supplemental Figure 2-1 RNA sequencing reads across the *Nab2* locus
Supplemental Figure 2-2 GO term enrichment among Nab2-regulated alternative splicing events
Supplemental Figure 2-3 RNA sequencing reads across the *CG13124* and *I_h channel* loci
Supplemental Figure 2-4 RNA sequencing reads across the *tra* and *dsx* loci

Supplemental Figure 2-5 Additional genetic interactions between *Nab2^{ex3} msl-2*, *roX1*, and *mle*
Supplemental Figure 2-6 Genomic PCR confirms the *Nab2^{ex3},Mettl3^{null}* recombinant
Supplemental Figure 2-7 Detailed schematic of the exon 2-3-4 *Sxl* locus
Supplemental Figure 2-9 Nab2 limits m^{6}A methylation of additional RNAs
Supplemental Figure 2-10 Heterozygosity for Mettl3 does not alter *Sxl* splicing in *control* or *Nab2^{ex3}* mutant female heads
Supplemental Figure 2-11 Neuronal overexpression of *Mettl3* RNA using the Gal4/UAS system.

Chapter 3

Figure 3-1. Loss of m^{6}A-reader proteins rescues *Nab2^{null}* defects in viability and adult locomotion
Figure 3-2. Nab2 and Mettl3 regulate splicing of the *trio* 5'UTR in the *Drosophila* head
Figure 3-3. Nab2 regulates Trio M protein level in the *Drosophila* head
Figure 3-4. Trio is altered in the *Nab2^{null}* mushroom body
Figure 3-5. Expression of Trio GEF2 rescues α/α' and β' defects in *Nab2^{null}* mushroom bodies.
Figure 3-6. Expression of Trio GEF2 rescues *Nab2^{null}* dendritic arborization defects in class IV ddaC sensory neurons.
Figure 3-7. Expression of Trio GEF2 rescues *Nab2^{null}* defects in viability and locomotion
Supplemental Figure 3-1. Trio is present in *Drosophila* Kenyon cell bodies and Caylx.
Supplemental Figure 3-2. Heterozygosity for Mettl3 does not dominantly rescue *Nab2^{null}* mushroom body phenotypes.
Supplemental Figure 3-3. Expression of Rac1 or Rho1/A in the mushroom body of *Nab2^{null}* flies is lethal.

Chapter 4

Figure 4-1 Outcrossing the *Nab2^{ex3}* allele to improve *Nab2^{ex3}* adult viability
Figure 4-2 Preliminary evidence suggests Sxl regulates mushroom body development in the female brain
Figure 4-3 Preliminary evidence suggests that loss of Nab2 causes ectopic methylation of the Exon 1-Intron 1- Exon 2 boundary of the *trio M* transcript

Appendix

Figure A-1 The considerations funnel

CHAPTER 1: General Introduction

This chapter was written by Carly L. Lancaster specifically for inclusion in this dissertation.

Table of Contents

ABSTRACT ..... ***vii***

ACKNOWLEDGEMENTS ..... ***ix***

CHAPTER 1: General Introduction ***1***

1.1 Regulation of gene expression **2**
1.1.a Regulation of gene expression in the Nucleus 3
1.1.b Nucleocytoplasmic transport 9
1.1.c Regulation of Gene Expression in the Cytoplasm 11

1.2 RNA binding proteins **20**
1.2.a RBPs in disease 22
1.2.b Regulation of RNA in the nervous system 23

1.3 Intellectual disability **24**

1.4 *Drosophila melanogaster* as a model for intellectual disability **26**
1.4.a The *Drosophila* Nervous System 28
1.4.b Mushroom Bodies 29
1.4.c Dendritic Arborization Neurons 31

1.5 ZC3H14-linked Intellectual Disability **32**
1.5.a Mammalian ZC3H14 32
1.5.b *Caenorhabditis elegans* Sut2 34
1.5.c *Saccharomyces cerevisiae* Nab2 34
1.5.d *Drosophila melanogaster* Nab2 37

1.6 Nab2 regulates splicing of select neuronally-enriched transcripts within the fly head. **40**
1.6.b Sex lethal (*Sxl*)- The master regulator of sex determination and dosage compensation in *Drosophila* ... 40
1.6.c The RhoGEF Trio 43

1.7 Scope of Dissertation **46**

1.8 Figures **49**

CHAPTER 2: The Drosophila Nab2 RNA binding protein inhibits m^{6}A methylation and male-specific splicing of Sex lethal transcript in female neuronal tissue ***68***

Abstract **69**

Introduction **70**

Results **72**
Nab2 loss affects levels and processing of a subset of RNAs in the transcriptome of the *Drosophila* head 72
Nab2 loss alters levels of transcripts linked to mRNA processing 74
Nab2^{ex3} females exhibit masculinized *Sxl* splicing in neuron-enriched tissues 76
The dosage compensation complex contributes to phenotypes in *Nab2^{ex3}* mutant females 79
Loss of the Mettl3 m^{6}A methyltransferase rescues *Nab2^{ex3}* phenotypes 80
Nab2 binds *Sxl* pre-mRNA and modulates m^{6}A methylation 82

Discussion **87**

Materials and Methods **93**

Acknowledgments **103**

Competing Interests **103**

Figures **104**

CHAPTER 3: The RNA binding protein Nab2 regulates levels of the RhoGEF Trio to govern axon and dendrite morphology ***125***

ABSTRACT **126**

Significance Statement **127**

INTRODUCTION **128**

RESULTS **132**

Loss of m^{6}A-reader proteins rescues *Nab2^{null}* defects in viability and adult locomotion 132
Nab2 and Mettl3 regulate splicing of the *trio* 5'UTR in the *Drosophila* head 133
Nab2 regulates levels of Trio M in the *Drosophila* head 136
Trio is altered in the *Nab2^{null}* mushroom body 137
Expression of Trio GEF2 rescues α/α' and β' defects in *Nab2^{null}* mushroom bodies 138
Expression of Trio GEF2 rescues *Nab2^{null}* dendritic arborization defects in class IV ddaC sensory neurons ... 140
Expression of Trio GEF2 rescues *Nab2^{null}* defects in viability and locomotion 140

DISCUSSION **141**

METHODS **148**

Acknowledgements **157**

CHAPTER 4: EXPANDED DATA ***171***

Outcrossing the *Nab2^{ex3}* allele to improve *Nab2^{ex3}* adult viability **171**

Preliminary evidence suggests Sxl regulates mushroom body morphology in the female brain **173**

Preliminary evidence suggests Nab2 causes ectopic methylation of the *trio M* transcript **176**

Nanopore direct sequencing of poly(A)+ RNA to map m^{6}A modifications within the *Drosophila* head transcriptome **178**

CHAPTER 5: DISCUSSION AND CONCLUSION ***184***

APPENDIX: How to Select a Graduate School for a Ph.D. in Biomedical Science ***194***

Abstract **195**

Author Biographies **196**

Introduction **197**

Ph.D. or Master's? **198**

Phase I: Research for Applications **199**

Phase II: The Interview **210**

Phase III: Follow-Up Research **219**

Acknowledgements **222**

REFERENCES ***224***

GENERAL INTRODUCTION

Parts of this introduction have been excerpted from a manuscript under review for publication in *WIREs RNA*:
Lancaster CL, Moberg KH, and Corbett AH. Post-transcriptional regulation of gene expression and the intricate life of eukaryotic mRNAs. *under review* for publication in *WIREs RNA*.

1.1 Regulation of gene expression

The expression of each gene is tightly controlled during the flow of genetic information from DNA, to RNA, to protein-- known as the central dogma of molecular biology[1]. The central dogma describes the process by which DNA is transcribed into messenger RNA (mRNA) and subsequently translated into protein (**Figure 1-1**)[1]. Proteins produced work in concert to execute a vast array of distinct cellular functions necessary for cell maintenance and survival.

It should be noted that DNA can also be transcribed into other classes of "non-coding" RNA (ncRNA) molecules including, but not limited to transfer RNA (tRNA), ribosomal RNA (rRNA), micro RNA (miRNA), small nuclear RNA (snRNA), small nucleolar RNA (snoRNA), piwi-interacting RNAs (piRNA), long noncoding RNAs (lncRNAs), and circular RNA (circRNA). All these distinct types of RNAs have critical functions necessary for cellular maintenance and survival. Importantly "coding" RNA, or mRNA, only makes up about ~2% of the transcriptome, whereas the remaining ~98% consists of ncRNA, which is mostly represented by rRNA [2-4]. In this thesis, I will focus primarily on mRNA processing, and briefly discuss some ncRNAs which can regulate multiple steps of mRNA processing.

Precise spatiotemporal regulation of gene expression is critical for cellular differentiation and establishment of cell-type specific functions for proper tissue development[5]. Although much of this regulation is achieved at the level of gene-specific

transcription, there are numerous post-transcriptional events that dictate cell-type specific expression patters to govern cellular function. Post-transcriptional regulation of gene expression includes a multitude of distinct pre-mRNA processing events including 5'capping, splicing, epitrancriptomic modification, polyadenylation, nuclear export, translation, and eventually mRNA decay in the cytoplasm (**Figure 1-2**)[5-8]. Each of these steps is intricately coordinated by a slew of RNA binding proteins (RBPs) that associate with RNA molecules throughout the lifecycle of the RNA.

1.1.a Regulation of gene expression in the Nucleus

Transcription

Transcription is the first step in gene expression, in which a DNA sequence is transcribed into a molecule of RNA by a multiprotein RNA polymerase (RNAP) complex. In eukaryotic organisms, transcription of protein-coding genes is carried out by RNA polymerase II (RNAPII/Pol II) with the help of a multitude of other proteins that act in concert to transcribe specific genes in response to intra- and extracellular signals. Transcription is critical for almost every cellular process, allowing constitutive production of "housekeeping" genes as well as the dynamic production of regulatory genes in response to specific cellular requirements. There are three intricately regulated phases of transcription: initiation, elongation, and termination[9] (**Figure 1-3**).

Transcription initiation by RNAPII requires several general transcription factors (GTFs) factors to properly position RNAPII at the transcription start site (TSS) and separate the DNA strands. These GTFs are designated TFIIA, -B, -D, -E, -F, and -H and together form the preinitiation complex on promoter DNA[10]. The promoter DNA strands

are separated, allowing RNAPII to access the template strand of the DNA and begin pre-mRNA synthesis. Once the pre-mRNA strand is approximately ~20-50 nucleotides in length, RNAPII pauses and other elongation factors bind RNAPII [10]. Once a stable elongation complex is formed transcription of the gene can ensue. After RNAPII has transcribed ~200nts from the TSS, elongation is highly processive through most genes. RNAPII does not terminate transcription until after a sequence is transcribed that directs cleavage and polyadenylation[10]. After transcription of the poly(A) addition site, transcription termination can occur at multiple sites within the following 0.5-2kb[10].

The C-terminal end of the largest subunit of RNAPII, RPB1, contains a heptapeptide repeat (Y-S-P-T-S-P-S) that is repeated multiple times known as the carboxyl terminal domain (CTD). Vertebrates contain 52 of these repeats which are essential for transcriptional regulation of gene expression. The CTD is involved in the initiation of DNA transcription, 5' capping, splicing (discussed in detail in later sections). Phosphorylation of serine 5 (Y-S-P-T-S-P-S) is required for transcription initiation, RNAPII pausing, and co-transcriptional capping of the 5' terminus of the pre-mRNA[9,10]. On the other hand, phosphorylation of serine 2 (Y-S-P-T-S-P-S) is necessary for attachment of the spliceosome for co-transcriptional splicing of the newly synthesized pre-mRNA and transcription termination[9,10]. Thus, the CTD of RPB1 is critical for the precise coordination of transcription and co-transcriptional pre-mRNA processing events.

5'Capping

Among the first steps of pre-mRNA regulation in the nucleus is the co-transcriptional addition of an N7-methylguanosine (m^7G) cap structure onto the emerging pre-mRNA transcript as soon as the incorporation of the first 25-30nts by RNA polymerase

II[11,12]. In this step, termed 5'capping, an m7G is linked to the first nucleotide of the nascent RNA via a reverse 5' to 5' triphosphate linkage[13] (**Figure 1-3**).

The 5' cap is an evolutionarily conserved modification that plays both protective and functional molecular roles in addition to its essential role in coordination of downstream RNA processing events such as splicing, polyadenylation, nuclear export, and in cap-dependent initiation of translation. The 5'cap is also required to protect the transcript from 5'-3' exonuclease degradation[11,14-19]. Failure of the nascent pre-mRNA transcript to be capped causes transcript instability, as the major RNA degredation pathways require removal of the cap prior to exonuclease cleavage [20,21]. Thus, the addition of the m7G cap is necessary for transcript stability and downstream RNA processing events.

Splicing

The pre-mRNA transcript is comprised of regions known as exons and introns. Exons are the nucleotide sequences that exit the nucleus, whereas introns are sequences that are removed before an mRNA exits the nucleus (**Figure 1-4**). A common misconception is that untranslated regions (UTRs) of mRNA are not exons, and that exons are sequences that encode protein. This is not the case. Both UTRs and coding sequences (CDS) exit the nucleus and are therefore considered exons (**Figure 1-4**).

For proper protein synthesis to occur, introns must be removed from the pre-mRNA transcripts and exons must be joined together in a process known as splicing. Splicing of pre-mRNA is a highly ordered process occurring co-transcriptionally and is performed by the spliceosome–a macromolecular machine made up of a multitude of various proteins and RNAs that orchestrate intron removal[22-24]. Small nuclear

ribonucleoproteins (snRNPs) of the spliceosome are responsible for both recognition of degenerate canonical splice site sequences at the 5' and 3' ends of the intron, as well as catalysis[24]. Accurate removal of the introns is accomplished by a two-part transesterification reaction[24] (**Figure 1-5A**). First, a lariat is formed via a nucleophilic attack of the phosphate group of the 5' splice site by the 3' hydroxyl group of the branch point adenosine located ~18-40 nucleotides from the 3'splice site[24-26]. Next, the free hydroxyl of the detached exon attacks the 3' splice site, thus forming a lariat intron and ligating adjacent exons[24-26]. Decades of research as well as the advent of sequencing technologies such as single-molecule and long-read sequencing have also uncovered several noncanonical splicing mechanisms[27,28]. These noncanonical splicing mechanisms include recursive splicing, backsplicing, and the splicing of microexons [29].

Recursive splicing is a mechanism by which long introns (>50kb) are removed in a multistep splicing process. This unique splicing mechanism was first described for the splicing of the 74kb intron found within the *ultrabithorax* gene of *Drosophila melanogaster* [30,31]. For proper splicing to occur the 5' and 3' splice sites must be in proximity, allowing the 2-step transesterification reaction to occur [32]. Thus, longer introns where the 5' and 3' splice sites are separated by thousands of bases or more, pose a unique challenge for the spliceosome. To solve this problem, the spliceosome utilizes recursive splice sites (also known as ratcheting sites) consisting of combined 3' and 5' splice sites to progressively remove the large intron in pieces (**Figure 1-5B**) [30-34]. These recursive splice sites are highly enriched within long introns (>20kb), illustrating their critical role in the accurate splicing of large intronic sequences[30].

Backsplicing is a noncanonical form of splicing whereby the 5' terminus of an upstream exon is covalently linked to the 3' terminus of a downstream exon (**Figure 1-5B**) generating a circularized RNA (circRNA) molecule[35]. The precise function of circRNAs remains elusive, however, recent evidence suggests a role for circRNAs in the sequestration of microRNAs (miRNAs) and in protein regulation[36-38]. Finally, the splicing of microexons refers to the splicing of very small exons (3-27nts) which insert only 1-9 amino acids into the resulting protein[39]. Recent evidence suggests that microexon inclusion requires specific U/C repeats and UGC motifs forming intronic splicing enhancers located upstream of the 3' splice site, necessary for recognition by spliceosomal proteins[40]. To date, several reviews have been published that provide an in-depth discussion of these distinct splicing mechanisms[29,41,42].

In addition to traditional splicing mechanisms, many pre-mRNA transcripts also undergo a process known as alternative splicing. Alternative splicing is a mechanism by which exons of a given pre-mRNA molecule are assembled in different ways (e.g., exon skipping or mutually exclusive cassette exons) (**Figure 1-5B**)[43]. In this process, the spliceosome utilizes alternative splice sites allowing variants of one gene to encode distinct proteins or include alternative regulatory sequences which can have disparate, or in some cases, even opposing functions[44]. Remarkably, over 90% of all human genes undergo alternative splicing, contributing to extraordinary transcriptome and proteome diversity[45-47]. This process like many other processes involved in the regulation of gene expression, requires interactions of the pre-mRNA molecule with a diverse set of RBPs that orchestrate the precise selection of exons to be included in the mature mRNA molecule occurring in a highly regulated, cell type-specific manner[43,48].

Endonucleolytic Cleavage and Polyadenylation

Akin to the processing steps that take place at the 5' end of the mRNA molecule, the 3' end of an mRNA transcript also undergoes a series of processing and maturation steps. The 3' ends of almost all eukaryotic mRNAs are generated in a two-step process: endonucleolytic cleavage followed by polyadenylation. Within the nucleus, pre-mRNAs are co-trasncriptionally cleaved at a polyadenylation signal (PAS) – a conserved sequence (typically AAUAAA or a similar variant) found within the 3' untranslated region (3'UTR) of the pre-mRNA. The PAS as well as downstream *cis* elements are responsible for the recruitment of cleavage and polyadenylation factors required to guide the formation of the poly(A) tail[49-51]. Poly(A) tails are non-templated additions of adenosine residues to the 3' end of the mRNA that serve several critical roles for downstream mRNA processing and transcript regulation. Cleavage of the pre-mRNA molecule takes place co-transcriptionally, approximately 10-30nt downstream of the PAS, allowing poly(A) polymerase (PAP) to catalyze the addition of adenosine residues onto the 3'end[52]. After the addition of 10-14 adenosine residues, a nuclear poly(A)-binding protein (PABN1) binds the growing poly(A) tail allowing for processive synthesis of a full-length poly(A) tail (~200-250nts in metazoans) by PAP[51-54].

The mRNA poly(A) tail is necessary for mature mRNA export from the nucleus and acts as a critical regulator of gene expression in the cytoplasm, contributing both to the translational status and the stability of the mRNA. For instance, the poly(A) tail can interact with the 5'cap structure to facilitate translation[55]. Transcripts with shorter poly(A) tails have reduced rates of translation in some specific cell types, thus deadenylation represses translation causing subsequent decay of the transcript [56]. Reciprocally, poly(A)

tails can be elongated in the cytoplasm to stabilize and stimulate translation of translationally repressed mRNAs[56,57]. Cumulatively, the dynamic nature of poly(A) tails is critical for fine-tuned regulation of gene expression and shapes the overall architecture of the cellular proteome.

1.1.b Nucleocytoplasmic transport

Eukaryotic cells segregate their RNA and protein synthesis into two distinct cellular compartments i.e., the nucleus and cytoplasm. The genetic materials within the nucleus are separated from the cytoplasmic contents by a highly regulated membrane known as the nuclear envelope. This compartmentalization necessitates nucleocytoplasmic exchange mechanisms which are mediated by the nuclear pore complex (NPC) – a cylindrical ring-like structure embedded within the nuclear envelope (**Figure 1-6**). The NPC is one of the largest macromolecular complexes (~120MDa) consisting of ~1,000 protein subunits called nucleoporins (Nups), which play critical roles in the regulation of transport across the membrane[57,58]. Nups contain phenylalanine-glycine repeat domains which create a permeability barrier preventing the passive diffusion of larger cargos (>60KDa), however, even smaller molecules, such as histones, require import into the nucleus in a carrier-mediated manner[59,60].

Nucleocytoplasmic transport is a complex mechanism involving a multitude of protein-protein interactions, regulatory mechanisms, and signaling pathways to efficiently import and export protein and transcript cargos. Nucleocytoplasmic transport of most cargoes involves karyopherin-mediated receptors, and the directionality of transport is determined by a RanGTP gradient (reviewed in:[61-63]). Unlike protein and other RNA cargoes, mRNA export is atypical and requires a mechanism distinct from other types of

cargoes. The export of mRNA is performed in three steps (1) packaging of mRNAs into mRNP complexes; (2) targeting and translocation of the mRNP; (3) intracytoplasmic release of the mRNPs for translation. Prior to export, newly synthesized mRNAs are packaged into mRNP complexes comprised of heterogeneous nuclear ribonucleoproteins (hnRNPs). In humans, the NFX1-NXT1 heterodimer acts as an export receptor for the mRNP and physically interacts with Nups to facilitate mRNP passage through the NPC [64-66]. Once the mRNP reaches the cytoplasmic face of the NPC, NFX1-NXT1 is released, and new proteins associate with the mRNP complex.

The Untranslated Regions

Although a majority of the mature transcript encodes the resulting protein, some exons instead play a regulatory role making up a region of the transcript known as the untranslated region (UTR). UTRs are found at both the 5' and 3' ends of the mRNA molecule (**Figure 1-7**) and play critical roles in post transcriptional regulation of gene expression. These transcribed, but not translated regions of the mRNA contain numerous *cis* regulatory elements that recruit *trans*-acting factors that govern critical steps in post-transcriptional gene expression including mRNA processing, stability, localization, and translation.

The 5' UTR contains several *cis*-regulatory elements including upstream open reading frames (uORFs), internal ribosomal entry sites (IRES), microRNA (miRNA) binding sites, as well as structural elements critical for regulation of splicing, mRNA stability, and famously, translation initiation. Dysregulation of the 5'UTR *cis*-regulatory elements or secondary structures can cause changes in gene expression that underlie a multitude of diseases, including cancer and neurodevelopmental disorders[67-69].

Moreover, the 5'UTR plays a crucial role in translation initiation (discussed in detail in the *Translation* section). Thus, precise regulation of the 5'UTR is critical for proper control of gene expression.

Like the 5'UTR, the 3'UTR is a critical regulator of gene expression, with important roles in modulating mRNA stability, localization, and translation[70]. Moreover, decades of work have identified functions for the 3'UTR in control of nuclear export[71], polyadenylation[72], subcellular targeting[73], and rates of degradation[74-76]. Alterations in 3'UTR-mediated functions can affect the expression of one or more genes and thereby underlie the pathogenesis of many diseases including myotonic dystrophy (DM)[77], inflammatory diseases[78], and cancers[79,80].

1.1.c Regulation of Gene Expression in the Cytoplasm

Translation

Translation is the process through which a protein is synthesized from the information contained within a mRNA molecule. Specifically, nucleotides encoded within the mRNA molecule are "decoded" by a macromolecular complex known as the ribosome, which directs the addition of amino acids onto an elongating polypeptide chain to generate a functional protein. Initiation of translation can occur via two distinct mechanisms: (1) a cap-dependent mechanism requiring a free 5' end and 5' cap, or (2) a cap-independent mechanism which utilizes an internal ribosome entry site (IRES), which is an RNA element that allows for translation initiation during conditions of cellular stress (e.g., hypoxia, apoptosis, starvation, or viral infection)[81-83].

Cap-dependent translation initiation is a four-step process that begins with recruitment of the 40S small ribosomal subunit and the associated eukaryotic initiation

factors (eIFs) to the 5' cap. First, the cap-binding complex is assembled wherein cap-binding protein eIF4E interacts with the scaffolding initiation factor eIF4G and the RNA helicase eIF4A. eIF4G interacts with cytoplasmic poly(A) binding protein (PABP) located on the 3' poly(A) tail, allowing circularization of the mRNA molecule to aid in translational control. Subsequently, eIF4G, via an interaction with eIF3, recruits the 43S pre-initiation complex consisting of eIF3, the 40S ribosomal subunit, the ternary complex (eIF2-GTP-Met-tRNA$_i$), eIF1, eIF1A, and eIF5 (Step 1). After the 43S pre-initiation complex binds near the 5'cap, the complex travels along the 5'UTR (an ATP-dependent process known as 'scanning'), until it encounters a start codon (typically, AUG) (Step 2). Next, the eIF4A RNA helicase travels along the mRNA molecule with the 43S complex to unwind any inhibitory secondary structures within the 5'UTR. The 48S initiation complex is then assembled after stable binding of 43S at the start codon, and triggers release of eIFs (Step 3). Finally, the 60S large ribosomal subunit joins the 40S small ribosomal subunit to form the elongation-competent 80S ribosome (Step 4), which then proceeds with translation elongation (discussed later in this section). The steps described above are reviewed in:[10,84,85].

Cellular stress conditions such as starvation or hypoxia, can inhibit the formation of the ternary complex thereby suppressing cap-dependent translation[82]. Thus, alternative translation mechanisms are required to synthesize proteins necessary for cellular survival under stress conditions. Non-canonical translation initiation mechanisms can vary with respect to cellular stress conditions. For example, ribosomal shunting requires the 5' cap as well as canonical initiation factors to load the 40S ribosomal subunit onto the mRNA molecule before translocating the 40S subunit downstream to initiate

translation[86]. On the other hand, IRESs can recruit a ribosome internally without the need for a 5' cap or a free 5' end. IRES translation initiation mechanisms have a range of initiation factor requirements depending on the type of IRES. For example, the simplest IRES studied (the *Dicistroviridae* intergenic region) requires no initiation factors[87], while others require all the initiation factors required for canonical translation initiation (such as the hepatitis A viral IRES)[88].

Translation elongation mechanisms are evolutionarily conserved and have been extensively studied in bacteria, with the key steps shared between bacteria and eukaryotes[89]. The ribosome contains three binding sites for tRNA: designated the A (aminoacyl) site, which accepts incoming aminoacylated tRNA; P (peptidyl) site, which holds the tRNA with the nascent peptide chain; and the E (exit) site, which holds the deacylated tRNA before it leaves the ribosome (**Figure 1-8A**). In eukaryotes, translation initiation concludes with the formation of the 80S initiation complex in which MET-$tRNA_i^{Met}$ is bound to the P site of the ribosome, with an empty A site. Aminoacylated tRNA is then brought to the A site as a ternary complex with eukaryotic elongation factor-1A (eEF1A) and GTP. Correct codon-anticodon interactions cause conformational changes in the ribosome that allow the A-site tRNA to translocate into the P-site. A peptide bond can then be formed through diacylation of the P-site tRNA and transfer of the peptide chain to the A-site tRNA. The deacylated tRNA in the P-site is then translocated to the E-site for exit from the ribosome. This process is repeated and translocation of the mRNA and the tRNA is facilitated by eEF2 (**Figure 1-8B**). Finally, translation termination occurs when the ribosome encounters a stop codon (typically UGA, UAG, or UAA). There are no tRNA molecules that can recognize these codons; thus, the ribosome recognizes that

translation is complete. Translation termination is mediated by release factors eRF1 and eRF3 which form a ternary eRF1/eRF3-GTP complex in which eRF1 recognizes the stop codon, and after hydrolysis of GTP by eRF3, mediates release of the nascent peptide[90]. The translation complex is disassembled, and the new chain of polypeptides is released and chaperone proteins aid in the folding of the protein into the correct structure. The steps described above are reviewed in:[10,90,91]

Transport/Trafficking/Localization

Once in the cytoplasm, the mRNA molecule can be trafficked to distinct subcellular locations for translation. Localization of mRNA to specific subcellular compartments provides a highly orchestrated mechanism for spatiotemporal control of gene expression, which is critical within highly polarized, asymmetric cells[92]. For example, in *Drosophila melanogaster* the localization of mRNAs that regulate developmental signaling, such as *bicoid*, *oskar*, and *nanos*, to the anterior and posterior poles of the oocyte to establish s morphogen gradient for proper embryonic development[93]. Similarly, mRNA encoding the *S. cerevisiae* transcriptional repressor Ash1 is transported to the bud tip of a dividing yeast cell such that only the daughter cell receives the *ASH1* mRNA, ensuring mother and daughter cells have distinct mating types[94]. Thus, localization of mRNAs to distinct subcellular locations allows spatial restriction of gene expression which is critical for many cellular and developmental processes.

The neuron is one type of highly polarized cell that relies extensively on mRNA trafficking mechanisms to regulate synaptic transmission and cell-cell communication. mRNA localization and local translation in neurons is crucial for a multitude of processes including polarization[95], neuronal development[96,97], and synaptic plasticity[98,99]. Neurons

contain four main parts: (1) dendrites, which receive messages from other neurons; (2) a cell body which contains the nucleus and cytoplasm; (3) an axon, which transmits information away from the nucleus; and (4) axon terminals, which transmit electrical and chemical signals to other neurons or effector cells (**Figure 1-9**). Unlike other cells in the body, many neurons must extend great lengths to perform their given functions, thus trafficking of mRNAs produced in the nucleus all the way to distal neurites for local protein synthesis is an intricate mechanism necessary for neuronal function. For example, the sciatic nerve is longest neuron in our body that stretches from our spinal cord all the way to our toes and can exceed one meter in length. Thus, our cells require intricate mechanisms to properly orchestrate the trafficking and localization of mRNA molecules across these great lengths.

After post-transcriptional processing and export from the nucleus, mRNAs are trafficked through the cytoplasm as mRNP complexes containing RBPs that regulate stability, localization and translation[100]. In many cases, this mRNP complex forms a part of a larger structure called an RNA transport granule which is transported through association with motor proteins, such as kinesin, dynein, and myosin along the cytoskeleton to the intended destination. Once the mRNA has arrived at its destination, local and regulated translation can ensue providing the cell with a spatially distinct proteome to govern a multitude of regulatory and developmental processes.

Decay

mRNA degradation is a highly regulated process that plays a crucial role in post-transcriptional regulation of gene expression. Evidence for mRNA turnover is highlighted by early studies demonstrating that mRNA steady-state levels do not directly correlate

with the rates of mRNA synthesis[101]. In general, mRNA is typically degraded at the end of its useful life, but mRNA molecules with defects in processing, folding, or assembly with proteins can also be rapidly recognized and degraded by RNA surveillance pathways to ensure the functional integrity of the cell[102]. Moreover, mRNA half-lives can differ significantly between mRNA transcripts[103]. For instance, mRNAs that encode housekeeping proteins tend to have longer half-lives than the average mRNA molecule[104]. Thus, intricate RNA surveillance pathways must be in place to regulate precise spatiotemporal degradation of mRNA.

Three major mRNA decay pathways exist in the mammalian cells: 5'-3' exonucleolytic-, 3'-5' exonucleolytic, and endonucleolytic decay. Deadenylation has long been considered the first and rate-limiting step during mRNA turnover[105,106], which is crucial for activation of decay in both the 3'-5' and 5'-3' directions[106]. The deadenylation complex (Ccr4-Not or Pan2-Pan3) is often recruited to the mRNA molecule to help accelerate deadenylation and thereby stimulate RNA decay[107]. Deadenylation also disrupts the closed circle of the mRNA molecule required for translation, and therefore removal of the poly(A) tail leads to translational repression[108]. After deadenylation, decapping factors are recruited to the 5'end of the mRNA molecule to efficiently remove the m^7G-methylguanosine cap[109,110]. Next, the 5'-3' exoribonuclease, XRN1, can recognize the 5' monophosphate and degrade the mRNA transcript[111,112]. Alternatively, the deadenylated mRNA can also be degraded by a multisubunit complex known as the RNA exosome, via the 3'-5' exonucleolytic subunit, DIS3L[113,114]. In particular cases, mRNA decay can also be initiated via endonucleolytic cleavage to trigger decay. Few endonucelases have been described in mammalian cells, but those that have been

defined include Pmr1, ZC3H12A, the NMD-specific endonuclease Smg6, and the siRNA/miRNA RNA-induced silencing complex (RISC)[115]. Each of these decay mechanisms is capable of endonucleolytic cleavage of the mRNA molecule to induce mRNA decay.

N6-methyladenosine

In recent years, there has been a growing appreciation for the critical and diverse roles that epigenetic modifications play in post-transcriptional regulation of gene expression. Post-transcriptional modifications of the pre-mRNA molecule chemically alter *cis* regulatory sequences to control several downstream processing events including splicing, localization, translation, and RNA stability. Presently, over 160 different types of chemical modifications of RNA have been identified[116], among which RNA methylation is the most prevalent[117]. To date, the most well-studied chemical modification on eukaryotic mRNA is known as N6-methyladenosine (m^6A)–a methylation modification deposited co-transcriptionally onto the N_6 position of select adenosine (A) residues (**Figure 1-10A**) and constitutes the most abundant internal modification on eukaryotic mRNAs[116,118]. Intriguingly, m6A is enriched within the brain and nervous system highlighting a key regulatory role for m^6A in nervous system development (discussed in detail in later sections)[119].

The m^6A methylation of mRNA was first observed in 1974[120], and decades of research following its discovery have uncovered a multitude critical functional roles for this epigenetic modification. Molecularly, m^6A modifications are deposited within DRACH sequence motifs (D=Uracil, Guanine, or Adenine, R=Guanine or Adenine, Adenosine, Cytosine, H=Uracil, Adenine, or Cytosine)[121-123] and are enriched near stop codons and

in 3' untranslated regions (3'UTRs; discussed in later section) [124-126]. Critically, m^{6}A has key post-transcriptional regulatory roles in mRNA splicing[127-129], alternative polyadenylation site selection[125], nuclear export[130], translation [131,132], and stability [133-135]. The spatiotemporal regulation of m^{6}A modifications is coordinated by three types of proteins called writers, readers, and erasers (**Figure 1-10B**)[136].

The m^{6}A writer machinery, also known as the methyltransferase complex, is responsible for catalyzing the addition of a methyl group from the donor *S*-adenosylmethionine (SAM) onto the N6 position of target adenosine residues[137]. The methyltransferase complex is a multi-subunit complex consisting of methyltrasferase-like protein 3 (METTL3; previously known as IME4 or MT-A70)[137,138], methyltrasferase-like protein 14 (METTL14)[139], Wilms' tunmor 1-associated protein (WTAP)[140], vir-like m6A methyltransferase-associated protein (VIRMA, also known as KIAA1429)[141], and RNA binding motifs protein 15/15B (RBM15/15B)[142]. METTL3 is the highly conserved core, catalytic subunit of the methyltransferase complex, which binds SAM[143]. Genetic depletion of *METTL3* in mammalian cells as well as plants, *Drosophila melanogaster* and yeast leads to complete or near complete loss of m^{6}A in polyadenylated RNA[144-147], defining METTL3 as the major m^{6}A forming enzyme for mRNA transcripts. METTL14 on the other hand is highly homologous to METTL3 and is required to support METTL3 structurally and enhance METTL3 catalytic activity[139]. WTAP is also a core component that associates with METTL3-METTL14 to enhance the catalytic activity of METTL3 [140,146], while VIRMA and RBM15/15B participate in regulating the catalytic activity of the complex and help aggregate the core components[141].

Protein readers, defined as m^{6}A recognition proteins, function through recognizing and binding m^{6}A modifications to modulate downstream RNA processing and fate[136,148]. Reader proteins recognize m^{6}A modifications via a YTH (YT521B homology) domain that selectively binds m^{6}A-modified RNA. Mammalian genomes contain five different YTH domain containing proteins that can bind m^{6}A: YTHDF1, YTHDF2, YTHDF3, YTHDC1, and YTHDC2[142]. The YTHDF proteins are highly similar to one another and are primarily localized within the cytoplasm. There have been conflicting studies seeking to define the precise function of the YTHDF family proteins. However, studies clearly demonstrate that YTHDF1 promotes translation and interacts with translation initiation factors (such as eIF3)[132]. On the other hand, YTHDF2 is the most abundant YTHDF family member in most cell types and has a well-established role as a regulator of mRNA stability[133]. Previous work illustrates that mRNAs in YTHDF2-depleted cells have increased half-lives, indicating a key role for YTHDF2 in mediating mRNA decay[124,145,149]. In contrast to YTHDF proteins, YTHDC1 is primarily nuclear and is the major m^{6}A reader protein within the cell [136]. YTHDC1 was originally identified as a regulator of splicing and subsequent studies have focused on elucidating the function of YTHDC1 in m^{6}A-mediated splicing[127]. On the other hand, YTHDC2 is a nucleocytoplasmic protein with poorly defined functions[136,142]. Several groups have resolved the structure of a YTH domain complexed with m^{6}A[121-123]. Intriguingly, these studies demonstrated that the affinity of YTH domain binding for m^{6}A is relatively weak (~1-2 μM)[121-123], suggesting that YTH-domain containing proteins may require additional factors to form a stable complex with m^{6}A.

Finally, m^{6}A eraser proteins are responsible for the demethylation of m^{6}A-modified RNAs. Two different enzymes have been identified with the ability to demethylate m^{6}A:

fat mass and obesity-associated protein (FTO)[150] and AlkB homolog H5 (ALKBH5)[151]. However, conflicting evidence suggests that the roles for these proteins in regulating m^6A methylation may be less exciting than initially perceived. For instance, FTO was the first enzyme linked to demethylation of m^6A, however, more recent studies suggest that FTO instead preferentially targets m^6A_m (a different highly prevalent methylation modification on mRNA)[152]. Moreover, analysis of m^6A levels in *Fto* knockout mice showed little to no change in m^6A levels across the transcriptome apart from a small subset of m^6A peaks[153], and FTO did not show a preference for m6A in its physiological consensus site[150]. Similarly, the degree to which ALKBH5 targets and demethylates m^6A-modifed RNAs remains unclear, and characterization of the enzymatic catalytic activity of ALKBH5 reported slow kinetics towards m^6A[151].

1.2 RNA binding proteins

RBPs are critical for nearly every aspect of RNA processing and regulation. RBPs associate with RNA molecules to form dynamic ribonucleoprotein (RNP) complexes that regulate every step of RNA processing from synthesis to decay. The specific RBPs that associate with a given RNA molecule change depending on cellular context or the functional state of the RNA.

RBPs bind mRNAs via evolutionarily conserved, modular RNA-binding domains (RBDs) including RNA recognition motifs (RRMs), zinc finger domains (ZnF), hnRNP K homology (KH) domains, and RGG-motifs among other binding domains[154]. The RRM is the most common and well-characterized RNA binding domain[154]. Over 9,000 RRMs have been identified with functions in most steps of gene expression[155]. Intriguingly, ~0.5-1%

of human genes encode an RRM, and there are typically multiple RRMs within a given gene[155]. Unlike RRMs, ZnFs are classical DNA-binding protein domains that can also bind RNA[156-160]. ZnFs are classified based on the amino acid residues that coordinate zinc binding: Cystine2Histidine2 (C2H2), CCH, CCHC. Like RRMs, these ZnF domains are typically present in multiple repeats within a single RBP. Similar to ZnFs KH-domains are typically found in multiple copies within a single RBD and can associate with DNA or RNA to regulate transcription and translation[161]. Finally, RGG-motifs are arginine-glycine-rich domains that bind RNA and are found in proteins critical for many cellular processes including translation, splicing, and apoptosis[162]. These RBDs as well as others not mentioned here associate with RNA in a sequence- and structure-dependent manner[154] and are critical for mediating the function of RBPs and their RNA targets to govern gene expression.

RBPs are critically important in governing RNA structure, regulatory functions, catalytic capacities (in the case of ncRNA), and all aspects of mRNA processing (as described in section 1). A wealth of literature documents critical roles for RBPs in RNA processing often in a dynamic, cell type-specific manner. Given the diverse functional roles for RBPs throughout mRNA processing, it is unsurprising that RBP loss or dysfunction has been linked to numerous diseases including neurological disorders, muscular atrophies, metabolic diseases, and cancer [163-165]. Thus, elucidating normal roles for RBPs during homeostasis or development will reveal important aspects of RBP function that are directly related to pathogenetic mechanisms underlying disease.

1.2.a RBPs in disease

RBPs are evolutionarily conserved and widely distributed across different tissues, consistent with their frequent housekeeping roles. However, despite the ubiquitous nature of RBP expression, loss of function (LOF) mutations within genes encoding RBPs often results in tissue-specific disease[166]. The tissue-specific nature of RBP-associated disease is attributed to multiple different factors. First, RBPs can act on RNA targets or with protein partners that display tissue-specific expression patterns[167]. Second, RBPs can bind target RNAs with a wide range of affinities and specificities leading to the formation of cell-type specific RNA regulatory complexes[168-171]. Finally, RBPs form extensive networks with their RNA targets and other regulatory proteins that are characterized by redundancy, as well as feedback and feedforward control[167]. Together, this complex network provides robust regulatory control such that RBP dysfunction may have distinct consequences in different cell types. Considering that RBPs coordinate elaborate networks of RNA-protein and protein-protein interactions that regulate key aspects of RNA processing, RBP dysfunction can negatively influence many different cellular pathways underlying disease phenotypes. A multitude of different diseases are associated with RBP dysfunction including muscular atrophies, cancer, and neurological disease[164,172,173].

The gene *PABPN1* encodes an RRM-type poly(A)-binding protein that regulates nuclear polyadenylation via association with adenosine molecules of a growing poly(A) tail and stimulating poly(A) polymerase (PAP)[174]. Abnormal expansion of a $(GCG)_n$ trinucleotide repeat in exon 1 of PABPN1 leads to the adult onset, autosomal dominant, degenerative disorder known as oculopharyngeal muscular dystrophy (OPMD)[174]. In unaffected individuals, $(GCG)_6$ codes for the first six alanine residues within a

homopolymeric stretch of ten alanines[175]. However, in individuals with OPMD, this $(GCG)_6$ is expanded to $(GCG)_{8-13}$ leading to a stretch of 12-17 alanines in mutant PABPN1[175]. The mutant PABPN1 then aggregates within the nuclei of skeletal muscle fibers causing progressive muscle weakness[174,175].

RBPs are key regulators of cell growth, differentiation, and proliferation. Thus, RBP dysfunction is implicated in a range of different cancers[176]. Cancer is a heterogeneous disease caused by mutations, chromosomal rearrangements, and gene amplifications resulting in altered activity of genes encoding tumor suppressors or oncogenes. One example of an RBP implicated in tumorgenesis is the altered expression of the mRNA cap binding protein eIF4E [177,178]. eIF4E is a key translation factor that is highly expressed within different tumor types[178]. Behaving as a proto-oncogene, overexpression of eIF4E causes malignant transformation leading to cancer[178].

1.2.b Regulation of RNA in the nervous system

The nervous system requires an intricate level of spatial and temporal regulation of gene expression for proper neuronal function. A neuron must rapidly modify synaptic function and connectivity to properly respond to external stimuli. However, the size, polarity, and structural complexity of neurons (**Figure 1-9**) presents unique challenges for fulfilling critical functions in development and plasticity. Thus, robust post-transcriptional regulatory mechanisms are required to enable rapid adaptation to the ever-changing demands of the nervous system. Activity-dependent control of gene expression within the neuron is established through intricate post-transcriptional regulation of mRNA expression via splicing, stability, trafficking, local translation, and degradation- all of which

require the function of RBPs to coordinate these diverse processing events in space and time.

RBPs regulate every step of mRNA processing and profoundly impact neurodevelopment and neuronal function. The importance of RBP function in neurons is underscored by the prevalence of neurological diseases that have been linked to defects within RBPs causing aberrant processing of RNAs that are necessary for proper neuronal function[166,172,173]. Moreover, transcriptomic analysis of human brain tissue indicates RNA processing defects are a common feature of neurological pathologies[179-182]. Thus, understanding the mechanisms by which RBPs impact the precisely regulated expression of neuronal mRNAs is key to elucidating neuronal disease pathogenesis.

1.3 Intellectual disability

Intellectual disability refers to a broad class of neurodevelopmental disorders characterized by significant limitations in intellectual functioning and impaired adaptive behavior. Clinically, these criteria are defined by an I.Q. score <70, limited independent functioning, and inability to adapt to the environment and social milieu. Intellectual disability affects ~1-3% of the world population and is etiologically heterogeneous associated with both environmental and genetic factors[183]. Environmental contributions to intellectual disability include asphyxia, prematurity, neonatal meningitis, trauma, extreme malnutrition, vascular accidents, intrauterine infections, and in utero drug exposure[184]. On the other hand, genetic etiology includes chromosomal, monogenic defects, such as X-linked, autosomal dominant, autosomal recessive, mitochondrial and imprinting epigenetic disorders[183]. Emerging evidence suggests that most genes linked

to intellectual disability converge on common molecular pathways, including those critical for axon guidance, synaptic structure, and plasticity, as well as neuronal morphology[185-189]. A growing list of over 700 genes has been linked to intellectual disabilities and interestingly, many of these genes encode RBPs with critical roles in post-transcriptional regulation of gene expression.

One key example of RBP dysfunction underlying intellectual disability is Fragile X Syndrome (FXS) [190]. FXS is the most common form of inherited intellectual impairment, developmental delay, and autism spectrum disorder (ASD)[173,191]. The molecular basis of FXS lies in a microsatellite repeat expansion of a cytosine-guanine-guanine (CGG) triplet within the 5'UTR of the Fragile X mental retardation 1 (*FMR1*) gene encoding Fragile X mental retardation protein (FMRP), an RBP that regulates mRNA translation and intracellular trafficking[173]. Under normal conditions, the 5'UTR of the *FMR1* gene contains 5-45 CGG repeats, however, the disease linked *FMR1* has over 200 CGG repeats causing abnormal methylation and subsequent transcriptional silencing[192-196].

FMRP is a largely cytoplasmic RBP, predominantly expressed within the granule layers of the hippocampus and cerebellum[197], that contains two KH domains and an RGG-type RBD[198,199]. Functionally, FMRP is responsible for translational repression of mRNA targes via ribosomal stalling and mRNA trafficking[200-203]. Given the role of FMRP in translational repression, elevated baseline global protein synthesis within the brain is a hallmark phenotype within FXS patients[204]. Moreover, several studies have demonstrated that FRMP is required for the trafficking of mRNAs with key neuronal functions (e.g., *CAMKIIa, Map1b,GABA-AR,* and *SAPAP4)* into dendrites and dendritic spines[201,205,206]. Given that FMRP-dependent mRNA trafficking is important in the

development of dendritic spines, FXS patients exhibit dendritic spines with long and thin immature morphologies compared to mature mushroom-shaped spines[207]. This example illustrates how defects in RNA post-transcriptional processing lead to neurological disease, however, further studies are required to precisely define molecular defects that underlie RBP-linked intellectual disability.

1.4 *Drosophila melanogaster* as a model for intellectual disability

Although the number of genes known to cause human monogenic intellectual disability is increasing rapidly[208], our understanding of the molecular mechanisms and neurodevelopmental pathways that are disrupted by these genetic aberrations is severely lacking. Moreover, studying these genetic aberrations in humans is extremely difficult for many reasons including our relatively long lifespan, uncontrollable environmental factors, and the plethora of ethical concerns (e.g. you cannot ethically dissect a human brain…especially if the person is still using it). In the words of my dear mentor, Dr. Anita Corbett, “humans are a crappy model organism”. Animal models are typically preferred because of their genetic similarity to humans, anatomy, and physiology. Also, animal models (with some exceptions) are often in unlimited supply and have great ease of manipulation. Of the various model organisms, *Drosophila melanogaster* has emerged as a powerful model to help us better understand the cellular and molecular underpinnings of genetic diseases, including intellectual disability. Despite the evolutionary distance between flies and humans, there is a strong conservation of genes, pathways, and regulatory networks. Approximately 75% of human disease genes have an orthologue in *Drosophila*[209] and a whopping 73% of the known intellectual disability

associated genes have a counterpart in flies[210]. Moreover, the *Drosophila* generation time is very quick at 10-12 days from egg laying to eclosion (**Figure 1-11**), and this rapid generation time allows for efficient screening of candidate alleles for genetic interaction. In contrast to mammalian models, the generation of fly mutants is easy, inexpensive and rapid, and the number of publicly available stocks and tools that can be utilized for experiments is increasing steadily[211].

In terms of genetic tools, flies have many well-established systems used to spatiotemporally control gene expression including the yeast-derived *Gal4/UAS* system (**Figure 1-12**) and the FLP-FRT system[212]. The *Gal4-UAS* system was adopted from yeast and allows researchers to control expression on transgenes in a cell-type specific manner[212]. This genetic tool is based on the finding that the Gal4 yeast transcription factor binds to upstream activating sequences (UAS) to activate gene expression[212]. Thus, a fly line carrying the UAS-cDNA construct of interest can be crossed into any number of fly lines expressing Gal4 in a tissue-specific pattern. The FLP/FRT system is another way to drive heritable overexpression of a transgene of interest. In this system, FLP recombinase catalyzes the site-specific recombination between FLP recombination target (FRT) sites[212]. A FLP-out construct contains several elements including a constitutive promoter, an FRT site, a marker gene with a transcription termination site, a second FRT site, and the cDNA of interest[212]. Once introduced to the genome, the expression of FLP recombinase by heat-shock inducible promoter excises the DNA between the FRT sites, leading to a random assortment of cells that overexpress the gene of interest[212].

Drosophila are particularly well-suited for intellectual disability research, as flies provide numerous approaches to investigate behavior as well as neuronal morphology

and function. A range of assays can be used to assess fly behavior including tracking larval crawling and motor development, negative geotaxis, phototaxis, and flight assays[213-215]. Moreover, complex cognitive behaviors such as learning, and memory can be investigated using olfactory learning and courtship conditioning paradigms. To investigate the role of genes in the organization of the brain and nervous system architecture, many studies analyze *Drosophila* nervous system structures in greater detail. For instance, studies of the fly neuromuscular junction are critical to our current understanding of synapse formation and neurotransmitter release mechanisms[216]. Moreover, *Drosophila* can be used to investigate molecular mechanisms regulating axon outgrowth and pathfinding through study of the *Drosophila* mushroom body development (discussed further in section 1.4.b). Finally, changes in dendritic arborization are commonly observed in patients exhibiting intellectual disability[217], and studies of *Drosophila* dendritic arborization (dA) neurons allow researchers to observe dendrite architecture and morphology (discussed in section 1.4.c). Taken together, these examples and many others not mentioned here illustrate that *Drosophila melanogaster* is a powerful model organism that provides many opportunities to advance our understanding of human intellectual disability and cognitive disease.

1.4.a The *Drosophila* Nervous System

Drosophila melanogaster are an excellent model organism for studying the molecular and genetic underpinnings of neurodevelopment and circuit formation[218]. Excitingly, vertebrate nervous systems function utilizing similar mechanisms, thus, the smaller, more simplistic *Drosophila* brain (**Figure 1-13**) provides a genetically tractable

model to enhance our understanding of human neurodevelopment and neuronal function [218]. To illustrate, the human brain contains over 86 billion neurons while the *Drosophila* brain contains only about 100,000 neurons [219], thereby making genetic manipulation and analysis more manageable.

The *Drosophila* brain contains neuronal bundles known as lineages. Lineages are formed from sibling neurons of a parent neuroblast that are bundled into distinct clonal units. The formation of neuronal lineages is advantageous as this provides the resolution necessary for study of critical neurodevelopmental events such as neuron development, axon formation, branch formation, and circuit formation. Moreover, these key neuronal events can be studied in an *in vivo* setting, in contrast to many studies of the mammalian brain where information about neuronal lineage remains elusive. Two neuronal structures commonly used to study axon pathfinding and dendritic arborization, respectively, are known as the mushroom body and larval dendritic arborization (dA) neurons.

1.4.b Mushroom Bodies

The mushroom body is the computational center of the *Drosophila* brain and is comprised of intricate neural circuits that allow the fly to store associative memories and process sensory and internal state information[220]. The mushroom body consists of a pair of twin neuropil structures conventionally viewed as regulators of associative olfactory learning and memory, but recent studies suggest more complex, multifaceted roles for the mushroom body in the regulation of *Drosophila* behavior[221-231]. The mushroom body begins developing in early embryonic stages of and continues until late pupal stages and undergoes extensive remodeling into its more complex adult form[232-234] (**Figure 1-13**).

Approximately 2000 intrinsic neurons known as Kenyon Cells (KCs) comprise the mushroom body. The unipolar KC cell bodies cluster in the posterior regions of the brain. The neurites of the KC cells extend anteriorly forming the peduncle. The neurites of the KC cells are considered axons, and harbor both pre-and post-synaptic sites, and the dendrites cluster and branch out near the cell bodies forming a structure known as the Calyx (**Figure 1-13**). The peduncle bifurcates to form three medial projecting lobes (γ, β, β') and two dorsal projecting lobes (α, α') (**Figure 1-13**). The axons that comprise the α and β lobes emanante from the αβ KCs, and the axons of the α' and β' lobes emanante from the α'β' KCs. On the other hand, axons from the γ KCs only extend medially to form the γ lobe. These three KC classes are further subdivided into subtypes. Each subtype is defined by their morphology and expression of different molecular markers. For instance, the αβ KCs have posterior (p), surface (s), middle (m), and core (c) subtypes; the α'β' KCs have anterior-posterior (ap1 and ap2) and middle (m) subtypes; and the γ KCs have dorsal (d) and main (m) subtypes. Each of these subtypes occupy distinct portions of their respective mushroom body lobe, and this characterization is essential to our understanding of mushroom body function[235].

Two classes of extrinsic neurons – dopaminergic neurons (DANs) and mushroom body output neurons (MBONs) – densely innervate the mushroom body[226,235,236]. DANs are primary input neurons projecting axons into the mushroom body thereby providing physiological state signals and reinforcement[225,226,228,230,231,237]. In contrast, MBONs are the primary output neurons that relay information from the mushroom body to other parts of the brain[226,235,236]. The mushroom body lobes are also innervated by several other neuron types including one GABAergic anterior posterior lateral neuron (APL), one

serotonergic dorsal paired medial neuron (DPM), and two octopamine-releasing neurons (OA-VPMs)[226,235,236]. Unlike DANs and MBONs, these neurons do not have zone-specific innervations. Instead, the neurites of APL and DPM branch into all of the lobes and the peduncle while the OA-VPMs only sparsely innervate the mushroom body lobes[226,235,236].

1.4.c Dendritic Arborization Neurons

Neurons of *Drosophila*, like many other insects, are primarily unipolar unlike most mammalian neurons. In the peripheral nervous system of *Drosophila* larvae, however, many neurons have multipolar morphologies[238]. Neuronal architecture complexity requires proper axon and dendritic guidance mechanisms which rely on a variety of cues to shape growth and projection[238,239]. One subgroup of multiple dendritic neurons are dendritic arborization (dA) neurons which are segmentally organized PNS neurons with elaborate dendritic arbors that tile the body wall of larvae[238,240]. These neurons are located between the basal muscle and the apical epidermal cells and are attached to the epidermal extracellular matrix (ECM) by integrin (dendritic) and laminin (epidermal) on the ECM, with a portion of the dendritic arbor in the epidermal cell[241]. There are four classes of da neurons, classes I-IV, with class I having the least elaborate arbors and class IV having the most complex arbors[241,242] (**Figure 1-14**). *Drosophila* larvae are segmented, and each segment contains 15 dA neurons that function in proprioception, muscle contraction, and nociception[241,242]. The dorsal most class IV neurons are known as ddaC neurons extend to anterior and posterior body segments and have traditionally been used to study dendritic arborization mechanisms in the fly[238]. Class IV dA neurons express the mechano-transducer Pickpocket (*ppk*), a Degenerin/Epithelial sodium channel subunit, thus using a *ppk*>Gal4 driving membrane tethered mCD8::GFP allows

for visualization of these neuronal architectures *in vivo* making this an ideal system to probe mechanisms of dendritic development[240,243] (**Figure 1-14**).

1.5 ZC3H14-linked Intellectual Disability

The recent evidence that intellectual disability-linked genes converge on a limited set of pathways suggests that disparate intellectual disabilities are unified by underlying molecular dysfunction. This convergence suggests that studies of monogenic, experimentally tractable forms of intellectual disability can provide molecular insight intro mechanisms common to all forms of the disease. A subset of monogenic intellectual disabilities are caused by mutations affecting genes that encode RBPs[244]. One such recessive, monogenic form of intellectual disability is caused by loss-of-function mutations within the gene encoding the evolutionarily conserved RBP, *ZC3H14*[215].

1.5.a Mammalian ZC3H14

Human *ZC3H14* encodes a ubiquitously expressed ZnF (see section 1.2), polyadenosine RBP, ZC3H14 (ZnF CysCysCysHis #14; Also known as Mammalian Suppressor of Tau-2, MSUT2), that is lost in a form of inherited non-syndromic, autosomal recessive intellectual disability[215]. Mutations in *ZC3H14* were discovered in a cohort of more than 200 consanguineous Iranian families via large-scale autozygosity mapping and linkage analysis[215]. Splice variants of *ZC3H14* give rise to four human ZC3H14 protein isoforms (Isoforms 1-4). ZC3H14 Isoforms 1-3 are ubiquitously expressed in all tissues and cell types, however, Isoform 4 is primarily expressed in the testes[245,246]. Several mutations in the *ZC3H14* gene have been linked to intellectual disability[215,247,248]. The most well characterized mutation leading to *ZC3H14*-linked intellectual disability (R154X;

Figure 1-15) creates a premature stop codon in exon 6 of *ZC3H14* causing loss of ZC3H14 Isoform 1-3 expression[215,245]. Other mutations including a frameshift (N309fs; **Figure 1-15**) and a 25bp deletion located 16-bp downstream of the 3'end boundary of exon 16 (Δ25bp) have been described. Human ZC3H14 Isoforms 1-3 contain an N-terminal proline-tryptophan-isoleucine (PWI)-like domain, a nuclear localization signal, and a C-terminal tandem CCCH ZnF domain ranging from 84-62 kDa[245] (**Figure 1-15**). The PWI-like domain serves as a protein-protein interaction domain, the nuclear localization signal (NLS) localizes these ZC3H14 isoforms to the nucleus, and the CCCH tandem zinc fingers bind polyadenosine RNA. Unlike ZC3H14 Isoforms 1-3, Isoform 4 is much smaller (~34kDa) and does not contain a predicted NLS and is localized to the cytoplasm[245].

Studies in human cell culture suggest that ZC3H14 affects the steady-state level of a small number of expressed transcripts (~1%)[249]. Specifically, loss of ZC3H14 reduces the stability of the *ATP5G1* transcript encoding the F_0 subunit of the mitochondrial ATP synthase [249]. These studies demonstrate that ZC3H14 binds and ensures proper nuclear processing and retention of *ATP5G1* pre-mRNA[249]. Consistent with the role of ATP5G1 as a rate-limiting component of ATP synthase activity, loss of ZC3H14, and therefore loss of *ATP5G1* processing causes reduced levels of cellular levels of ATP as well as mitochondrial fragmentation[249]. Together, these data suggest that human ZC3H14 modulates pre-mRNA processing of select transcripts and regulates cellular energy levels, which likely has broad implications for proper neurodevelopment and function.

1.5.b *Caenorhabditis elegans* Sut2

Several studies have utilized the nematode *Caenorhabditis elegans* to explore roles for Sut2 (Suppressor of tau pathology-2), an orthologue of human ZC3H14/MSUT2. These studies identified a role for Sut2 in modulating Tau toxicity in a *C. elegans* Taupathy model [250-252]. Tauopathies are diseases defined by the accumulation of insoluble Tau or hyperphosphorylation of Tau which, in part, cause neurodegeneration within the central nervous system[253]. Tau dysfunction has been implicated in several neurodegenerative disorders, including Alzheimer's disease (AD) and frontotemporal dementia (FTD)[253]. *C. elegans* expressing mutant human Tau exhibit a plethora of defects including movement defects and neurodegeneration that worsen as nematodes age[252]. Intriguingly, *sut-2* was identified in a mutant screen as a modifier of these behaviors. Indeed, homozygous loss of *sut-2* restores movement of Tau-expressing nematodes back to control-levels. Furthermore, loss of *sut-2* reduces Tau aggregation, mitigates neurodegenerative changes, and restores motor function[252]. These studies have been extended to human cell culture models whereby high Tau levels lead to increased expression of mammalian SUT-2 (MSUT2) and RNAi knockdown of MSUT2 in cells overexpressing Tau, causes a decrease in Tau aggregation[251]. Taken together, insights from these functional studies suggest that SUT-2/MSUT2 influences neuronal vulnerability to Taupathies, thus, neuroprotective strategies that target MSUT2 may be of therapeutic interest in targeting tauopathy-linked disease[251,254].

1.5.c *Saccharomyces cerevisiae* Nab2

Numerous molecular functions for the Saccharomyces cerevisiae orthologue of human ZC3H14, Nab2, have been defined. Original studies illustrate that Nab2 is an

essential heterogeneous nuclear ribonucleoprotein (hnRNP) in yeast that co-purifies with polyadenosine RNA[255]. Nab2 shuttles between the nucleus and cytoplasm and is required for both polyadenylation and nuclear export as evidenced by extended poly(A) tails and nuclear accumulation of poly(A) RNA in *nab2* mutant yeast cells[255-258]. Subsequent studies reveal that the Nab2 zinc finger domain mediates sequence specific binding of Nab2 to poly(A) RNA with nanomolar affinity (~30 nM)[259].

Like human ZC3H14, Nab2 contains several key domains: an N-terminal domain, a Q-rich domain, an RGG domain, and a C-terminal tandem zinc finger domain[255,256] (**Figure 1-15**). The N-terminal domain of Nab2 forms a five alpha-helix bundle with a PWI-like fold which facilitates poly(A) RNA export[255,260]. The Q-rich domain is not essential and has no defined function to date[256]. The RGG domain is important for nuclear import and mediates interaction with the import receptor, Kap104[256,261-263]. Finally, the C-terminal zinc finger domain contains seven CCCH-type ZnFs that mediate high affinity binding to poly(A) RNA[255,256,259,264]. Functionally, the N- and C-terminal domains are the most well characterized and play roles in mRNA export and poly(A) tail length control, respectively.

The N-terminal domain of Nab2 is critically important for poly(A) RNA export in budding yeast[256,257], where *nab2* mutants that lack the N-terminal domain (*nab2*-Δ*N*) exhibit severely impaired growth and accumulation of bulk poly(A) RNA in the nucleus[256,257]. Intriguingly, *nab2*-Δ*N* cells also demonstrate extended poly(A) tails, suggesting that the N-terminus may play a role in restriction of poly(A) tail length[264]. Alternatively, this observation my reflect hyperadenylation of mRNA transcripts due to nuclear residence time. The N-terminal domain of Nab2 also interacts with two nuclear pore-associated protein, Mlp1 and Gfd1[260,265-267]. Mlp1 localizes to the nuclear side of the

NPC and functions in pre-mRNA retention, whereas Gfd1 localizes to the cytoplasmic face of the nuclear pore and facilitates mRNP disassembly[260,268-272]. These interactions reflect the ability of Nab2 to concentrate correctly processed mRNAs to the nuclear side of the nuclear pore complex for export via interactions with Mlp1, and tether mRNPs at the cytoplasmic face for disassembly via interactions with Gfd1.

As mentioned previously, the C-terminal CCCH-type ZnF domain recognizes poly(A) RNA and is critical for regulation of poly(A) tail length[259,264]. Biochemically, ZnFs 5-7 of yeast Nab2 are necessary and sufficient for high affinity binding to polyadenosine RNA[256,264]. To illustrate, cells expressing *nab2* ZnF domain mutants, *nab2-21* (Loss of ZnF6 and ZnF7)*, nab2-C437S* (C437S in ZnF6)*,* or *nab2-*$C_{5\text{-}7}$*→A* (C415A in ZnF5, C437A in ZnF6, and C458A in ZnF7) exhibit cold-sensitive growth phenotypes and extended poly(A) tails[256,264]. Together, these data illustrate that Nab2 binds poly(A) RNA via the ZnF domain and facilitates targeting of these transcripts to the nuclear pore complex via the N-terminal PWI-like domain.

In addition to the roles of Nab2 in regulation of poly(A) tail length and nuclear export, further studies implicate Nab2 in mRNA splicing[273,274]. Nab2 associates with early branch point factors Mud2 and Msl5 and *nab2* mutant yeast cells exhibit an increase in unspliced pre-mRNA and a significant decrease in total RNA levels[273]. Together, with proteomic evidence that human ZC3H14 associated with the U2AF2/U2AF spliceosome protein, these data provide a physical link between Nab2/ZC3H14 and the spliceosome and indicate that Nab2 plays an important role in the regulation of pre-mRNA splicing[273].

1.5.d *Drosophila melanogaster* Nab2

As mentioned above (section 1.4), *Drosophila melanogaster* provide a powerful model for studying mechanisms of neurodevelopment and provide invaluable insight into the molecular pathways disrupted in neurodevelopmental disease. By exploiting *Drosophila* evolutionary conservation and ease of manipulation, crucial insights have been made to our understanding of RBP-linked intellectual disabilities, including Fragile X syndrome[275] and Angelman syndrome[276,277]. Our labs have similarly employed a *Drosophila* model to elucidate ZC3H14 function via study of the *Drosophila* orthologue, Nab2[215,274,278-282]. A Nab2 mutant fly model (hereafter referred to as $Nab2^{null}$ or $Nab2^{ex3}$) was generated via imprecise excision of a P-element (*EY08422*) located at the 5'end of the *Nab2* genomic locus[215,283]. This excision removes a large portion of the *Nab2* gene including the transcriptional start site (TSS), generating flies functionally null for Nab2 RNA and protein[215]. Unlike the four ZC3H14 protein isoforms in humans, *Drosophila* express only one isoform of Nab2[215]. Although *Drosophila* Nab2 shares only 41% amino acid identity with human ZC3H14, the structure is highly conserved within critical functional domains including the N-terminal domain, PWI-like domain, predicted NLS, and the five CCCH-ZnF RNA-binding domains[215] (**Figure 1-15**). Our labs have extensively exploited this *Drosophila* model of ZC3H14-linked intellectual disability to uncover the functional relevance of this critical and conserved RBP.

We have elucidated several key developmental roles for Nab2. Loss of Nab2 causes severe reductions in adult viability as only 3-5% of $Nab2^{null}$ homozygotes eclose from their pupal casings (the majority die in late pupal stages)[215]. The flies that emerge completely exhibit severely reduced lifespans of ~10-15 days compared to the average

Drosophila lifespan of ~60-80 days[215]. These flies exhibit severe morphological defects reminiscent of other RBP mutants, including a wings-held-out phenotype, in which flies fail to properly fold their wings over the dorsal side of their thorax and abdomen[215]. Moreover, these flies exhibit disorganization and kinking of their thoracic bristles. *Nab2^{null}* homozygotes do not exhibit viability, morphological, or behavioral defects through mid-pupal development[215]. Intriguingly however, embryos lacking germline contribution of *Nab2* die in early embryogenesis, indicating that *Nab2* is required for embryonic viability and development[215]. In addition to these developmental and phenotypic defects, *Nab2^{null}* flies also exhibit flight impairment and compromised locomotor capabilities[215]. Experiments probing tissue-specific requirements for Nab2 illustrate that pan-neuronal knockdown of *Nab2* mimics defects of *Nab2^{null}* homozygotes, illustrating that Nab2 is required in neurons for normal behavior[215]. Moreover, courtship-conditioning assays used to assess the pan-neuronal requirement for Nab2 in short-term memory acquisition illustrate that Nab2 regulates pathways critical for short-term memory formation[284]. Significantly, transgenic expression of human ZC3H14-isoform 1 only in fly neurons is sufficient to rescue a variety of *Nab2^{null}* defects, supporting a model in which *Drosophila* Nab2 and Human ZC3H14 share critical molecular roles and mRNA targets.

In addition to the phenotypic and behavioral defects observed in *Nab2^{null}* flies, previous studies revealed a role for Nab2 in the regulation of *Drosophila* neuronal morphology in mushroom bodies of the central nervous system, (CNS; as discussed in 1.4.b) and dA neurons of the peripheral nervous system (PNS; as discussed in 1.4.c) [281,284]. Within Kenyon cells of the mushroom body Nab2 localizes primarily to the nucleus, in foci reminiscent of nuclear speckles. Germline, pan-neuronal (*Elav-Gal4*), and

mushroom body-specific (*OK107-Gal4*) loss of *Nab2* causes axonal projection defects in Kenyon cells of the mushroom body. Specifically, *Nab2*^{null} flies exhibit thinning or loss of α lobes and thinning, loss, or midline crossing of β lobes[284]. To date, defects in the γ lobe structures have not been observed[284]. In **Chapter 3** of this dissertation, we describe the first observation of disrupted α' and β' structures in *Nab2* mutant flies which exhibit a characteristic axonal defasciculation phenotype. Together, these data illustrate a requirement (in some cases cell-autonomous) for Nab2 in the regulation of *Drosophila* mushroom body morphology. Nab2 also limits dendritic arborization of class IV dA neurons through a mechanism that involves the planar cell polarity (PCP) pathway in the *Drosophila* PNS, as loss of Nab2 in class IV ddAC neurons (*UAS-Nab2RNAi, ppk*-Gal4) and *Nab2*^{null} homozygotes exhibit severe overarborization defects[281].

Several molecular roles for *Drosophila* Nab2 have been described by our labs. For example, loss of Nab2 moderately increases bulk poly(A) tail length in *Drosophila* heads, indicating that fly Nab2, like both yeast Nab2 and mammalian ZC3H14, plays a role in regulating poly(A) tail length[215,278,279]. Moreover, Nab2 physically and functionally interacts with the well-known translational repressor Fmr1 (the *Drosophila* homolog of FMRP) to support axonal morphology and olfactory memory[278]. In support of roles for Nab2 in translational repression (potentially in concert with Fmr1), knockdown of Nab2 increases fluorescence from a transgenic *CaMKII* 3'UTR reporter construct. Nab2 also interacts with the neuronal translational regulator Ataxin-2 (Atx-2), which has dual functions to suppress or activate translation of RNA transcripts in neurons, further linking molecular functions for Nab2 to the regulation of translation[282]. Epitope-tagged Nab2 RNA immunoprecipitation (RIP; *Nab2-FLAG*) reveals that Nab2-associated transcripts encode

proteins of various neuronal and neurodevelopmental functions, linking Nab2 dysfunction to a variety of *Nab2*^{null} phenotypes[282]. In support of Nab2 as a polyadenosine RBP, these studies also confirm that Nab2-assocoated transcripts are over-represented for A-rich sequence motifs (outside of the poly(A) tail). Although these recent advances have shed invaluable light on our understanding of Nab2 function, the precise molecular roles of Nab2 and the specific neuronal mRNA targets that Nab2 governs to guide neurodevelopment remain elusive.

1.6 Nab2 regulates splicing of select neuronally-enriched transcripts within the fly head.

In **Chapter 2** of this thesis, we describe a novel function for Nab2 in the regulation of splicing of select neuronally-enriched transcripts within the fly head. Thus, dysregulation of transcripts critical for neuronal function may help explain, in part, the numerous neuronal-specific defects observed in *Nab2*^{null} flies. Many of the mRNA transcripts with disrupted levels or splicing patterns upon loss of Nab2 encode factors with roles in behavior, neurodevelopment, and/or neural function. We focus on two transcripts in this thesis known as *Sex lethal* (*Sxl*) and *trio*.

1.6.b Sex lethal (*Sxl*)- The master regulator of sex determination and dosage compensation in *Drosophila*

Sex determination is essential for sexual dimorphism, the anatomical, physiological, and behavioral differences between sexes of the same species. Like many organisms, *Drosophila melanogaster* sex determination is governed by the inheritance of sex chromosomes (X and/or Y chromosomes) where males have one X and one Y

chromosome (XY), and females have two X chromosomes (XX). This means that females (XX) have twice the “dose” of the X chromosome than males (XY). Humans born with two X chromosomes undergo a process known as X inactivation in which transcription from one X chromosome is silenced in each somatic cell to “equalize” gene transcription from the X chromosome between sexes. This process is the essentially the opposite in *Drosophila* where males undergo a process known as dosage compensation in which transcription on their single X chromosome is increased to equal that of transcription of two X chromosomes[285]. Dosage compensation in *Drosophila* hinges on expression of the RBP Sex lethal (Sxl) to govern sex determination and sexual dimorphism in the fly[285].

The *Sxl* gene encodes an RBP that governs both RNA splicing and translational regulation necessary and sufficient for female sexual identity in both somatic and germline cells[285,286]. In somatic cells, transcription from the *Sxl* “establishment” or “early” promoter (SxlPe) is activated only in the presence of two X chromosomes and occurs in the early embryonic stages. Splicing of *SxlPe* is performed by default splicing machinery yielding an early pulse of functional Sxl protein. Transcription from the *Pe* promoter is turned off as the embryo develops and transcription from the *Sxl* “maintenance” promoter *Pm* is turned on[285,286]. Unlike the *Pe* promoter, transcription from *Pm* occurs in both XX and XY animals[285,286]. Unlike *SxlPe*, *SxlPm* requires alternative splicing that is dependent on Sxl itself[286]. Given that only XX animals have early Sxl protein, only XX animals can initiate this positive feedback loop. In this sex determination cascade[285,286] (**Figure 1-16**), Sxl produced from *SxlPe* induces female-specific skipping of *SxlPm* exon 3 which contains a premature termination codon. Thus, functional Sxl protein from the Pm promoter is only produed in XX animals.

The expression of functional Sxl protein in XX animals directs a female-specific sex-determination cascade via regulation of sex-specific splicing patterns. Sxl directs the female-specific splicing of the *transformer* (*tra*) transcript giving rise to functional Tra protein. Together, Tra and Tra-2 (*tra-2* does not undergo sex-specific splicing) bind an exonic splicing enhancer (ESE) of the female-specific exon of the *doublesex* (*dsx*) transcript thereby acitivating a weak 3' splicing site to generate female-type DSX (DSX^F) [285,286]. On the other hand, lack of functional Sxl in XY animals causes male-specific splicing of *tra*, which similar to *Sxl*, contains a premature termination codon. Thus, no functional Tra is produced in males[285,286]. The absence of Tra in XY animals causes default splicing of *dsx* to generate male-type DSX (DSX^M) protein. Both DSX^F and DSX^M govern sex-specific transcription of target genes that regulate *Drosophila* sexual dimorphism. Moreover, Sxl inhibits production of male-specific lethal-2 (Msl-2) protein at the post-transcriptional level[287]. Thus, Msl-2 is only expressed in XY animals where it associates with other factors forming the MSL complex to enhance transcription from the X chromosome[287].

Intriguingly, proper splicing of the *Sxl* transcript to govern sex-determination is regulated by m^6A (N-6 methyladenosine; discussed in detail in 1.1.a) [129]. Previous studies illustrate that loss of *Mettl3* (previously known as *Ime4*) which encodes the catalytic subunit of the methyltransferase complex, causes masculinized splicing of the *Sxl* transcript in female heads[129]. Consistent with these findings, splicing of *tra* and *msl-2* is also disrupted in female heads[129]. Moreover, various alleles perturbing function of the methyltransferase complex cause masculinized splicing of *Sxl* in female tissue, illustrating

that the methyltransferase complex plays a critical role in sex determination in *Drosophila* (discussed in detail in **Chapter 2**)[129,147,288-290].

1.6.c The RhoGEF Trio

The Rho (Ras homolog) family of proteins are integral members of the RAS superfamily of guanine nucleotide-binding proteins. As master regulators of the cytoskeleton, Rho family proteins control almost all fundamental cellular processes in eukaryotes including gene expression, morphogenesis, cell division, cell polarity, and cell migration[291]. Rho GTPases serve as molecular switches cycling between a GDP-bound inactive state, and a GTP-bound active state. Active GTP-bound Rho GTPases can then activate downstream effector proteins to regulate a diverse array cellular functions. Regulation of this of this GTPase cycle involves Rho guanine nucleotide exchange factors (GEFs), which activate Rho GTPases by accelerating the exchange of GDP for GTP[292]. On the other hand, Rho GTPases are inactivated by Rho GTPase-activating proteins (GAPs) which stimulate GTP hydrolysis[292] (**Figure 1-17**). Given the diverse roles of Rho family proteins in the regulation of cellular processes, mutations in Rho family proteins are implicated in numerous diseases including, immunological diseases, cardiovascular disorders, cancer, and neurodevelopmental disease (including intellectual disability)[293-296]. Although the molecular mechanisms of Rho GTPase regulation have been well characterized, how loss of GTPase regulatory proteins disrupts cellular function and development remains poorly understood.

Rho GTPases respond to a variety of external stimuli including growth factors, hormones, and cytokines, and RhoGEF proteins are responsible for relaying these external stimuli by activating Rho GTPases[297,298]. There are two distinct classes of

RhoGEFs known as Dbl proteins and the DOCK proteins[298,299]. The Dbl family of proteins is comprised of 70 members sharing a catalytic Dbl Homology (DH) domain and a Pleckstrin-Homology (PH) domain that regulates GEF activation and localization[300]. In addition to this DH domain, Dbl family GEFs typically contain various catalytic or protein-protein interaction motifs through which GEFs connect Rho GTPase signaling to upstream molecular pathways[301]. Unlike the large number of Dbl proteins, there are only 11 members of the DOCK family of RhoGEFs[302]. DOCK family proteins contain a catalytic DHR-2 or CZH domain restricted to activation of Rac1 and Cdc42, in contrast to Dbl domains that can also activate RhoA[303].

One unique RhoGEF with critical roles in regulation of Rac1 and RhoA to govern neuronal development, is known as Trio[303]. Trio is a member of the Dbl family of GEF proteins and contains three catalytic domains, hence the name Trio (**Figure 1-18**). In humans, the Trio protein is comprised of a SEC14 domain, 9 spectrin repeats, an N-terminal GEF domain (GEF1), two SH3 domains, a C-terminal GEF domain (GEF2), and Ig-like domain, and a C-terminal serine-threonine kinase domain (**Figure 1-18**)[304]. Trio is enriched within the nervous system and notably, the Trio A and Trio D isoforms which lack the second SH3 domain (SH3-2), the Ig-like domain, and the serine threonine kinase domain are more highly expressed in the brain than full-length Trio (Trio-FL)[304]. Importantly, loss- and gain-of-function mutations in the human *TRIO* gene are linked to genetically dominant forms of intellectual disability[305-308].

Trio is unique in that it contains two GEF domains which target the Rac1 and RhoA (also known as Rho1) small RhoGTPases. Specifically, the GEF1 domain of Trio activates Rac1 while the GEF2 domain of Trio activates RhoA[295,303,304,308-318]. Rac1 and RhoA are

among the most widely studied RhoGTPases and play critical roles as cytoskeletal regulators critical for proper neuronal development and function[310]. Intriguingly, Rac1 and RhoA activate antagonistic downstream pathways that cooperate via precise spatiotemporal control to execute a variety of coordinated cytoskeletal processes during neurodevelopment[310,319]. In general, Rac1 activation promotes neurite outgrowth while RhoA activation restricts neurite outgrowth[310,319,320]. In axons, Rac1 is critical for axon formation and elongation with *Rac1* conditional knock-out mice exhibiting dramatically impaired axon formation and routing[321-323]. In contrast, conditional knock-out of *RhoA* causes significantly longer axonal projections[324]. In dendrites, Rac1 is considered a positive regulator of dendritic arbor growth while RhoA typically acts as a negative regulator of dendritic arbor growth[320,325-329]. Together, these studies highlight important roles for both Rac1 and RhoA in fine-tuning of neurite projection throughout development, and as a dual GEF, Trio is uniquely positioned to provide precise spatiotemporal control of Rac1 and RhoA activation to govern proper neurodevelopment.

Studies in *Drosophila melanogaster* have significantly enhanced our understanding of Trio function in neurodevelopment. The *Drosophila* Trio amino acid sequence and modular protein structure is similar to human Trio, sharing the N-terminal domain, spectrin-repeats, a GEF1 and GEF2 domain, and an SH3 domain (**Figure-18**). Unlike human Trio, however, *Drosophila* Trio lacks the Ig-like domain and the serine-threonine kinase domain. Two variants of Trio highly enriched in the *Drosophila* nervous system are known as Trio Long (Trio L) and Trio Medium (Trio M). Trio L is most similar to human Trio A consisting of the N-terminal domain, spectrin-repeats, a GEF1 and GEF2 domain, and an SH3 domain (**Figure-18**). On the other hand, *Drosophila* Trio M consists

only of the SH3 domain, and the GEF2 domain (**Figure-18**). Previous studies investigating *Drosophila* Trio focused on the role of Trio L which acts primarily via the GEF1 domain to illicit downstream neuronal patterning. However, little is known about the function of the Trio M protein and any role in *Drosophila* neurodevelopment (Discussed in detail in **Chapter 3**). Previous studies in *Drosophila* have demonstrated that Trio is enriched within the nervous system where it regulates axon pathfinding and dendritic morphology. Specifically, loss of Trio function causes mistargeting of individual axons within the CNS and PNS[313,316,330,331], and previous work defines a critical role for Trio-GEF1 and -GEF2 functions in patterning dA neurons within the *Drosophila* PNS (discussed in detail in **Chapter 3**)[320]. In the *Drosophila* brain, Trio is enriched within the mushroom body α', β', and γ lobes where it directs proper axon pathfinding during neurodevelopment PNS (discussed in detail in **Chapter 3**)[313]. Taken together, these studies highlight an important role for Trio in neurodevelopment and illustrate that investigation of Trio function in *Drosophila* can help shed light on Trio-dependent neurodevelopmental mechanisms disrupted in neuronal diseases such as intellectual disability.

1.7 Scope of Dissertation

The mechanism by which critical RNAs are post-transcriptionally regulated during neurodevelopment and in the context of neurodevelopmental disease has long been an active area of research. The RNA binding protein ZC3H14/Nab2 is necessary for proper post-transcriptional processing of RNAs and plays key roles in metazoan development. Using *Drosophila melanogaster* as a model organism, key developmental and molecular

functions for Nab2 have been described including roles in polyadenylation, translation, neurodevelopment, and cognitive function. Despite these advances in our understanding of the diverse roles for Nab2, few insights have been made into how disruption of specific Nab2-target mRNAs may lead to perturbations in molecular and developmental function required for proper neurogenesis. Thus, defining key mRNA targets of Nab2 and exploring how these transcripts are regulated is key to elucidating elevated roles for Nab2 in the developing nervous system.

The overarching goal of the research presented in this dissertation, as well as the research that has preceded my time as a graduate student, is to investigate the role of the Nab2 RBP in the post transcriptional regulation of RNAs to govern neurodevelopment. In this thesis, I build on previous studies from our group and others to investigate the role of Nab2 in the *Drosophila* nervous system. In doing so, I address a gap in our understanding of Nab2 function by defining key neuronal mRNA targets of Nab2 and define potential mechanisms by which they are regulated by this conserved RBP (**Figure 1-19**). In culmination, the studies presented here help to elucidate how perturbations in human ZC3H14 expression impact human neurodevelopment underlying neurodevelopmental disease.

In **Chapter 2**, I address a function of Nab2 in the brain by revealing that Nab2 regulates splicing and transcript levels of neuronally-enriched transcripts within the fly head. I focus our studies on retention of a male-specific exon in *Sxl* occurring in the heads of female flies. Intriguingly, this analysis further identifies genetic interactions between Nab2 and components of the methyltransferase machinery and unveils a role for Nab2 in the regulation of m^6A methylation on the *Sxl* transcript. These studies suggest

that Nab2 and Mettl3 may act on the similar RNA targets to regulate downstream RNA processing events at by modulating levels of m^6A methylation. In **Chapter 3**, we build on the work presented in **Chapter 2** as well as work from our previous studies[215,278-282,284,332] by focusing on how Nab2 and Mettl3 regulation of *trio* pre-mRNA processing shapes axon guidance and dendritic arbor development within the *Drosophila* nervous system. In **Chapter 4** I share some of the painstaking research I performed that will probably never see the light of day (apart from this thesis, of course), including how to "clean-up" a lethal stock of *Nab2^{null}* flies, the first evidence that *Sxl* regulates mushroom body development, my thoughts on the limitations of DART for analysis of pre-mRNA methylation states and preliminary evidence that Nab2 regulates methylation of the *trio* transcript, and a pilot experiment for nanopore direct-RNA sequencing of the *Nab2^{null}* head transcriptome. Finally, in **Chapter 5** I discuss the findings from this dissertation, providing overarching context and future directions for our studies.

1.8 Figures

Figure 1-1

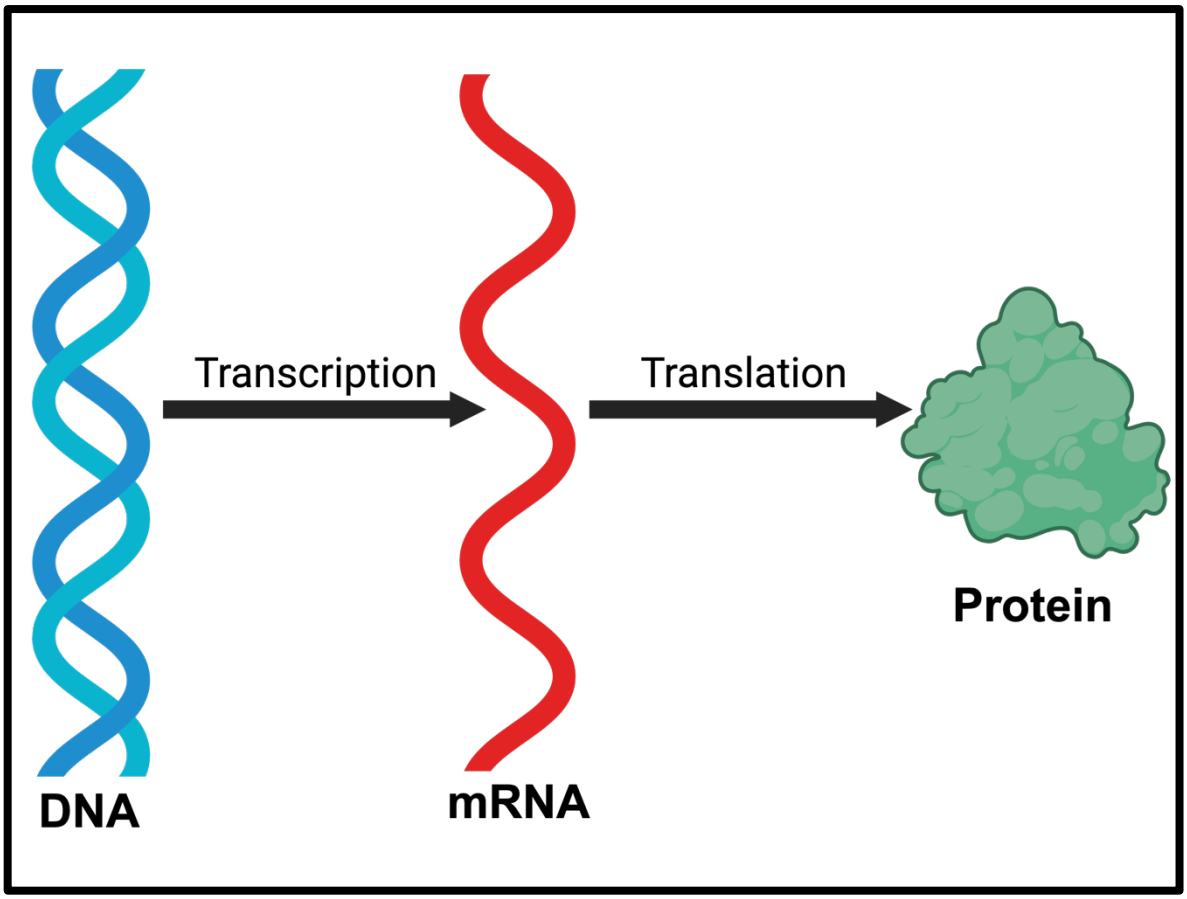

Figure 1-1. The Central Dogma. The central dogma of molecular biology illustrates the flow of genetic information in which DNA is transcribed into messenger RNA (mRNA) and subsequently translated into protein.

Figure 1-2

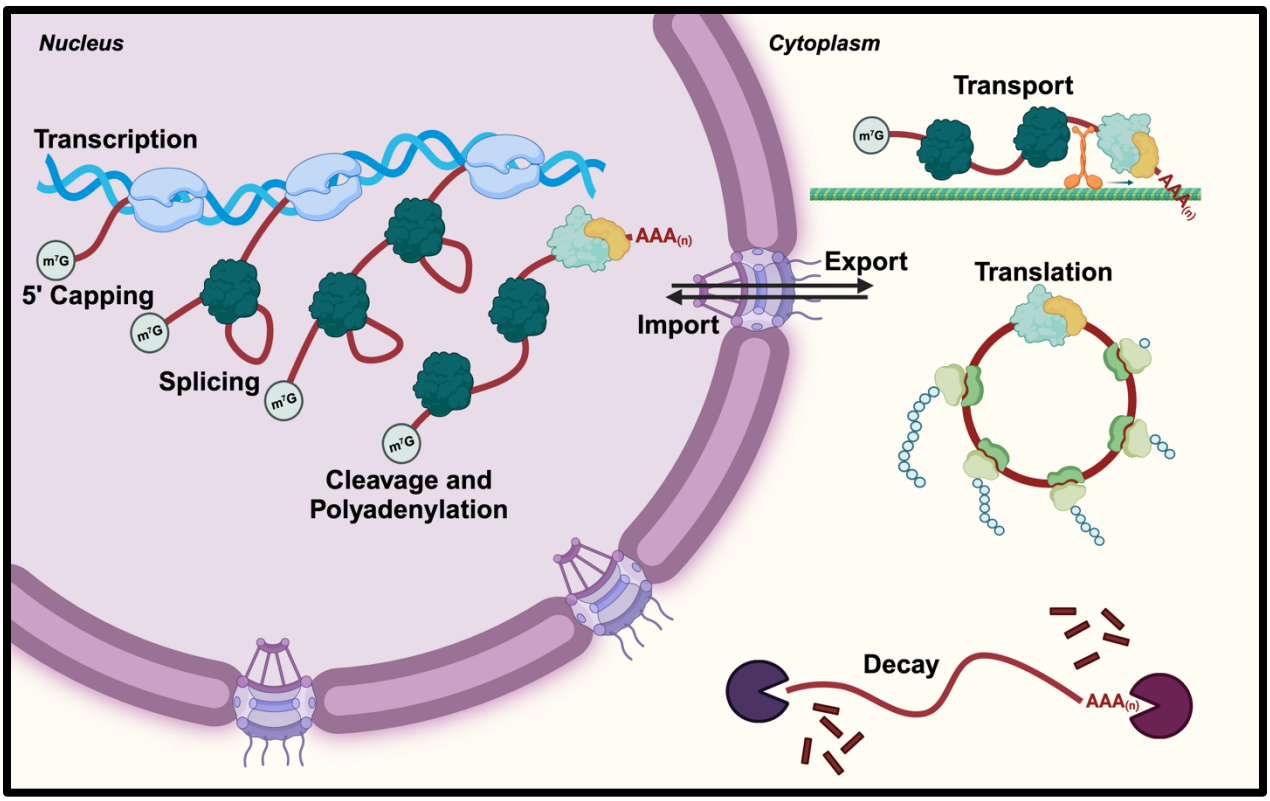

Figure 1-2. Regulation of Gene Expression Regulation of gene expression occurs both in the nucleus and the cytoplasm. Transcription of the nascent pre-mRNA molecule occurs in the nucleus where it undergoes co-transcriptional 5' capping, splicing, and cleavage followed by polyadenylation. The mature mRNA is then exported from the nucleus to the cytoplasm, through the nuclear pore. Within the cytoplasm, the mRNA is transported, translated, and undergoes decay. The nucleus is denoted by the purple background and the cytoplasm is denoted by the light-yellow background. The large purple cylinders indicate the nuclear envelope, and the cage structures represent the nuclear pore.

Figure 1-3

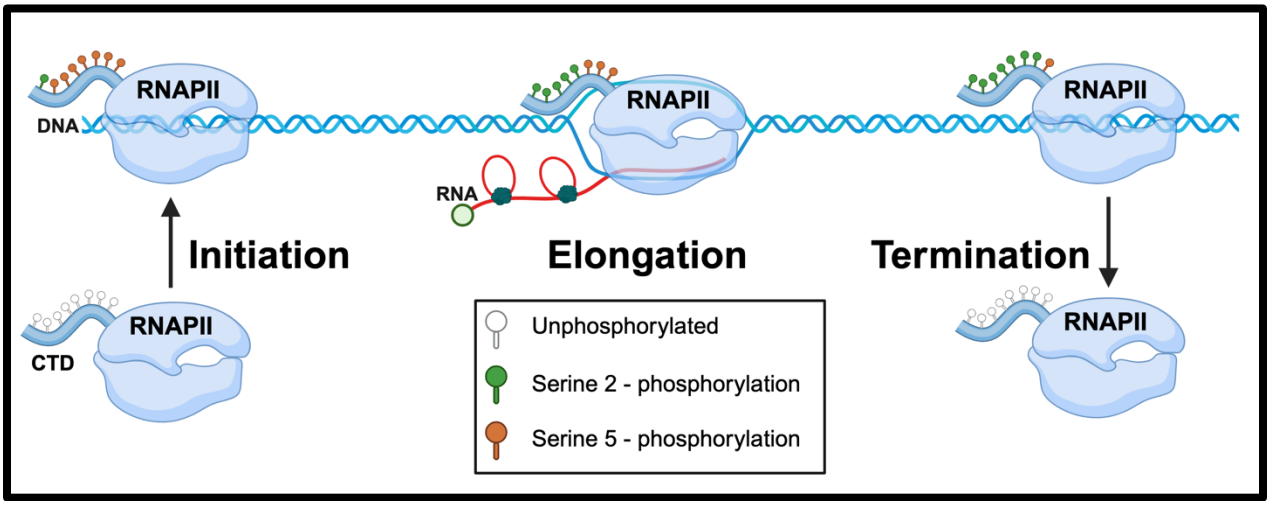

Figure 1-3. Transcription. Initiation: Hypophosphorylated RNA polymerase II (RNAPII) is recruited to a gene promoter into the preinitiation complex (not pictured) and is phosphorylated on serine 5. Elongation: RNAPII synthesizes an RNA molecule from the template DNA and serine 2 is phosphorylated. Termination: RNAPII halts RNA synthesis and nobth RNAPII and RNA are released from the template DNA and serine 2 phosphorylation is more prevalent [9].

Figure 1-4

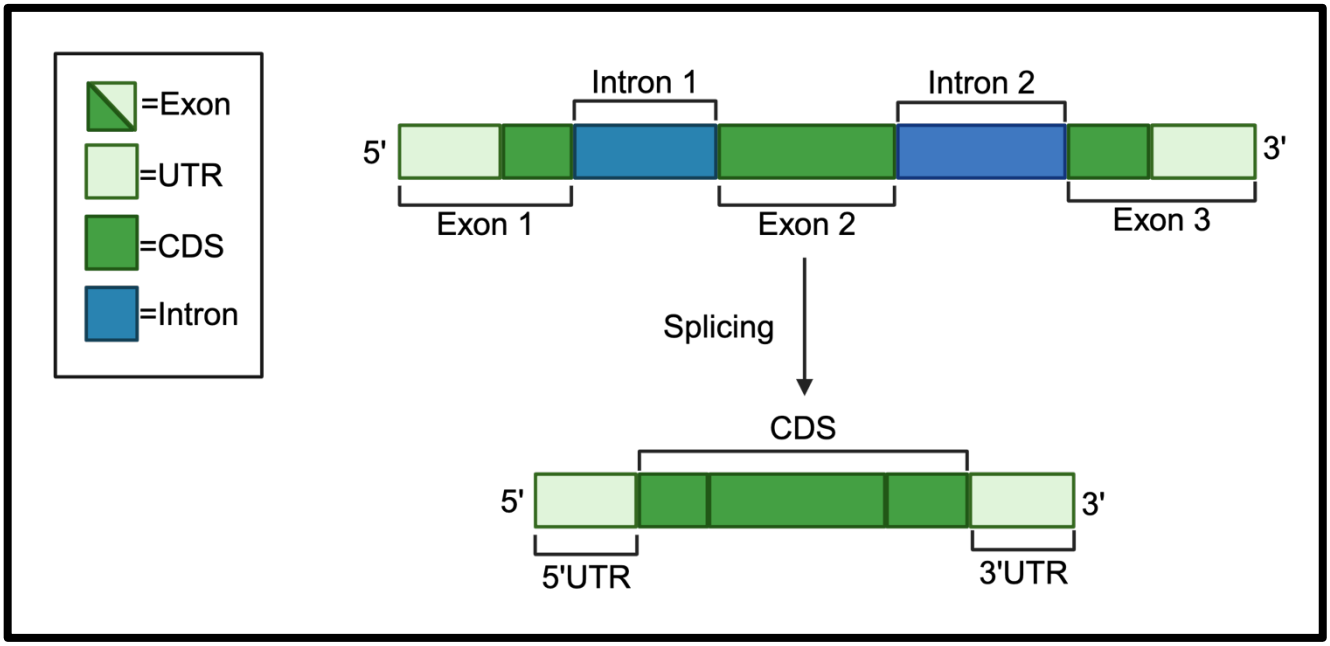

Figure 1-4 Untranslated regions are exons too. Exons (light green and dark green) are sequences that exit the nucleus including untranslated regions (UTRs; light green) and the coding sequence (CDS). Introns (blue) are removed during splicing and do not exit the nucleus

Figure 1-5

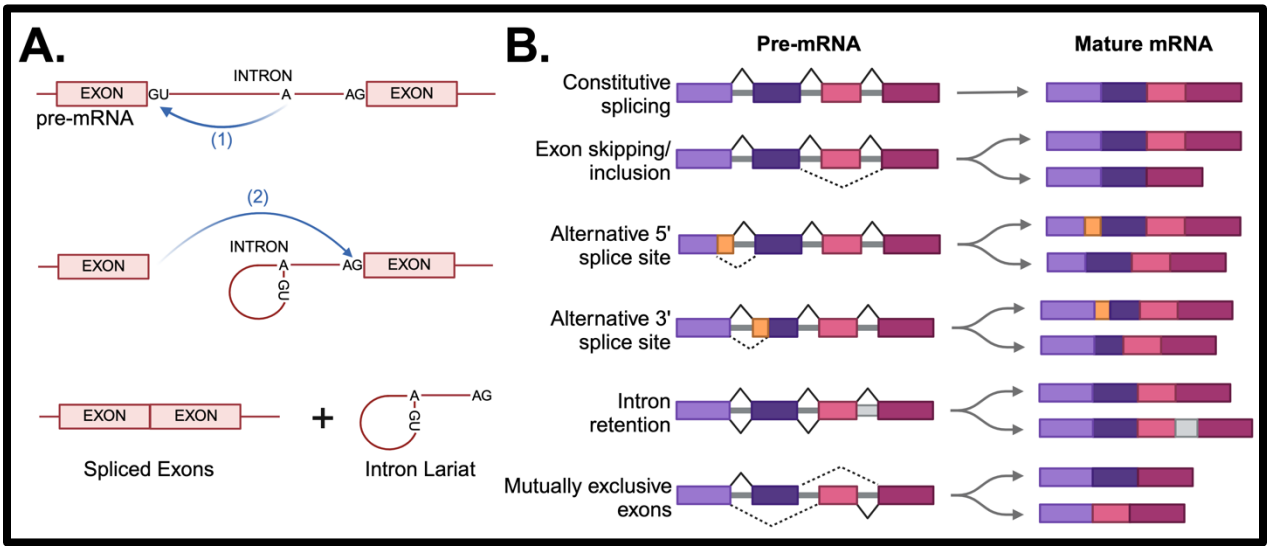

Figure 1-5. RNA splicing. A. Pre-mRNA splicing occurs through a two-step transesterification reaction to remove introns. **B.** There are multiple different types of alternative splicing including constitutive splicing, exon skipping/inclusion, alternative 5' or 3' splice sites, intron retention, and mutually exclusive exons.

Figure 1-6

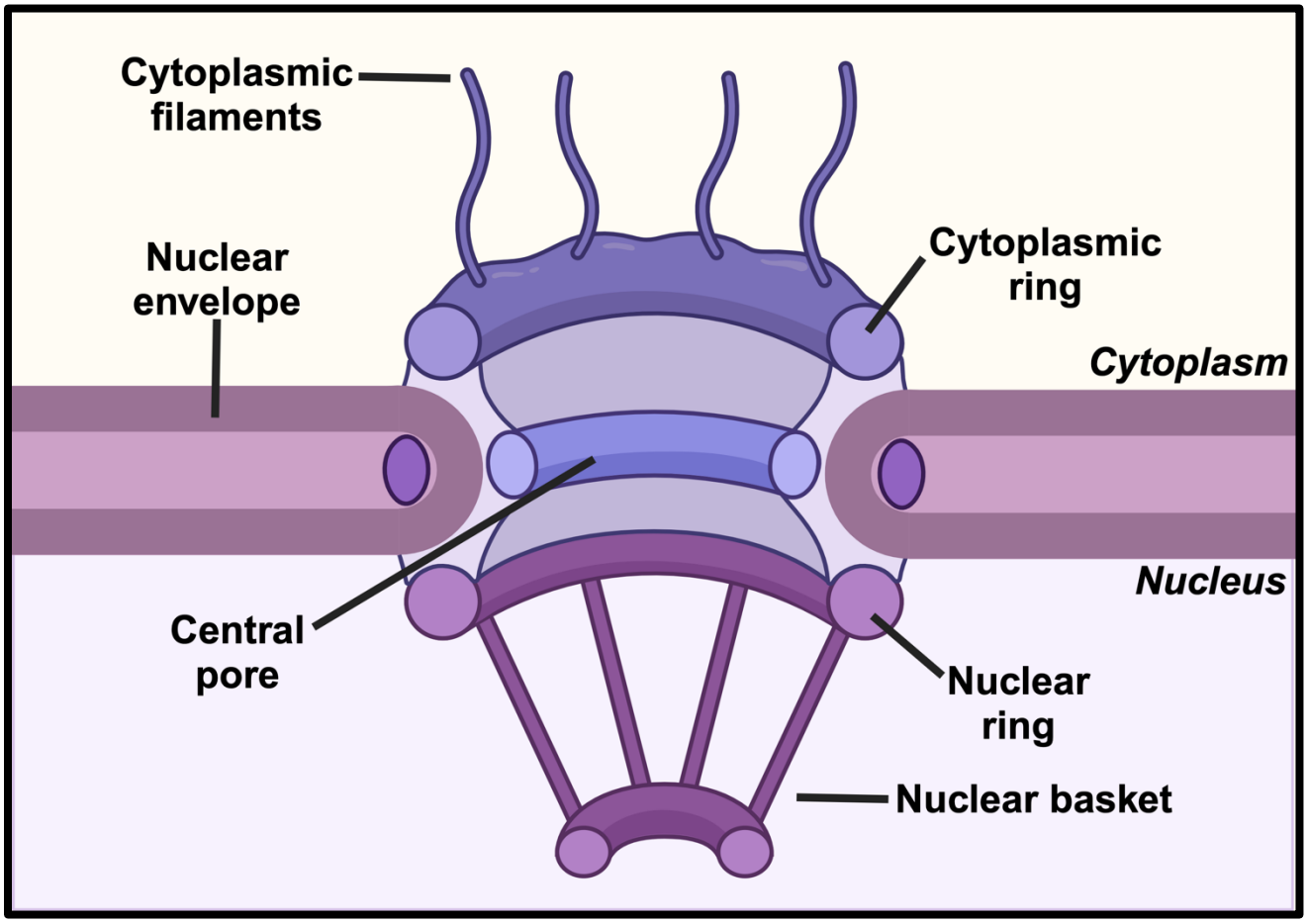

Figure 1-6. The Nuclear Pore. Schematic cross-section of the nuclear core complex embedded within the nuclear envelope showing major components.

Figure 1-7

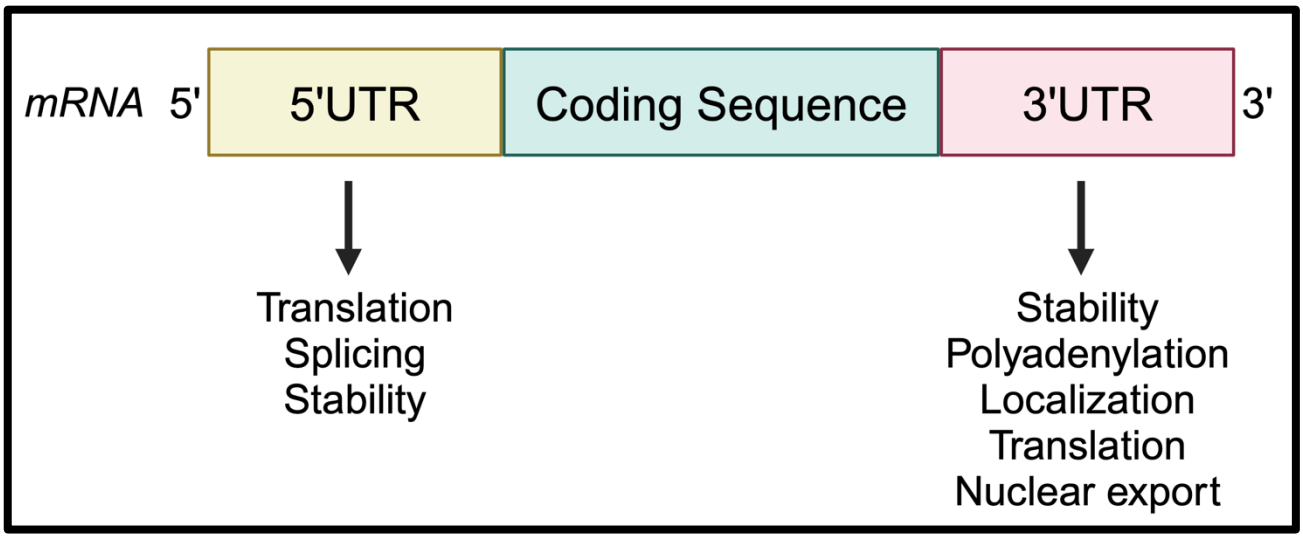

Figure 1-7 Untranslated Regions. The generic structure of eukaryotic mRNA, illustrating the 5' and 3' untranslated regions (UTRs) and their respective roles in regulation of gene expression.

Figure 1-8

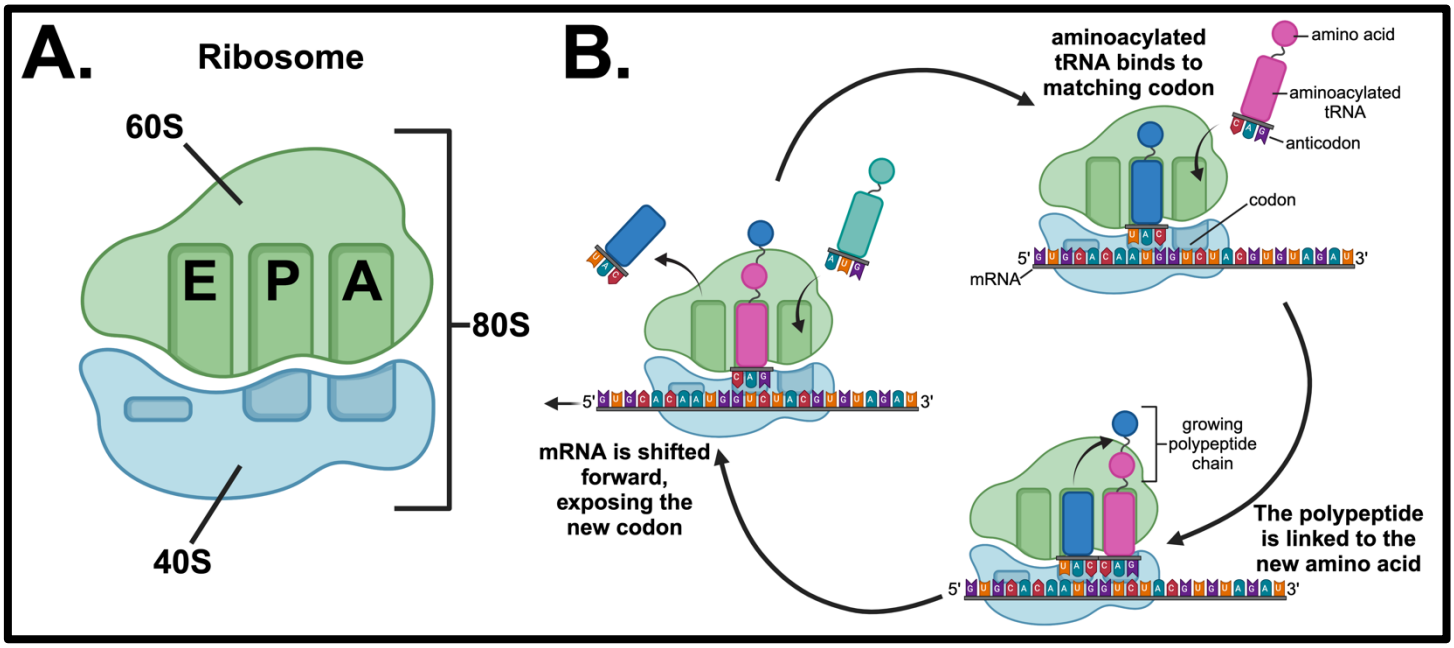

Figure 1-8 Translation A. The ribosome is made up of a 40S small subunit and a 60S large subunit that come together to form the translation-competent 80S ribosome. The ribosome contains three binding sites for tRNA: designated the A (aminoacyl) site, which accepts incoming aminoacylated tRNA; P (peptidyl) site, which holds the tRNA with the nascent peptide chain; and the E (exit) site, which holds the deacylated tRNA before it leaves the ribosome **B.** Overview of translation. An aminoacylated tRNA binds to the codon. Next, the exisiting polypeptide chain is linked to the aminoacid of the tRNA via a chemical reaction. Finally, the mRNA is shifted one codon over in the ribosome, exposing a new codon and the deacylated tRNA leaves the ribosome.

Figure 1-9

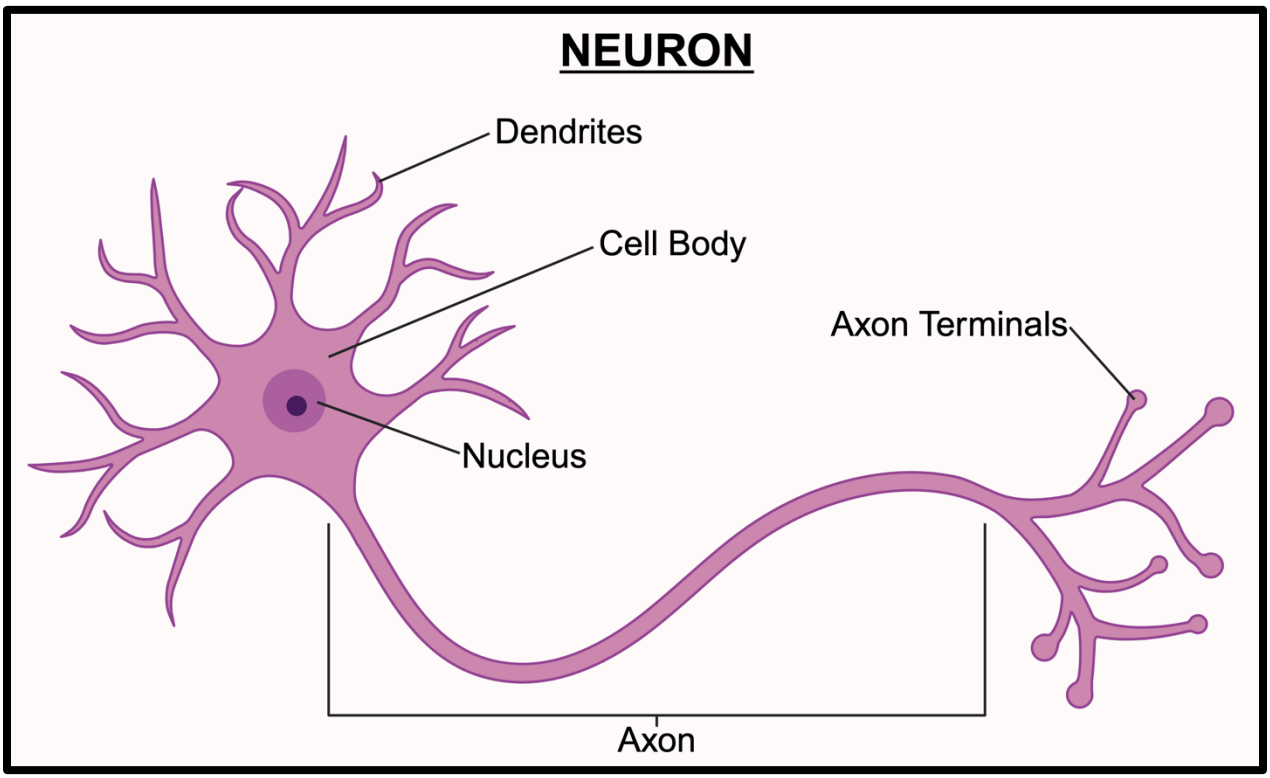

Figure 1-9 Anatomy of a Neuron The generic structure of a neuron consists of dendrites, which receive messages from other neurons; a cell body which contains the nucleus and cytoplasm; an axon, which transmits information away from the nucleus; and axon terminals, which transmit electrical and chemical signals to other neurons or effector cells.

Figure 1-10

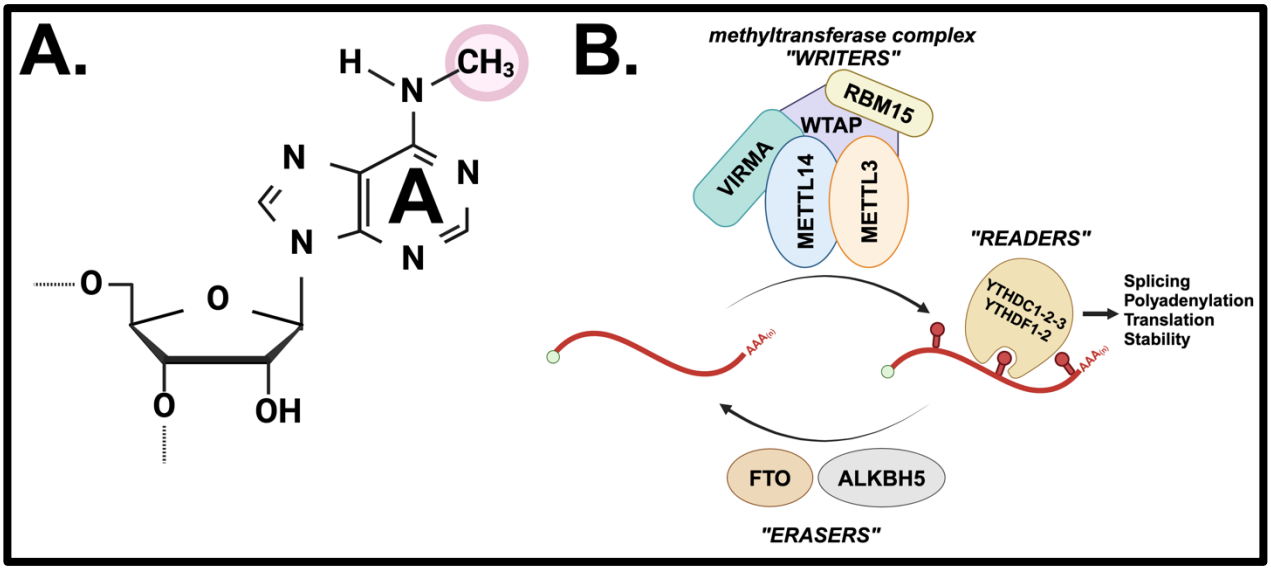

Figure 1-10. N6-methyladenosine and the m^{6}A mRNA pathway A. Molecular structure of Adenosine residue with m^{6}A methylation modification on the N6 position (pink circle). **B.** The methyltransferase complex ("writer") is composed of five factors and deposits a methyl group onto target adenosine residues. YTH domain-containing m^{6}A "reader" proteins recognize m^{6}A methylated RNA and regulated downstream RNA fate. "Eraser" proteins mediate the removal of m^{6}A methylation on target RNAs.

Figure 1-11

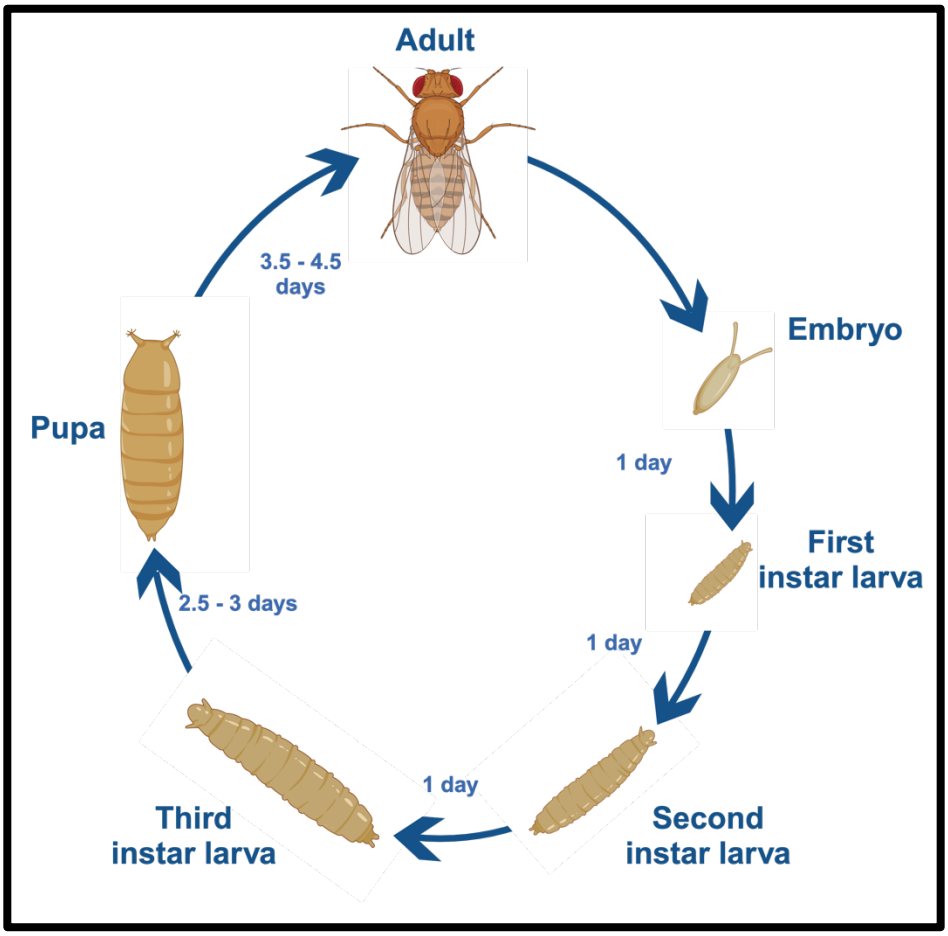

Figure 1-11 The *Drosophila melanogaster* Life CycleThe whole lifecycle of *Drosophila melanogaster* is relatively quick and takes 10-12 days. Development of the fruit fly is divided into various stages including: embryo, larva (first, second, and third instars), pupa, and adult.

Figure 1-12

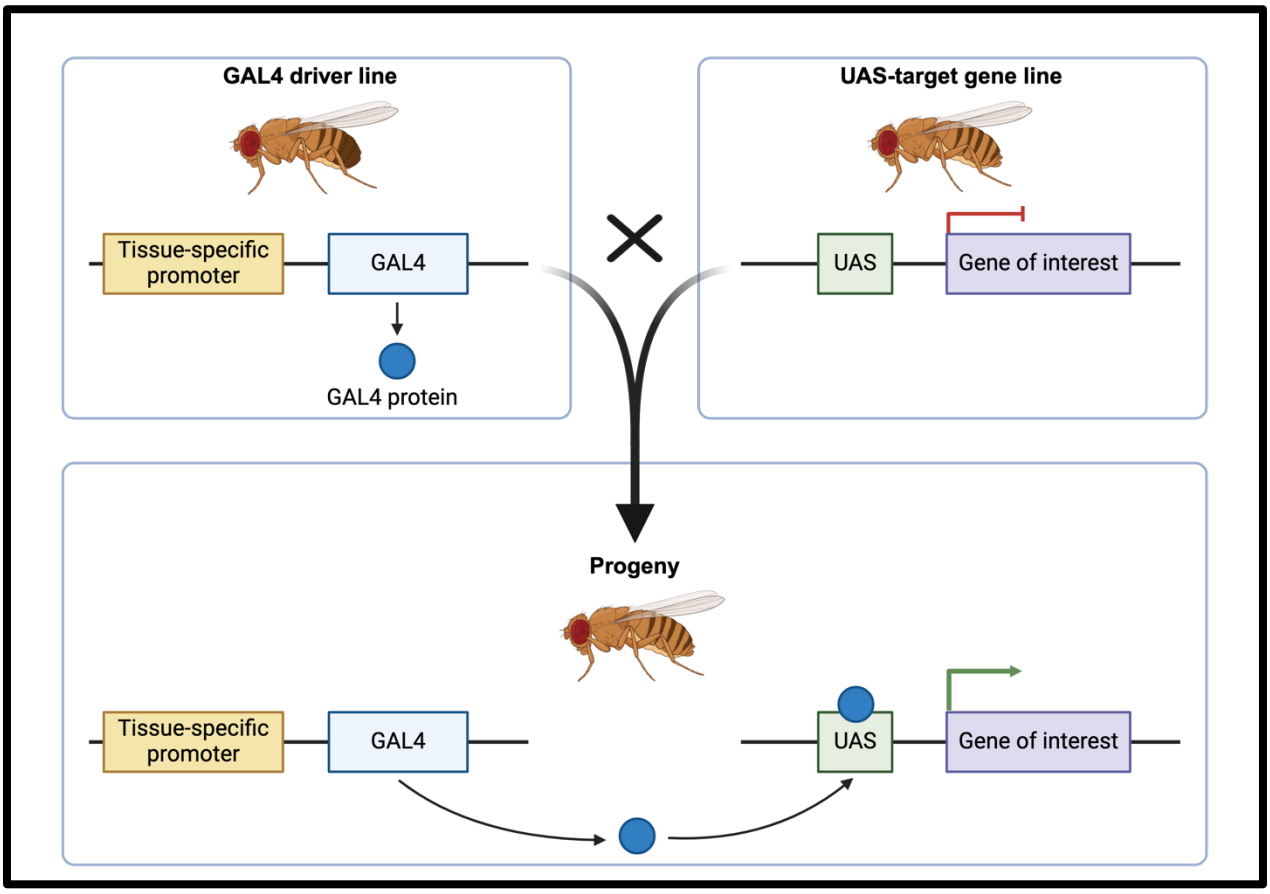

Figure 1-12 The *Gal4/UAS* System. The Gal4/UAS system is used to modulate spatial expression of transgenes in specific tissues. To express a transgene or RNAi construct in a certain tissue or type of cell, a fly carrying a "driver" with a tissue specific promoter placed upstream of the Gal4 transcription factor is mated to a fly carrying the gene of interest downstream of an upstream activating sequence (UAS). UAS is activated by Gal4. Thus, progeny of this cross will carry both transgenes and the tissue-specific promoter will drive expression of Gal4, which binds UAS driving expression of the gene of interest in the specified tissue. This system can also be used to express a hairpin RNA to knockdown a gene in the target tissue.

Figure 1-13

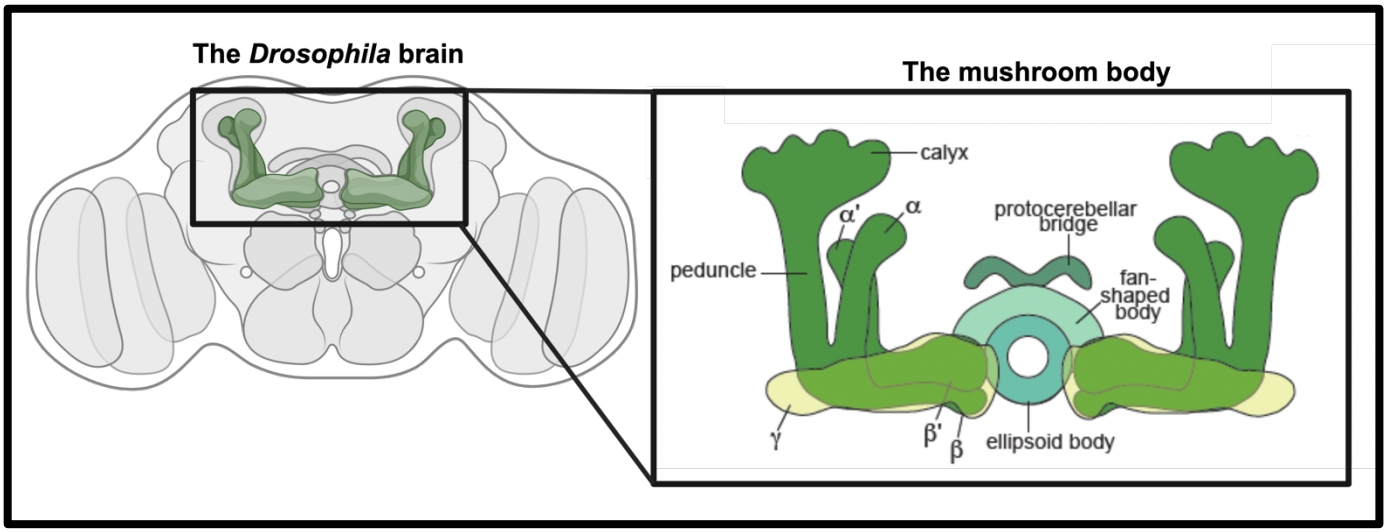

Figure 1-13 The Drosophila brain and mushroom body. Schematic of the *Drosophila* brain containing the centrally located mushroom body, a twin neuropil structure that regulates associative olfactory learning and memory. The adult mushroom body is composed of several distinct stuctures including the calyx, penuncle, protocerebellar bridge, fan-shaped body, ellipsoid body, and axons of the vertically projecting alpha (α), alpha prime (α') neurons, the medially projecting gamma (γ), beta (β), and beta prime (β') neurons.

Figure 1-14

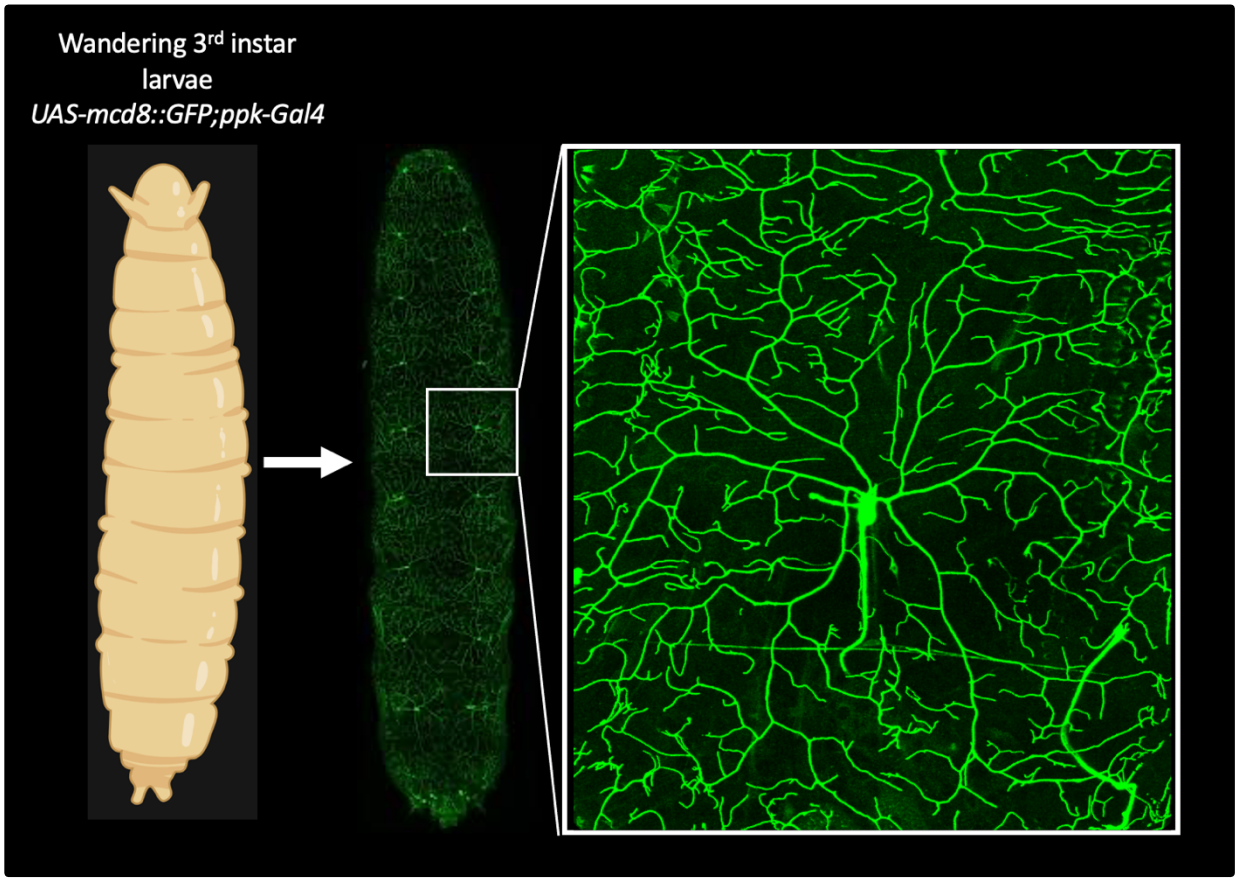

Figure 1-14 Class IV ddaC neurons. *Drosophila* dendritic arborization (dA) neurons provide an excellent system to investigate dendritic development and morphology. There are multiple types of da neurons, and this thesis specifically focuses on class IV dorsal dendritic arbor C (ddaC) neurons, as pictured. ddaC neurons have some of the largest and most elaborate dendritic arbors covering the body wall of the larvae. These ddaC neurons are marked in green with mCD8::GFP (live cell imaging methods are described in detail in **Chapter 3** of this thesis).

Figure 1-15

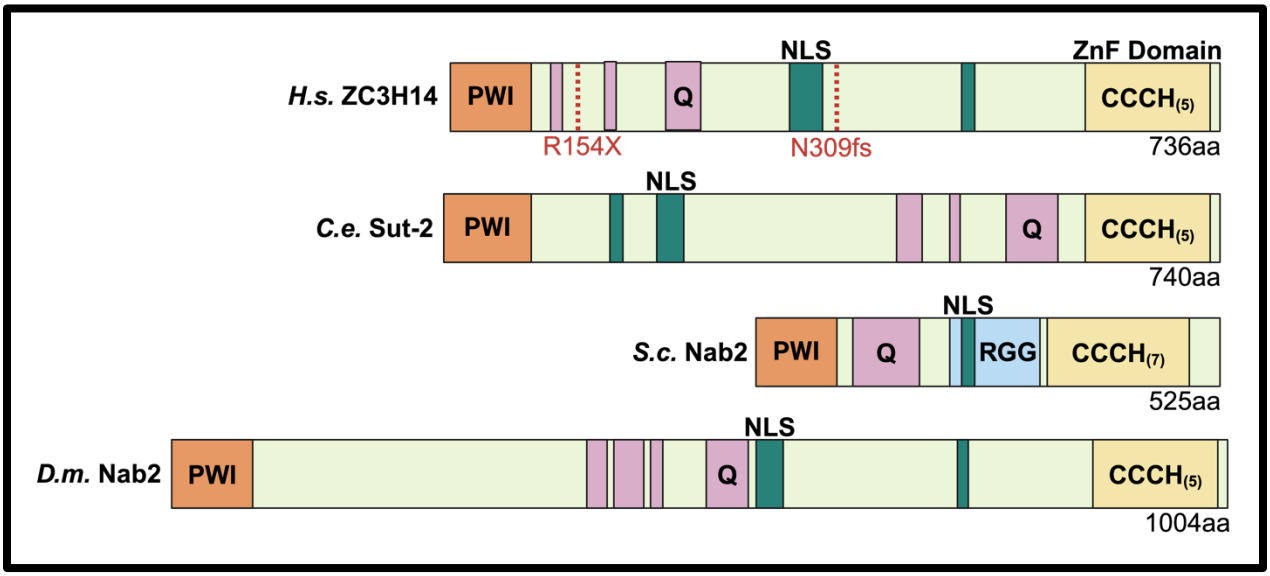

Figure 1-15 Orthologues of ZC3H14. Nab2 orthologues share a common domain structure based on N-terminal PWI-fold domain (orange), which serves as a protein-protein interaction domain, a Q-rich region (purple), a nuclear localization signal (NLS; teal), and a C-terminal zinc finger (ZnF) domain (yellow) containing a series of Zn fingers that bind to polyadenosine RNA. Additionally, *S.c.* Nab2 contains an RGG domain (blue) that functions in nuclear import. The nonsense mutation (R154X) and frameshift mutation (N309fs) are highlighted in red.

Figure 1-16

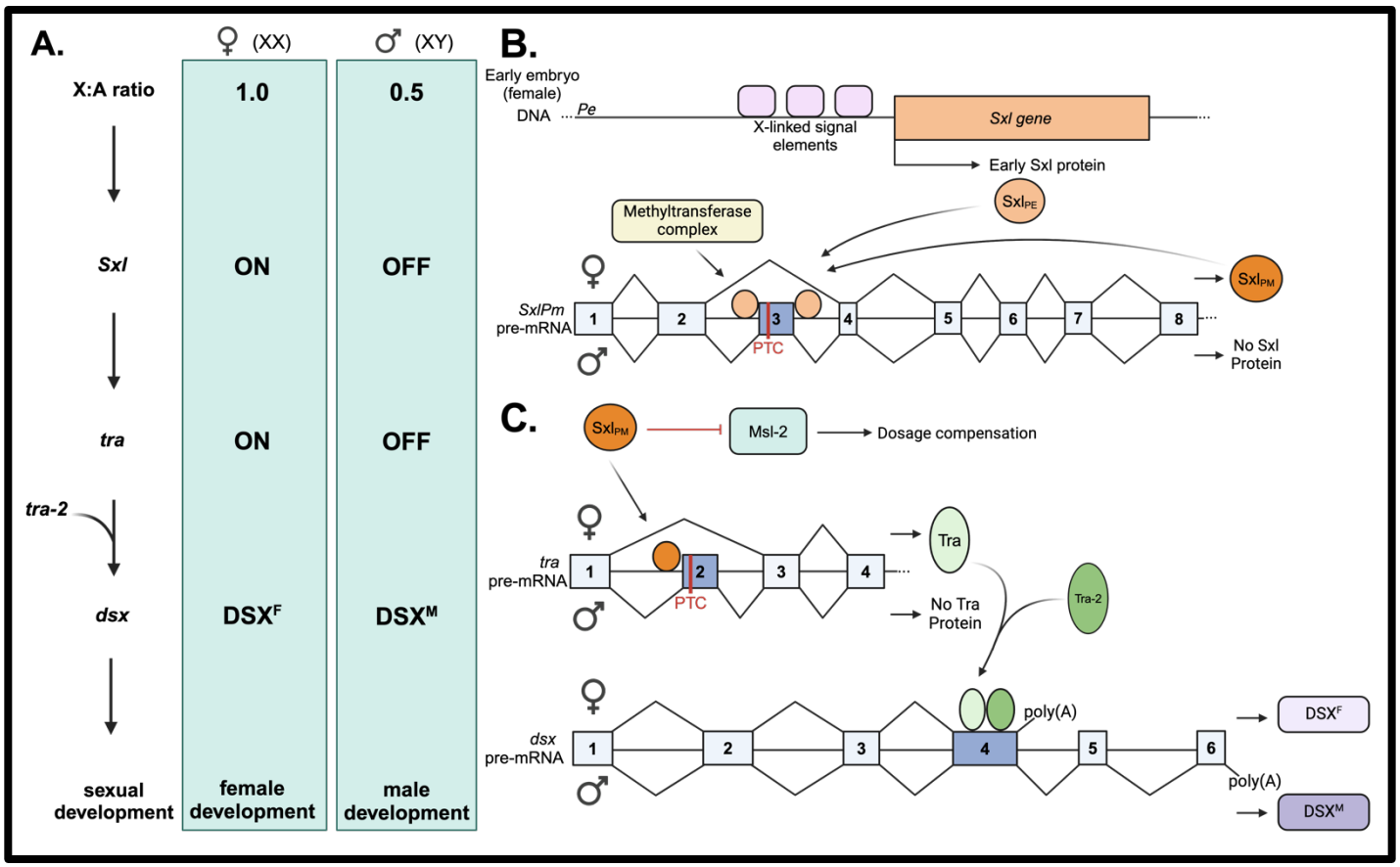

Figure 1-16 Sex determination cascade in *Drosophila* A. The primary genetic signal for sex determination is the ratio of X chromosomes to sets of autosomes (X:A). The sex determination cascade, composed of *Sxl*, *tra, tra-2*, and *dsx* is dependent on this ratio. **B.** Transcription from the *Sxl* establishment promoter (*Pe*) is activated during early embryonic development in XX animals. The Sxl protein encoded by the transcripts from the early promoter (Sxl_{PE}) induces female-specific splicing of *Sxl* from the maintenance promoter to produce functional Sxl protein (Sxl_{PM}). Lack of Sxl in males causes male-specific inclusion of *Sxl* exon 3 which contains a premature termination codon (PTC), thus, no functional Sxl protein is made. In females, Sxl protein binds its own pre-mRNA forming an autoregulatory loop to maintain female-specific splicing. **C.** Sxl directs female-specific splicing of *tra* giving rise to functional Tra protein. Lack of functional Sxl causes male-specific splicing of *tra* pre-mRNA which contains a PTC, thus, no functional Tra is made. Tra protein that acts in concert with Tra-2 to bind an exonic splicing enhancer of *dsx* thereby activating a weak 3' splic site to generate female-specific DSX protein (DSX^F). In the absence of Tra, *dsx* pre-mRNA undergoes default splicing patterns to produce male-specific DSX protein (DSX^M).

Figure 1-17

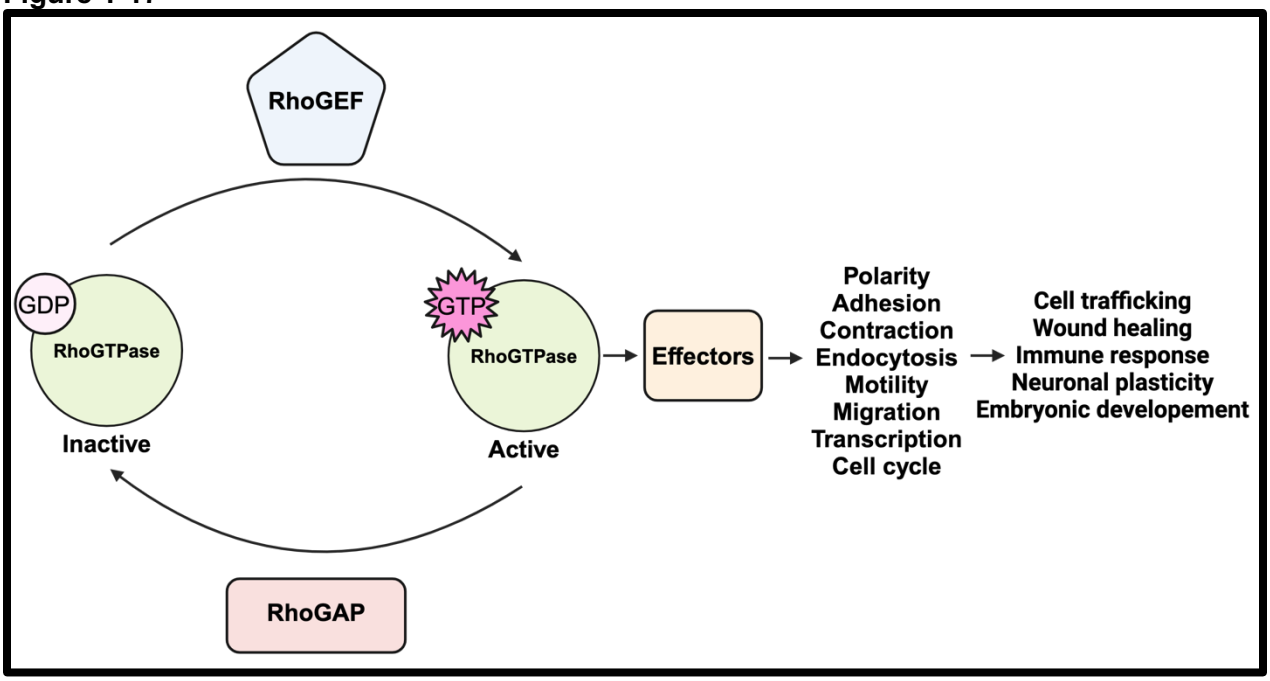

Figure 1-17 The GTPase cycle. Most RhoGTPases act as molecular switches by cycling through a GDP-bound, inactive state and a GTP-bound, active state. Rho guanine nucleotide exchange factors (RhoGEFs) activate RhoGTPases by accelerating the exchange of GDP for GTP, thereby switching ON signal transduction. On the other hand, RhoGTPase-activating proteins (GAPs) negatively regulate RhoGTPases by stimulating GTP hydrolysis thereby switching OFF signal transduction.

Figure 1-18

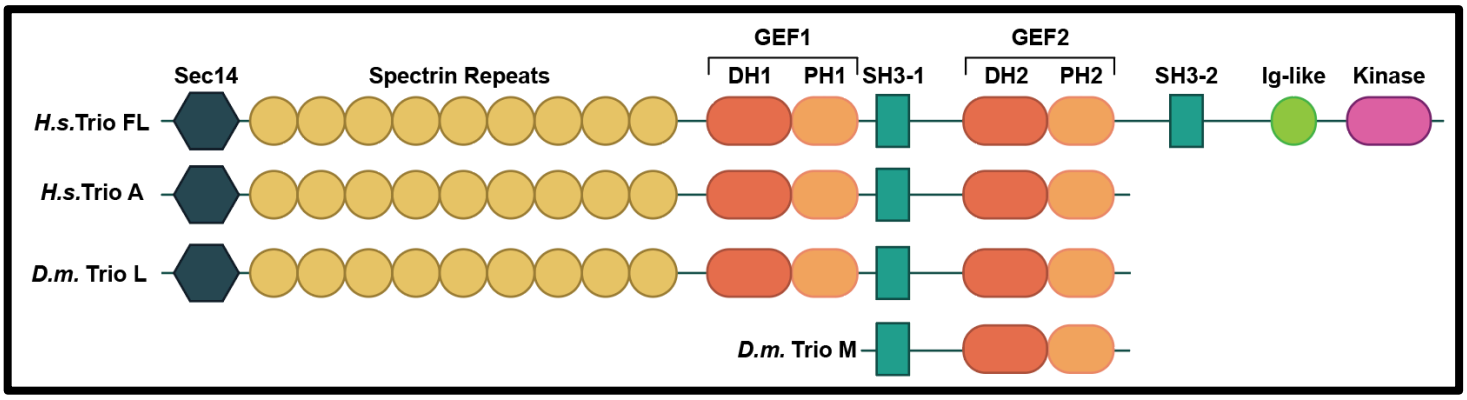

Figure 1-18 Schematic of human and *Drosophila* Trio proteins. Schematic of the human (*H.s.*) Trio FL and Trio A and *Drosophila melanogaster* (*D.m.*) Trio L and Trio M proteins. Trio contains a Sec14 domain, nine spectrin repeats, two Src homology 3 (SH3-1 and SH3-2) domains, and two catalytic GEF domains (GEF1 and GEF2), comprised of tandem Dbl homology (DH) and pleckstrin homology (PH) domains, an immunoglobulin like domain (Ig-like), and a serine-threonine kinase domain.

Figure 1-19

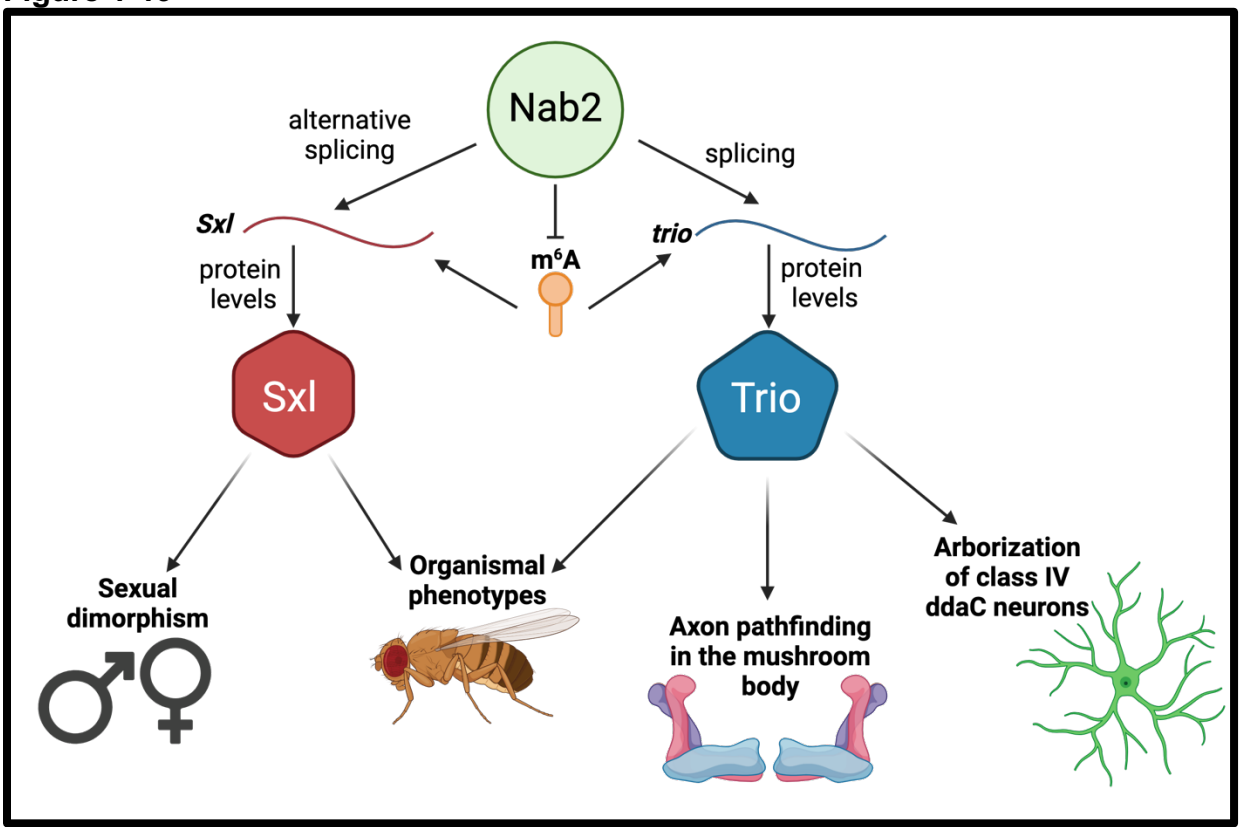

Figure 1-19 Model Figure. Nab2 regulates splicing and protein levels of Sxl and Trio to govern sexual development, organismal phenotypes, and neuronal development in *Drosophila melanogaster*.

CHAPTER 2: The *Drosophila* Nab2 RNA binding protein inhibits m^{6}A methylation and male-specific splicing of *Sex lethal* transcript in female neuronal tissue

Binta Jalloh[1,2,3†], Carly L. Lancaster[1,2,4†], J. Christopher Rounds[1,2,3‡], Brianna E. Brown[1,2‡], Sara W. Leung[1], Ayan Banerjee[1], Derrick J. Morton[1,5], Rick S. Bienkowski[1,2,3], Milo B. Fasken[1], Isaac J. Kremsky[1], Matthew Tegowski[6], Kate D. Meyer[6,7], Anita H. Corbett[1*], and Kenneth H. Moberg[2*]

[1] Department of Biology, Emory University, Atlanta, Georgia, USA
[2] Department of Cell Biology Emory University School of Medicine
[3] Graduate Program in Genetics and Molecular Biology, Emory University
[4] Graduate Program in Biochemistry, Cell and Developmental Biology, Emory University
[5] Emory Institutional Research and Academic Career Development Award (IRACDA), Fellowships in Research and Science Teaching (FIRST) Postdoctoral Fellowship
[6] Department of Biochemistry, Duke University School of Medicine, Durham, North Carolina, USA
[7] Department of Neurobiology, Duke University School of Medicine

[†]These authors contributed equally to this study.
[‡]These authors contributed equally to this study
*Co-corresponding authors

This chapter has been excerpted from a manuscript published in *eLife*:
Jalloh B, Lancaster CL, Rounds JC, Brown BE, Leung SW, Banerjee A, Morton DJ, Bienkowski RS, Fasken MB, Kremsky IJ, Tegowski M, Meyer K, Corbett A, Moberg K. The *Drosophila* Nab2 RNA binding protein inhibits m^{6}A methylation and male-specific splicing of *Sex lethal* transcript in female neuronal tissue. Elife. 2023 Jul 17;12:e64904. doi: 10.7554/eLife.64904.

Author Contributions:
Carly L. Lancaster authored Figures 2-3C, 2-3D, 2-3E, 2-5A, 2-5B, 2-5C, 2-5D, 2-5E, 2-5F, 2-5G, 2-6D, 2-6E, 2-6F, 2-6H, and Supplemental Figures 2-10A, 2-10B, and 2-11. J. Christopher Rounds was the bioinformatics lead on the RNA-Sequencing experiment and analyses described in this chapter. He authored Figures 2-1A, 2-1C, 2-1D and 2-2A. He contributed to analyses underlying Figures 2-1B, 2-1E, 2-2B, 2-3A, and 2-3G. He administratively coordinated the RNA-Seq with the sequencing core. He also wrote the RNA-Sequencing Methods Table and multiple RNA-Sequencing Methods subsections. For the RNA-Sequencing experiment, Binta Jalloh collected samples and performed RNA extractions; the Georgia Genomics and Bioninformatics core prepared cDNA libraries and performed sequencing; Isaac J. Kremsky performed MISO, RBM, and other bioinformatic analyses; and Kenneth H. Moberg contributed to IGV analyses and DEX-Seq. All other experiments were performed and associated text was written and edited by authors other than Carly L. Lancaster, especially Binta Jalloh, J. Christopher Rounds, Anita H. Corbett, and Kenneth H. Moberg.

Abstract

The *Drosophila* polyadenosine RNA binding protein Nab2, which is orthologous to a human protein lost in a form of inherited intellectual disability, controls adult locomotion, axon projection, dendritic arborization, and memory through a largely undefined set of target RNAs. Here, we show a specific role for Nab2 in regulating splicing of ~150 exons/introns in the head transcriptome and focus on retention of a male-specific exon in the sex determination factor *Sex-lethal* (*Sxl*) that is enriched in female neurons. Previous studies have revealed that this splicing event is regulated in females by N6-methyladenosine (m^6A) modification by the Mettl3 complex. At a molecular level, Nab2 associates with *Sxl* pre-mRNA in neurons and limits *Sxl* m^6A methylation at specific sites. In parallel, reducing expression of the Mettl3, Mettl3 complex components, or the m^6A reader Ythdc1 rescues mutant phenotypes in *Nab2* flies. Overall, these data identify Nab2 as an inhibitor of m^6A methylation and imply significant overlap between Nab2 and Mettl3 regulated RNAs in neuronal tissue.

Introduction

RNA binding proteins (RBPs) play important roles in guiding spatiotemporal patterns of gene expression that distinguish different cell types and tissues within organisms. There are an estimated ~1500 RBPs that distribute between the nucleus and cytoplasm [333], and each has the potential to interact with RNAs to modulate post-transcriptional gene expression. Such regulation is particularly critical in highly specialized cells such as neurons[334] where regulated alternative splicing of coding regions and 3'UTRs, cleavage/polyadenylation, trafficking and local translation contribute to precise regulation of gene expression[166]. The critical roles of RBPs in neurons is highlighted by many studies that reveal the importance of this class of proteins in brain development and function [335] and by the prevalence of human neurological diseases linked to mutations in genes encoding RBPs [166]. Many of these RBPs are ubiquitously expressed and play multiple roles in post-transcriptional regulation. Thus, defining the key neuronal functions of these proteins is critical to understanding both their fundamental roles and the links to disease.

Among the RBPs linked to human diseases are a group of proteins that bind with high affinity to polyadenosine RNAs, which are termed poly(A) RNA binding proteins or Pabs [264]. Functional studies of classical nuclear and cytoplasmic Pabs, which utilize RNA recognition motifs (RRMs) to recognize RNA, have uncovered diverse roles for these proteins in modulating mRNA stability, alternative cleavage and polyadenylation and translation [336]. A second, less well-studied, group of Pabs uses zinc-finger (ZnF) domains to bind target RNAs. Among these is the Zinc Finger Cys-Cys-Cys-His-Type Containing 14 (ZC3H14) protein, which binds with high affinity to poly(A) RNAs via a set of C-terminal tandem Cys-Cys-Cys-His type zinc-finger domains [245]. ZC3H14 is broadly expressed in

many tissues and cell types but mutations in the human *ZC3H14* gene are associated with a heritable form of intellectual disability [215], implying an important requirement for this protein in the central nervous system.

ZC3H14 has well-conserved homologs in eukaryotes, including *S. cerevisiae* Nuclear poly(A)-binding protein 2 (Nab2), *Drosophila melanogaster* Nab2, *C. elegans* SUT-2 and murine ZC3H14[337]. Zygotic loss of *ZC3H14* in mice and *Drosophila* impairs neuronal function[215,338], while neuron-specific depletion of *Drosophila* Nab2 is sufficient to replicate these effects [215]. Reciprocally, expression of human ZC3H14 in Nab2-deficient neurons rescues this defect, demonstrating a high degree of functional conservation between human ZC3H14 and *Drosophila* Nab2 [279]. Collectively, these data focus attention on what are critical, but poorly understood, molecular roles for ZC3H14/Nab2 proteins in neurons.

Neuronal ZC3H14/Nab2 can be divided into two pools, a nuclear pool that accounts for the majority of ZC3H14/Nab2 in the cell, and a small cytoplasmic pool of protein detected in mRNA ribonucleoprotein particles (mRNPs) of axons and dendrites [245,278,338]. Depletion of both pools in *Drosophila* neurons cause defects in axon projection within the brain mushroom bodies (MBs)[284], a pair of neuropil structures involved in olfactory learning and memory[232,339], and excess branching of dendrites on peripheral sensory neurons[281]. The Nab2 requirement in MBs is linked to a physical association between Nab2 and the *Drosophila* Fragile-X mental retardation protein homolog[275] in the neuronal cytoplasm and translational repression of shared Nab2-Fmr1 target RNAs[278]. Genetic data indicate that Nab2 limits dendritic branching through effects on the cytoplasmic planar cell polarity pathway [281]. Despite these insights into a cytoplasmic

functions of Nab2, a molecular role of the abundant pool of Nab2 protein in neuronal nuclei remains undefined.

Here, we employ a broad and an unbiased RNA sequencing approach to identify transcriptome-wide changes in the heads of *Nab2* loss-of-function mutant flies. While the steady-state levels of most transcripts are not significantly changed, we find a striking effect on splicing of a subset of neuronal RNA transcripts. We focus our analysis on a well-characterized sex-specific alternative splicing event in the *Sex-lethal* (*Sxl*) transcript [286,340,341]. Results reveal that *Nab2* plays a novel role in regulating the alternative splicing of *Sxl* in a sex-specific manner. Recent work has revealed a role for m^6A RNA methylation by the enzyme Mettl3 in modulating this splicing event[129,288]. Similar to *Mettl3*, the requirement for *Nab2* in alternative splicing of *Sxl* is only essential for neuronally-enriched tissues. Genetic and biochemical experiments support a functional link between m^6A methylation and Nab2 in which Nab2 limits m^6A on target RNAs. These results demonstrate the role for *Drosophila Nab2* in RNA alternative splicing as well as RNA methylation and sex determination in neurons.

Results

Nab2 loss affects levels and processing of a subset of RNAs in the transcriptome of the *Drosophila* head

To assess the role of Nab2 in regulating the central nervous system transcriptome, a high-throughput RNA Sequencing (RNA-Seq) analysis was carried out in triplicate on *Nab2* null mutant heads (*Nab2*^{ex3} imprecise excision of *EP3716*) [215] and isogenic control heads (*Nab2*^{pex41} precise excision of *EP3716*). To capture any sex-specific differences, heads were collected from both male and female flies of each genotype. Briefly, total RNA from

1-day old adults was rRNA-depleted and used to generate stranded cDNA libraries that were sequenced (150 cycles) on a NextSeq 500 High Output Flow Cell. This generated a total of approximately 1.1 billion 75 base-pair (bp) paired-end reads (91 million/sample) that were mapped onto the Dmel6.17 release of the *Drosophila* genome using RNA STAR [342]. Read annotation and per-gene tabulation was conducted with featureCounts [343] and differential expression analysis was performed with DESeq2 [344].

RNA sequencing reads across the *Nab2* gene are almost completely eliminated in $Nab2^{ex3}$ mutants, confirming the genetic background and integrity of this analysis pipeline (**Supplemental Figure 2-1**). Principal component analysis (PCA) performed with DESeq2 output data confirms that the 12 RNA-seq datasets distribute into four clusters that diverge significantly from one another based on genotype ($Nab2^{ex3}$ vs. $Nab2^{pex41}$ control; PC1 58% variance) and sex (male vs. female; PC2 26% variance) (**Figure 2-1A**). The DESeq2 analysis detects 3,799 and 1,545 genes in females and males, respectively, that exhibit statistically significant differences in RNA abundance between $Nab2^{ex3}$ and control (BH adjusted *p*-value/false discovery rate (FDR)<0.05). Comparison of fold-changes ($Nab2^{ex3}$ vs. control) among these significantly different RNAs reveals a high degree of correlation in female vs. male samples (R=0.79), particularly among RNAs whose levels are most elevated upon Nab2 loss (**Figure 2-1B**). Applying a 2-fold change cutoff ($|\log_2[\text{fold-change}]| \geq 1$) trims these sets to 453 significantly changed RNAs in females (294 ‘up’, 159 ‘down’), and 305 significantly changed RNAs in males (150 ‘up’, 155 ‘down’) (**Figure 2-1C**), which merge into a combined set of 570 significantly affected RNAs that trend similarly in heatmap analysis of mutant vs. control samples (**Figure 2-1D**). A majority of the 453 affected ‘female’ RNAs are mRNAs (439) and the remaining

are snoRNAs (8), snRNAs (1), pre-rRNAs (1), and tRNAs (4) (**Figure 2-1E**). A similar distribution occurs in male heads: a majority of the affected RNAs are mRNAs (297) and the remainder are snoRNAs (4), snRNAs (1), pre-rRNAs (1), and tRNAs (2) (**Figure 2-1E**). Overall, the number of significantly changed RNAs ($(|\log_2[\text{fold-change}]| \geq 1$ and FDR<0.05) in *Nab2*^{ex3} female and male heads represents a small fraction of RNAs detected in heads (2.2% and 3.7% in males and females, respectively), suggesting that Nab2 normally contributes to RNA-specific regulatory mechanisms in *Drosophila* head tissue.

Nab2 loss alters levels of transcripts linked to mRNA processing

To identify functional groups within Nab2-regulated RNAs, Gene Set Enrichment Analysis (GSEA) [345,346] was performed with the goal of defining enriched gene ontology (GO) terms [347,348] among the significantly changed female and male RNAs identified by DESeq2. This filtering uncovers significant enrichment (p<0.05) for “RNA splicing” GO (GO:0008380) within the upregulated group of RNAs in both sexes (**Figure 2-2A**). In *Nab2*^{ex3} females, 32 of 155 genes annotated under this term are present among upregulated RNAs; whereas in males, 75 of 159 genes annotated under this term are present among upregulated RNAs (**Figure 2-2A**). This enrichment for upregulated splicing-related factors indicates that Nab2 loss could shift splicing patterns in the adult head. Consistent with this hypothesis, MISO (mixture of isoforms) analysis [349] of annotated alternative splicing events confirms that Nab2 loss significantly alters splicing patterns within a small number of transcripts in female (48) and male (50) heads (**Supplemental File 2-2**) that fall into a variety of GO terms (**Supplemental Figure 2-2**). These MISO-called alternative splicing

events include 5' and 3' alternative-splice site usage, intron retention events, and previously annotated exon skipping events, some of which are detected in the same transcripts (**Figure 2-2B**).

To test whether Nab2 loss results in unannotated or aberrant splicing events among head RNAs, DEXSeq analysis[350] was performed to scan for differential abundance of individual exons relative to other exons within the same transcript. This analysis detects 151 affected RNAs in *Nab2*^{ex3} females and 114 in *Nab2*^{ex3} males, with many top-ranked transcripts encoding factors with roles in behavior, neurodevelopment, and/or neural function. Re-analysis with a lower significance threshold yielded additional transcripts that show evidence of altered post-transcriptional processing in *Nab2* mutant heads but did not alter the group of RNAs identified as most significantly affected by Nab2 loss. Among the 151 most affected RNAs, the most statistically significant exon usage change in either sex is female-specific inclusion of exon 3 in the *Sex lethal* (*Sxl*) mRNA (p=3.08x10^{-235}). This effect on *Sxl* mRNA in *Nab2*^{ex3} females is followed in rank order of statistical significance by enhanced inclusion of exons 1 and 2 of the MIF4GD homolog transcript *CG13124*, exons 1 and 2 of the voltage-gated ion channel transcript I_h *channel* (I_h), and exon 1 of the synaptic enzyme transcript *Acetylcholine esterase* (*Ace)*. In *Nab2*^{ex3} males, the top four events are enhanced inclusion of exon 1 of the *Ace* transcript*,* exon 1 of the *Protein kinase C at 53E* (*Pkc53E*) transcript, exons 1 and 2 of the Rab GTPase *pollux* (*plx*) transcript, and exons 1 and 2 of *Protein kinase N* (*Pkn*) transcript. In a number of cases, identical exons are affected in both *Nab2*^{ex3} sexes and accompanied by retention of the intervening intron (e.g., see *CG13124* and I_h traces in **Supplemental Figure 2-3**). The robust increase in *Sxl* exon 3 in *Nab2*^{ex3} females is noteworthy both for the central

role that differential inclusion of *Sxl* exon 3 plays in *Drosophila* sex determination[351] and because DEXSeq did not detect changes in exon 3 inclusion or abundance in *Nab2*^{ex3} males. In light of this sex-specific effect of Nab2 loss on alternative splicing of *Sxl* exon 3, subsequent analyses focused on the role of Nab2 in *Sxl* mRNA splicing in female heads.

Nab2^{ex3} females exhibit masculinized *Sxl* splicing in neuron-enriched tissues

The Sex lethal (Sxl) protein is a female-specific, U-rich RNA binding protein that is best defined for its role acting through the *tra-dsx* and *msl-2* pathways to promote female somatic and germline identity [352,353]. *Sxl* pre-mRNA is expressed in both males and females, but alternative splicing regulated by m^{6}A RNA methylation and several RBPs leads to female-specific skipping of exon 3 during splicing[129,341,354]. Because exon 3 includes an in-frame translation 'stop' codon, full-length Sxl protein is only made and active in female cells[355]. The inclusion of *Sxl* exon 3 in *Nab2*^{ex3} mutants would thus implicate Nab2 as a novel component of molecular machinery that controls *Sxl* pre-mRNA splicing.

Visualizing *Sxl* RNA-Seq reads with IGV Viewer[356] confirms a large increase in exon 3 reads in *Nab2*^{ex3} females (*Nab2*^{ex3} F) relative to control females (control F), and also reveals retention of ~500 bases of intron 3 sequence in *Nab2*^{ex3} females (**Figure 2-3A**). Normal splicing patterns are detected across all other *Sxl* intron-exon junctions in both genotypes of males and females, including female-specific exon 9 inclusion. Quantification of reads across the entire *Sxl* locus detects an ~1.5-fold increase in the overall abundance of the *Sxl* mRNA in *Nab2*^{ex3} females compared to control females.

Parallel reverse transcription polymerase chain reaction (RT-PCR) on fly heads using *Sxl* primers that detect exon 2-exon 4 (control females) and exon 2-exon 3-exon 4 (control males) confirms the presence of the mis-spliced exon 2-exon 3-exon 4 mRNA transcript in *Nab2*^{ex3} females (**Figure 2-3B**). The exon 2-exon 3-exon 4 mRNA transcript appears to be more abundant in *Nab2*^{ex3} female heads than in female heads lacking *Mettl3*, which encodes the catalytic component of the m^{6}A methyltransferase complex that promotes exon 3 skipping in nervous system tissue [129,288,341]. RT-PCR also reveals a ~1kb band in *Nab2*^{ex3} females (arrowhead, **Figure 2-3B**) that sequencing identifies as aberrantly spliced transcript that incorporates 503 bases of intron 3 leading up to a cryptic 5' splice site (i.e., exon 2-exon 3-intron 3^{503}-exon 4), which matches the *Sxl* intron 3 sequencing reads observed in IGV (see **Figure 2-3A**).

qRT-PCR confirms a statistically significant increase in the inclusion of the male-specific exon 3 in females with a concomitant decrease in the level of correctly spliced (exon 2-exon 4) transcript in both *Nab2*^{ex3} and *Mettl3*^{null} female heads (**Figure 2-3C**). Because *Sxl* exon 3 includes an in-frame translation 'stop' codon, we tested whether full-length Sxl protein levels decrease in *Nab2*^{ex3} female heads. Indeed, immunoblotting analysis reveals reduced levels of Sxl protein in *Nab2*^{ex3} female heads compared to control or *Mettl3* null heads (**Figures 2-3D-E**). Together, these data implicate Nab2 in post-transcriptional regulation of *Sxl* splicing and control of Sxl protein levels within female heads.

As all the analysis carried out thus far employed heads as source material, we tested whether Nab2-dependent splicing changes were also detected in other tissues. Significantly, RT-PCR analysis of *Sxl* mRNA in dissected control and *Nab2*^{ex3} females

detects exon 3 retention in *Nab2*^{ex3} samples prepared from the thorax, but little to no retention in the abdomen and ovary (**Figure 2-3F**). This result implies that Nab2 is only necessary to direct *Sxl* exon 3 exclusion in specific tissues or cell types such as neurons, which are enriched in the head (brain) and thorax (ventral nerve cord). In sum, these data reveal a tissue-specific role for Nab2 in blocking *Sxl* exon 3 inclusion in females and regulating 5'-splice site utilization at the exon 3-exon 4 junction.

As Sxl is itself an RBP with roles in alternative splicing[352,355], we performed a bioinformatic scan for RBP motifs enriched in proximity to the Nab2-dependent alternative splicing events identified by MISO analysis (see **Figure 2-2B**). Input sequences were composed of retained introns plus 25nt extending into each flanking exon, and alternative splice sites with 25nt of exon plus 1kb of adjacent intron (see schematic, **Figure 2-3G**). This unbiased scan detected candidate Sxl binding sites as the single most abundant RBP motif within the Nab2-regulated MISO events in females (**Figure 2-3G**). Notably, Sxl motifs were not detected as enriched in the male *Nab2*^{ex3} MISO dataset, which otherwise strongly resembles the remaining group of female-enriched RBP motifs [(e.g., the hnRNPL homolog *smooth* (*sm*), *RNA binding protein-9* (*Rbp9*), the U1-SNRNPA homolog *sans fille* (*snf*), and the U2-SNRNP component (*U2AF50*)]. The female-specific enrichment for Sxl binding sites raises the possibility that Nab2 regulates a portion of the alternative splicing events indirectly via control of a Sxl-regulated splicing program, or that Sxl and Nab2 proteins target common splicing events. Intriguingly, the Sxl target *transformer* (*tra*) and the Tra target *double-sex* (*dsx*) [357,358] were not recovered in the *Nab2*^{ex3} MISO or DESeq2 datasets, and IGV reads show little evidence of altered structure of *tra* and *dsx* RNAs as compared to *Nab2*^{pex41} controls (**Supplemental Figure**

2-4). Together, these data suggest that Sxl may not control the *tra-dsx* pathway in the adult head, or that *tra* and *dsx* splicing are only altered in a subset of *Nab2*^{ex3} head cells and thus not detectable by bulk RNA-Seq analysis.

The dosage compensation complex contributes to phenotypes in *Nab2*^{ex3} mutant females

The decrease in Sxl protein in *Nab2*^{ex3} female heads suggests that aberrant inclusion of *Sxl* exon 3 could contribute to *Nab2*^{ex3} phenotypes by reducing Sxl activity. To test this hypothesis, the constitutively female-spliced *Sxl*^{M8} allele[359] was placed as a heterozygote into the background of *Nab2*^{ex3} animals. *Sxl*^{M8} contains a 110bp deletion spanning the 3'-end of intron 2 and 5'-end of exon 3, and consequently undergoes constitutive splicing to the feminized exon 2-exon 4 variant regardless of sex (top panel, **Figure 2-4A**). Consistent with the original report describing *Sxl*^{M8} [359], the allele is male-lethal in both control and *Nab2*^{ex3} backgrounds. However, heterozygosity for *Sxl*^{M8} produces strong rescue of *Nab2*^{ex3} mutant female viability from ~4% to 71% (*Sxl*^{M8}*/+;;Nab2*^{ex3}) (**Figure 2-4A**). Female *Nab2*^{ex3} siblings that did not inherit the *Sxl*^{M8} allele also exhibit elevated viability (64%), perhaps due to maternal loading of *Sxl* mRNA. *Sxl*^{M8}*/+;;Nab2*^{ex3} females also show improved locomotion in a negative geotaxis assay (**Figure 2-4B**) and lengthened lifespan (**Figure 2-4C**) relative to *Nab2*^{ex3} females. This female-specific rescue of *Nab2*^{ex3} by *Sxl*^{M8} indicates that partial restoration of Sxl expression can compensate for Nab2 loss.

The absence of any effect on *tra* or *dsx* transcripts upon loss of Nab2 (**Supplemental Figure 2-4**) prompted us to analyze the other major role of Sxl, which is to bind to the *male-specific lethal-2* (*msl-2*) mRNA and inhibit its translation in female

somatic and germline tissues [360,361]. As a result, Msl-2 protein is only expressed in male cells, where it promotes assembly of a chromatin modifying complex termed the Dosage Compensation Complex (DCC; composed of Msl-1, Msl-2, Msl-3, Mof, Mle and *roX1* and *roX2* non-coding RNAs), which is recruited to the male X chromosome to equalize X-linked gene expression between males and females [360,361]. A number of DCC components are expressed at high levels in the adult nervous system [362], which correlates with the tissue-restricted link between Nab2 and *Sxl* splicing (as in **Figure 32-F**). As a functional test of interactions between Nab2 and the DCC pathway, the *msl-2*^{kmA} (*msl-2*$^{killer\ of\ males\text{-}A}$) male lethal EMS allele [363] was tested for dominant effects on *Nab2*^{ex3} female phenotypes. A single copy of *msl-2*^{kmA} significantly rescues defects in viability (**Figure 2-4D**), locomotion (**Figure 2-4E**), and lifespan (**Figure 2-4F**) in *Nab2*^{ex3} females. Furthermore, a second *msl-2* mutant allele over a deficiency that uncovers the *msl-2* locus (*msl-l*^{227}*/Exel7016*) [364], as well as *roX1* and *mle* loss-of-function alleles, rescue *Nab2*^{ex3} mutant phenotypes (**Supplemental Figure 2-5**). Given that Msl-2 is not normally active in adult female tissues [362,365] and its forced expression reduces female viability [366], rescue of *Nab2*^{ex3} females by these *msl-2*, *mle*, and *roX1* alleles provides evidence that the DCC pathway is inappropriately activated upon Nab2 loss. Of note, the *msl-2*, *mle* and *roX1* RNAs appear similar in IGV reads from both control and *Nab2*^{ex3} adult heads (**Supplemental Figure 2-4**), suggesting that genetic interactions between these loci are not through direct effects of Nab2 loss on post-transcriptional processing of these RNAs in a large fraction of cells.

Loss of the Mettl3 m^{6}A methyltransferase rescues *Nab2*^{ex3} phenotypes

Genetic interactions between *Nab2*, *Sxl*, and *msl-2* alleles are consistent with a role for Nab2 protein in regulating sex-specific splicing of *Sxl* exon 3. One mechanism that promotes exon 3 exclusion in females is based on N^6-methylation of adenosines (m^6A) in *Sxl* pre-mRNA by the Methyltransferase like-3 (Mettl3)-containing methyltransferase complex[129,341]. Inactivating mutations in components of this m^6A 'writer' complex masculinize the pattern of exon 3 splicing in female flies in a manner similar to $Nab2^{ex3}$ and molecular studies indicate that the Mettl3 complex promotes exon 3 exclusion in females by depositing m^6A within *Sxl* exon 3 and flanking introns[129,147,288,341].

To assess Nab2-Mettl3 functional interactions, the $Mettl3^{null}$ allele (formerly known as $Ime4^{null}$) [129] was carefully recombined with $Nab2^{ex3}$ (the loci are less than 1cM apart; **Supplemental Figure 2-6**) Multiple recombinant $Nab2^{ex3},Mettl3^{null}$ chromosomes were found to be lethal at pre-larval stages but semi-viable over the $Nab2^{ex3}$ chromosome; we therefore analyzed phenotypes in $Nab2^{ex3},Mettl3^{null/+}$ mutant females. Consistent with prior work[129,288,341], homozygosity for the $Mettl3^{null}$ allele reduces adult viability (**Figure 2-5A**), decreases locomotion in a negative geotaxis assay (**Figure 2-5B**), and shortens lifespan (**Figure 2-5C**). However, $Mettl3^{null}$ heterozygosity has the inverse effect of suppressing each of these defects in $Nab2^{ex3}$ females: $Nab2^{ex3},Mettl3^{null}$/+ mutant females show approximately 3-fold higher viability (**Figure 2-5A**), 6-fold higher climbing rates (at the 30 sec time point; **Figure 52-B**), and 1.75-fold longer lifespan (**Figure 2-5C**) than $Nab2^{ex3}$ mutant females. As both Nab2 and Mettl3 act within the *Drosophila* nervous system[129,147,278,280,288,367], we sought to test whether this rescue of $Nab2^{ex3}$ by reduced *Mettl3* stems from cell autonomous roles for both factors within neurons. To address this hypothesis, we expressed a *UAS-Mettl3-RNAi* transgene in $Nab2^{ex3}$ neurons using the

pan-neuronal driver *elav-Gal4*[368] (i.e., *elav-Gal4*;*UAS-Mettl3-RNAi;Nab2*^{ex3}). Notably, this depletion of Mettl3 only in neurons was sufficient to suppress *Nab2*^{ex3} associated defects in both viability (**Figure 2-5D**) and locomotion (**Figure 2-5E)** in female flies, consistent with a functional interaction between Nab2 and Mettl3 in neurons. Similarly, we reasoned that reducing other components of the m6A 'writer' complex could rescue *Nab2*^{ex3} defects. Indeed, we observed that heterozygous loss of two other components of the methyltransferase complex required for *Sxl* exon 3 skipping, *female-lethal(2)d* (*fl(2)d*) and *virilizer* (*vir*)[369-371], also suppresses *Nab2*^{ex3} mutant phenotypes (**Figure 2-5F-G**). Heterozygous loss of *fl(2)d* in a *Nab2*^{ex3} mutant suppresses defects in female locomotion but not viability, while heterozygous loss of *virilizer* dominantly suppresses defects in both viability and locomotion.

Nab2 binds *Sxl* pre-mRNA and modulates m^{6}A methylation

The finding that reduced Mettl3 expression rescues viability, lifespan, and locomotor defects in *Nab2*^{ex3} females indicates that the Mettl3 m^{6}A 'writer' complex is required to promote developmental and behavioral defects in Nab2 mutants. However, loss of the same Mettl3 m^{6}A 'writer' complex normally causes developmental and behavioral defects that resemble Nab2 mutant phenotypes documented here (**Figures 2-4 and 2-5**), and that are accompanied by *Sxl* exon 3 inclusion due to hypomethylation of *Sxl* mRNA[129,147,288,341]. This paradox could be explained if *Sxl* exon 3 inclusion in *Nab2*^{ex3} females accumulate excess m^{6}A on the *Sxl* pre-mRNA. To test this hypothesis, a series of primer sets were designed to examine *Sxl* pre-mRNA and mRNA transcripts by RNA-immunoprecipitation (RIP) and anti-m^{6}A-RIP (MeRIP) (**Figure 2-6A**). As illustrated in

Figure 2-6A, the *Sxl* transcript contains candidate binding sites for both Sxl protein (polyuridine tracts=**red** ticks) and the polyadenosine RNA binding protein Nab2 protein ($AC(A)_{13}$ tract=**green** tick). Approximate mapped sites of m^6A methylation (**yellow** ticks) in the *Drosophila* head transcriptome are also indicated [147] (see **Supplemental Figure 2-7** for a more detailed schematic).

To assess the m^6A status of total *Sxl* RNA, MeRIP precipitates from female head lysates (control, $Nab2^{ex3}$, and $Mettl3^{null}$) were analyzed by reverse transcription-real time quantitative PCR (RT-qPCR) with the exon 2-exon 2 (E2-E2) primer pair, which amplifies both pre-mRNA and mature mRNA ($Sxl^{E2\text{-}E2}$ in **Figure 2-6B**). This approach detects reduced *Sxl* m^6A in $Mettl3^{null}$ heads relative to controls, which is consistent with prior studies [129,147,288,341], and an increase in *Sxl* transcript recovered from MeRIP of $Nab2^{ex3}$ heads, consistent with increased *Sxl* m^6A modification. As additional controls for m^6A status, two m^6A-methylated Mettl3-target RNAs, *Act5c* and *Usp16* [129,147,288] were analyzed. MeRIP-qPCR indicates that both mRNAs show decreased m^6A in $Mettl3^{null}$ and show increased m^6A in $Nab2^{ex3}$ flies (**Supplemental Figure 2-9**). Shifting this analysis to qPCR with the *Sxl* E2-E4 primer set ($Sxl^{E2\text{-}E4}$ in **Figure 2-6B**), which detects spliced *Sxl* mRNA, reveals a similar pattern of elevated *Sxl* m^6A in $Nab2^{ex3}$ heads. Together, these MeRIP-qPCR data argue that Nab2 either inhibits Mettl3-mediated m^6A deposition or promotes m^6A removal from *Sxl* mRNA. A prediction of this model is that Nab2 loss should result in increased levels of m^6A on *Sxl* pre-mRNA. MeRIP analysis using the I2-E3 primer pair ($Sxl^{I2\text{-}E3}$ in **Figure 2-6C**) or the I3-E4 primer pair ($Sxl^{I3\text{-}E4}$ in **Figure 2-6C**) reveals moderate (1.5-fold) enrichment for intron 2-containing *Sxl* RNAs in $Nab2^{ex3}$ heads, and

stronger (4.5-fold) enrichment for intron 3-containing RNAs, consistent with elevated m^{6}A on *Sxl* pre-mRNAs that contain introns 2 and 3.

To more precisely define how loss of Nab2 alters the relative abundance and/or location of m^{6}A deposition along the *Sxl* transcript in female heads, we utilized *in vitro* DART-Sanger sequencing (Deamination adjacent to RNA modification Targets followed by Sanger sequencing) [372,373] (**Figure 2-6D-F**). This method overcomes several limitations of traditional antibody-based methods including limited sensitivity and selectivity, and struggle to distinguish m^{6}A from other RNA modifications (i.e., m^{6}Am) [372]. Briefly, *in vitro* DART-Sanger sequencing involves incubating RNA with a chimeric fusion protein consisting of the deaminating enzyme APOBEC1 fused to the m^{6}A-binding YTH domain of m^{6}A 'reader' proteins. As m^{6}A-modified adenosine (A) residues are followed by a cytosine (C) residue in the most common consensus sequence [126,372,374], the APOBEC-YTH fusion recognizes m^{6}A-modified A and deaminates the neighboring C, creating a uracil (U) base which is read as a thymine (T) during Sanger sequencing. Therefore, C-to-U transitions and the frequency at which they occur permit mapping of m^{6}A location and relative abundance. Thus, this method enables us to define the m^{6}A modification status of the *Sxl* transcript in control and *Nab2^{ex3}* heads. For this experiment, we treated RNA extracted from female control or *Nab2^{ex3}* heads with APOBEC1-YTH, and subsequently performed RT-PCR with primers that amplify *Sxl* exon 3-intron 3[503] (E3-I3 as illustrated in **Figure 2-6F**). Sanger sequencing and subsequent analysis of C-to-U transitions revealed the presence of seven m^{6}A sites (sites #1-7) within this region (**Figure 2-6D-F,** denoted by asterisk in **Figure 2-6D**). These sites fall within or adjacent to sites mapped in a previous study of *Drosophila* head RNAs [147]. Of the seven m^{6}A modifications

mapped within this region, four sites show a statistically significant increases C-to-U transition in *Nab2*^{ex3} female heads compared to control (**Figure 2-6D;** four sites are denoted by red color in **Figures 2-6E-F**). Specifically, sites 1-3 and 7 show ≥2.00 ratio of m^{6}A modification (calculated as %C-to-U *Nab2*^{ex3}/%C-to-U *control*), providing evidence that these sites are methylated to a greater extent in *Nab2*^{ex3} female heads as compared to control heads. Notably, the m^{6}A modification mapped to site 7 falls within the first adenosine residue of the proposed Nab2 AC(A)$_{13}$ binding site (see schematic in **Figure 2-6A,F**). These results are consistent with a role for Nab2 in inhibiting m^{6}A levels on *Sxl* pre-mRNA and suggest that modulation of m^{6}A levels may link Nab2 to other RNA targets within the *Drosophila* head transcriptome. To test whether Nab2 physically associates with *Sxl* pre-mRNA as a potential mechanism to limit m^{6}A levels, an anti-Flag IP of FLAG-Nab2 was performed from head lysates of adult females expressing N-terminally tagged Nab2 specifically in neurons (*elav>Flag:Nab2*). RT-qPCR of precipitates analyzed with *Sxl* I3-E4 primers, provides evidence that Nab2 associates with unspliced *Sxl* pre-mRNA (**Figure 2-6G**). In sum, these data provide a molecular framework to interpret *Nab2-Mettl3-Sxl* genetic interactions in which Nab2 associates with the *Sxl* pre-mRNA, perhaps via the AC(A)$_{13}$ site located in I3 (**green** tick; **Figure 2-6A**) and limits levels of m^{6}A on this transcript.

In light of these m^{6}A data, we revisited the effect of altered *Mettl3* gene dosage on *Sxl* RNA structure. Reducing *Mettl3* levels by half (*Mettl3*$^{null/+}$) does not significantly alter *Sxl* splicing patterns in either control females or *Nab2*^{ex3} females (**Supplemental Figure 2-10**). Because complete removal of Mettl3 is lethal in animals that also lack Nab2, we considered whether overexpressing Mettl3 is sufficient to reproduce *Sxl* splicing defects

we observe in *Nab2*^{ex3} female heads. To test this possibility, we compared patterns of *Sxl* splicing between *Nab2*^{ex3} female heads and heads from animals overexpressing Mettl3 in neurons using a *UAS-Mettl3* [129] transgene driven by *elav-Gal4* [368] (**Supplemental Figure 2-11**). As shown in **Figure 2-6H**, RT-PCR using primers located in *Sxl* exon 3 and exon 4 detect misspliced exon 3-exon 4 RNA (green boxes) and the aberrant exon 3-intron 3^{503}-exon 4 (red-grey boxes) product in *Nab2*^{ex3} homozygous heads, with none or very low levels of these two RNA species in control (*elav-Gal4* alone) and *Nab2*^{ex3} heterozygous heads. However, overexpression of Mettl3 in neurons is sufficient to produce the exon 3-exon 4 and exon 3-intron 3^{503}-exon 4 RNAs in both control and *Nab2*^{ex3} heterozygote heads, thus replicating the effect of Nab2 loss on *Sxl* splicing. This analysis also identified a *Sxl* exon 3-exon 4 splicing intermediate in female heads that is approximately 60nt smaller than the expected exon 3-exon 4 product, which is lost in *Nab2*^{ex3} female heads (grey arrow, **Figure 2-6H**). Sanger sequencing of this product revealed the presence of a Nab2-regulated cryptic 3' splice site located within exon 3 that corresponds to the *Sxl-RZ*, *RK* and *RQ* RNAs (see Flybase).

The increase in m^{6}A levels detected on *Sxl* pre-mRNA upon loss of Nab2 provides evidence that Nab2 normally limits methylation on some RNAs. Excess m^{6}A on transcripts in *Nab2*^{ex3} heads could lead to over-recruitment of the nuclear m^{6}A YTH-domain containing 'reader' protein, Ythdc1 (or YT521-B), which regulates nuclear processing of many pre-mRNA targets including the removal of *Sxl* exon 3 in females[128]. Thus, we tested whether reducing levels of Ythdc1 with the *Ythdc1*$^{\Delta N}$ null allele[129] could rescue the lethality of *Nab2*^{ex3} mutants. Indeed, heterozygous loss of *Ythdc1* increases viability of *Nab2*^{ex3} females approximately 5-fold (**Figure 2-6I**). This finding is consistent with

biochemical evidence that Nab2 represses m^{6}A levels on the *Sxl* RNA and provides additional evidence that Nab2 interacts genetically with multiple elements of the m^{6}A machinery.

Discussion

Through an unbiased high-throughput RNA sequencing approach, we identify a set of head-enriched RNAs in *Drosophila* whose levels or structure are significantly affected by loss of the Nab2 RBP, with the latter effect on RNA structure traced to splicing defects (including intron retention, alternative 5' and 3' splice site usage, and exon skipping) in a small group of approximately 150 transcripts. The top ranked Nab2-regulated splicing event is skipping of *Sxl* exon 3 in females, which prior studies [129,288,341] have shown to be guided by m^{6}A methylation of specific sites in the *Sxl* pre-mRNA. Our biochemical studies reveal that Nab2 inhibits hypermethylation of sites in and around *Sxl* exon3, and genetic data show that developmental and behavioral phenotypes resulting from Nab2 loss are rescued by decreasing levels of the Mettl3 methyltransferse, other components of the Mettl3 complex, or the nuclear m^{6}A reader protein Ythdc1. Data suggest that Nab2-Mettl3 coregulation of *Sxl* splicing is most significant in neurons - the effect of Nab2 on *Sxl* splicing is strongest in tissues that contain CNS components (e.g., brain and ventral nerve cord), while Mettl3 overexpression only in neurons is sufficient to replicate *Sxl* splicing defects seen in *Nab2* mutant heads. This apparent tissue specificity of the link between Nab2 and Mettl3 may help explain neurological defects in mice and humans lacking the Nab2 ortholog ZC13H14, although lethality of animals lacking both Nab2 and Mettl3 is consistent with only partial overlap between RNA targets of these two RBPs.

Because *Sxl* exon 3 contains a translational termination (stop) codon, inclusion of this exon disrupts female-specific expression of Sxl protein, a U-rich RNA binding protein that controls somatic and germline sexual identity via effects on splicing and translation of target mRNAs rev. in [352,375]. Multiple lines of evidence suggest that *Sxl* mRNA may be a particularly significant target of Nab2 in neurons: mis-spliced RNAs in *Nab2* mutant female heads are enriched for bioinformatically predicted Sxl binding motifs, and the Sxl^{M8} allele that constitutively skips exon 3 [359] substantially reverses developmental and behavioral defects in *Nab2* null females (**Figure 2-4**). Moving downstream of Sxl, alleles of male-specific dosage compensation complex (DCC) components, including the direct Sxl target *msl-2* [376,377], also rescue phenotypic defects in *Nab2* mutant females (**Figure 2-4** and **Supplemental Figure 2-5**). Given that these DCC components are not normally expressed or active in females, these data provide evidence that masculinized *Sxl* splicing and DCC activity contribute to developmental and behavioral defects in *Nab2* mutant female flies. Elevated DCC activity could contribute to axon projection defects in female MBs, but this seems unlikely given that $Nab2^{ex3}$ males develop similar MB axonal defects [284]. Overall, these data imply a specific link between Nab2 and the *Sxl* exon 3 splicing machinery, which is confirmed by strong genetic interactions between *Nab2* and the *Mettl3* methyltransferase that promotes exon 3 skipping by depositing m^6A on *Sxl* pre-mRNA [129,288,341].

Molecular assays provide key insight into the Nab2-Sxl interaction. A tagged form of Nab2 protein associates with unspliced *Sxl* pre-mRNA when expressed in brain neurons, and Nab2 loss results in excess m^6A on *Sxl* mRNA as detected by two independent assays used to map m^6A sites, meRIP-qPCR and DART. The high resolution

of the DART technique allowed us to map m^{6}A sites in the *Sxl* exon 3-intron 3-exon 4 region that are more highly methylated in *Nab2* mutants than in controls, consistent with Nab2 inhibiting m^{6}A accumulation at sites normally modified by the Mettl3 complex. Significantly, these Nab2-regulated methylation sites lie under or adjacent to anti-m^{6}A-CLIP peaks mapped in the *Sxl* RNA from adult female heads [147] and thus complement and extend our knowledge of m^{6}A patterns on *Sxl* mRNAs expressed in the adult head. Given the known role of m^{6}A in promoting *Sxl* exon 3 excision [129,288,341], these data collectively support a model in which Nab2 interacts with the *Sxl* pre-mRNA in the nucleus and opposes m^{6}A methylation by the Mettl3 complex, thus ensuring a level of m^{6}A necessary to guide *Sxl* exon 3 skipping in the female nervous system. We term this a 'Goldilocks' model in which either too little or too much m^{6}A methylation of the region surrounding *Sxl* exon 3 can result in its retention in the developing female brain. These data provide the first evidence that the highly conserved Nab2 RBP is a key regulator of splicing in the adult brain, and that Nab2 is required to limit m^{6}A modification of an RNA.

Studies employing the *Sxl^{M8}* allele indicate that altered *Sxl* splicing and decreased Sxl protein contribute to *Nab2* mutant phenotypes in females. As Sxl is itself an RBP that can control splicing, some fraction of the mis-sliced mRNAs detected by *Nab2^{ex3}* high throughput sequencing may thus be Sxl targets. This hypothesis is supported by the substantial rescue conferred by the *Sxl^{M8}* allele and the enrichment for candidate Sxl-binding sites among mis-spliced mRNAs in *Nab2* mutant female heads. However, splicing of the Sxl target RNA *tra* is unaffected in the *Nab2* mutant RNA-Seq datasets. The lack of effect on *tra* could be due to lack of read depth in the RNA-seq data, although this does not seem to be the case (see **Supplemental Figure 2-4**), or to alternative Sxl target RNAs

in adult heads. Unbiased screens for Sxl target RNAs have carried out in ovaries [378] and primordial germ cells [379], but a similar approach has not been taken in the adult nervous system, where Sxl targets may differ from other tissue types. In this regard, the group of Nab2-regulated RNAs identified here may be enriched for neuronal RNAs that are directly regulated by Sxl.

Although this study focuses on *Sxl* as a female-specific Nab2 regulated RNA, a large majority of other mis-splicing events in *Nab2* mutant head RNAs occur in both males and females. This evidence of a Nab2 role in non-sex specific splicing events parallels evidence of accumulation of ~100 intron-containing pre-mRNAs in *nab2* mutant *S. cerevisiae* cells [273]. Rescue of *Nab2* mutant males and females by neuron-restricted expression of human ZC3H14 [279] implies that this specificity may be a conserved in ZC3H14 proteins in higher eukaryotes. Indeed, knockdown of ZC3H14 in cultured vertebrate cells results in pre-mRNA processing defects and intron-specific splicing defects in the few RNAs that have been examined [249,380]. The basis for Nab2 target specificity in *Drosophila* heads is not clear but could be due selectivity in binding to nuclear pre-mRNAs (e.g., *Sxl*) or interactions between Nab2 and partner proteins that define splicing targets.

Site-specific hypermethylation of *Sxl* resulting from Nab2 loss could arise by several mechanisms, including Nab2 modulating m^6A deposition by blocking access of the Mettl3 complex to its target sites, or to Nab2 recruitment of an m^6A ‘eraser’. However, recent studies demonstrating that Nab2 and ZC3H14 each co-purify at nearly stoichiometric levels with the exon junction complex (EJC) [381,382] and that the EJC binding locally excludes Mettl3-mediated m^6A deposition on pre-mRNAs [134,383,384], suggest an

alternate model in which Nab2 inhibits m^{6}A deposition in cooperation with the EJC. Notably, the human homolog of the *Drosophila* protein Virilizer, which is an m^{6}A methyltransferase subunit and splicing factor [370,371], was recovered in an IP/mass-spectrometry screen for ZC3H14 nuclear interactors [380]. This finding raises an additional possibility that ZC3H14/Nab2 modulates m^{6}A methylation via interactions with both the Mettl3 complex and the EJC. Moreover, evidence that m^{6}A modulatory role of Nab2 is not restricted to the *Sxl* mRNA (see **Figure 2-6B** and **Supplemental Figure 2-6**) raises the additional hypothesis that changes in abundance or structure of the group of Nab2-regulated RNAs defined in this study (see **Figures 2-1** and **2-2**) are due in part to changes in m^{6}A status.

Prior work has shown that almost all developmental and behavioral defects caused by Nab2 loss can be traced to a Nab2 role within central nervous system neurons [215,279,281,284,367]. Suppression of these phenotypes by heterozygosity for *Sxl^{M8}* or *Mettl3^{null}* alleles or by neuron-specific *Mettl3* RNAi is thus consistent with a mechanism in which Nab2 inhibits steady-state m^{6}A levels on a group of neuronal RNAs, and that *Sxl* is one of these RNAs in the female brain. However, the lack of statistically significant rescue of *Sxl* splicing defects by *Mettl3* heterozygosity **(Supplemental Figure 2-10)** implies that *Sxl* splicing is only rescued in a small subset of cells or that *Sxl^{M8}* and *Mettl3^{null}* heterozygosity rescue *Nab2* mutant phenotypes through different mechanisms. While *Sxl^{M8}* specifically restores a single splicing event in a single mRNA, the *Mettl3^{null}* allele has the potential to broadly affect m^{6}A levels on multiple RNAs with subsequent effects on multiple m^{6}A-dependent processes in the cytoplasm, including mRNA export to the cytoplasm and translation. One potential candidate mRNA of this type is *Wwox*, which

encodes a conserved WW-domain oxidoreductase that accumulates in brains of *Nab2* mutant flies [280] and is mutated in human spinocerebellar ataxia type-12 [385,386]. Significantly, the *Wwox* RNA has a 3'UTR intron that is retained in *Nab2* mutant heads (this study) and contains a candidate m^{6}A site [147], suggesting that *Wwox* RNA may be a target of both Nab2 and Mettl3. Elevated Wwox protein is also detected in the hippocampus of *ZC3H14* knockout mice, raising the possibility that Nab2 and ZC3H14 share some common RNA targets across species [338]. ZC3H14 has to date not been linked to the m^{6}A mark in mouse or human cells. However, the enrichment for *Sxl* mis-splicing in neuronal tissue (see **Figure 2-3F**) and rescue by *ZC3H14* when expressed in neurons of otherwise *Nab2* deficient animals [284] supports the hypothesis that the Nab2/ZC3H14 family of RBPs may share an m^{6}A inhibitory role that is specific to neurons, and that excessive m^{6}A methylation of RNAs also contributes to neurological deficits in mice and humans lacking ZC3H14.

Materials and Methods

Drosophila stocks and genetics

Drosophila melanogaster stocks and crosses were maintained in humidified incubators at 25ºC with 12hr light-dark cycles. The alleles *Nab2*^{ex3} (null), *Nab2*^{pex41} (*precise excision 41*; control) and *UAS-Flag-Nab2* have been described previously [215,279]. Lines from Bloomington *Drosophila* Stock Center (BDSC): *GMR-Gal4 (*#1350), *elav*^{C155}*-Gal4* (#458), *msl-2*^{227} (#5871), *msl-2*^{kmA} (#25158), *mle*^{9} (#5873), *roX1*^{ex6} (#43647), *UAS-Mettl3, UAS-Mettl3-RNAi* (#80450), *fl(2)d*^{2} (#36302)*, vir*^{2F} (#77886). The *Mettl3*^{null}*, UAS-Mettl3,* and *Ythdc*$^{\Delta N}$ alleles were all kind gifts of J-Y. Roignant. The *Nab2*^{ex3},*Mettl3*^{null} and *Nab2*^{ex3}*, Ythdc*$^{\Delta N}$ chromosomes were generated by meiotic recombination and confirmed by genomic PCR. A total of 200 recombinant lines were screened to identify *Nab2,Mettl3* double mutants.

RNA Sequencing (RNA-Seq) on *Drosophila* heads

RNA-Seq was performed on three biological replicates of 60 newly-eclosed adult female and male *Drosophila* heads genotype (control and *Nab2*^{ex3} mutants). Heads were collected on dry ice, lysed in TRIzol (ThermoFisher), phase-separated with chloroform, and ran through a RNeasy Mini Kit purification column (QIAGEN). Samples were treated with DNase I (QIAGEN) to remove DNA contamination and transported to the University of Georgia's Genomics and Bioinformatics Core for sequencing. rRNA was depleted using a Ribo-Zero Gold Kit (Illumina) and cDNA libraries were prepared using a KAPA Stranded RNA-Seq Kit (Roche). Quality control steps included initial Qubit quantification along with RNA fragment size assessment on an Agilent 2100 Bioanalzyer before and after rRNA depletion. The cDNA libraries were then sequenced for 150 cycles on a NextSeq 500

High Output Flow Cell (Illumina) set to generate paired-end, 75 base-pair (bp) reads. Total sequencing yield across all samples was 81.48 Gbp, equivalent to about 1.1 billion reads in total and 91 million reads per sample. Sequencing accuracy was high; 93.52% of reported bases have a sequencing quality (Q) score greater than or equal to 30.

Read mapping, differential expression, and visualization

Raw read FASTA files were analyzed on the Galaxy web platform usegalaxy.org [387]. The BDGP6 release *Drosophila melanogaster* genome [388] from release 92 of the Ensembl database [389] was used as input for subsequent read mapping, annotation, and visualization. Briefly, reads from all four NextSeq500 flow cell lanes were concatenated using the Galaxy *Concatenate datasets tail-to-head (cat)* tool and mapped using RNA STAR [342] with default parameters with some modifications. For each Galaxy tool, version numbers and exact parameters used are detailed in the Table below:

Galaxy software and parameters:

Tool	Concatenate datasets tail-to-head (cat)	Default parameters
	Galaxy Version 0.1.0	
Tool	RNA STAR	Default parameters with the following exceptions:
	Galaxy Version 2.5.2b-0	read type: *paired*
		reference genome: *from history (using Ensembl FASTA and GTF referenced in text)*
Tool	featureCounts	Default parameters with the following exceptions:
	Galaxy Version 1.6.0.3	gene annotation file: *history (Ensembl GTF referenced in text)*
		count fragments instead of reads: *enabled*
		GFF gene identifier: *gene_name*
		strand specificity: *stranded-reverse*
Tool	DESeq2	Default parameters with the following exceptions:
	Galaxy Version 2.11.40.1	factors: *4 levels, each a group of three biological replicates*
		output normalized counts table-*true*
		output all levels vs all levels-*true*
Tool	DEXSeq-Count	Default parameters with the following exceptions:
	Galaxy Version 1.20.1	In 'read count' mode: strand specific library-*yes, reverse*
Tool	DEXSeq	Default parameters with the following exception:
	Galaxy Version 1.20.1	visualize results? - *no*

Gene Ontology (GO) software and parameters

Tool	GO2MSIG	Parameters:
	web interface	data source: *NCBI gene2go*
		taxon ID- *7227*
		evidence codes: *include—EXP, IDA, IEP, IGI, IMP, IPI, ISS, TAS*
		propagate associations - *true*
		use gene- *symbol*
		repress IDs - *no*
		create genesets for - *[1 top level domain only]*
		max. geneset size - *700*
		min. geneset size - *15*
		output format - *gmt*
		database release - *April 2015*
Tool	GSEA Desktop for Windows	Default parameters with the following exceptions:
	v4.0.3	*For up- and downregulated transcripts in Nab2^{ex3} vs. control:*
	GSEA-Preranked	zip-report - *true*
		plot top x - *100*
		create svgs - *true*
		collapse - *No collapse*
		For alternatively spliced transcripts in Nab2^{ex3} vs. control:
		zip-report - *true*
		minimum gene set size - *5*
		create svgs - *true*
		collapse - *No collapse*
Tool	AmiGO 2	Default parameters
	web interface	

Mapped reads were assigned to exons and tallied using featureCounts [343] default parameters with some modifications noted above. Differential expression analysis was conducted for all 12 samples using DESeq2 [344] (Galaxy Version 2.11.40.1) and default parameters with some modifications noted above. Differential exon usage was analyzed using Galaxy Version 1.20.1 of DEXSeq [350] and the associated Galaxy tool DEXSeq-Count in both "*prepare annotation*" and "*count reads*" modes. Both tools were run with the

Ensembl GTF with default parameters with some modifications noted above. Unlike with DESeq2, female samples and male samples were compared in independent DEX-Seq analyses. Outputs from all tools were downloaded from Galaxy for local analysis, computation, and visualization.

Custom R scripts were written to generate volcano plots and heatmaps. Additional R packages used include ggplot2 [390] and ggrepel [391]. R scripts were written and compiled in RStudio [392]. Principal component analysis was conducted on Galaxy. Mapped reads were visualized in the Integrative Genomics Viewer (IGV) [356] and annotated based on data available on Flybase [393]. Significant fold change values in either male or female from DESeq2 (adj. *p*-val<0.05 and $|\log_2 FC|>1$) were plotted, with the color indicating the fold change threshold reached in either males or females. Significantly DE genes (adj. *p*-val<0.05 and $|\log_2 FC|>1$) were classified by type, as indicated by their gene ID.

Mixtures of Isoforms (MISO) Analysis

Mixtures of isoforms (MISO) [349] version 0.5.4 was used to determine percent spliced in (PSI) PSI values for annotated alternative 3' splice sites, alternative 5' splice sites, and retained introns for each sample separately as follows. Alternative splicing annotations were generated using the rnaseqlib (a direct link to script is provided here) (https://rnaseqlib.readthedocs.io/en/clip/) script, gff_make_annotation.py, with flags--flanking-rule commonshortest --genome-label dm6. Replicates for each sample were pooled, and only full-length, mapped reads (76 bp) were used for the MISO analysis as MISO requires all reads input to be of the same length. MISO was run with the flag-prefilter, and the output was then input into the script, summarize_miso, with the flag --summarize-samples. Next, differential, alternative 5' and 3' splice sites, and differential

retained introns, were determined comparing *Nab2*^{ex3} and control for males and females, separately, using the script, compare_miso, with flag --compare-samples. The output of compare miso was then input into the script, filter_events, with the flags --filter --num-inc 10 --num-exc 10 --num-sum-inc-exc 50 --delta-psi 0.3 --bayes-factor 10, to obtain the final differential PSI values.

Gene ontology (GO) analysis

Gene Set Enrichment Analysis (GSEA) software [346] was employed for Gene Ontology (GO) analysis [348]. For clarity, analyses were conducted separately for each of the three top-level GO domains: *molecular function*, *biological process*, and *cellular component*. GSEA-compatible GO term gene sets for *Drosophila melanogaster* were acquired using the GO2MSIG web interface [394]. GSEA Desktop for Windows, v4.0.3 (Broad Institute) was then used to identify two distinct classes of GO terms, independently for females and for males: (1) terms enriched among up- and downregulated transcripts in *Nab2*^{ex3} compared to controls, and (2) terms enriched among transcripts alternatively spliced in *Nab2*^{ex3} compared to controls. For the first class, inputs consisted of all genes whose expression could be compared by DESeq2 (i.e., adjusted *p*-value ≠ NA). For the second class, inputs consisted of all genes with previously annotated alternative splicing events according to MISO. To identify the first class of GO terms, genes were ranked by $\log_2$ (fold change) calculated by DESeq2 and analyzed by the GSEA-Pre-ranked tool. To identify the second class of GO terms, genes with were ranked by the absolute value of the difference in PSI (Percent Spliced In) comparing *Nab2*^{ex3} and control calculated by MISO. This second ranking was analyzed by the GSEA-Preranked tool. Enriched GO terms (nominal *p*-value<0.05) identified for the first class were evaluated manually, surfacing multiple terms

directly related to splicing. Enriched GO terms (nominal *p*-value<0.05) for the second class were ordered by normalized enrichment score (NES) and evaluated to identify the top “independent” GO terms. Terms were defined as “independent” by reference to their position in the GO hierarchy as reported on each term’s “Inferred Tree View” page of the AmiGO2 GO database web tool [395]. “Independent” terms had no parent, child, or sibling terms in the GO hierarchy associated with a higher NES than their own.

RBPs Motif Enrichment Analysis using Mixture of Isoforms (MISO) Analysis

RNA sequences were analyzed at differentially retained introns and alternative 3’ and 5’ splice sites obtained from the MISO analysis on males and females separately (*Nab2*^{ex3} mutants vs. control). The sequence for each of these went 25 bp into the exon(s) of interest and 1 kb into the intron of interest. In the case of alternative 3’ and 5’ splice sites, the sequences went 25 bp into the exon starting from the alternative spice site that is closest to the center of the exon (i.e., the inner-most splice site), and 1 kb into the intron starting from that inner-most spice site. To convert these to RNA sequences, DNA sequences were first obtained using fastaFromBed [396], and then all T’s were converted to U’s with a custom script. To obtain putative binding sites for RBPs at these sequences, the sequences were then input into fimo using the flags --text --max-strand and the ”Ray2013_rbp_Drosophila_melanogaster.meme” file [397].

RNA isolation for reverse transcription (RT) PCR and real-time qPCR

Total RNA was isolated from adult tissues with TRIzol (Invitrogen) and treated with DNase I (Qiagen). For RT-PCR, cDNA was generated using SuperScript III First Strand cDNA Synthesis (Invitrogen) from 2 µg of total RNA, and PCR products were resolved and

imaged on 2% agarose gels (BioRad Image). Quantitative real-time PCR (qPCR) reactions were carried out in biological triplicate with QuantiTect SYBR Green Master Mix using an Applied Biosystems StepOne Plus real-time machine (ABI). Results were analyzed using the ΔΔCT method, normalized as indicated (e.g., to *Act5C*), and plotted as fold-change relative to control.

Primers used for RT and qPCR analysis:

Name	Sequence	Detects
Sxl pre-mRNA	Fwd: AGAACCAAAACTCCCTTACAGC Rev: GTGAGTGTCTTTCGCTTTTCG	intron 2-exon 3
Sxl pre-mRNA	Fwd: ACCAATAACCGACAACACAATC Rev: ACATCCCAAATCCACGCCCACC	intron 3-exon 4
Sxl mRNA	Fwd: GCTGAGCGCCAAAACAATTG Rev: AGGTGAGTTTCGGTTTTACAGG	exon 2-exon 2
Sxl RT-PCR	Fwd: ACACAAGAAAGTTGAACAGAGG Rev: CATTCCGGATGGCAGAGAATGG	exon 2-3-4
Sxl RT-PCR	Fwd: CTCTCAGGATATGTACGGCAAC Rev: CATTCCGGATGGCAGAGAATGG	exon 2-3-4
Sxl RT-PCR	Fwd: AGTATGTAGTTTTTATTTGCACGGG Rev: CATTCCGGATGGCAGAGAATGG	exon 3-4
Sxl mRNA exon 2-4 transcript	Fwd: GATTGAATCTCGATCATCGTTC Rev: CATTCCGGATGGCAGAGAATGG	exon 2-exon 4
Sxl mRNA exon 3-4 transcript	Fwd: CGAAAAGCGAAAGACACTCACTG Rev: CATTCCGGATGGCAGAGAATGG	exon 3-exon 4
Act5C	Fwd: GAGCGCGGTTACTCTTTCAC Rev: ACTTCTCCAACGAGGAGCTG	*Actin5C*
USP-16-45-RF	Fwd: ACACTTGGTCACGTCGTTCA Rev: GGGCGCGCTCTTGAATTTAC	*USP-16*

Immunoblotting

For analysis of Sxl protein levels, *Drosophila* were reared at 25°C. Heads of newly eclosed flies were collected on dry ice. Protein lysates were prepared by homogenizing heads in 0.5mL of RIPA-2 Buffer (50 mM Tris-HCl, pH 8; 150 mM NaCl; 0.5% sodium deoxtcholate; 1% NP40; 0.1% SDS) supplemented with protease inhibitors (1mM PMSF;

Pierce Protease Inbinitors [Thermo Fisher Scientific]). Samples were sonicated 3 X 10 seconds with 1 minute on ice between repetitions, and then centrifuged at 13,000*g* for 15 min at 4°C. Protein lysate concentration was determined by Pierce BCA Protein Assay Kit (Life Technologies). Head lysate protein samples (40-60 µg) in reducing sample buffer (50 mM Tris HCl, pH 6.8; 100 mM DTT; 2% SDS; 0.1% Bromophenol Blue; 10% glycerol) were resolved on 4-20% Criterion TGX Stain-Free Precast Polyacrylaminde Gels (Bio-Rad), transferred to nitrocellulose membranes (Bio-Rad), and incubated for 1hr in blocking buffer (5% non-fat dry milk in 0.1% TBS-Tween) followed by overnight incubation with anti-Sxl monoclonal antibody (1:1000; DHSB #M18) diluted in blocking buffer. Primary antibody was detected using species-specific horse-radish peroxidase (HRP) conjugated secondary antibody (Jackson ImmunoResearch) with enhanced chemiluminescence (ECL, Sigma).

Viability and lifespan analysis

Viability at 25°C was measured by assessing eclosion rates of among 100 wandering L3 larvae collected for each genotype, and then reared in a single vial. Hatching was recorded for 5-6 days. At least three independent biological replicates per sex/genotype were tested and significance was calculated using grouped analysis on GraphPad (Prism). Lifespan was assessed at 25°C as described previously [398]. In brief, newly eclosed animals were collected, separated by sex, placed in vials (10 per vial), and transferred to fresh vials weekly. Survivorship was scored daily. At least three independent biological replicates per vial of each genotype were tested and significance was calculated using grouped analysis on GraphPad (Prism).

Locomotion assays

Negative geotaxis was tested as previously described [398]. Briefly, newly eclosed flies (day 0) were collected, divided into groups of 10 male or females, and kept in separate vials for 2-5 days. Cohorts of age-matched flies were then transferred to a 25-ml graduated cylinder for analysis. At least three biological replicates per sex were analyzed per genotype using GraphPad (Prism).

Flag and m^{6}A RNA immunoprecipitation (Flag-RIP and MeRIP)

The FLAG-RIP and MeRIP protocols were performed using previously described protocols [278] and [129] with some modification. Briefly, three replicates of 30 newly eclosed female flies were collected in 1.5 ml Eppendorf tubes and frozen in dry ice. Heads were removed with a 5.5 Dumont tweezer and homogenized with a mortar/pestle in Isolation buffer (50 mM Tris-HCl pH 8.1, 10 mM EDTA, 150 mM NaCl, and 1% SDS, 50 mM NaCl). This preparation was diluted into IP buffer (50 mM HEPES, 150 mM NaCl, 5 mM EDTA, 0.5 mM DTT, 0.1% NP-40) supplemented with protease inhibitors (Roche) and RNasin Plus Inhibitor (Promega). Lysates were incubated with anti-Flag (M2 clone; Sigma) or anti-m^{6}A (Synaptic Systems) antibody and recovered on magnetic Protein G Dynabeads (Invitrogen). After overnight incubation at 4^{o}C with rocking, beads were washed 5x in IP buffer and RNA was isolated from antibody-bead precipitates, or controls (input samples) using TRIzol (ThermoFisher). Samples were treated with DNase-I and RNA was purified using RNeasy Kit (Qiagen).

Deamination adjacent to RNA modification targets (DART)

APOBEC-YTH and APOBEC-YTH^{mut} were purified and *in vitro* DART-Sanger sequencing assays were performed as previously described [373] with minor modifications. Briefly, total RNA was isolated from adult heads with TRIzol (Invitrogen) and treated with DNase I (NEB). RNA was isolated once more with TRIzol (Invitrogen) to remove DNase I and DNase I Buffer (NEB). Next, 200 ng of purified RNA from *Drosophila* heads was incubated with 1000 ng of purified DART protein in DART buffer (10mM Tris-HCl, pH 7.4, 50 mM KCl, 0.1 M $ZnCl_2$) and 1 µL of RNaseOUT (Invitrogen) in a total volume of 200 µL for 4 hours at 37°C. RNA was isolated with the Qiagen Plus Micro Kit (Qiagen) and stored at -80°C before being thawed for downstream Sanger sequencing analysis. cDNA was made using iScript Reverse Transcription Supermix (BioRad). PCR amplification of *Sxl* pre-mRNA was carried out with Phusion High Fidelity PCR Kit (NEB). The resulting PCR product was PCR-purified using the Qiagen PCR Purification Kit (Qiagen). Samples were submitted for Sanger sequenceing (McLabs) and %C-to-U editing was quantified using EditR software [399].

Primers used for DART PCR and Sanger sequencing:

Name	Sequence	Detects
Sxl DART-PCR	Fwd:ACATATTTTTTTTCACAGCCCAG Rev:TCAAAACGATCCCCCAGTTAT	exon 3-intron 3
Sxl DART Sanger Seq	Fwd:TTTTCACAGCCCAGAAAGAAGC	exon 3-intron 3

Statistical Analysis

Group analysis on biological triplicate experiments was performed using Two-way ANOVA (Turkey's multiple comparison test) on GraphPad (Prism) Version 8.4.2(464). Sample

sizes (n) and *p*-values are denoted in the text, figures, and/or figure legends and indicated by asterisks (e.g., *$p<0.05$).

Acknowledgments

Stocks obtained from the Bloomington Drosophila Stock Center/BDSC (NIH P40OD018537) were used in this study. We thank members of the Moberg and Corbett Labs for helpful discussions and advice, and B. Bixler, J. Tanquary, and C. Bowen for their contributions. We also thank M. Alabady (Georgia Genomics and Bioinfomatics Core) for technical support, and T. Lence and J.-Y. Roignant (Lausanne) for the gift of the *Mettl3* allele, and T. Cline (Berkeley) for discussions and insights on the *Sxl[M8]* allele. This work was funded by grants from the National Institute of Health to K.H.M. and A.H.C (R01 MH10730501), K.D.M. (NIGMS RM1 HG011563; R01 MH118366), J.C.R. (F31 HD088043), B.J. (F31 NS103595), and C.L.L (F31 NS127545). B.J. and B.E.B were also supported during portions of the study by The Emory Initiative to Maximize Student Development (NIH R25 GM125598).

Competing Interests

The authors declare no competing interests.

Figures

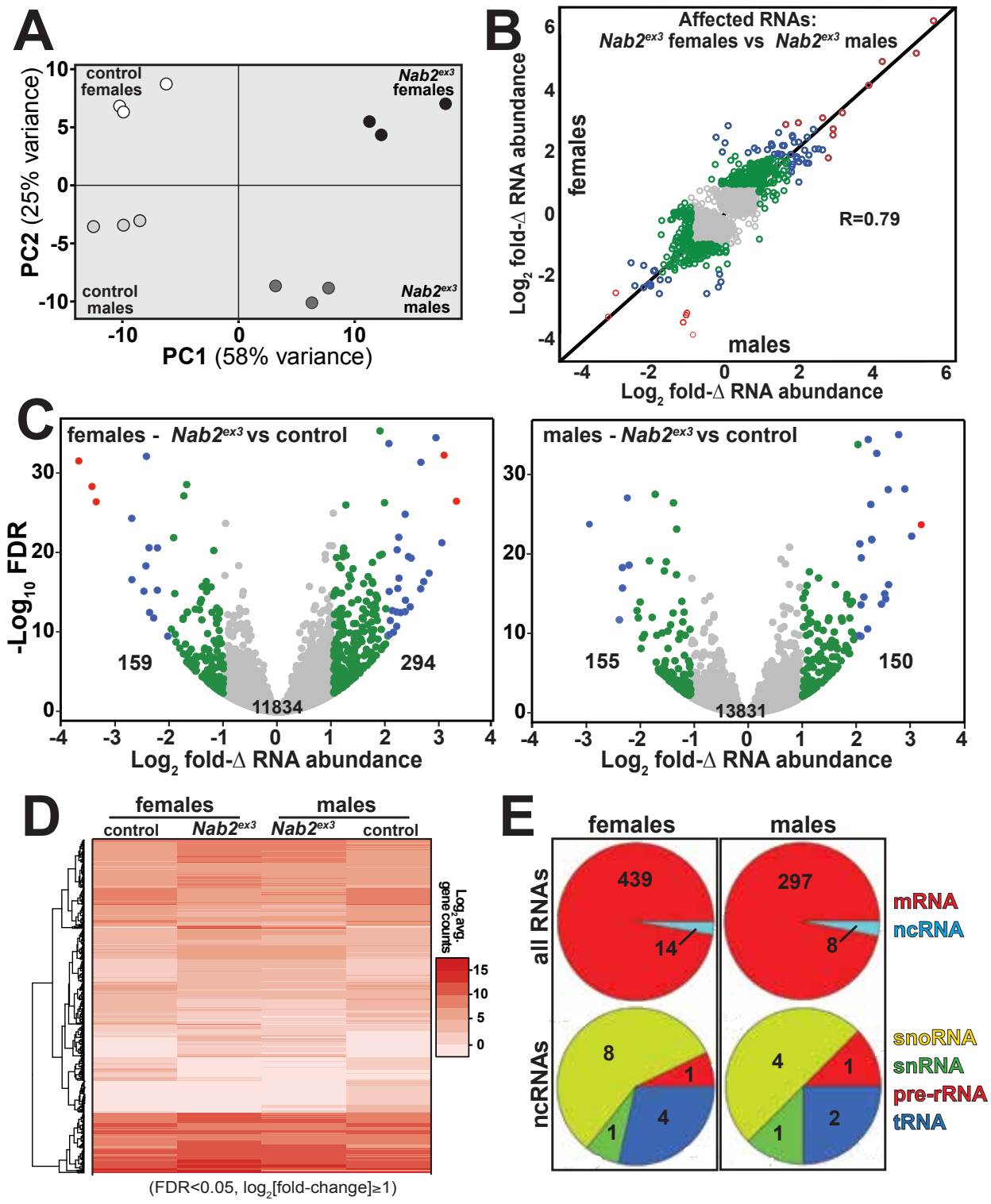
A
control females
Nab2ex3 females
control males
Nab2ex3 males
PC2 (25% variance)
PC1 (58% variance)
B
Affected RNAs:
Nab2ex3 females vs Nab2ex3 males
R=0.79
females
males
Log2 fold-Δ RNA abundance
C
females - Nab2ex3 vs control
159
294
11834
males - Nab2ex3 vs control
155
150
13831
-Log10 FDR
Log2 fold-Δ RNA abundance
D
females
males
control
Nab2ex3
Nab2ex3
control
Log2 avg. gene counts
(FDR<0.05, log2[fold-change]≥1)
E
females
males
all RNAs
ncRNAs
439
14
297
8
8
1
4
1
4
1
2
1
mRNA
ncRNA
snoRNA
snRNA
pre-rRNA
tRNA

Figure 2-1. RNA sequencing detects effects of Nab2 loss on the head transcriptome. (A) Principal component analysis (PCA) of RNA-seq data from three biological replicates of control and *Nab2* mutant (*Nab2*^{ex3}) male and female heads. **(B)** Correlation scatter plot of $\log_2$ fold change (Δ) in abundance of affected RNAs in males and females ($\log_2$ average gene counts: **grey**<1, $1\leq$**green**<2, $2\leq$**blue**<3, **red**≥ 3). **(C)** Volcano plots of fold-Δ in abundance vs false discovery rate (FDR $-\log_{10}$) of affected RNAs in *Nab2*^{ex3} females and males (dot plot color coding as in **B**). Elevated (≥ 1), reduced (≤ -1), and total RNAs are indicated. **(D)** Heatmap comparison of significantly changed gene counts (FDR<0.05;$|\log_2$ fold-$\Delta| \geq 1$) in *Nab2*^{ex3} females and males vs sex-matched controls. **(E)** Pie chart distribution of RNA classes among significantly affected RNAs detected in **C** and **D**.

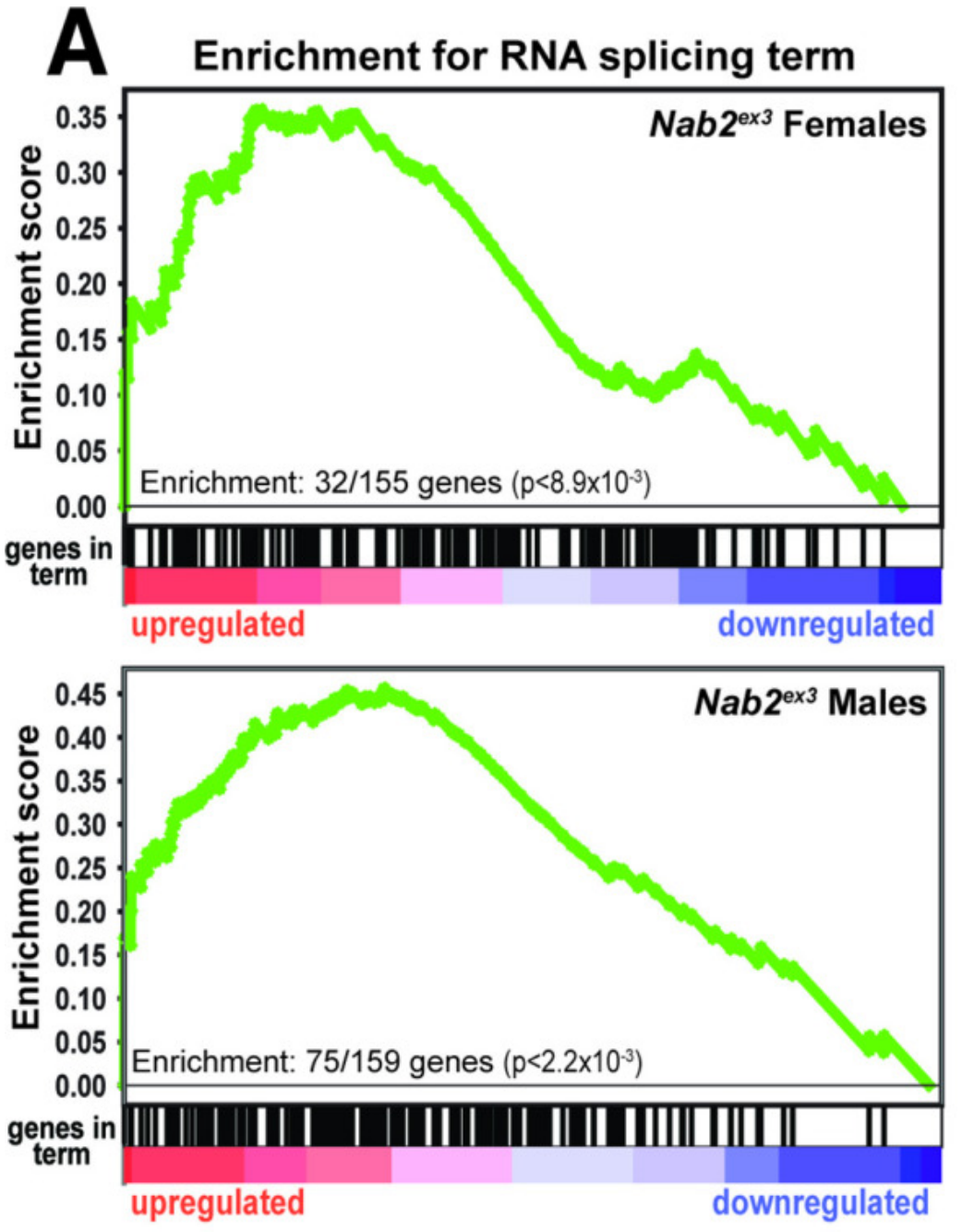
A
Enrichment for RNA splicing term
Nab2ex3 Females
Enrichment score
0.35
0.30
0.25
0.20
0.15
0.10
0.05
0.00
Enrichment: 32/155 genes (p<8.9x10-3)
genes in term
upregulated
downregulated
Nab2ex3 Males
Enrichment score
0.45
0.40
0.35
0.30
0.25
0.20
0.15
0.10
0.05
0.00
Enrichment: 75/159 genes (p<2.2x10-3)
genes in term
upregulated
downregulated

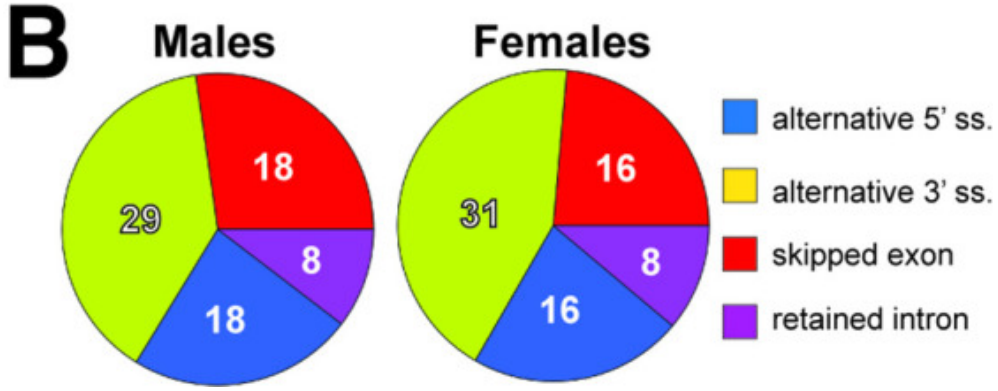
B
Males
Females
18
29
8
18
16
31
8
16
alternative 5' ss.
alternative 3' ss.
skipped exon
retained intron

Figure 2-2. Significantly up/down-regulated RNAs in *Nab2*^{ex3} heads are enriched for predicated splicing factors. (A) Gene set enrichment analysis (GSEA) detects enrichment for the 'RNA splicing' GO term in up- and down-regulated gene sets in both female (top) and male (bottom) *Nab2*^{ex3} datasets. Gene enrichments are indicated with corresponding p-values. **(B)** Pie chart illustrating the distribution of previously annotated alternative splicing RNA splicing events that are significantly altered in *Nab2*^{ex3} mutant female and male heads (ss=splice site).

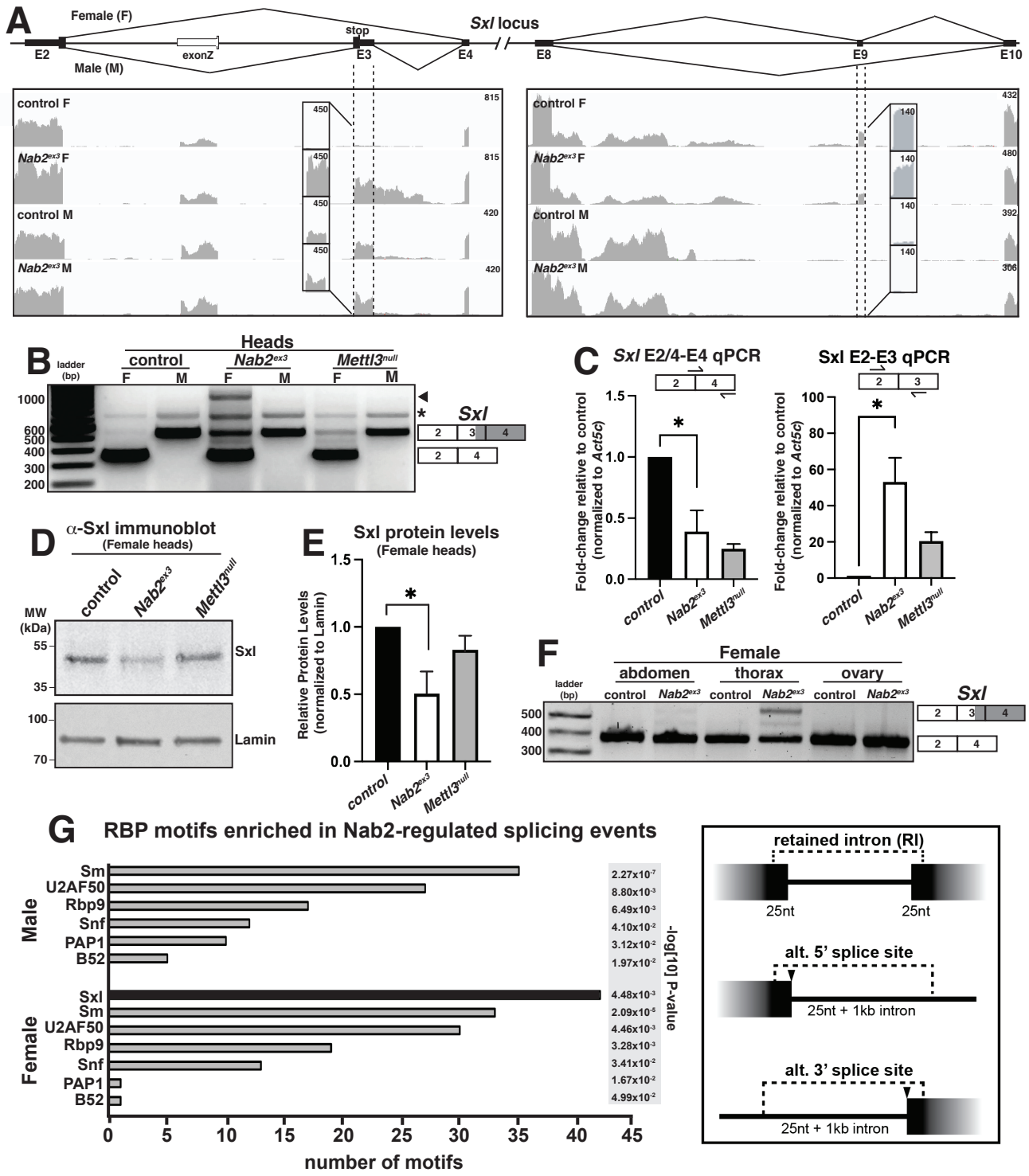
A
Female (F)
Male (M)
Sxl locus
stop
E2
exonZ
E3
E4
E8
E9
E10
control F
Nab2ex3 F
control M
Nab2ex3 M
B
Heads
ladder (bp)
control
Nab2ex3
Mettl3null
F
M
Sxl
C
Sxl E2/4-E4 qPCR
Sxl E2-E3 qPCR
Fold-change relative to control (normalized to Act5c)
D
α-Sxl immunoblot
(Female heads)
MW (kDa)
Sxl
Lamin
E
Sxl protein levels
(Female heads)
Relative Protein Levels (normalized to Lamin)
F
Female
abdomen
thorax
ovary
G
RBP motifs enriched in Nab2-regulated splicing events
Male
Female
Sm
U2AF50
Rbp9
Snf
PAP1
B52
Sxl
-log[10] P-value
number of motifs
retained intron (RI)
25nt
alt. 5' splice site
25nt + 1kb intron
alt. 3' splice site

Figure 2-3. *Sxl* alternative splicing and protein levels are disrupted in *Nab2*^{ex3} female heads. **(A) Top panel:** normal *Sxl* alternative splicing patterns across exon 2-4 and exon 8-10 regions in Female (F) and Male (M). **Bottom panel:** corresponding sequencing reads across the *Sxl* locus in the indicated sexes and genotypes. Dotted lines and boxed insets highlight exon 3 and exon 9 reads. **(B)** RT-PCR analysis of *Sxl* mRNA in control, *Nab2*^{ex3} and *Mettl3*^{null} Female (F) and Male (M) heads. Exon 2-3-4 and exon 2-4 bands indicated. Arrowhead denotes exon 2-3-intron-4 product noted in text. Asterisk (*) is non-specific product. **(C)** RT-qPCR analysis of *Sxl* transcripts in adult female, control *Nab2*^{ex3}*, and Mettl3*^{null} heads using the indicated primer sets. Asterisk indicates results that are statistically significant at p-value <0.05. **(D)** Immunoblot of protein samples from control, *Nab2*^{ex3}*,* and *Mettl3*^{null} female heads. Antibody against female-specific Sxl protein isoform was used to detect Sxl in each sample. Lamin serves as a loading control. Molecular weights are given in kDa and indicated to the left. **(E)** Quantification of Sxl protein levels in **D** using ImageLab software. Protein levels are normalized to control, with the value for control set to 1.0. Asterisk indicates results that are statistically significant at p-value <0.05. **(F)** RT-PCR analysis of *Sxl* mRNA in adult female control and *Nab2*^{ex3} tissues with exon 2-3-4 and 2-4 bands indicated. **(G)** RNA binding protein (RBP) motif enrichment analysis detects predicted Sxl binding sites as the most frequent motif among Nab2-regulated splicing events in female heads. Other enriched motifs are similar between male and female heads. Regions used for motif analysis (retained introns, and alternative 5' or 3' splice sites plus flanking sequence) are described in the text and illustrated in the schematic to the right.

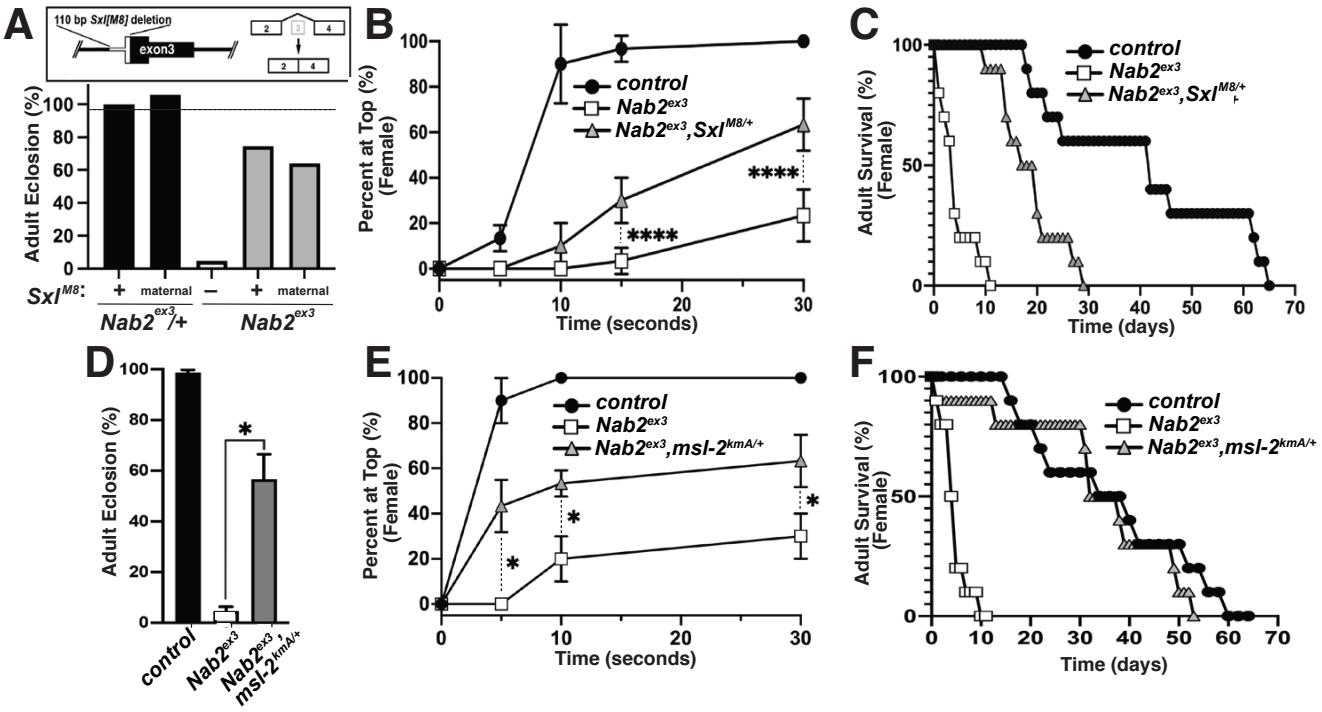

Figure 2-4. Alleles of *Sxl*^{M8} or the DCC component *male-specific lethal-2* (*msl-2*) rescues *Nab2* phenotypes. (A) A single copy of the *Sxl*^{M8} allele, which harbors a 110bp deletion that causes constitutive exon 2-4 splicing, partially suppresses lethality of *Nab2*^{ex3}, both zygotically and maternally (calculated as #observed/#expected). **(B-C)** *Sxl*^{M8} dominantly (i.e., *M8/+*) suppresses previously defined **(B)** locomotion (as assessed by negative-geotaxis) and **(C)** lifespan defects in age-matched *Nab2*^{ex3} females. **(D)** Percent of control, *Nab2*^{ex3}, or *msl-2*^{kmA}*/+;;Nab2*^{ex3} (*msl-2* is on the X chromosome) that eclose as viable adults (calculated as #observed/#expected). **(E-F)** *msl-2*^{kmA} dominantly (i.e., *kmA/+*) suppresses previously defined **(E)** locomotion (as assessed by negative-geotaxis) and **(F)** lifespan defects in age-matched *Nab2*^{ex3} females. Significance values are indicated (**p*<0.05, *****p*<0.0001).

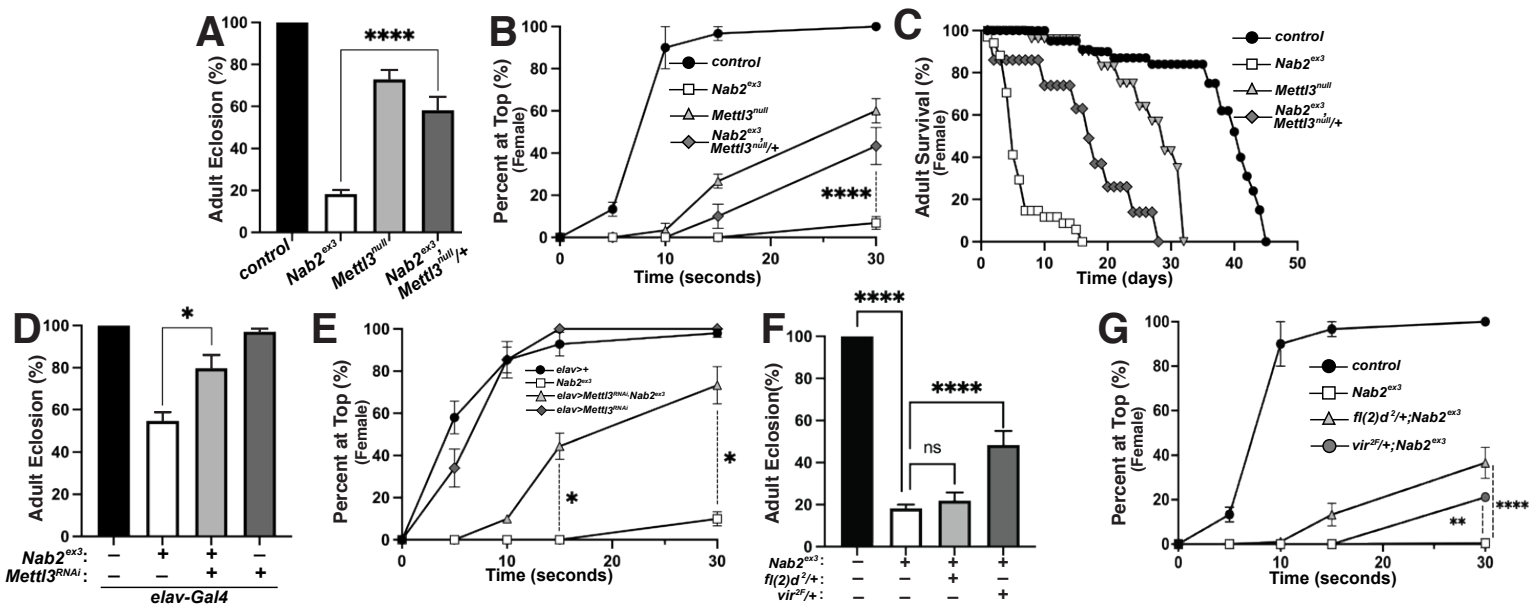

Figure 2-5. Reduction of the Mettl3 m^{6}A transferase suppresses viability and behavioral defects in *Nab2* mutant females. (A) Percent of control, *Nab2^{ex3}*, and *Nab2^{ex3},Mettl3$^{null/+}$* flies that eclose as viable adults (calculated as #observed/#expected). **(B)** Negative geotaxis of age-matched adult females of the indicated genotypes over time in seconds. **(C)** Survival of age-matched adult female flies of the indicated genotypes over time in days. **(D)** Percent of *elav>Gal4* alone control, *elav-Gal4;;Nab2^{ex3}*, *elav-Gal4;UAS-Mettl3-RNAi;Nab2^{ex3}*, and *elav-Gal4;UAS-Mettl3-RNAi* flies that eclose as viable adults (calculated as #observed/#expected). Note that baseline *Nab2^{ex3}* viability is elevated in the background of the *elav-Gal4* transgene, and significantly suppressed by inclusion of *UAS-Mettl3* RNAi. **(E)** Negative geotaxis assay for age-matched adult females of the indicated genotypes over time in seconds. **(F)** Percent of control, *Nab2^{ex3}*, *Nab2^{ex3},fl(2)d$^{2/+}$*, or *Nab2^{ex3},vir$^{2F/+}$* flies that eclose as viable adults (calculated as #observed/#expected). **(G)** Negative geotaxis of age-matched adult females of the indicated genotypes over time in seconds. Significance values are indicated (*p<0.05, **p<0.01,****p<0.0001).

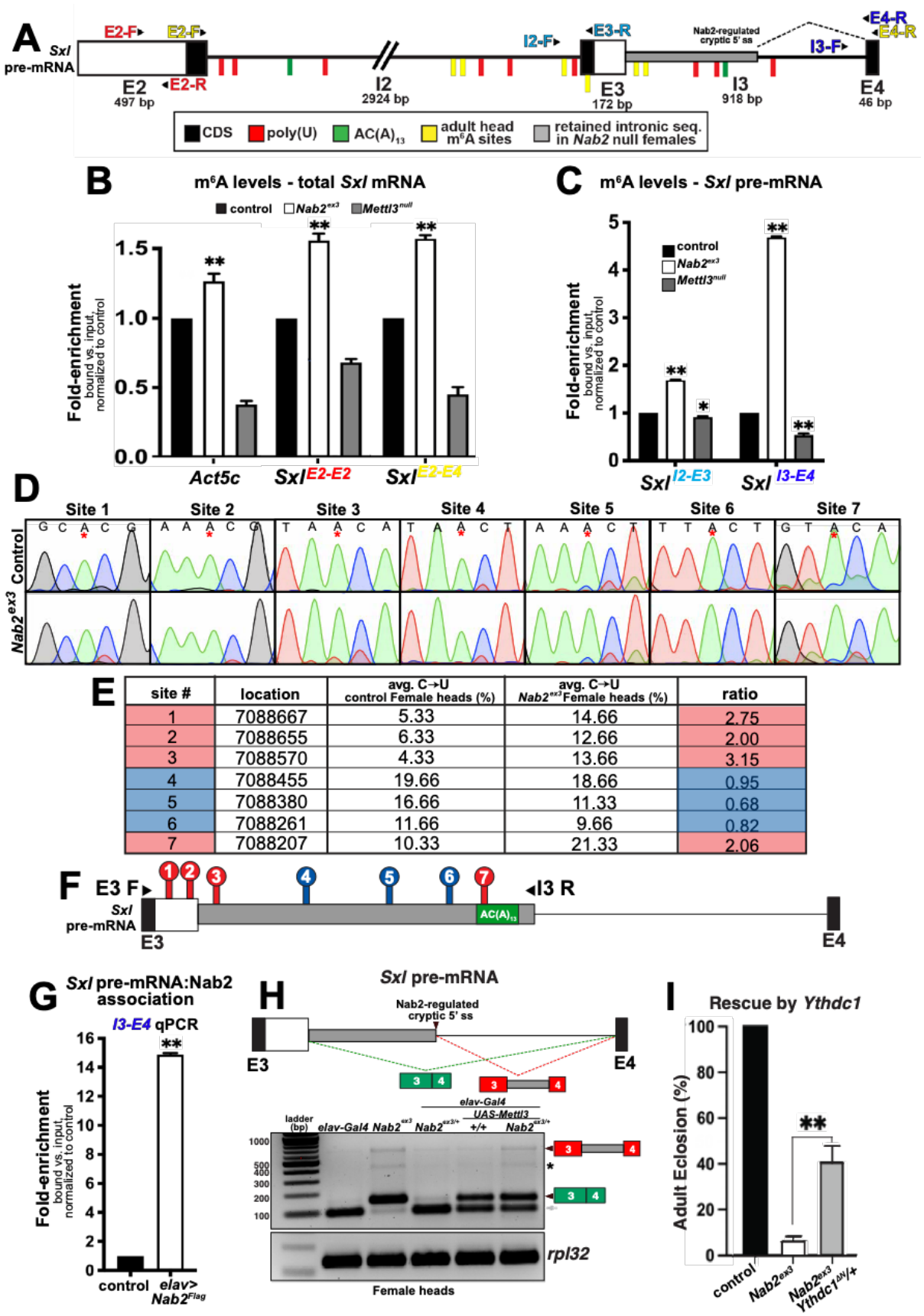
A
Sxl pre-mRNA
E2-F
E2-F
E2-R
E2
497 bp
I2
2924 bp
I2-F
E3-R
E3
172 bp
Nab2-regulated cryptic 5' ss
I3
918 bp
I3-F
E4-R
E4-R
E4
46 bp
CDS
poly(U)
AC(A)13
adult head m6A sites
retained intronic seq. in Nab2 null females
B
m6A levels - total Sxl mRNA
control
Nab2ex3
Mettl3null
Fold-enrichment
bound vs. input, normalized to control
Act5c
Sxl E2-E2
Sxl E2-E4
C
m6A levels - Sxl pre-mRNA
control
Nab2ex3
Mettl3null
Fold-enrichment
bound vs. input, normalized to control
Sxl I2-E3
Sxl I3-E4
D
Site 1
Site 2
Site 3
Site 4
Site 5
Site 6
Site 7
Control
Nab2ex3
E
site #
location
avg. C→U control Female heads (%)
avg. C→U Nab2ex3 Female heads (%)
ratio
1 7088667 5.33 14.66 2.75
2 7088655 6.33 12.66 2.00
3 7088570 4.33 13.66 3.15
4 7088455 19.66 18.66 0.95
5 7088380 16.66 11.33 0.68
6 7088261 11.66 9.66 0.82
7 7088207 10.33 21.33 2.06
F
E3 F
I3 R
Sxl pre-mRNA
E3
E4
AC(A)13
G
Sxl pre-mRNA:Nab2 association
I3-E4 qPCR
Fold-enrichment
bound vs. input, normalized to control
control
elav> Nab2Flag
H
Sxl pre-mRNA
Nab2-regulated cryptic 5' ss
E3
E4
elav-Gal4
UAS-Mettl3
ladder (bp)
elav-Gal4
Nab2ex3
Nab2ex3/+
+/+
Nab2ex3/+
rpl32
Female heads
I
Rescue by Ythdc1
Adult Eclosion (%)
control
Nab2ex3
Nab2ex3 Ythdc1Δ9/+

Figure 2-6. Nab2 associates with the *Sxl* mRNA and inhibits its m^{6}A methylation (A) Diagram of exons (E2,E3,E4) and introns (I2 and I3) of the *Sxl* pre-mRNA annotated to show coding sequence (CDS; black), the retained intronic region in *Nab2^{ex3}* female (grey), and location of color-coded primer pairs (E2-F(orward) and E2-R(everse), E2-F and E4-R, I2-F and E3-R, I3-F and E4-R), poly(U) sites (red lines), AC(A)$_{13}$ site (green line), and mapped m^{6}A positions in *Drosophila* heads (yellow lines) (Kan et al. 2021). **(B)** RT-qPCR analysis of *Act5c* and *Sxl* mRNA present in anti-m^{6}A precipitates of control (*control*; black), *Nab2^{ex3}* (white), or *Mettl3^{null}* (grey) female heads. The position of *Sxl* primer pairs is indicated (E2-F+E2-R and E2-F+E4-R). **(C)** Similar analysis as in (**B)** using I2-F+E3-R and I3-F+E4-R primer pairs to detect unspliced *Sxl* transcripts in anti-m^{6}A precipitates of control (black), *Nab2^{ex3}* (white), or *Mettl3^{null}* female heads. **(D)** Sanger sequencing traces showing C-to-U editing adjacent to m^{6}A sites in control and *Nab2^{ex3}* female head RNA samples subjected to DART-sanger sequencing [372] within the retained intronic region of *Sxl* pre-mRNA. m^{6}A sites are indicated by red asterisks. **(E)** Table of the m^{6}A sites (red=hypermethylated in *Nab2^{ex3}*, blue=no change in *Nab2^{ex3}*) mapped by DART-sanger sequencing in (**D)** with the corresponding location (dm6), average C-to-U editing fraction (%), and ratio of C-to-U editing for *Nab2^{ex3}* to control female head samples. Data are representative of three biological replicates. **(F)** Schematic showing the location of the m^{6}A sites mapped by DART within exons (E3 and E4) and intron 3 of *Sxl* pre-mRNA. Site numbering corresponds to numbering in **(E). (G)** RT-qPCR analysis with the I3-F+E4-R primer pair in **(A)** from anti-Flag precipitates of control and *elav-Gal4,UAS-Nab2:Flag* female heads. **(H)** Top: Schematic of the exon3-exon4 region of *Sxl* mRNA showing the intron region retained in *Nab2^{ex3}* (grey fill) and the normal exon 3-exon 4 splicing product (green fill) and the aberrant exon 3-intron 3^{503}-exon 4 (red-grey fill). Bottom: RT-PCR analysis of *Sxl* using the E3-E4 primer pair and RNAs harvested from female heads of the indicated genotypes: *elav-Gal4* alone, *elav-Gal4+Nab2$^{ex3/+}$*, *Nab2^{ex3}* mutant, *Nab2^{ex3}*/+, *UAS-Mettl3* alone, or *elav>Mettl3+Nab2$^{ex3/+}$*. Arrowheads denote exon3-exon4 and exon3-intron3^{503}-exon4 bands are indicated. Small grey arrow indicates Nab2-dependent splice variant. Asterisk marks a non-specific band. **(I)** Percent of control, *Nab2^{ex3}*, or *Nab2^{ex3};Ythdc1$^{\Delta N}$*/+ flies that eclose as viable adults (calculated as # observed/# expected).

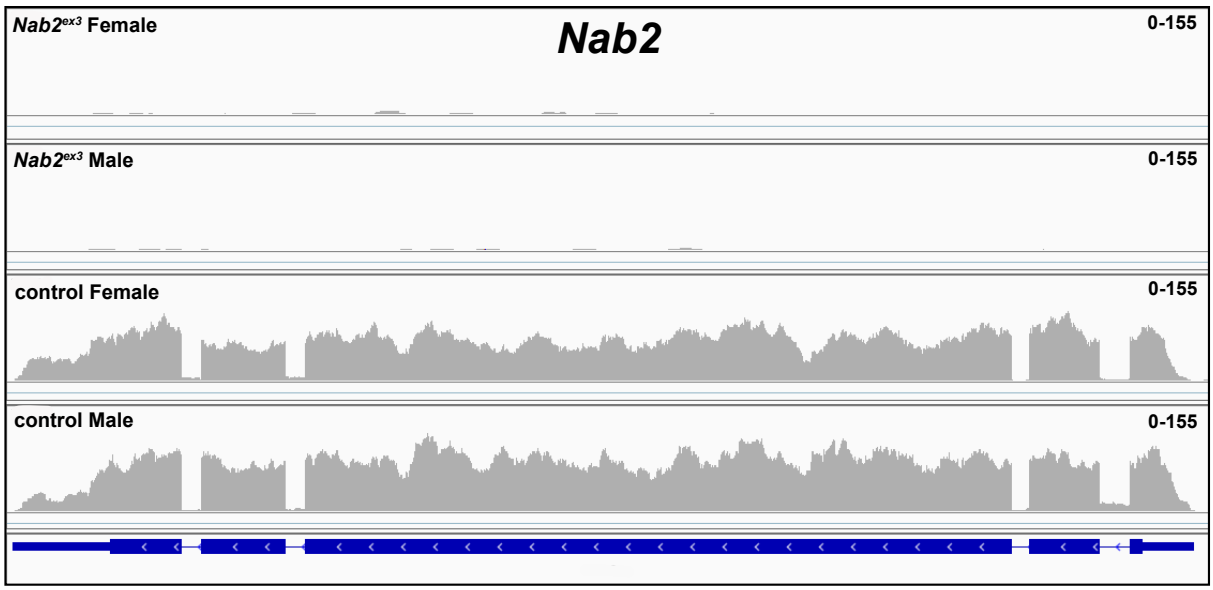

Supplemental Figure 2-1 RNA sequencing reads across the *Nab2* locus. IGV image of RNA sequencing reads across the *Nab2* locus in *Nab2*^{ex3} (top tracks) and control (*Nab2*^{pex41}) adult female and male heads. Intron-exon structure is indicated at bottom. Read depth scale is indicated (0-155).

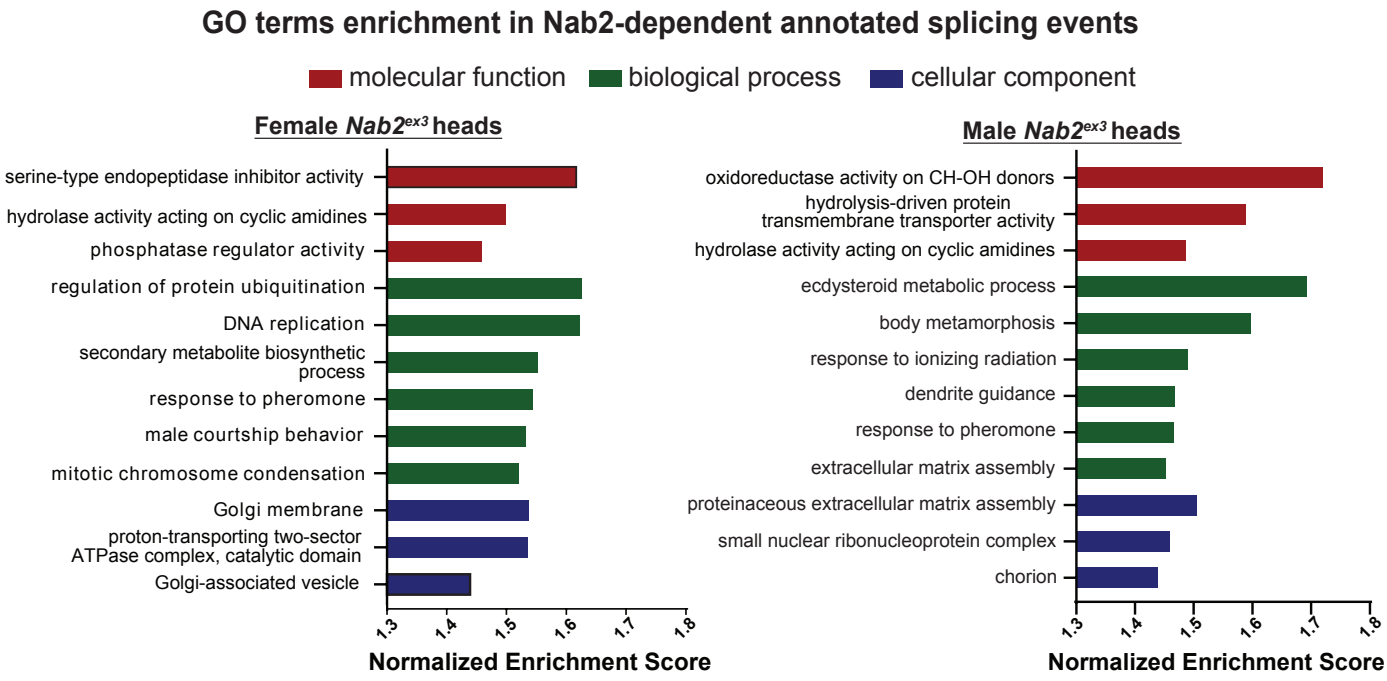

Supplemental Figure 2-2 GO term enrichment among Nab2-regulated alternative splicing events. Chart illustrating gene ontology (GO) terms enriched in the 'molecular function', 'biological process' and 'cellular component' categories among altered alternative splicing events detected by MISO in female and male *Nab2*^{ex3} head RNAs.

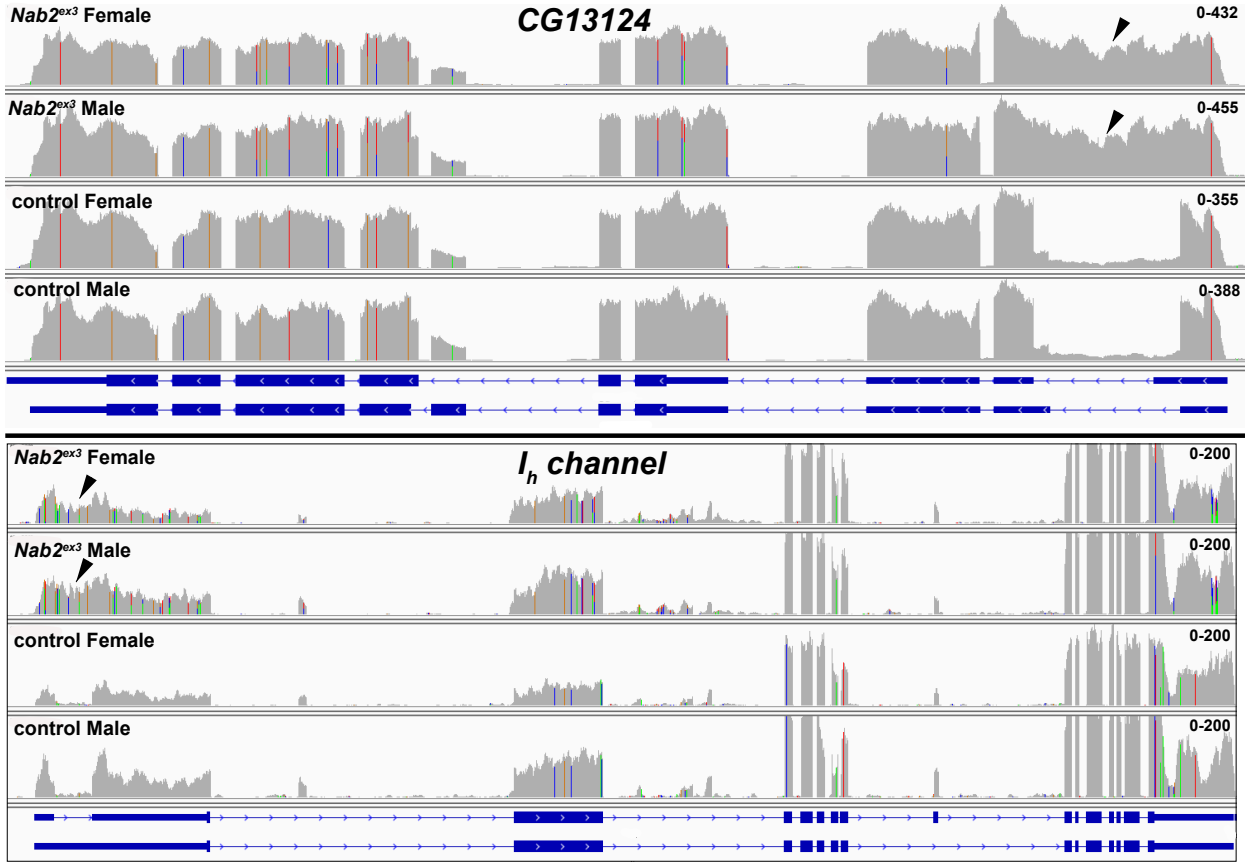

Supplemental Figure 2-3. RNA sequencing reads across the *CG13124* and I_h *channel* loci. IGV images of RNA sequencing reads across *CG13124* and I_h *channel* in $Nab2^{ex3}$ (top tracks) and control ($Nab2^{pex41}$) adult female and male heads. Intron-exon structure is indicated at bottom. Read depth scales are indicated. Arrowheads indicate reads across the first intron of each gene. Also related to data displayed in Table 1.

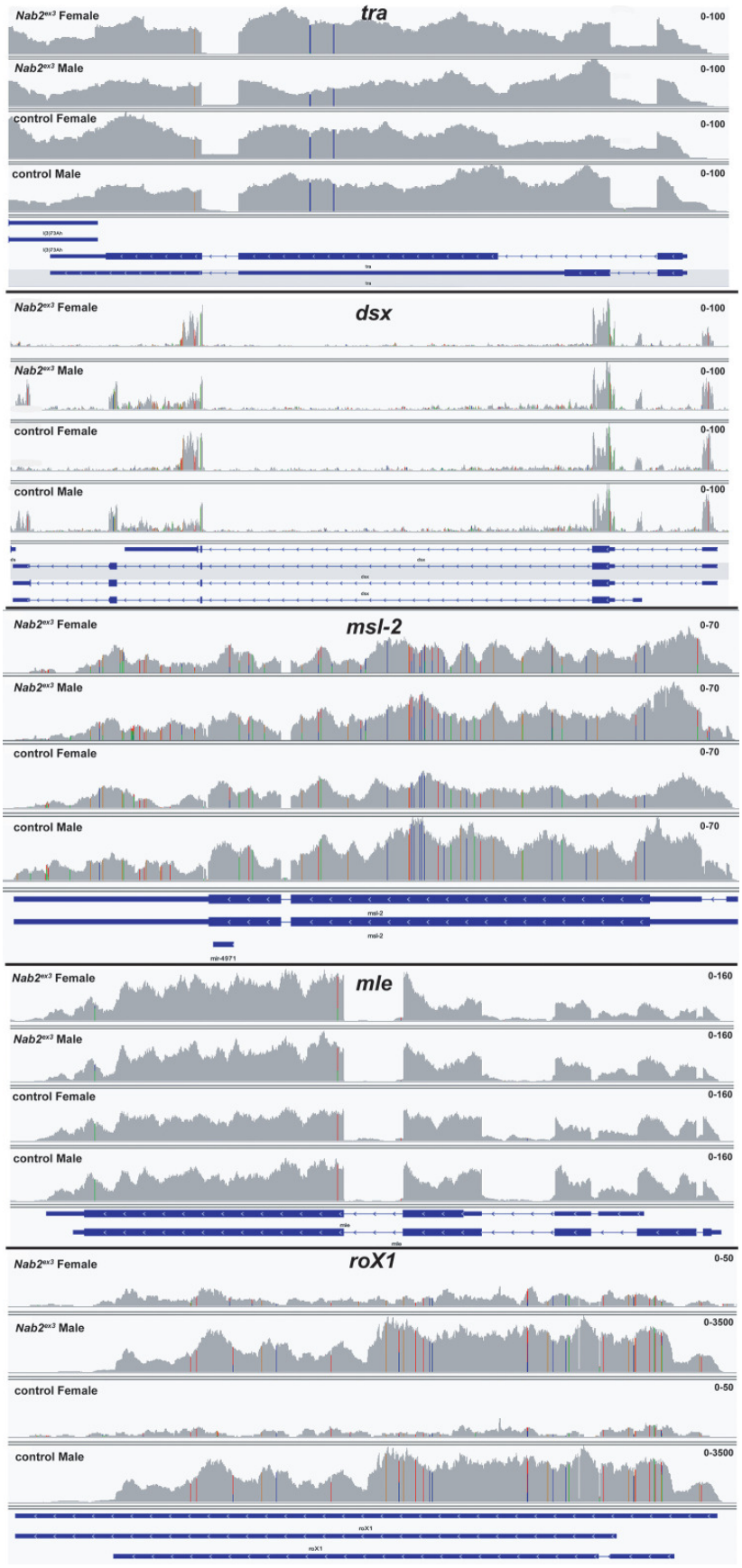
tra
Nab2ex3 Female
0-100
Nab2ex3 Male
0-100
control Female
0-100
control Male
0-100
dsx
Nab2ex3 Female
0-100
Nab2ex3 Male
0-100
control Female
0-100
control Male
0-100
msl-2
Nab2ex3 Female
0-70
Nab2ex3 Male
0-70
control Female
0-70
control Male
0-70
mle
Nab2ex3 Female
0-160
Nab2ex3 Male
0-160
control Female
0-160
control Male
0-160
roX1
Nab2ex3 Female
0-50
Nab2ex3 Male
0-3500
control Female
0-50
control Male
0-3500

Supplemental Figure 2-4 RNA sequencing reads across the *tra* and *dsx* loci. IGV images of RNA sequencing reads across *tra*, *dsx*, *msl-2*, *mle* and *roX1* in *Nab2*^{ex3} (top tracks) and control (*Nab2*^{pex41}) adult female and male heads. Intron-exon structure is indicated at bottom. Read depth scales are indicated.

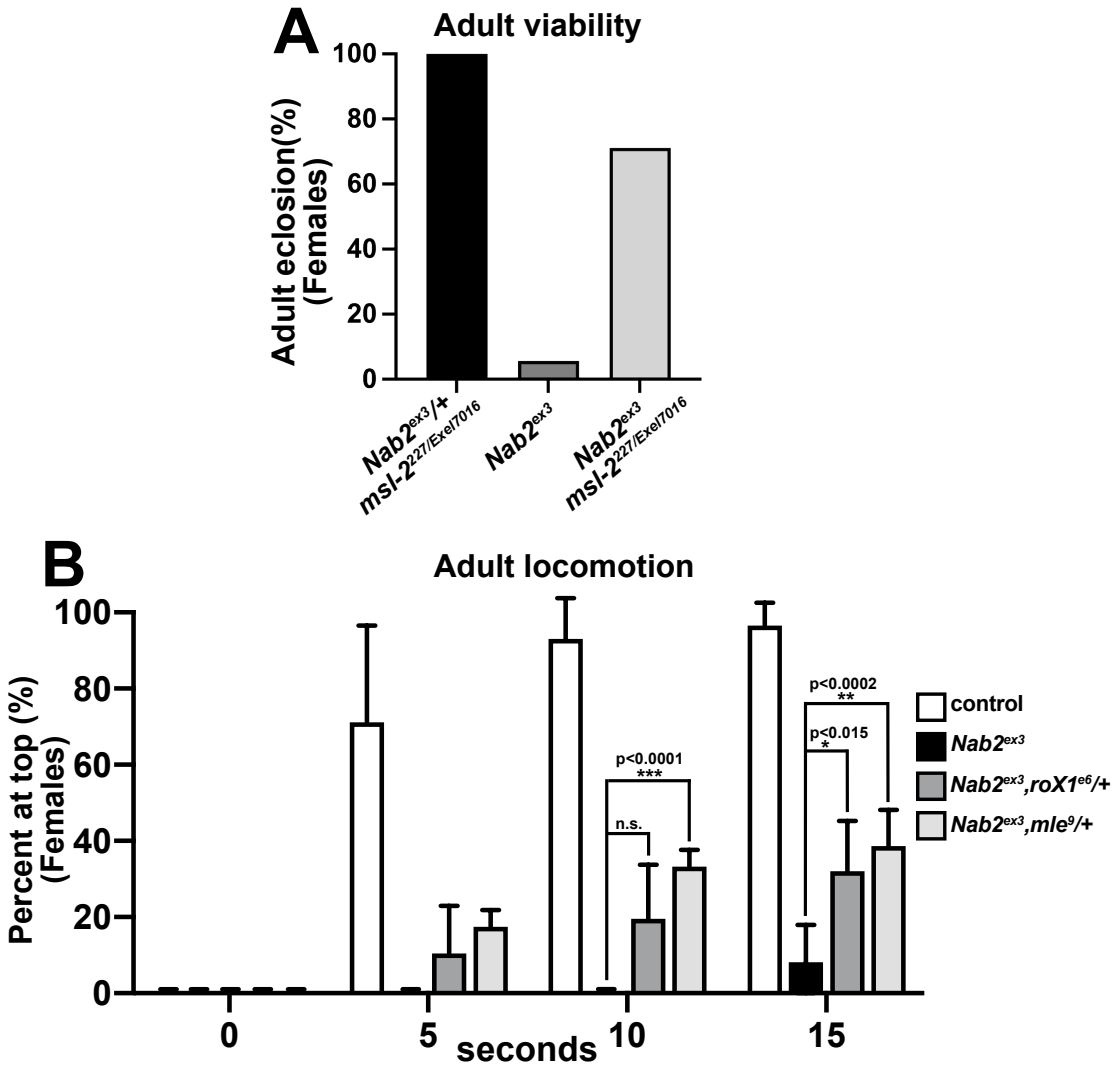

Supplemental Figure 2-5 Additional genetic interactions between *Nab2^{ex3}* *msl-2*, *roX1*, and *mle* (A) Adult viability of control females (**black** bar) with one copy of *Nab2^{ex3}* in a *msl-2* deficient background (*msl-2^{227}* truncating allele over *Exel7016* deletion), females lacking Nab2 (*Nab2^{ex3}*, **dark grey** bar), or *Nab2^{ex3}* mutant females in *msl-2^{227}/Exel7016* background (**light grey** bar). **(B)** Negative geotaxis of age-matched adult female controls (*Nab2^{pex41}*), *Nab2^{ex3}* mutants, or *Nab2^{ex3}* mutants carrying single copies of the *roX1^{e6}* or *mle^{9}* loss-of-function alleles at 5sec, 10sec, and 15 sec timepoints. Significance values between indicated groups are indicated at the 30sec timepoint (p-values are indicated; n.s.=not significant).

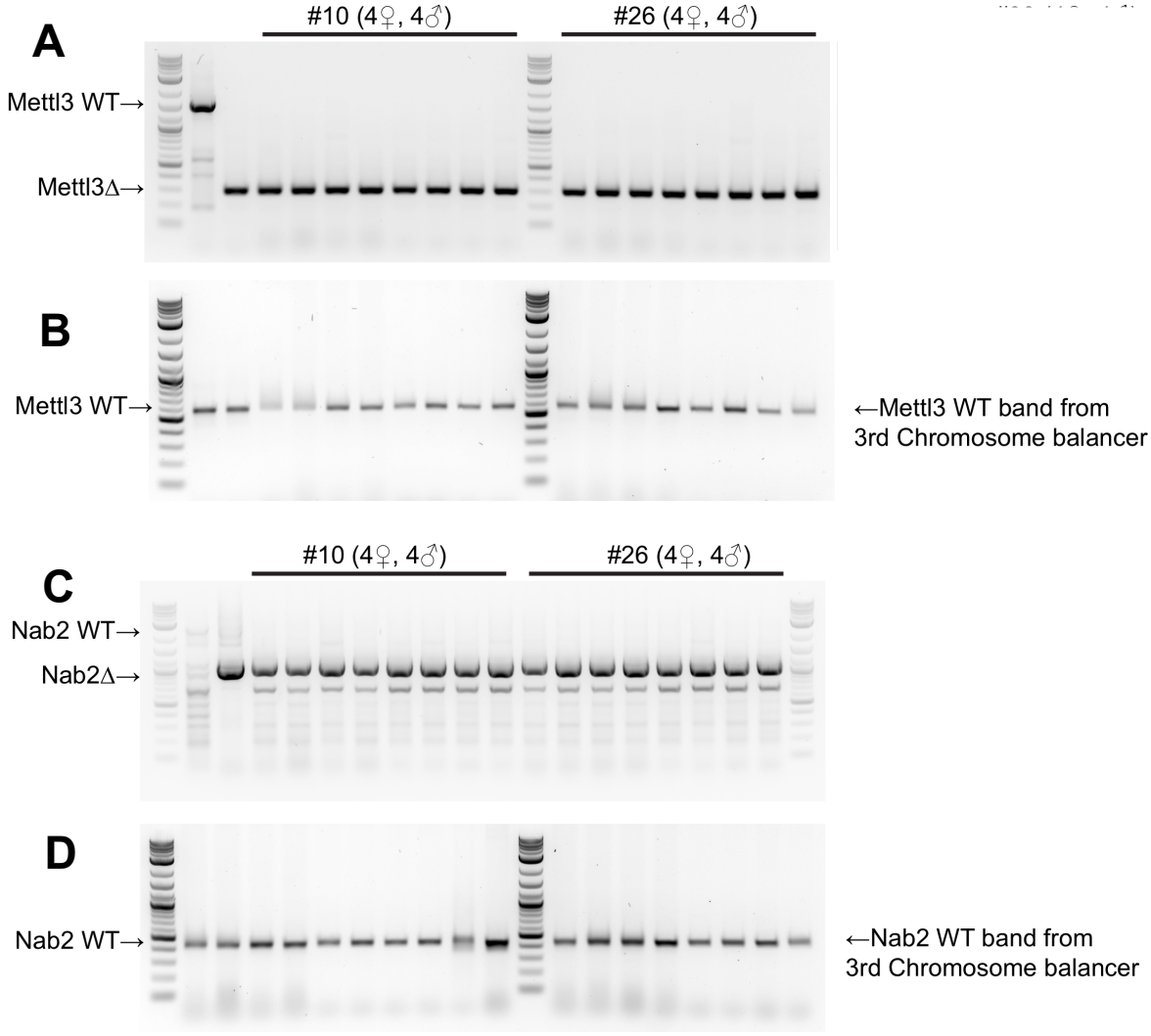

Supplemental Figure 2-6 Genomic PCR confirms the *Nab2^{ex3},Mettl3^{null}* recombinant
Genomic PCR of two different isolates (#10, #26) of the *Mettl3^{null},Nab2^{ex3}* double mutant chromosome balanced over *TM6B*. **(A)** and **(C)** show PCR products generated from each isolate using primers that flank the deletions in each gene; the normal wt product from *TM6B* and truncated products (Δ) are indicated. **(B)** and **(D)** show PCR products generated from each isolate using primers that lie within the deleted regions of each gene; the wt products from *TM6B* are indicated. Numbers of adults used for extraction of gDNA is indicated

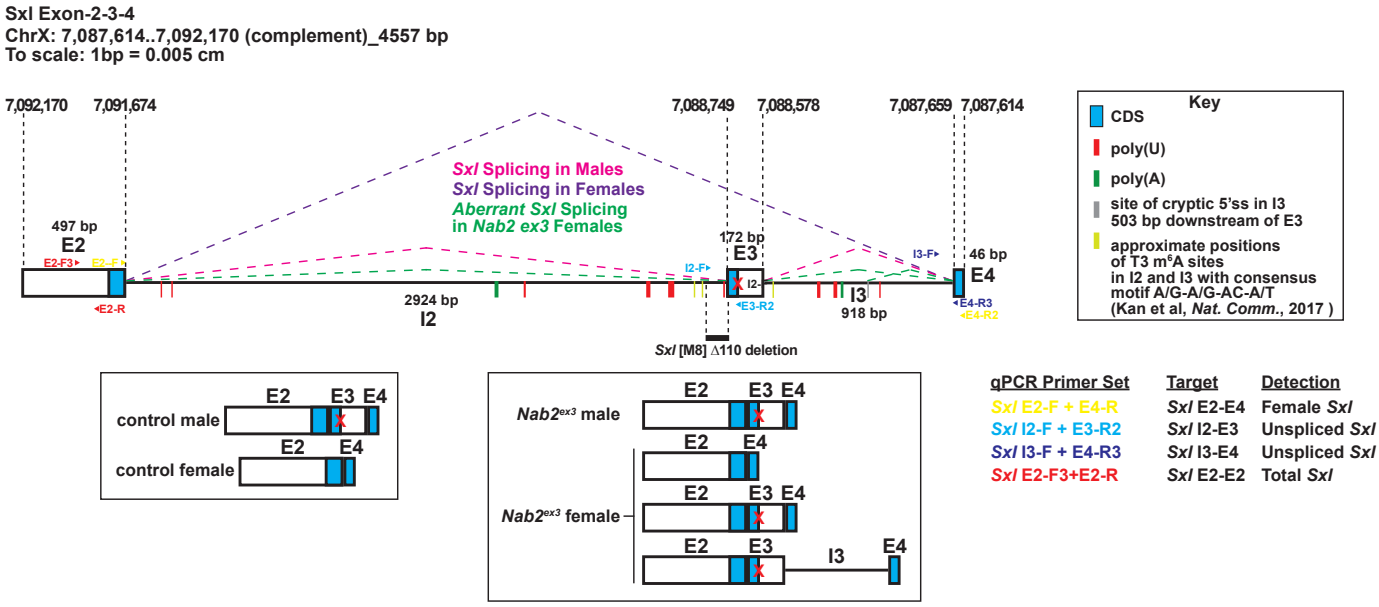

Supplemental Figure 2-7. Detailed schematic of the exon 2-3-4 *Sxl* locus with annotated locations of introns and exons annotated to show coding sequence (CDS; blue), the retained intronic region in *Nab2*^{ex3} females (grey), and locations of color-coded primer pairs (E2-F and E2-R, E2-F and E4-R, I2-F and E3-R, I3-F and E4-R), poly(U) sites red lines, poly(A) sites green lines, and mapped m^{6}A locations in *Drosophila* embryos yellow lines [288]. Colored dotted lines indicated sex-specific splicing in wildtype adults and the altered splicing documented in this study. Boxed areas below summarize exon-intron structure in wild type heads and *Nab2*^{ex3} heads. Base pair coordinates are indicated (Dm Release 6).

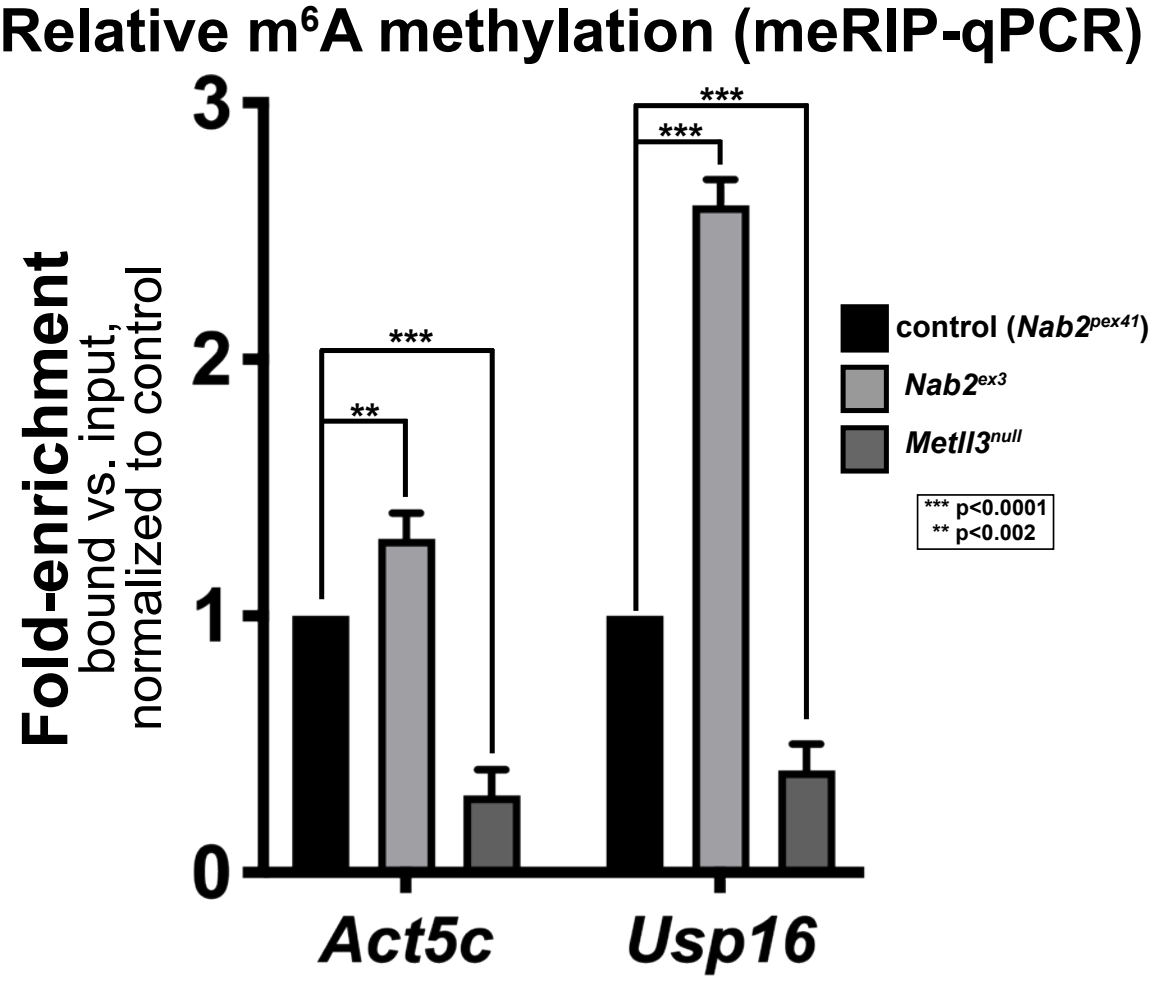

Supplemental Figure 2-9 figure supplement 2. Nab2 limits m^{6}A methylation of additional RNAs Quantitative real-time PCR analysis of *Act5c* and *Usp16* mRNAs present in anti-m^{6}A precipitates of control (*Nab2*^{pex41}; black), *Nab2*^{ex3} (grey), *Mettl3*^{null} (dark grey) adult female heads. 1-day old female heads were used in three biological replicates, and data represent bound vs. input ratios normalized to control (*Nab2*^{pex41}). p-values are indicated (n.s.=not significant).

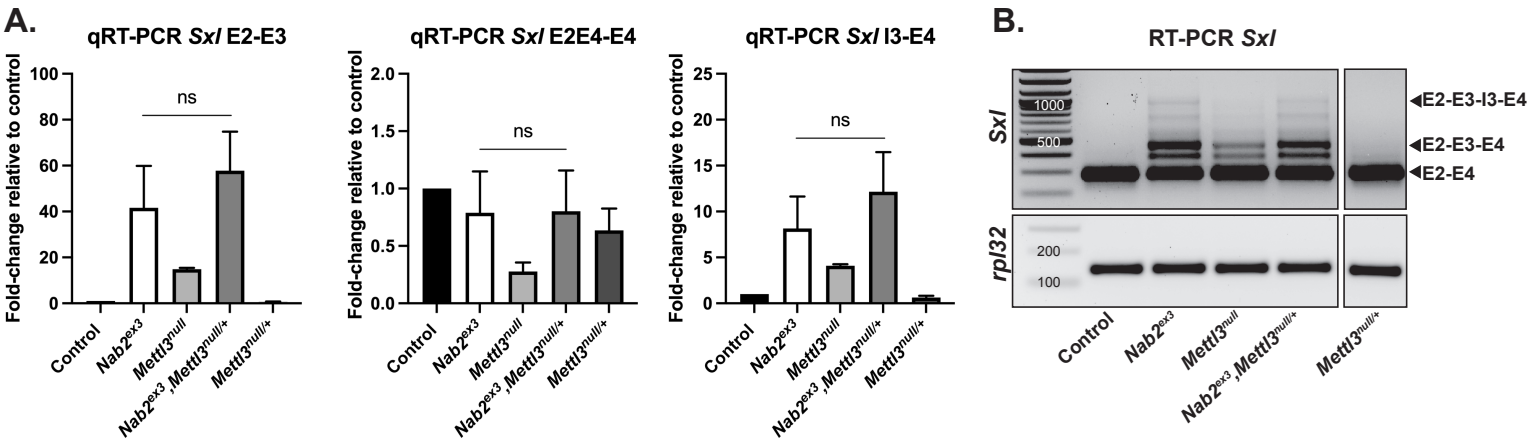

Supplemental Figure 2-10 Heterozygosity for Mettl3 does not alter *Sxl* splicing in *control* or *Nab2^{ex3}* mutant female heads. (A) qRT-PCR analysis of RNAs harvested from adult female heads of the indicated genotypes with primers that amplify spliced *Sxl* exon 2-exon 3 (E2-E3) or exon 3- exon 4 (E3E4-E4). The E3E4 primer spans the exon 3-exon 4 junction. Fold-change is calculated relative to 'control' (*Nab2^{pex41}*) and normalized to CT values of *Act5c*. *ns* = not specific. **(B)** Semi-quantitative RT-PCR analysis of *Sxl* (top) or control *RpL32* (bottom) in adult female head RNA of the indicated genotypes. *Sxl* was analyzed with a E2-E4 primer pair that detects *Sxl* RNAs indicated by arrowheads. Genotypes and nt size ladder are indicated.

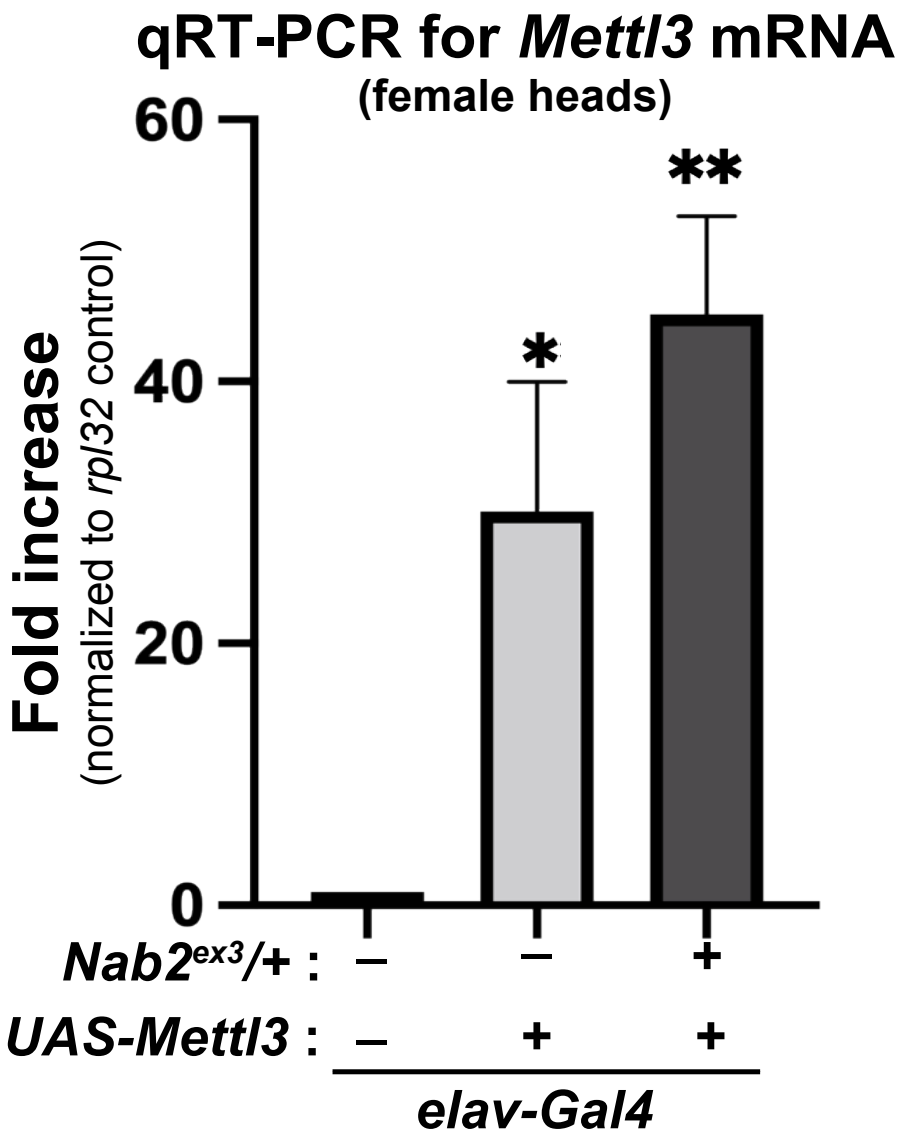

Supplemental Figure 2-11 Neuronal overexpression of *Mettl3* RNA using the Gal4/UAS system. qRT-PCR analysis of *Mettl3* RNA levels in heads of control w^{1118} (lane 1), or *Mettl3* overexpressing (*elav-Gal4,UAS-Mettl3)* adult females in the absence (lane2) or presence (lane 3) of a single $Nab2^{ex3}$ allele. *p*-values ∗<0.05, ∗∗<0.005

CHAPTER 3: The RNA binding protein Nab2 regulates levels of the RhoGEF Trio to govern axon and dendrite morphology

Carly L. Lancaster[1,2,3], Pranav S. Yalamanchili[1,2], Jordan N. Goldy[1,2,3], Sara W. Leung[1], Anita H. Corbett[1]*, and Kenneth H. Moberg[2]*

[1] Department of Biology, Emory College of Arts and Sciences, Atlanta, Georgia, USA
[2] Department of Cell Biology Emory University School of Medicine
[3] Graduate Program in Biochemistry, Cell and Developmental Biology, Emory University

Running Title: Nab2 regulates Trio levels

Abbreviations: RNA binding protein (RBP), polyadenosine binding protein (Pab), zinc finger Cys-Cys-Cys His type containing 14 (ZC3H14), nuclear polyadenosine RNA binding protein 2 (Nab2), guanine nucleotide exchange factor (GEF)

This chapter has been excerpted from a manuscript published in *MBoC*:
Lancaster CL, Yalamanchili PS, Goldy JN, Leung SW, Corbett AH, Moberg KH. The RNA-binding protein Nab2 regulates levels of the RhoGEF Trio to govern axon and dendrite morphology. Mol Biol Cell. 2024 Aug 1;35(8):ar109. doi: 10.1091/mbc.E24-04-0150. Epub 2024 Jul 10.

*For correspondence:
acorbe2@emory.edu
Emory College of Arts and Sciences, Department of Biology
1510 Clifton Rd, Atlanta, GA 30322

*For correspondence:
kmoberg@emory.edu
Emory University School of Medicine, Department of Cell Biology
615 Michael St, Atlanta, GA, 30322

ABSTRACT

The *Drosophila* RNA binding protein (RBP) Nab2 acts in neurons to regulate neurodevelopment and is orthologous to the human intellectual disability-linked RBP, ZC3H14. Nab2 governs axon projection in mushroom body neurons and limits dendritic arborization of class IV sensory neurons in part by regulating splicing events in ~150 mRNAs. Analysis of the *Sex-lethal* (*Sxl*) mRNA revealed that Nab2 promotes an exon-skipping event and regulates m^6A methylation on *Sxl* pre-mRNA by the Mettl3 methyltransferase. Mettl3 heterozygosity broadly rescues $Nab2^{null}$ phenotypes implying that Nab2 acts through similar mechanisms on other RNAs, including unidentified targets involved in neurodevelopment. Here, we show that Nab2 and Mettl3 regulate the removal of a 5'UTR intron in the *trio* pre-mRNA. Trio utilizes two GEF domains to balance Rac and RhoGTPase activity. Intriguingly, an isoform of Trio containing only the RhoGEF domain, GEF2, is depleted in $Nab2^{null}$ nervous tissue. Expression of Trio-GEF2 rescues projection defects in $Nab2^{null}$ axons and dendrites, while the GEF1 Rac1-regulatory domain exacerbates these defects, suggesting Nab2-mediated regulation Trio-GEF activities. Collectively, these data indicate that Nab2-regulated processing of *trio* is critical for balancing Trio-GEF1 and -GEF2 activity and show that Nab2, Mettl3, and Trio function in a common pathway that shapes axon and dendrite morphology.

Significance Statement

- *Drosophila* Nab2, ortholog of the human RBP ZC3H14 lost in inherited intellectual disability, acts through unknown RNA targets to control axon and dendrite morphology.

- This study shows that Nab2 and the Mettl3 methyltransferase guide splicing of *trio* mRNA, which encodes a conserved GEF-domain protein. Loss of Nab2 is associated with an imbalance in levels of Trio GEF domains in Nab2-deficient neurons. Restoring this balance partially rescues neuronal defects.

- These findings suggest that Nab2 control of Trio levels is required to pattern axon and dendrite growth and suggests that ZC3H14 may play a similar role in the vertebrate brain.

INTRODUCTION

RNA binding proteins (RBPs) associate with nascent RNA transcripts and govern expression via a multitude of mechanisms, including regulation of splicing, polyadenylation, nuclear export, translation, and stability [6,400-402]. These RNA-RBP interactions are particularly important in highly specialized cells such as neurons which require fine-tuned spatiotemporal control of gene expression to ensure proper development and function of the nervous system [167,244,334,403,404]. The importance of RBP function in neurons is highlighted by the prevalence of neurodevelopmental diseases that have been linked to defects in RBPs, leading to aberrant processing of RNAs encoding neurodevelopment factors [163,215,244,335,403,405-407]. Intriguingly, many of these RBPs are ubiquitously expressed and have roles in relatively common RNA processing mechanisms [408-413]. Therefore, defining roles for these RBPs in neurons has become key to understanding why they are linked to neurological disease.

One important family of post-transcriptional regulatory proteins consists of polyadenosine binding proteins (Pabs) [264]. Conventional Pab family members bind polyadenosine RNA via RNA recognition motifs (RRMs) and modulate a multitude of RNA processing events such as splicing, export, polyadenylation, translation, and stability [174,414,415]. Another less well-studied group of Pabs utilize zinc finger (ZnF) domains to bind specific RNA motifs and modulate downstream processing events [259,264,279]. One such ZnF Pab termed zinc finger Cys-Cys-Cys-His-type containing 14 (ZC3H14; also termed MSUT2) is expressed ubiquitously and binds tracts of polyadenosine RNA with high affinity via tandem ZnF domains [245,259,264,279,416]. Despite ubiquitous expression, mutations in human *ZC3H14* cause a form of inherited non-syndromic autosomal recessive

intellectual disability, which implies a specific requirement for ZC3H14 in the developing brain [215,332].

The ZC3H14 protein is evolutionarily conserved among eukaryotes and has been studied in *Mus musculus* (*Zc3h14*) [215,251,273], *Caenorhabditis elegans* (*sut-2*) [252], *Sacchromyces cerevisiae* (Nab2) [255-259,264,273,417], *Sacchromyces pombe* (Nab2) [418], and *Drosophila melanogaster* (Nab2) [215,Jalloh and Lancaster et al., [274,280-282,284,337,419]. These studies have collectively uncovered molecular and neuronal functions for this conserved ZnF Pab. For example, *Zc3h14* loss impairs working memory in mice where ZC3H14 protein localizes to synaptosomes in hippocampal neurons and regulates the abundance of synaptic proteins, including CaMK2α [420,421]. Moreover, studies in *C. elegans* identified SUT-2 as a modulator of Tau-induced toxicity, as loss of *sut-2* robustly rescues the toxic consequences of Tau overexpression in worms [252,422], a function of ZC3H14/MSUT2 that extends to mice [423]. On the other hand, yeast *NAB2* is essential for viability [255] and has critical functions in regulating transcription termination [424], nuclear export [258], and transcript stability [337,417,424,425]. Moreover, *NAB2/Nab2* loss leads to increases in bulk poly(A) tail length in yeast, mice, and flies supporting a conserved function for Nab2 in restricting poly(A) tail length [257,258,264,279]. Taken together, these findings suggest that ZC3H14/Nab2 is involved in multiple aspects of post-transcriptional RNA metabolism and that these roles may be particularly significant in neurons.

Drosophila melanogaster is a genetically tractable system in which to define molecular and developmental roles of the ZC3H14 invertebrate homolog, Nab2 [215]. Our prior studies have determined that Nab2 function is necessary in neurons, as pan-neuronal expression of *Drosophila* Nab2 or human ZC3H14 is sufficient to rescue viability

and locomotor defects associated with zygotic loss of Nab2 [215,279]. Moreover, Nab2 has a cell-autonomous role in Kenyon cells to pattern axonal projections from these cells into the mushroom bodies [284], a twin neuropil structure that regulates *Drosophila* associative olfactory learning and memory [339,426-428]. Biochemical studies show that Nab2 interacts with Fmr1, the fly homolog of Fragile X Syndrome RBP, FMRP [275], and that these two RBPs co-regulate mushroom body morphology and olfactory memory through a mechanism likely to involve translational repression of shared Nab2-Fmr1 target RNAs [278]. Beyond the brain, Nab2 limits dendritic branching of class IV dorsal dendritic arborization (ddaC) sensory neurons through a mechanism involving the planar cell polarity (PCP) pathway [281], suggesting that Nab2 controls RNA targets encoding regulators of the actin cytoskeleton. Our recent work studying the effect of Nab2 loss on the brain transcriptome revealed that Nab2 is required for proper splicing of ~150 mRNAs Jalloh and Lancaster et al., [274]. Furthermore, Nab2 limits methylation at the N-6 position of adenosine (m^6A) on key mRNAs, including the alternatively spliced *Sex-lethal* (*Sxl*) transcript Jalloh and Lancaster et al., [274]. However, Nab2-regulated transcripts encoding factors that guide axon and dendrite morphology have not been identified.

A recent study uncovered multiple Nab2-regulated candidate transcripts with key functions in neurodevelopment Jalloh and Lancaster et al., [274]. Specifically, this work revealed significant retention of a 5'UTR intron in the *trio* transcript. Trio is a member of the Dbl homology (DH) family of guanine nucleotide exchange factor (GEF) proteins with well-conserved orthologues in *C. elegans* and mammals that control F-actin polymerization through the Rac and Rho small GTPases [*305,308,313,314,316,330,331,429-432*]. As a result of these roles, Trio loss affects axon guidance and dendritic branching as well as

synaptic transmission and plasticity [305,306,320,430,433]. Notably, *Drosophila* Trio is enriched in the brain mushroom bodies where it controls axon projection and Trio also regulates arborization of sensory ddaC neurons in the larval peripheral nervous system (PNS) [313,320,434]. Moreover, several recent studies have identified loss- and gain-of-function mutations in the human *TRIO* gene and its paralogue *KALRN* that lead to genetically dominant forms of intellectual disability and neurodevelopmental disease [305,307,308,431].

Trio contains two GEF domains, GEF1 and GEF2, that differentially activate Rac1 or RhoA/Rho1 GTPases, respectively [309,432,435]. Trio-GEF1 activation of Rac1 regulates motor neuron axon guidance, cell migration and axon outgrowth [316,330,430,436,437]. Comparatively, little is known about the function of Trio-GEF2; however, recent work suggests that it promotes growth cone collapse through RhoA/Rho1 [429]. Supporting this model of opposing roles for Trio GEF1 and GEF2 function, studies in *Drosophila* ddaC neurons suggest that Trio promotes dendritic branching via GEF1 and restricts this process via GEF2 [320]. Despite insight into Trio GEF specificity for Rac and RhoA/Rho1, how these two opposing Trio activities are modulated within axons and dendrites remains unclear.

Here, we exploit both genetic and molecular approaches to assess the role of Nab2 and the m^{6}A machinery in regulating expression of the neuronally enriched protein Trio in the adult fly brain. Consistent with our previous findings that Nab2 limits m^{6}A methylation on specific transcripts, reduced levels of either *Drosophila* m^{6}A reader protein – the nuclear reader Yt521-B or the cytoplasmic reader Ythdf – is sufficient to rescue *Nab2^{null}* viability and locomotion defects, indicating that m^{6}A-mediated changes in RNA nuclear processing and cytoplasmic metabolism contribute to defects in Nab2 mutants. Focusing

on the *trio* mRNA, we find that Nab2 and the m^{6}A methyltransferase, Mettl3, each promote an intron-excision event within the 5'UTR of a *trio* mRNA species encoding only the GEF2 (RhoGEF) domain. Intriguingly, levels of the corresponding Trio-GEF2 protein drop in heads of *Nab2^{null}* but not *Mettl3^{null}* flies, consistent with a model in which Nab2 modulates both nuclear splicing and cytoplasmic metabolism of the GEF2-only variant of *trio* mRNA. Critically transgenic expression of Trio-GEF2 rescues axon projection defects in *Nab2^{null}* mushroom body neurons and class IV ddaC neurons while Trio-GEF1 has the opposite effect of exacerbating *Nab2^{null}* axon projection defects. Together, these data identify Nab2 and Mettl3 as key regulators of *trio* 5'UTR structure and provide evidence that altered expression of Trio-GEF2 contributes to axon and dendrite defects in *Drosophila* lacking Nab2.

RESULTS

Loss of m^{6}A-reader proteins rescues *Nab2^{null}* defects in viability and adult locomotion

Nab2 loss causes severe defects in *Drosophila* viability, adult locomotion, and lifespan [215]. Building on the previous finding that Nab2 loss elevates m^{6}A methylation on select mRNAs Jalloh and Lancaster et al., [274], we hypothesized that some *Nab2^{null}* organismal phenotypes could result from ectopic recruitment of m^{6}A reader proteins onto affected mRNAs. These m^{6}A reader proteins recognize m^{6}A-modified adenosines via a YTH-domain [123] and act downstream of the methyltransferase machinery to bind and regulate the fate of methylated RNAs [121-123,438,439]. Unlike more complex mammalian systems, *Drosophila* have a single nuclear m^{6}A reader protein, YT-521-B (or Ythdc1) and a single cytoplasmic m^{6}A reader protein, Ythdf [128,288].

To assess roles of nuclear Yt521-B and cytoplasmic Ythdf in *Nab2* mutant phenotypes, the *yt521-B*$^{\Delta N}$ and *ythdf*$^{\Delta YTH}$ alleles [129,440] were individually recombined with a zygotic *Nab2*^{null} allele (also known as *Nab2*^{ex3}; imprecise excision of *EP3716*) [215] and assessed for effects on viability, adult locomotion, and lifespan. Homozygous double mutant *yt521-B*$^{\Delta N/\Delta N}$*,Nab2*^{null} flies show increase viability compared to *Nab2*^{null} flies indicating that the nuclear m^{6}A reader is required for the effect of Nab2 loss of viability (**Figure 3-1A**). The *ythdf*$^{\Delta YTH}$ *,Nab2*^{null} double mutants are inviable; furthermore, heterozygous reduction of cytoplasmic Ythdf (*ythdf*$^{\Delta YTH/+}$*, Nab2*^{null}) does not improve *Nab2*^{null} viability (**Figure 3-1A**). In contrast, homozygous loss of nuclear Yt521-B has no effect on *Nab2*^{null} locomotion, whereas heterozygous reduction of cytoplasmic Ythdf rescues *Nab2*^{null} climbing rates by approximately 6-fold as assessed in a negative geotaxis assay (at the 30s time point; **Figure 3-1B**). Despite the ability of reader alleles (e.g., *yt521-B*$^{\Delta N/\Delta N}$ or *ythdf*$^{\Delta YTH\ /+}$) to rescue viability or adult locomotion, neither mutant alone rescues *Nab2*^{null} lifespan defects (**Figure 3-1C**). Together, these genetic rescue data provide evidence that neurological effects of Nab2 loss require nuclear and cytoplasmic m^{6}A readers, and suggest that each of these mechanisms may involve different mRNAs.

Nab2 and Mettl3 regulate splicing of the *trio* 5'UTR in the *Drosophila* head

In light of the effects of Nab2 loss on axon and dendrite development [278,281,284,367], we mined our high-throughput RNA sequencing (RNA-seq) analysis of adult heads from *Nab2*^{null} mutants (zygotic null; imprecise excision of *EP3761*) and isogenic Controls (precise excision of *EP3716*) [215,Jalloh and Lancaster et al., [274] to identify potential Nab2

target transcripts regulated by m^{6}A with functions in neurodevelopment. One transcript identified in this analysis was *trio*, which encodes a Rho guanine nucleotide exchange factor (RhoGEF) that activates specific downstream Rho family GTPases [314,432]. There are multiple different variants of the *trio* transcript, two of which are readily detected in adult fly heads: hereafter referred to as *trio Medium* (*trio M*) and *trio Long* (*trio L*) (**Figure 3-2A, top panel**). Visualization of RNA-seq reads from *Nab2^{null}* and Control heads using Integrative Genomics Viewer (IGV) [356] reveals an increase in reads in introns within the 5'UTR of both *trio M* and *trio L* in *Nab2^{null}* heads relative to Control (**Figure 3-2A**). Normal splicing patterns are detected across all other *trio* intron-exon junctions. Utilizing a publicly available me-RIP-Seq dataset from *Drosophila* heads [147], we bioinformatically identified three m^{6}A sites in the *trio M* 5'UTR (**Figure 3-2A,** red lollipops), but none in the *trio L* 5'UTR. These data suggest that Nab2 is required for removal of 5'UTR introns in *trio M* and *trio L* and present the possibility that the removal of the *trio M* 5'UTR could also involve m^{6}A.

To experimentally test this prediction, we first analyzed the *trio M* transcript using reverse transcription polymerase chain reaction (RT-PCR) analysis with primers that detect the *trio M* 5'UTR intron (exon 1-intron 1 and intron 1-exon 2) (**Figure 3-2B**, blue and orange primer pairs). This analysis reveals that the *trio M* 5'UTR intron-retaining transcript is enriched in adult heads of *Nab2^{null}* flies as well as in heads lacking *Mettl3,* the catalytic subunit of the methyltransferase complex (**Figure 3-2C**) with concomitant reduction or loss of properly spliced *trio M* 5'UTR (exon 1-exon 2) (**Figure 3-2B**, red primer pair; see **Figure 3-2C**). Primers that detect correctly spliced exon 1-exon 2 *trio M* transcript (**Figure 3-2B**, red primer pair) also amplify a ~550bp band in *Nab2^{null}* heads

that is an aberrantly spliced product corresponding to the *trio M* pre-mRNA transcript (**Figure 3-2C**). This RT-PCR analysis did not detect the ~4kb *trio M* 5'UTR intron-retaining transcript, possibly due to the large size of the expected product. To quantitate these results, we performed reverse transcription quantitative PCR (RT-qPCR) analysis, which confirms a significant increase in the levels of the *trio M* 5'UTR intron-retaining transcript in both $Nab2^{null}$ and $Mettl3^{null}$ heads (**Figure 3-2D**). Reciprocal RT-qPCR analysis to quantify the levels of properly spliced *trio M* confirms reduced levels of the properly spliced transcript in $Nab2^{null}$ heads and a complete loss of the properly spliced transcript in $Mettl3^{null}$ heads (**Figure 3-2E**).

Shifting the analysis to the *trio L* 5'UTR intron using primers to detect exon 1-exon 2 confirms the presence of the *trio L* 5'UTR intron-retaining transcript (exon 1-intron 1-exon 2) in $Nab2^{null}$ heads and reduced levels of the properly spliced transcript (exon 1-exon 2) (**Figure 3-2F,** green primer pair; **Figure 3-2G**). In contrast, only properly spliced *trio L* 5' UTR is detected in heads of flies lacking *Mettl3* (**Figure 3-2G**). RT-qPCR analysis confirms increased levels of the *trio L* 5'UTR intron-retaining transcript in $Nab2^{null}$, but not $Mettl3^{null}$ heads, as compared to Control (**Figure 3-2H**). Reciprocally, RT-qPCR analysis using primers that detect levels of properly spliced *trio L* 5'UTR show reduced transcript levels in $Nab2^{null}$ heads and no change in $Mettl3^{null}$ heads compared to Control (**Figure 3-2I**). Collectively, these data confirm that splicing of the *trio M* and *trio L* 5'UTR introns are both Nab2-dependent, but that only splicing of the *trio M* 5'UTR and not the *trio L* 5'UTR is Mettl3-dependent.

Nab2 regulates levels of Trio M in the *Drosophila* head

The *Drosophila* Trio L protein is most similar to a form of human Trio protein (Trio A) that is enriched in the human brain and nervous system [304]. As illustrated in **Figure 3-3A**, Trio L contains a Sec14 domain, nine spectrin repeats, one Src homology 3 (SH3) domain, and two catalytic GEF domains comprised of tandem Dbl homology (DH) and pleckstrin homology (PH) domains, referred to as GEF1 and GEF2. The *Drosophila* Trio M protein corresponds to the C-terminal end of Trio L, including only the SH3 domain and the GEF2 catalytic domain (**Figure 3-3A**).

Based on the finding that Nab2 regulates splicing of the *trio L* and *trio M* 5'UTR introns and that Mettl3 only regulates splicing of the *trio M* 5'UTR intron, we tested whether these intron retention events affect levels of Trio L or Trio M proteins in the fly head. Immunoblotting analysis reveals that Trio L and Trio M are the major isoforms of Trio in Control brains, and that Nab2 loss reduces levels of Trio M but has no apparent effect on Trio L protein levels relative to Control (**Figure 3-3B**). Densitometry analysis of the Trio L and Trio M protein levels demonstrates that the decrease in the steady-state level of Trio M protein is statistically significant (**Figure 3-3C**). Although loss of *Mettl3* or *Nab2* results in *trio M* 5'UTR intron retention (**Figure 3-2C-E**), only loss of Nab2 causes a concomitant drop in Trio M protein levels (**Figure 3-3B&C**). These results imply an independent effect of Nab2 on post-splicing metabolism of the *trio M* 5'UTR intron retaining mRNA, suggesting additional roles for Nab2 in the regulation of *trio M* translation, trafficking, or turnover.

Trio is altered in the *Nab2^{null}* mushroom body

Previous studies demonstrated that Trio is enriched in the mushroom bodies [313], which are divided into five lobes per hemisphere (α/α', β/β' and γ) that project anteriorly from the dorsally located Kenyon cells (**Figure 3-4A**) [441,442]. The α/α' lobes project dorsally, while the β/β' and γ lobes project medially, towards the central ellipsoid body (EB) (**Figure 3-4A**). As demonstrated previously, loss of Nab2 causes defects in α and β lobe structures, specifically loss or thinning of the α lobes and midline fusion of the β lobe structures [281,282,284] (**Figure 3-4B**). To visualize Trio in these structures, we stained Control brains overexpressing membrane tethered GFP in α/β/γ lobes (*201Y-Gal4, UAS-mcd8::GFP*) with an α-Trio antibody, which recognizes both Trio L and Trio M protein [313] (**Figure 3-4B**). This analysis confirms that Trio is enriched in γ lobes, Kenyon cell bodies, and the calyx as shown by colocalization with GFP, but absent or below the level of detection in α and β lobes [313] (**Figure 3-4B** and **Supplemental Figure 3-1**). Intriguingly, Trio accumulates in dysplasic axons near the midline that are not labeled with the *201Y-Gal4* driver (which exclusively drives mcd8::GFP expression in α/β/γ lobes), suggesting these dysplasic axons belong to the β' lobe (**Figure 3-4B**, middle panel, bottom row).

We extended this analysis to explore how loss of Nab2 impacts Trio localization. Trio is lost in the GFP-positive γ lobes of *Nab2^{null}* brains (**Figure 3-4B**, bottom row). Given the strong reduction of Trio M protein detected by immunoblotting of *Nab2^{null}* heads (see **Figure 3-2B**), this result suggests that Trio M may be the primary isoform of Trio present in mushroom body γ lobes.

To explore the localization of Trio specifically in the α' and β' lobe structures, we utilized the Gal4-UAS system to overexpress GFP (*UAS-mcd8::GFP*) using a prime lobe

specific Gal4 driver (*Cka*^{C305a}*-Gal4;* exclusively drives mcd8::GFP expression in α'and β' lobes) (**Figure 3-4C**). As reported previously, Trio is enriched in α' and β' axons, and is also detected in γ lobe axons and ellipsoid body of Control brains [313] (**Figure 3-4C**, top row). *Nab2*^{null} brains show complete loss or thinning of the α' lobe axons as well as a distinct defasciculation phenotype in the β' lobe structures (**Figure 3-4C**). These morphological phenotypes are accompanied by Trio loss in *Nab2*^{null} γ lobe axons and ellipsoid body, and Trio accumulation in the distal portion of β' lobe axons closest to the brain midline (**Figure 3-4C**, middle panel, bottom row).

Expression of Trio GEF2 rescues α/α' and β' defects in *Nab2*^{null} mushroom bodies

The reduced level of Trio M protein in *Nab2*^{null} heads (**Figure 3-3B**) raises the possibility that an imbalance in the relative dose of Trio-GEF1 and Trio-GEF2 activities contributes to mushroom body morphology defects observed in *Nab2*^{null} flies [284]. This model is based on the established role of the Trio protein in patterning of axons in the mushroom body [313], and predicts that loss of Trio M lowers Trio-GEF2 activity within specific mushroom body lobes.

To test this model, transgenes encoding specifically the Trio-GEF1 (*UAS-Trio*-GEF1; **Figure 3-3A,** AAs 1287-1583 tagged at the 3'end with 8 copies of the tag MYC) or -GEF2 domain (*UAS-Trio-GEF2*; **Figure 3-3A,** AAs 1945-2246 tagged at the 3'end with 8 copies of the tag MYC) [313,316], were expressed in all mushroom body lobes of *Nab2*^{null} brains using the *OK107-Gal4* driver. As previously reported [278,280-282,284] and shown in **Figures 3-5A-C**, *Nab2*^{null} mutant brains have highly penetrant defects in the structure of the mushroom body α lobes (missing or thinned) and β lobes (missing, thinned, or midline

crossed) as detected by α-FasII staining, which specifically recognizes the α, β and weakly the γ lobes [443]. Transgenic expression of Trio-GEF2 alone has no effect on mushroom body structure in a control background. Intriguingly, transgenic expression of Trio-GEF2 does not rescue *Nab2*^{null} β lobe defects, but significantly suppresses *Nab2*^{null} α lobe defects (**Figure 3-5A-C**). In contrast, mushroom body expression of Trio-GEF1 in control brains causes complete loss of axonal projection from the Kenyon cells (no lobe structures were detected in any of the brains analyzed; n=25) and is completely lethal in a *Nab2*^{null} background (**Figure 3-5A-C**). Thus, Nab2 loss sensitizes mushroom body axons to the dose of Trio GEF domains such that expression of Trio-GEF2 rescues α lobe axons and expression of extra Trio-GEF1 is lethal to the animal; neither effect is observed in Control brains, indicative of a tight link between Nab2 and Trio GEF dosage in the developing mushroom body.

Given the enrichment of Trio protein in the α' and β' lobes (see **Figure 3-4B**), we also tested whether transgenic expression of the Trio GEF1 or GEF2 domain could autonomously rescue *Nab2*^{null} α' or β' lobe morphology as visualized with the *Cka*^{C305a}-*Gal4* driver (with *UAS-mcd8::GFP*). As with Trio-GEF1 or Trio-GEF2 expression in the α, β, and γ lobes using the *201Y-Gal4* driver, expression of Trio-GEF2 alone has no effect on α' and β' lobe morphology in Control brains but rescues *Nab2*^{null} defects in α' lobe structure and strongly reduces β' lobe defasciculation (**Figure 5D-G**). Expression of Trio-GEF1 in α' and β' lobes has the inverse effect of late larval lethality in both Control and *Nab2*^{null} animals (**Figure 5D**). These data are consistent with a model in which Nab2 acts through Trio-GEF2 to guide axon projection and fasciculation in the α' and β' lobes.

Expression of Trio GEF2 rescues *Nab2^{null}* dendritic arborization defects in class IV ddaC sensory neurons

Nab2 normally restricts branching of sensory dendrites in larval class IV ddaC neurons in body wall neurons [281]. Significantly, Trio-GEF1 promotes and Trio-GEF2 restricts branching of dendrites from these same class IV ddaC neurons (**Figure 3-6A,B**) [320]. Thus, we reasoned that an imbalance of Trio-GEF1 and Trio-GEF2 activities in *Nab2^{null}* ddaC neurons might contribute to dendritic defects. To test this model, we employed a *pickpocket* (*ppk*)-*Gal4*,*UAS-mcd8::GFP* system to visualize class IV ddaC cell bodies and dendritic trees. As observed previously, loss of Nab2 [281] or transgenic expression of Trio-GEF1 [320] individually increases dendritic branch complexity, while transgenic expression of Trio-GEF2 reduces dendritic branch complexity [320] (**Figure 3-6A,B**). Significantly, combining Nab2 loss (*Nab2^{null}*) with ddaC-specific expression of Trio-GEF2 rescues over-arborization normally observed in *Nab2^{null}* larvae (**Figure 3-6A,B**). Intriguingly, transgenic expression of Trio-GEF1 in *Nab2^{null}* larvae causes an increase the variance between arborization phenotypes among the neurons analyzed (**Figure 3-6B**). Together, these data indicate that loss of Trio-GEF2 in *Nab2^{null}* larvae likely contributes to *Nab2^{null}* ddaC overarborization defects.

Expression of Trio GEF2 rescues *Nab2^{null}* defects in viability and locomotion

Given the genetic interactions between the *UAS-Trio-GEF1* and *UAS-Trio-GEF2* transgenes and *Nab2*, we assessed whether transgenic expression of these distinct Trio GEF domains in the mushroom body (*OK107-Gal4, UAS-Trio-GEF1* or *UAS-Trio-GEF2*) affects the organismal phenotypes of viability, adult locomotion, and lifespan. Confirming

our previous findings [215], we detected severe reductions in viability, adult locomotion, and lifespan in *Nab2*^{null} flies compared to Control (**Figure 3-7A-C**). As previously noted, expression of Trio-GEF1 in mushroom bodies is lethal at late larval stages (**Figure 3-7A**). In contrast, transgenic expression of Trio-GEF2 in mushroom bodies strongly suppresses *Nab2*^{null} defects in viability and suppresses defects in adult locomotion but does not significantly alter lifespan (**Figure 3-7A-C**), indicating that a deficit in Trio-GEF2-regulated cytoskeletal dynamics within *OK107*-expressing brain neurons contributes to developmental and post-developmental defects in *Drosophila* lacking Nab2.

DISCUSSION

Here, we identify a role for the *Drosophila* Nab2 RBP and Mettl3 m^{6}A methyltransferase in regulating the *trio* mRNA, which encodes a conserved RhoGEF protein that is altered in human intellectual disability and regulates axon guidance and dendritic arborization through two GEF domains that individually control the cytoskeletal regulators Rac and RhoA/Rho1 [291,309,314,320,331,430,432,435]. The data presented provide strong evidence that the *trio* transcript is a key downstream target of Nab2 in neurons based on an m^{6}A- and Nab2-dependent splicing event and identifies specific effects of each Trio GEF domain within axons and dendrites that develop from neurons lacking Nab2. The results of this study combine with our previous work Jalloh and Lancaster et al., [274,281] to support a model in which Nab2 regulates transcripts that encode key regulators of neurodevelopment, including the conserved GEF, Trio. In the broader context, the phenotypic consequences of loss of an RBP result from the collective changes to numerous target transcripts, and defining the mechanistic basis of these

phenotypes requires systematic analysis of how individual targets, such as *trio*, are impacted. In the case of Nab2, evidence now supports both m^{6}A-dependent and independent roles in *trio* mRNA splicing as well as potential effects on downstream processing such as cytoplasmic metabolism of *trio* mRNA. Taken together, these findings support a model where RBPs such as Nab2/ZC3H14 regulate a collection of target transcripts, potentially through multiple mechanisms, that all contribute to downstream phenotypes.

Previous work illustrating broad rescue of *Nab2^{null}* phenotypes by Mettl3 heterozygosity Jalloh and Lancaster et al., [274] suggested that other regulators of m^{6}A-modified transcripts could also contribute to *Nab2^{null}* defects in viability, adult locomotion, and lifespan. Here, we demonstrate that loss of nuclear or cytoplasmic m^{6}A reader function rescues some, but not all, organismal phenotypes associated with loss of Nab2 (**Figure 3-1**). Homozygous loss of the nuclear m^{6}A reader YT521-B suppresses *Nab2^{null}* defects in viability, but not locomotion or lifespan, whereas heterozygous loss of the cytoplasmic m^{6}A reader Ythdf dominantly suppresses *Nab2^{null}* defects in locomotion, but not viability or lifespan. Collectively, these data suggest that mRNA targets of Nab2 responsible for these behavioral phenotypes may be differentially regulated between cell types and in an m^{6}A-dependent manner. For instance, Nab2-regulated transcripts encoding proteins that govern *Drosophila* viability could rely more heavily on nuclear m^{6}A regulatory mechanisms, such as splicing or export. On the other hand, Nab2-regulated transcripts encoding proteins that govern *Drosophila* negative geotaxis could more heavily require cytoplasmic m^{6}A regulatory mechanisms, such as translation or stability. Moreover, the inability of *YT521-B* or *Ythdf* loss to rescue *Nab2^{null}* defects in lifespan

suggests that Nab2-regulated transcripts that govern lifespan may not by modified by m^{6}A, or that Nab2 plays m^{6}A-independent roles in regulating transcripts critical to control lifespan.

Previous studies demonstrated that loss of m^{6}A regulatory proteins disrupts axon projection in the *Drosophila* mushroom body [147,440]. Although *Mettl3* heterozygosity broadly rescues *Nab2^{null}* behavioral defects Jalloh and Lancaster et al., [274], a decrease in Mettl3 does not dominantly suppress mushroom body morphology defects (**Supplemental Figure 3-2**). This finding suggests that Mettl3 heterozygosity is insufficient to reduce m^{6}A methylation on Nab2-target transcripts to a degree necessary for rescue of axonal projection defects. Given the ability of m^{6}A writer and reader alleles to broadly rescue *Nab2^{null}* phenotypes, future studies will aim to further define the relationship between m^{6}A machinery and Nab2 in relation to regulation of *Drosophila* mushroom body morphology. Moreover, a genome-wide approach to assess transcriptomic changes in m^{6}A in *Nab2^{null}* flies will help delineate the neuronal, Nab2-regulated transcripts that exhibit changes in m^{6}A methylation.

A number of *trio* transcript variants exist in the *Drosophila* brain [313]. Here, we demonstrate that both Nab2 and Mettl3 are required for proper splicing of the 5'UTR intron of *trio M*. On the other hand, splicing of the 5'UTR intron of *trio L* is dependent on Nab2 but not Mettl3. These data align with previously published RNA-seq data from *Nab2^{null} Drosophila* heads Jalloh and Lancaster et al., [274], as well as a publicly available mi-CLIP-seq dataset that mapped m^{6}A sites in the *trio M* 5'UTR intron, but not in the *trio L* 5'UTR intron [147]. Notably, our data reveal that disruptions in splicing of the *trio* 5'UTR due to loss of Nab2 or Mettl3 do not correspond with perturbations in steady-state levels of Trio L and

Trio M proteins. These results show that the intron retention event in the 5'UTR of *trio M* is associated with a significant reduction in the level of Trio M protein in the *Nab2^{null}* fly head. Surprisingly, the steady-state level of Trio M protein is unaffected in *Mettl3^{null}* heads even though *trio* 5'UTR intron retention is comparable to the levels observed in *Nab2^{null}* heads. These data imply that Nab2 may regulate *trio M* protein levels in a manner independent of *trio M* 5'UTR splicing. However, given previously defined roles for Nab2 as a negative regulator of m^{6}A methylation Jalloh and Lancaster et al., [274], this observation more likely suggests that excess m^{6}A on the *trio M* pre-mRNA upon loss of Nab2 may disrupt subsequent translation, trafficking, or stability. In contrast, retention of the *trio L* 5'UTR intron that occurs upon loss of Nab2 does not affect the steady-state level of the Trio L protein, suggesting this intron retention event may not disrupt translation. Alternatively, the remaining level of the properly spliced *trio L* in *Nab2^{null}* heads may be sufficient to maintain the steady-state level of Trio L protein. Further studies expanding to additional co-regulated Nab2 and Mettl3 targets will be required to define how these factors regulate post-transcriptional events.

Given that Nab2 regulates splicing and downstream processing of numerous neuronally-enriched mRNAs Jalloh and Lancaster et al., [274], morphological defects observed in *Nab2^{null}* mushroom bodies are likely due to collective processing defects that affect multiple RNAs critical for axon development. Our results support a model where loss of Trio M, and therefore GEF2 function, contributes to morphological defects in mushroom bodies of *Nab2^{null}* flies. Previous studies demonstrated that Trio is a critical regulator of mushroom body morphology and Trio is enriched in the α', β' and γ lobes, but is virtually absent in the α and β lobes [313]. We confirm these findings and further

demonstrate that upon loss of Nab2, Trio levels are depleted in the γ lobes. Despite the established functions of Trio in regulating γ lobe formation [313], γ lobe defects are not detected upon loss of Nab2 [284]. Given that Trio M is the only isoform of Trio depleted in *Nab2*^{null} brains (**Figure 3-3B**) and γ lobes show no defects (**Figure 3-5A**), this finding suggests that Trio L, and therefore GEF1 function, is responsible for patterning γ lobe axons in the developing brain.

Studies of axon pathfinding mechanisms in the mushroom body demonstrate that the α' and β' lobes guide development of the α and β lobes [444]. Given that Trio is enriched in the α'/β'/γ lobes of the mushroom body, our data suggest that loss of Trio M, and therefore GEF2 levels, in α'/β' lobes contributes to *Nab2*^{null} α/β lobe defects. We demonstrate that transgenic expression of Trio-GEF2 in α'/β' lobes (*C305a-Gal4*) of *Nab2*^{null} mushroom bodies rescues α' lobe defects and β' lobe defasciculation phenotypes in a cell autonomous manner (**Figure 3-5**). Moreover, expression of Trio-GEF2 in all mushroom body lobes (*OK107-Gal4*) rescues *Nab2*^{null} α lobe defects; however, whether this rescue occurs in a cell autonomous manner remains unknown (**Figure 3-5**). Collectively, these data demonstrate that Trio-GEF2 rescue is limited to some mushroom body lobes (α, α', β') and not others (β), implying that Trio-GEF2 is required for projection of only some *Nab2*^{null} axons. In this regard, misprojection defects in *Nab2*^{null} β axons are not rescued by multiple genetic manipulations that rescue α axon defects (e.g., by transgenic expression of Trio-GEF2 [this study] or by single copy alleles of *fmr1*, *Atx2*, or PCP components [278,281,284,367]). These findings imply specific roles for Nab2 in these two types of Kenyon cell projections and suggest that Nab2 regulates different mRNAs to govern development of distinct mushroom body lobes.

Previous studies established that the Trio-GEF1 domain acts primarily through activation of Rac1 to promote axon outgrowth and pathfinding, while Trio-GEF2 acts primarily through RhoA/Rho1 to restrict neurite outgrowth [314,319,320]. Given that loss of Nab2 disrupts the ratio of GEF1 and GEF2 in *Drosophila* heads by decreasing the level of Trio M but not Trio L, we hypothesized that expression of the GEF1 effector, Rac1, in mushroom body neurons would exacerbate *Nab2^{null}* phenotypic and morphological defects, whereas expression of the GEF2 effector, RhoA/Rho1, would rescue these same defects. Intriguingly, we observed that expression of either Rac1 or RhoA/Rho1 in the absence of Nab2 in Trio-enriched mushroom body neurons is lethal (**Supplemental Figure 3-3**). These data suggest that further expression of Rac1 in *Nab2^{null}* flies in which GEF1 levels, and therefore likely Rac1 activation, dominates is detrimental to nervous system development and the lethality induced by expression of RhoA/Rho1 upon loss of Nab2, indicates that Trio-GEF2 may act via other unknown effectors to govern mushroom body development. On the other hand, alternative RhoGEFs may compensate for the loss of Trio M protein in the mushroom body thereby leading to the lethality of *Nab2^{null}* animals transgenically expressing Rac1 or RhoA/Rho1. In sum, further studies are required to elucidate how loss of Nab2 alters Rac1 and RhoA/Rho1 activity in the *Drosophila* brain.

Nab2 and Trio have established roles in sculpting dendritic arborization of class IV ddaC neurons in the *Drosophila* peripheral nervous system [281,320]. Here, we demonstrate that transgenic expression of the Trio-GEF2 domain rescues overarborization defects in *Nab2^{null}* class IV ddaC neurons. In line with previous studies [320], we validate that transgenic expression of Trio-GEF1 in class IV ddaC neurons causes dramatic

overarborization defects, while transgenic expression of Trio-GEF2 causes underarborization defects compared to control animals. Interestingly, we also demonstrate that expression of Trio-GEF1 in class IV ddaC neurons of *Nab2*^{null} flies results in a wide range of arborization phenotypes. Very few of these animals survive to the wandering 3rd instar larval stage and no animals survive to adulthood. Given these observations, disruption of Nab2-regulated mRNAs in these neurons as well as over-activation of Rac1 by GEF1 may severely disrupt ddaC development such that arborization defects are highly variable from animal-to-animal. Overall, these data support a role for Trio M, and therefore GEF2 loss, in contributing to the established overarborization defects in *Nab2*^{null} class IV ddaC neurons [281].

In aggregate, these data reveal a role for Nab2 and Mettl3 in regulating splicing and protein levels of the RhoGEF Trio to support proper nervous system development. Genetic interactions between the m^{6}A machinery and Nab2 support a role for Nab2 in the regulation of m^{6}A methylation. We show for the first time that loss of Trio M, and therefore GEF2 levels, in *Nab2*^{null} flies contributes to several *Nab2*^{null} defects, including neuronal defects, such as mushroom body morphology and class IV ddaC arborization. Moreover, we demonstrate that transgenic expression of Trio-GEF2 broadly rescues *Nab2*^{null} viability and adult locomotion. This regulatory relationship between Nab2 and Trio-GEF2 could be cell autonomous, but further experiments are required determine the nature of this interaction. Given that mutations in human *ZC3H14* and *TRIO* are both linked to intellectual disabilities [215,305], dysregulation of Trio function in neurons is one potential mechanism to explain axonal and dendritic phenotypes observed in *Nab2*^{null} *Drosophila*

[215,]Jalloh and Lancaster et al., [274,278,280,281,284] and *Zc3h14* mutant mice [420], as well as the cognitive defect observed in human patients lacking ZC3H14 [215].

METHODS

RESOURCES TABLE

REAGENT or RESOURCE	SOURCE	IDENTIFIER
Antibodies		
Mouse monoclonal 9.4A anti-Trio	University of Iowa Developmental Studies Hybridoma Bank	RRID:AB_528494
Mouse monoclonal ADL101 anti-Lamin	University of Iowa Developmental Studies Hybridoma Bank	RRID:AB_528332
Mouse monoclonal 1D4 anti-Fasciclin II	University of Iowa Developmental Studies Hybridoma Bank	RRID: AB_528235
Rabbit Polyclonal Anti-Green Fluorescent Protein (GFP)	ThermoFisher Scientific	Cat#A-11122
Alexa Fluor® 488 AffiniPure Polyclonal Goat Anti-rabbit IgG	Jackson ImmunoResearch Laboratories	RRID: AB_2338046
Cy™3 AffiniPure Polyclonal Goat Anti-Mouse IgG	Jackson ImmunoResearch Laboratories	RRID: AB_2338690
Chemicals, peptides, and recombinant proteins		
TRIzol reagent	Invitrogen	Cat#15596018
1-Bromo-3-chloropropane	Scientific Laboratory Supplies	Cat# B9673
2-propanol/isopropanol	Fisher Scientific	Cat#A416-1
Ethanol 200 proof	Fisher Scientific	Cat#04-355-233
Diethyl pyrocarbonate (DEPC)	Sigma-Aldrich	Cat#D5758
Agarose LE, Quick Dissolve	Genesee Scientific	Cat#20-102QD
Red Safe	iNtRON Biotechnology	Cat# 21141
NaCl	Sigma-Aldrich	Cat#S7653
KCl	Sigma-Aldrich	Cat#P3911
$ZnCl_2$	Sigma-Aldrich	Cat#208086
Polysorbate 20 (Tween® 20)	Fisher Bioreagents	Cat#BP-337-500
Triton X-100	Sigma-Aldrich	Cat#T8787
Tris Base Ultrapure	USBiological Life Sciences	Cat#T8600
Sodium Dodecyl Sulfate	Fisher Bioreagents	Cat#YBP166500
Sodium deoxycholate	Thermo Scientific	Cat#89905
NP-40	Thermo Scientific	Cat#85124
Dithiothreitol (DTT)	Thermo Scientific	Cat#R0861

Bromophenol Blue	Thermo Scientific Chemicals	Cat#A18469-18
Glycerol	USBiological Life Sciences	Cat#G8145
RNaseOUT	Invitrogen	Cat#10777019
p-Coumaric acid	Sigma-Aldrich	Cat#C9008
Luminol	Sigma-Aldrich	Cat#A8511
Acetic Acid, Glacial	Fisher Scientific	Cat# A38-212
EDTA	USBiological Life Sciences	Cat#E2210
Paraformaldehyde	Electron Microscopy Sciences	Cat#15713
VECTASHEILD mounting medium	Vector Laboratories Inc.	REF#H-1000
Normal Goat Serum	Jackson ImmunoResearch Laboratories	RRID:AB_2336990
Diethyl Ether Anhydrous (stabilized with BHT)	Tokyo Chemical Industry (TCI) America	Cat#D3497
Halocarbon oil 27	Sigma-Aldrich	Cat#H8773
Critical commercial assays		
DNase I, Amplification Grade	Invitrogen	Cat#18068015
M-MLV Reverse Transcriptase	Invitrogen	Cat#28025013
Taq DNA Polymerase (1000U)	Qiagen	Cat# 201205
QuantiTect SYBR Green PCR Kit	Qiagen	Cat# 204145
MicroAmp™ Fast Optical 96-Well Reaction Plate with Barcode, 0.1 ml	Applied Biosystems	Cat# 4346906
MicroAmp™ Optical Adhesive Film	Applied Biosystems	Cat# 4311971
4–20% Mini-PROTEAN® TGX Stain-Free™ Protein Gels	Bio-Rad	Cat#4568093
Nitrocellulose Membrane, 0.2 µm	Bio-Rad	Cat#1620112
iScript Reverse Transcriptase Supermix	Bio-Rad	Cat#1708841
Phusion High Fidelity PCR	Thermo Scientific	Cat#F530S
Pierce BCA Protein Assay Kit	Thermo Scientific	Cat#23225
SuperFrost Plus slides	Fisher Scientific	Cat# 12-550-15
Il90p-Experimental models: Organisms/Strains		
D. melanogaster: w-;;Nab2^{pex41} (Control);	[215]	N/A
D. melanogaster: w-;;Nab2^{ex3} (*Nab2^{null}*); (Zygotic loss of Nab2)	[215]	N/A
D. melanogaster: w-;;Mettl3^{null};	[129]	N/A
D. melanogaster:YT521-B$^{\Delta N}$	[129]	N/A
D. melanogaster: Ythdf$^{\Delta YTH}$ (Ythdf^{0})	[440]	N/A
D. melanogaster:w^{1118};;Df(3R)BSC655 (ythdf deficiency)	Bloomington Drosophila Stock Company	BDSC:26507
D. melanogaster: y^{1}w^{67c23};UAS-mcd8::GFP, 201Y-Gal4;;	Bloomington Drosophila Stock Company	BDSC:64296

D. melanogaster:w;Cka^{c305a}-Gal4*	Bloomington Drosophila Stock Company	BDSC:30829
D. melanogaster: y^{1}w;UAS-mcd8::GFP;;*	Bloomington Drosophila Stock Company	BDSC:5137
D. melanogaster: w;;;OK107-Gal4*	Bloomington Drosophila Stock Company	BDSC:854
D. melanogaster:y^{1}w:UAS-trio-GEF1-myc* (Trio-GEF1 domain; AAs 1287-1583 tagged at the 3'end with 8 copies of the tag MYC)	Bloomington Drosophila Stock Company	BDSC:9133
D. melanogaster: y^{1}w:UAS-trio-GEF2-myc* (Trio-GEF2 domain; AAs 1945-2246 tagged at the 3'end with 8 copies of the tag MYC)	Bloomington Drosophila Stock Company	BDSC:9134
D. melanogaster:w;;ppk-Gal4*	Bloomington Drosophila Stock Company	BSDC:32079
D. melanogaster:w;UAS-Rac1*	Bloomington Drosophila Stock Company	BSDC:6293
D. melanogaster:w;UAS-Rho1*	Bloomington Drosophila Stock Company	BSDC:58819
Oligonucleotides		
RT-PCR *trio L* Forward: AACAAAACAGAGAGCGCCC	This study	N/A
RT-PCR *trio L* Reverse: GATGGGCACTGCAGCATAA	This study	N/A
RT-qPCR *trio L* Intron Retention Forward: 5'-TTAGCCCGCGTCAAGTC-3'	This study	N/A
RT-qPCR *trio L* Intron Retention Reverse: 5'-CTGCTTGTGCCACCAAAT-3'	This study	N/A
RT-qPCR *trio L* Properly Spliced Forward: 5'-GTTGTGTTGACAAAAGAGTG-3'	This study	N/A
RT-qPCR *trio L* Properly Spliced Reverse: 5'-GATGGGCACTGCAGCATAA-3'	This study	N/A
RT-PCR *trio M* Intron Retention (1) Forward: 5'-CAGCAGTCTCTTCTTCACTAA-3'	This study	N/A
RT-PCR *trio M* Intron Retention (1) Reverse: 5'-ACTCGGATTGTTGTTTCACTTT-3'	This study	N/A
RT-PCR *trio M* Intron Retention (2) Forward: 5'-GACTGCGCAAACATAGCATTA-3'	This study	N/A
RT-PCR *trio M* Intron Retention (2) Reverse: 5'-ATCCGCTCGTTGAGAAACT-3'	This study	N/A
RT-PCR *trio M* Properly Spliced Forward: 5'-CGCTAAAGAGGAGCGCAATA-3'	This study	N/A
RT-PCR *trio M* Properly Spliced Reverse: 5'-CTTCTTAACACTCTTCATGATTCG-3'	This study	N/A
RT-qPCR *trio M* Intron Retention Forward: 5'-TTGAGTGAACCCGCTAAAG-3'	This study	N/A
RT-qPCR *trio M* Intron Retention Reverse: 5'-CTTTGGAGTGCTTGTTCTTATC-3'	This study	N/A
RT-qPCR *trio M* Properly Spliced Forward: CGTCCATAAATTGAGTCGGAGAAC	This study	N/A

RT-qPCR *trio M* Properly Spliced Reverse: 5'-CTTCTTAACACTCTTCATGATTCG-3'	This study	N/A
RT-PCR and RT-qPCR *rpl32* Forward: AAGATGACCATCCGCCCAGCATAC	This study	N/A
RT-PCR and RT-qPCR *rpl32* Reverse: ACGCACTCTGTTGTCGATACCCTT	This study	N/A
Software and algorithms		
Fiji/ImageJ	[445,446]	https://imagej.net/
Integrated Genome Viewer (IGV)	[447]	https://igv.org/
Image Lab	Bio-Rad	https://image-lab-4-0.software.informer.com/
GraphPad (Prism)		
Other		
ChemiDoc	BioRad	Cat#12003153
Humidified Incubators	Shel Lab	SRI20PF
#5 Dumont Fine Forceps	Ted Pella Inc.	Prod#5622
Motorized Pestle	Argos Technologies	Cat#A0001
NanodropOne	Thermo Fisher	N/A

RESOURCE AVAILIABILTY

Lead contact

Further information and requests for resources and reagents should be directed to and will be fulfilled by the Lead Contact, Ken Moberg (kmoberg@emory.edu).

Materials availability

The *Drosophila melanogaster* lines generated in this study are available by contacting the Lead Contact.

Data and code availability

This study did not generate any dataset or codes.

EXPERIMENTAL MODEL AND SUBJECT DETAILS

Flies (*Drosophila melanogaster)* were raised on standard cornmeal agar medium and maintained in an incubator set at 25ºC with a 12-hour light/dark cycle. Crosses were

reared under the same conditions, and standard medium was supplemented with dry yeast. The GAL4-UAS binary transgenic system was used to express transgenes of interest. Details of genotypes can be found in the Key Resources Table. One to five day-old flies were used for experiments in this study. An equal number of males and females was used for all experiments.

METHOD DETAILS

Drosophila melanogaster stocks and genetics

Drosophila melanogaster stocks were raised on standard cornmeal agar and maintained in humidified incubators (SRI20PF, Shel Lab) at 25ºC with 12-hour light/dark cycles. Crosses were reared under the same conditions and supplemented with dry yeast. The strains used in this study are described in the Key Resources Table.

Viability and lifespan analysis

Viability at 25ºC was measured by assessing eclosion rates of 100 wandering L3 larvae collected for each genotype, and then reared in a single vial. Hatching was recorded for 5-6 days. At least three independent biological replicates per genotype were tested for significance and calculated using group analysis on GraphPad (Prism). Lifespan was assessed at 25ºC as described previously [398]. In brief, newly eclosed flies were collected, placed in vials (10 flies per vial), and then transferred to fresh vials weekly, or as needed. Survivorship was scored daily. At least three independent biological replicates were tested for each genotype, and significance was calculated using group analysis on GraphPad (Prism).

Locomotion assays

Negative geotaxis was tested as previously described [398]. Briefly, newly eclosed flies (day 0) were collected, and kept in vials for 2-5 days. Cohorts of 10 age-matched flies were transferred to a 25 ml graduated cylinder for analysis. Flies in graduated cylinders were tapped to bring flies to the bottom of the vial and the rate at which the flies traveled to the top of the vial (25 ml mark) was measured at 5, 10, 15, and 30s). At least three biological replicates per genotype were analyzed and significance was calculated using grouped analysis on GraphPad (Prism).

***Drosophila* decapitation**

CO_2-anesthetized flies were collected and frozen at -80ºC for approximately five minutes. Frozen flies were then placed on a metal plate over dry ice. Gently, #5 Dumont fine forceps (Ted Pella, Inc.) were placed between the *Drosophila* head and thorax to remove the head from the remainder of the body. Heads were carefully placed in Eppendorf tubes, on ice, for subsequent processing.

RNA isolation for RT-PCR and real-time qPCR

Total RNA was isolated from ~25 adult fly heads using the TRIzol (Invitrogen) method. Briefly, *Drosophila* heads were homogenized in 0.1 ml TRIzol using a motorized pestle (Argos Technologies) on ice. TRIzol was added to samples to bring to a total volume of 0.5 ml and 0.1 ml of 1-Bromo-3-chloropropane (Scientific Laboratory Supplies) was added. Samples were vortexed on high speed for 10s and incubated at room temperature

for 15 min. Next, samples were centrifuged for 15m at 13,000 x g at 4ºC. The top, aqueous layer was removed and placed into a clean Eppendorf tube. An equal volume of 2-propanol (~250 μL) was added. Samples were inverted 10 times and incubated at room temperature for 10 min. Next, samples were centrifuged for 15m at 13,000 x g at 4ºC. The supernatant was removed, and 0.5 ml of 75% ethanol was added. Samples were centrifuged a final time for 15 min at 13,000 x g at 4°C**.** The supernatant was removed, and the samples were allowed to air dry until the remaining ethanol evaporated (~5 min). The pellet was resuspended in 10-20 μL of DEPC water. RNA concentration and purity was assessed using a Spectrophotometer (Thermo Fisher). Total RNA (1 μg) was treated with DNaseI (Qiagen). cDNA was generated using M-MLV Reverse Transcriptase (Invitrogen). Qiagen *Taq* polymerase (Qiagen) was used for PCR amplification of target transcripts and products were resolved and imaged on 1-2% agarose gels (Chemi-Doc). Quantitative real-time PCR reactions were carried out in technical triplicate with QuantiTect SYBR Green Master Mix using Applied Biosystems StepOne Plus real-time machine (ABI). Results were analyzed using ΔΔCT method, normalized to loading Control (e.g., *rpl32*), and plotted as relative levels normalized to Control. At least three independent biological replicates were performed for each genotype, and significance was calculated using group analysis on GraphPad (Prism). Primers used for all PCR reactions are listed in the Key Resources Table.

Immunoblotting

For analysis of Trio protein levels, ~25 adult fly heads (1-5 days old) were decapitated and collected on dry ice. Protein lysates were prepared by homogenizing heads in 0.5 ml

of RIPA-2 Buffer (50 mM Tris-HCl, pH 8; 150 mM NaCl; 0.5% sodium deoxycholate; 1% Igepal CA-630 0.1% SDS) supplemented with protease inhibitors (1 mM PMSF; Pierce Protease Inhibitors; Thermo Fisher Scientific) and 1% SDS. Samples were sonicated 3 x 10 s with 1 min on ice between repetitions, and then centrifuged at 13,000 x g for 15 min at 4ºC. Protein lysate concentration was determined by Pierce BCA Protein Assay Kit (Life Technologies). Head lysate protein samples (40–60 µg) in reducing sample buffer (50 mM Tris-HCl, pH 6.8; 100 mM DTT; 2% SDS; 0.1% Bromophenol Blue; 10% glycerol) were resolved on 4–20% Criterion TGX Stain-Free Precast Polyacrylamide Gels (Bio-Rad), transferred to nitrocellulose membranes (Bio-Rad), and incubated for 1 hr in blocking buffer (5% non-fat dry milk in 0.1% TBS-Tween) followed by overnight incubation with anti-Trio monoclonal antibody (1:1000; DHSB #9.4A) diluted in blocking buffer. Primary antibody was detected using species-specific horse-radish peroxidase (HRP) conjugated secondary antibody (Jackson ImmunoResearch) with enhanced chemiluminescence (ECL,Sigma). Densitometry analysis was performed using Image Lab software (Bio-Rad). At least three independent biological replicates were performed for each genotype, and significance was calculated using group analysis on GraphPad (Prism).

Drosophila brain dissection, immunohistochemistry, visualization, and statistical analysis

For *Drosophila* mushroom body morphology imaging, brains were dissected using #5 Dumont fine forceps (Ted Pella, Inc.) in PBS supplemented with 0.1% Triton X-100 (0.1% PBS-T). The proboscis was removed to provide a forceps grip point, and the remaining cuticle and trachea were peeled away from the brain. Brains were submerged in 1X PBS

on ice until all brains were dissected. Dissected brains were fixed in 4% paraformaldehyde for 30 min and then permeabilized in 0.3% PBS-Triton X-100 (0.3% PBS-T) for 30 min, on ice. Brains were carefully transferred to 0.5 ml Eppendorf tubes in 0.1% PBS-T. For both primary and secondary antibody incubations, brains were left rocking at 4ºC for 24-72 hours (see list of dilutions and incubation times below) in 0.1% PBS-T supplemented with normal goat serum (Jackson ImmunoResearch) at a 1:20 dilution. Immunostained brains were mounted on SuperFrost Plus slides in Vectasheild (Vector Laboratories) using a coverslip bridge. Brains were imaged on a Nikon A1R confocal microscope. ~25 brains were analyzed for each genotype, for each experiment. Maximum intensity projections were generated using Fiji ImageJ software.

Antibody: Mouse monoclonal 9.4A anti-Trio, **Incubation time:** 48-72hr, **Dilution:** 1:50

Antibody: Mouse monoclonal 1D4 anti-Fasciclin II, **Incubation time:** 48-72hr, **Dilution:** 1:50

Antibody: Rabbit Polyclonal Anti-Green Fluorescent Protein (GFP), **Incubation time:** Overnight-24hr, **Dilution:** 0.125:100

Antibody: Alexa Fluor® 488 AffiniPure Polyclonal Goat Anti-rabbit IgG, **Incubation time:** Overnight-24hr, **Dilution:** 1:100

Antibody: Cy™3 AffiniPure Polyclonal Goat Anti-Mouse IgG, **Incubation time:** Overnight-24hr, **Dilution:** 1:100

Drosophila neuron live imaging confocal microscopy, neuronal reconstruction, data analysis, and statistical analysis

Live imaging of class IV ddaC neurons was performed as described previously [320]. Briefly, ~10 wondering 3rd instar *ppk-Gal4,UAS-mcd8::GFP* labeled larvae were mounted in 1:5 (v/v) diethyl ether: halocarbon oil under an imaging bridge of 22 x 22mm glass coverslips

topped with a 22 x 55mm glass coverslip. The ddaC images were captured on a Nikon A1R inverted Confocal microscope. Maximum intensity projections were generated using Fiji ImageJ software. Quantitative morphological data were compiled using the Simple Neurite tracer (SNT) plugin for Fiji [448,449]. Batch processing was completed using a custom Fiji macro and Rstudio script created and gifted by Dr. Atit A. Patel (Dr. Dan Cox Lab, Georgia State University) [450] and the resulting data were exported to Excel (Microsoft).

Statistical Analysis

Group analysis on biological triplicate experiments was performed using One-Way or Two-Way ANOVA (Tukey's multiple-comparison test) on GraphPad (Prism). Sample sizes (n) and p-values are denoted in text, figures, and/or figure legends and indicated by asterisks (e.g., *p<0.05).

Acknowledgements

This work was supported by the Emory University Emory Integrated Cellular Imaging Core Facility (RRID:SCR_023534). The authors thank Dr. Dan Cox, GA State Neuroscience Institute, and his lab members Drs. Erin Lottes and Atit Patel for training, reagents, and discussions. We also thank the members of the Moberg and Corbett laboratories, especially Dr. Milo Fasken for insightful discussions.

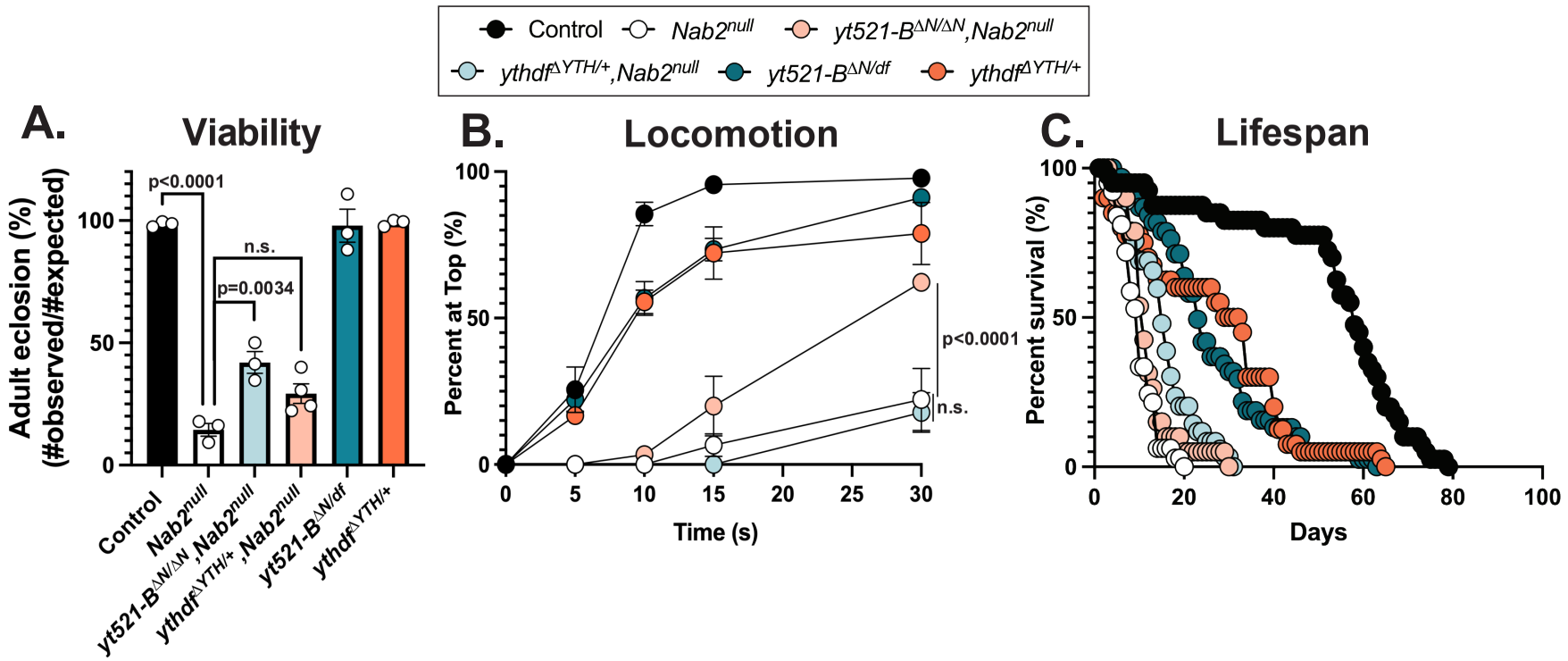

Figure 3-1. Loss of m^{6}A-reader proteins rescues *Nab2^{null}* defects in viability and adult locomotion. (**A**) Percent of Control, *Nab2^{null}*, *yt521-B$^{ΔN/ΔN}$Nab2^{null}*, *yhdf$^{ΔYTH/+}$Nab2^{null}*, *yt521-B$^{ΔN/df}$*, and *ythdf$^{ΔYTH/+}$* that eclose as viable adults (calculated as #observed/#expected). At least 100 larvae were analyzed for each biological replicate. (**B**) Negative geotaxis as a measure of locomotion of age-matched adult flies of indicated genotypes over time in seconds (s) taken to reach the top of a vial. The negative geotaxis was observed for at least 10 animals for each biological replicate.(**C**) Survival of age matched adult flies of the indicated genotypes over time in days. The survival of at least 10 flies was observed for each biological replicate. At least three biological replicates were tested for each genotype and experiment. Significance values are indicated.

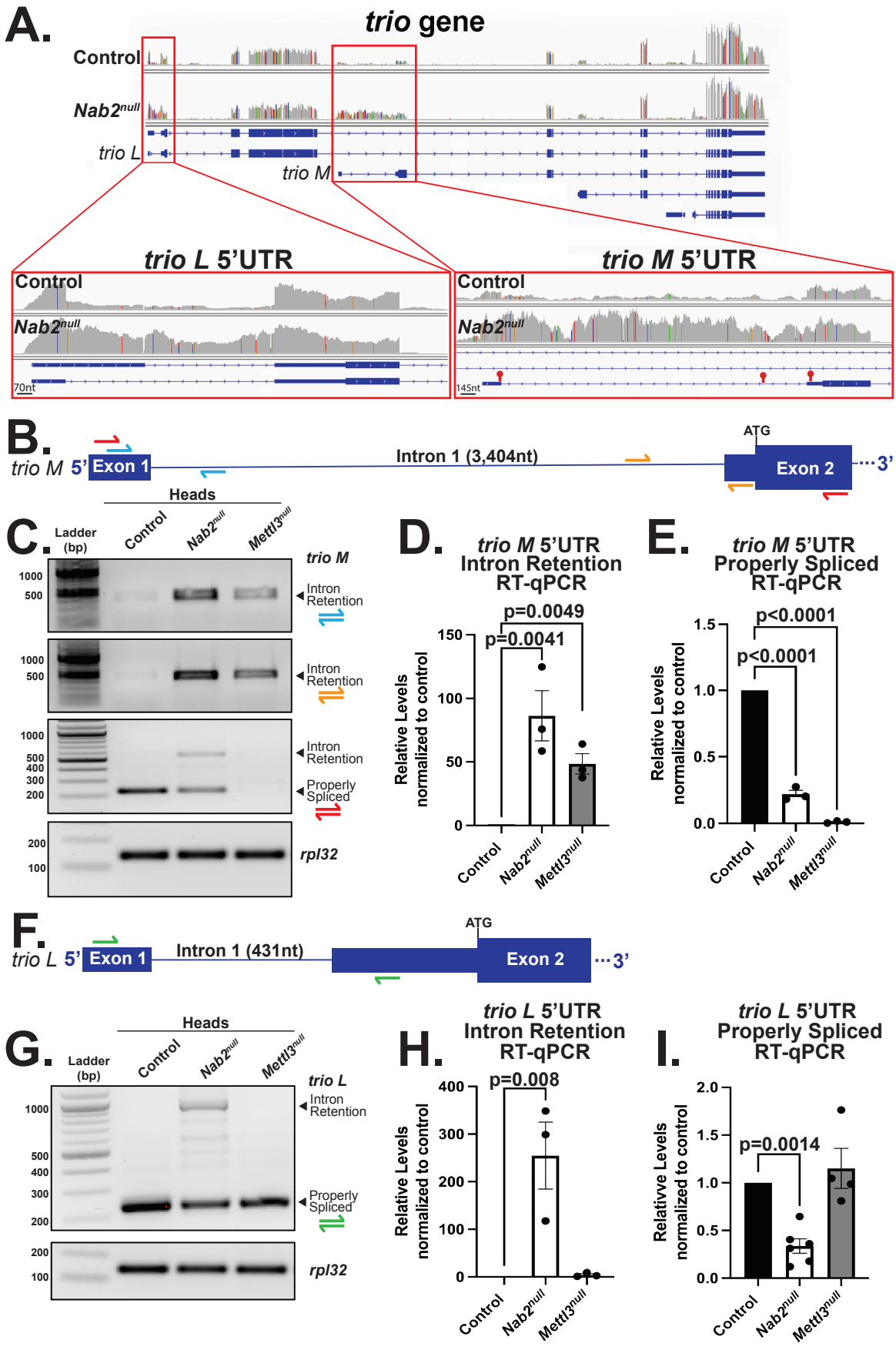
A.
trio gene
Control
Nab2null
trio L
trio M
trio L 5'UTR
trio M 5'UTR
70nt
145nt
B.
trio M 5'
Exon 1
Intron 1 (3,404nt)
ATG
Exon 2
3'
C.
Heads
Ladder (bp)
Control
Nab2null
Mettl3null
trio M
Intron Retention
Properly Spliced
rpl32
D.
trio M 5'UTR Intron Retention RT-qPCR
p=0.0049
p=0.0041
Relative Levels normalized to control
E.
trio M 5'UTR Properly Spliced RT-qPCR
p<0.0001
p<0.0001
F.
trio L 5'
Intron 1 (431nt)
G.
trio L
H.
trio L 5'UTR Intron Retention RT-qPCR
p=0.008
I.
trio L 5'UTR Properly Spliced RT-qPCR
Relativve Levels normalized to control
p=0.0014

Figure 3-2. Nab2 and Mettl3 regulate splicing of the *trio* 5'UTR in the *Drosophila* head. (**A**) RNA sequencing reads across the *trio* locus in Control and *Nab2*^{null} fly heads Jalloh and Lancaster et al [274]. Boxed insets highlight the sequencing reads from the *trio L* (scale bar=70nt) and *trio M* (scale bar=145nt) 5'UTR. Red lollipops denote location of mapped m^{6}A sites. (**B**) Diagram of the *trio M* 5'UTR annotated to show location of color-coded primer pairs. The position of the ATG is also indicated (**C**) RT-PCR analysis of *trio M* mRNA from Control, *Nab2*^{null}, and *Mettl3*^{null} heads. Properly spliced transcript and intron reattaining transcript bands are indicated. *Rpl32* serves as a control. RT-qPCR analysis detecting levels of (**D**) intron retaining or (**E**) properly spliced *trio M* transcript from Control, *Nab2*^{null}, and *Mettl3*^{null} heads, where control is set to 1.0. (**F**) Diagram of the *trio L* 5'UTR annotated to show location of color-coded primer pairs. (**G**) RT-PCR analysis of *trio L* mRNA from Control, *Nab2*^{null}, and *Mettl3*^{null} heads. Properly spliced and intron retaining transcript bands are indicated. (**H**) RT-qPCR analysis detecting levels of intron retaining and (**I**) properly spliced *trio L* transcript in Control, *Nab2*^{null}, and *Mettl3*^{null} heads. RNA from 25 heads was extracted from each genotype for each biological replicate. At least three biological replicates were performed for each experiment. Significance values are indicated.

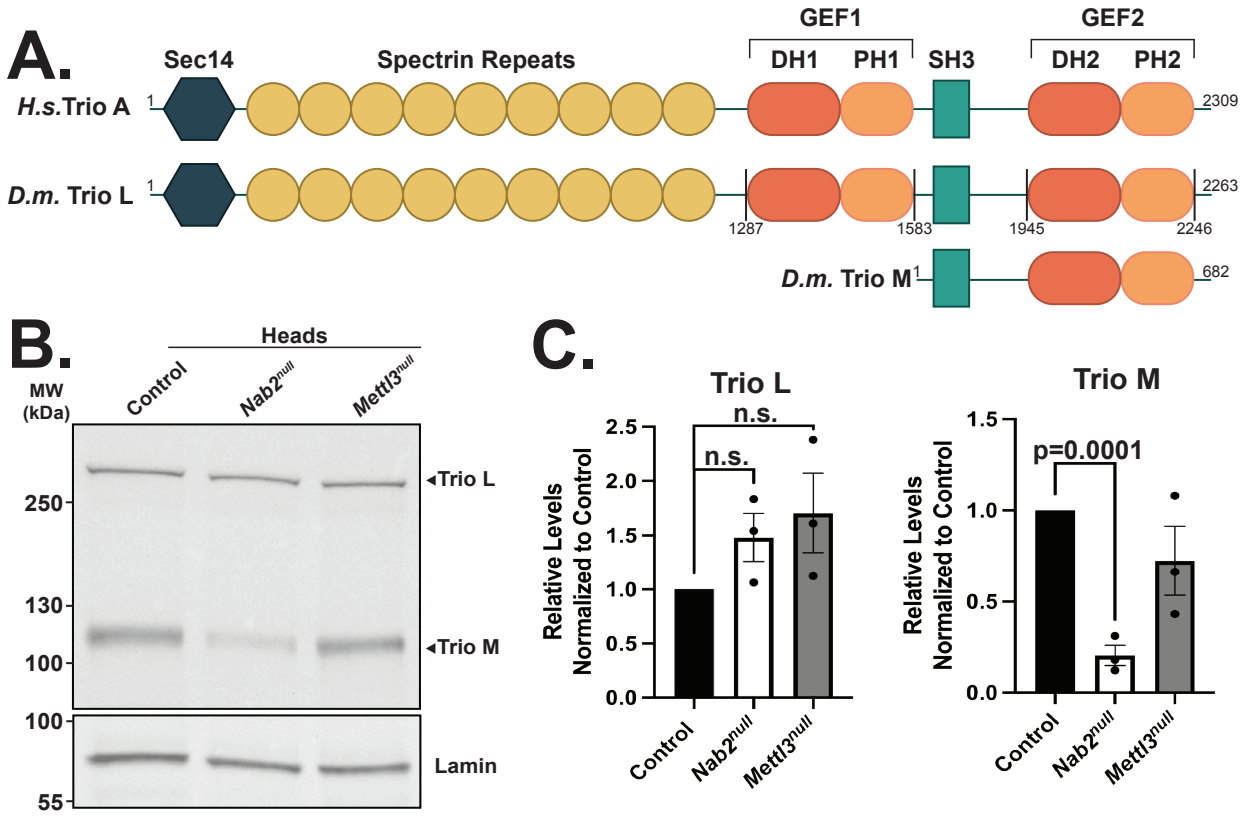

Figure 3-3. Nab2 regulates Trio M protein level in the *Drosophila* head. (**A**) Schematic of the human (*H.s.*) Trio A and *Drosophila melanogaster* (*D.m.*) Trio L and Trio M proteins. Trio contains a Sec14 domain, nine spectrin repeats, one Src homology 3 (SH3) domain, and two catalytic GEF domains (GEF1 and GEF2), comprised of tandem Dbl homology (DH) and pleckstrin homology (PH) domains. Amino acid lengths are indicated for each Trio protein and the amino acids corresponding to Trio GEF1 and GEF2 are indicated in the schematic for Drosophila Trio L. (**B**) Immunoblotting analysis of Trio L and Trio M protein levels from Control, *Nab2*^{null}, and *Mettl3*^{null} heads. Lamin serves as a loading Control. Molecular weights in kDa are indicated to the left. (**C**) Quantification of Trio L (left) and Trio M (right) protein levels in (**B**) using Image Lab software. Protein levels are normalized to Control, with the value for Control set to 1.0. Protein from at least 25 heads was extracted from each genotype for each biological replicate. Three biological replicates were performed. Significance values are indicated.

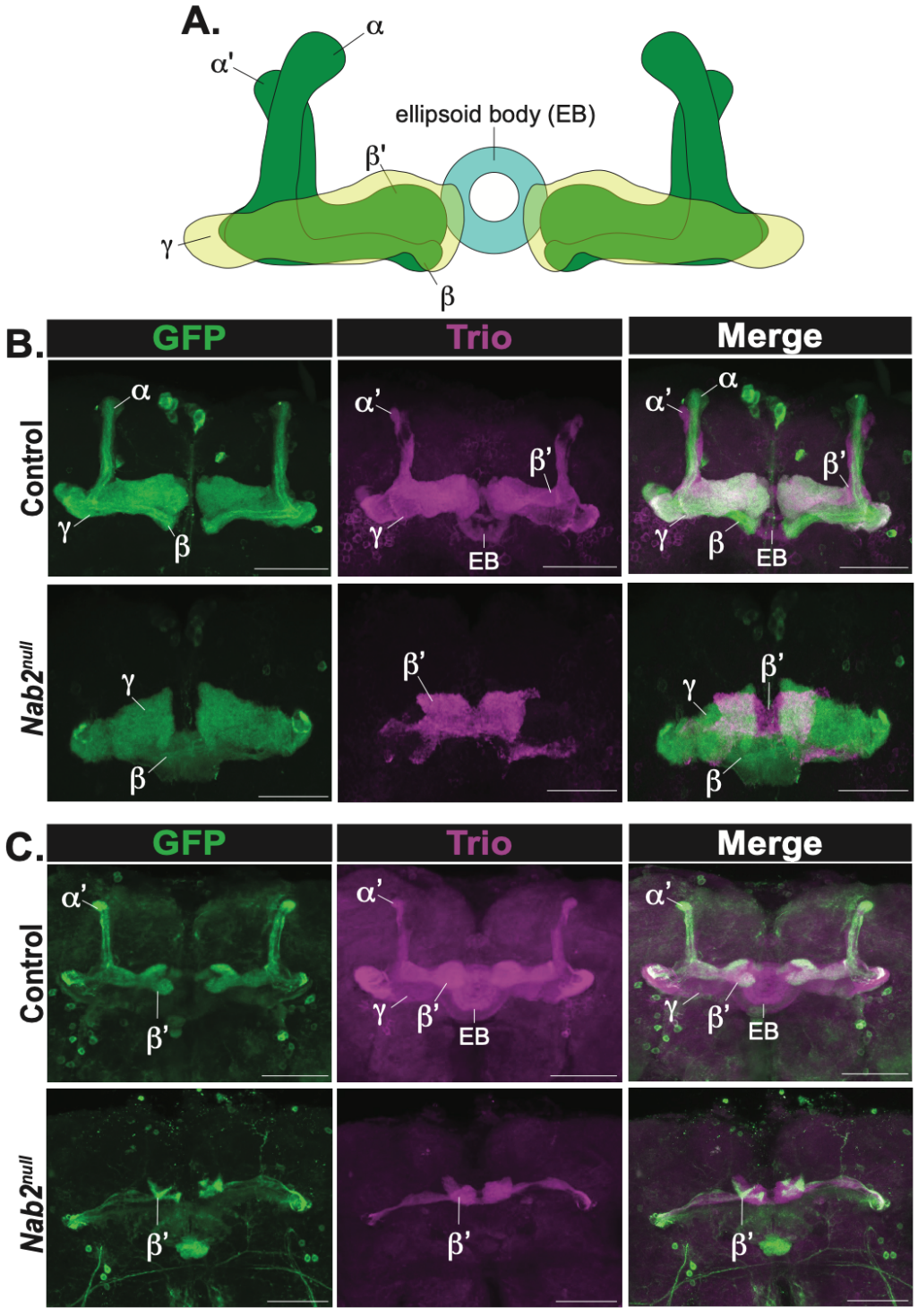

Figure 3-4. Trio is altered in the *Nab2*^{null} mushroom body. (**A**) Diagram of the adult *Drosophila* mushroom body lobes depicting axons of the medially projecting gamma (γ) neurons, the vertical alpha (α) and alpha prime (α') neurons, the medially projecting beta (β) and beta prime (β') neurons, and the ellipsoid body (EB).(**B**) Immunofluorescence images of Control (*w-;UAS-*

mcd8::GFP/201Y-Gal4;;) and *Nab2*^{null} (*w-;UAS-mcd8::GFP/201Y-Gal4;Nab2*^{null}*;*) mushroom bodies driving *UAS-mcd8::GFP* under the α, β, γ lobe-specific mushroom body *201Y-Gal4* driver. (**C**) Immunofluorescence images of Control (*w-;UAS-mcd8::GFP/C305a-Gal4;;*) and *Nab2*^{null} (*w-;UAS-mcd8::GFP/C305a-Gal4;Nab2*^{null}*;*) mushroom bodies driving *UAS-mcd8::GFP* under the α' and β' lobe-specific mushroom body *C305a-Gal4* driver. False colored panels show fluorescence corresponding to α-GFP (green, mcd8::GFP), α-trio (purple), and merges of the channels. At least 25 brains were analyzed for each genotype. Scale bar = 50 μm.

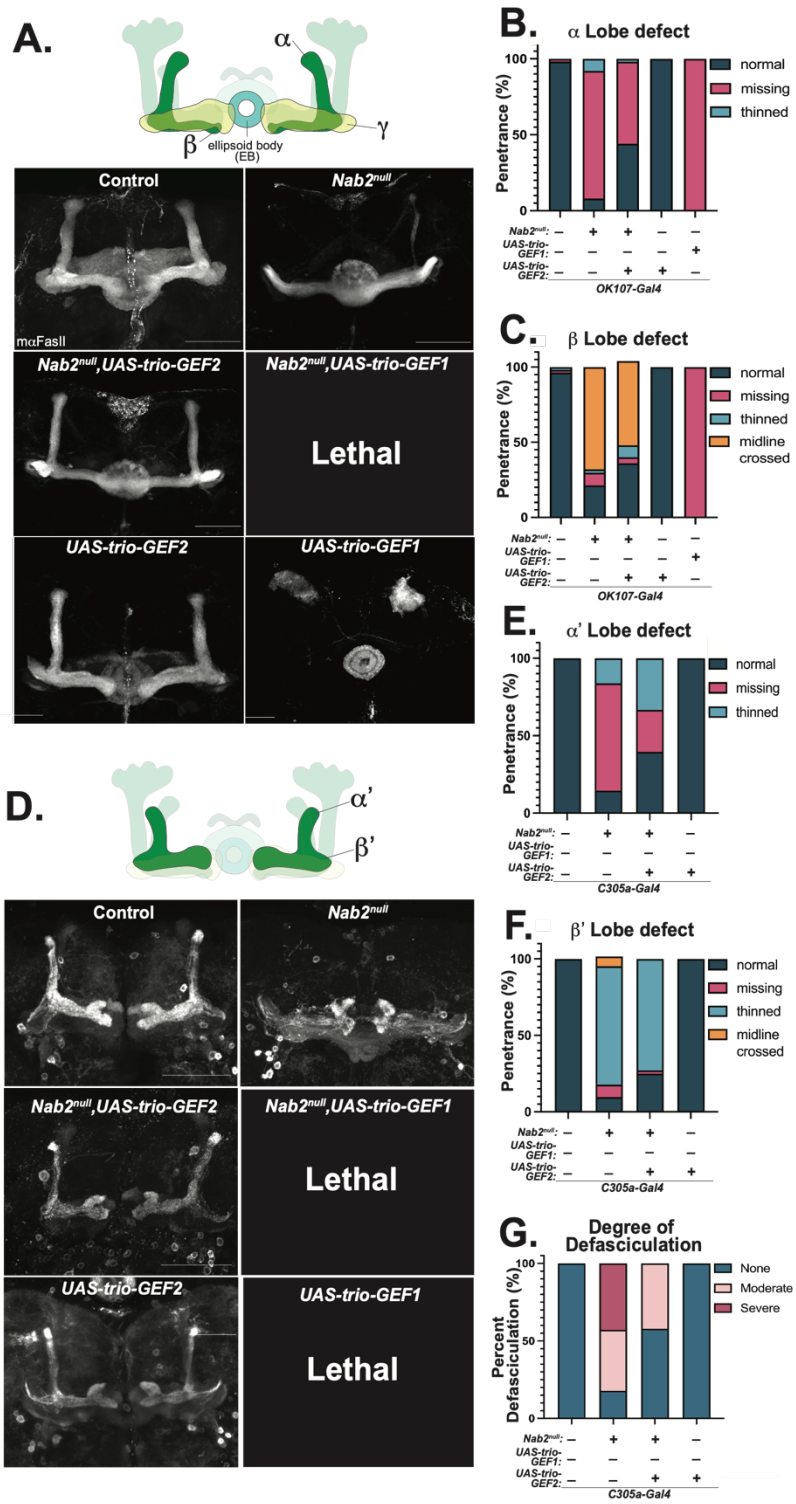

Figure 3-5. Expression of Trio GEF2 rescues α/α' and β' defects in *Nab2*^{null} mushroom bodies. **(A)** Top: Schematic of the *Drosophila* mushroom body with lobes stained by α-Fasciclin II (FasII) highlighted. Bottom: Representative max projections of mushroom bodies of indicated genotypes

stained by α-FasII. (**B**) Quantification of frequency of α lobe defects in each indicated genotype. (**C**) Quantification of frequency of β lobe defects in indicated genotypes. (**D**) Top: Schematic of the *Drosophila* mushroom body with lobes overexpressing *mcd8::GFP* under the *C305a-Gal4* driver highlighted. Bottom: Representative max projections of mushroom bodies of indicated genotypes stained with α-GFP. (**E**) Quantification of frequency of α' lobe defects in each indicated genotype. (**F**) Quantification of frequency of β' lobe defects in indicated genotypes. (**G**) Quantification of defasciculation phenotype severity in the indicated genotypes. At least 25 brains were analyzed for each genotype. Scale bar = 50 μm.

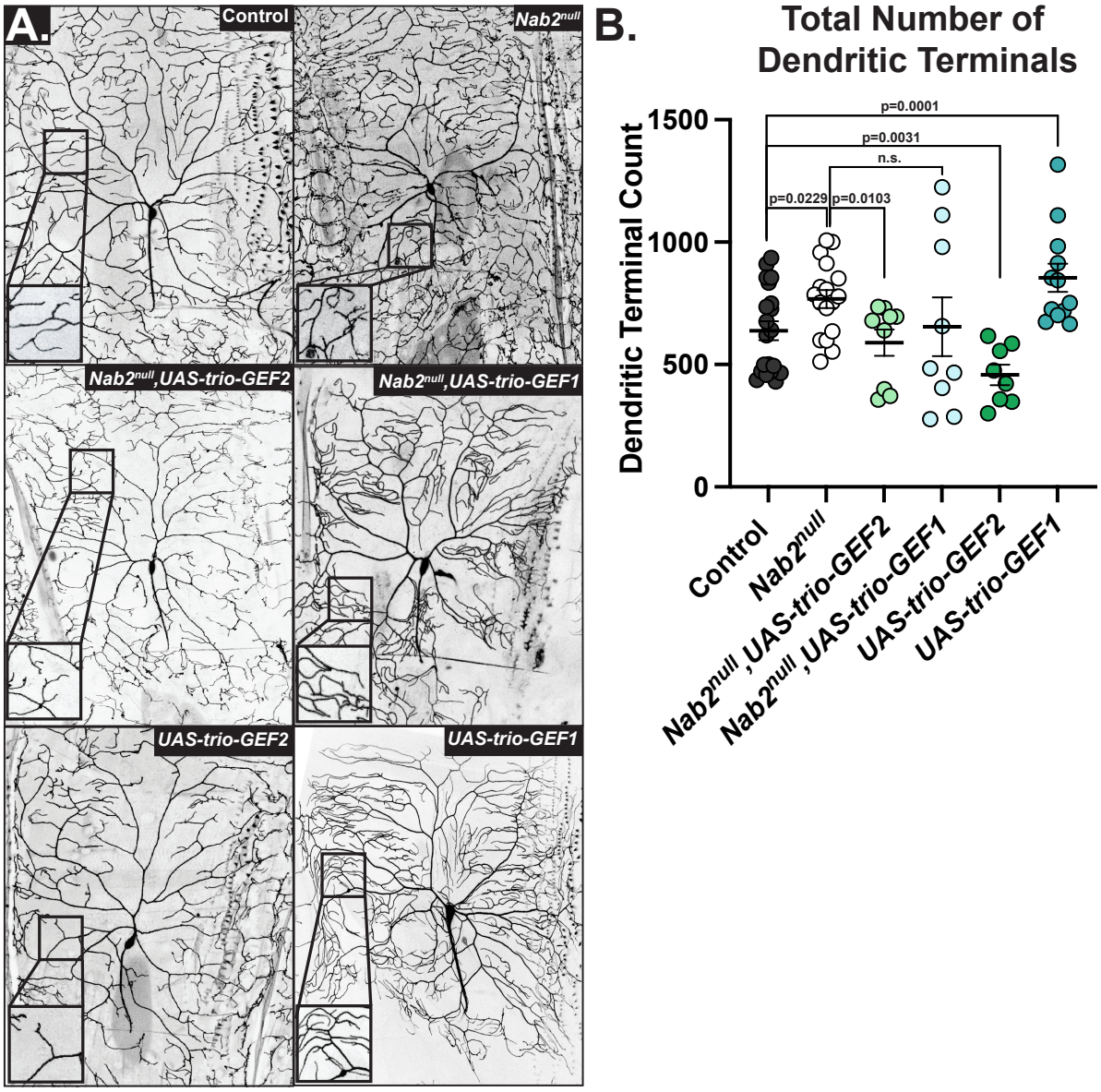

Figure 3-6. Expression of Trio GEF2 rescues *Nab2*^{null} dendritic arborization defects in class IV ddaC sensory neurons. (**A**) Maximum intensity projections of *Drosophila* class IV ddaC neurons from Control, *Nab2*^{null}, *Nab2*^{null} *UAS-Trio-GEF2, Nab2*^{null} *UAS-Trio-GEF1, UAS-Trio GEF2, and UAS-Trio-GEF1* L3 larvae. Inset black boxes show high magnification views of dendritic arbors. (**B**) Quantification of total number of dendritic terminals for each genotype. At least 8 neurons were measured for each genotype. Significance values are indicated.

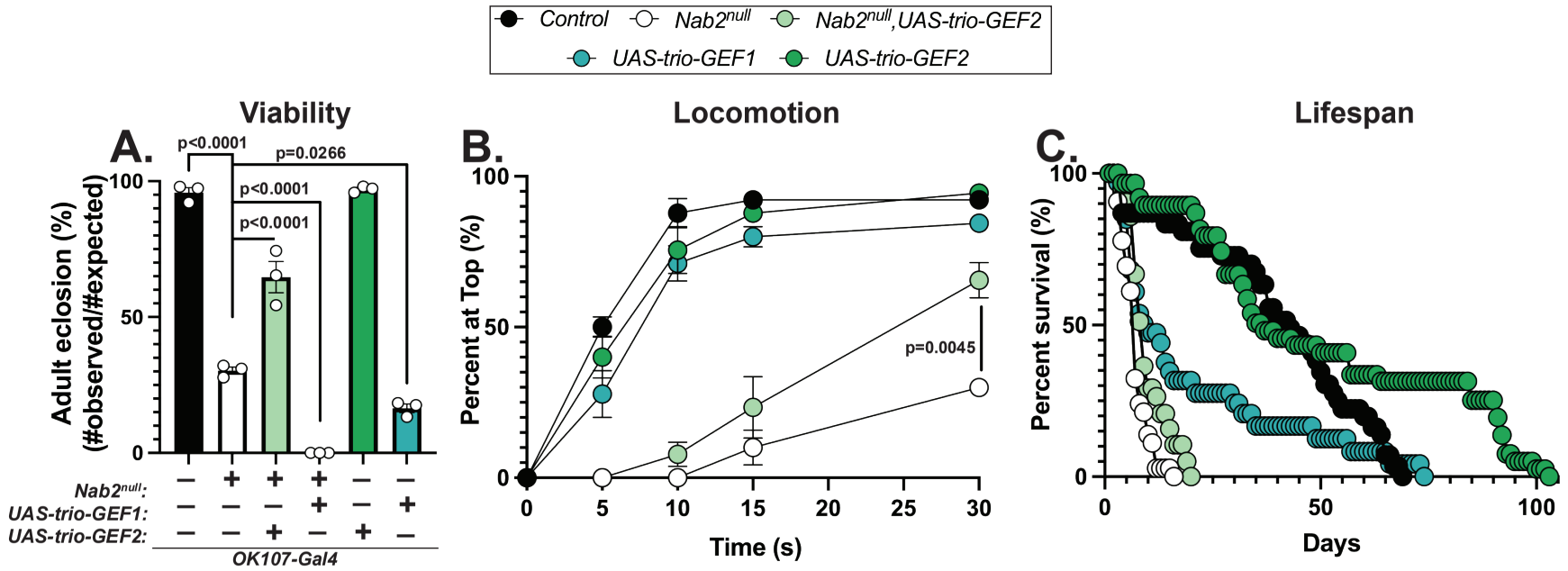

Figure 3-7. Expression of Trio GEF2 rescues *Nab2*^{null} defects in viability and locomotion. (**A**) Percent of Control, *Nab2*^{null}, *Nab2*^{null} *UAS-Trio-GEF2, UAS-Trio GEF2,* or *UAS-Trio-GEF1* that eclose as viable adults (calculated as #observed/#expected) using the *OK107-Gal4* mushroom body driver. (**B**) Negative geotaxis of age-matched adult flies of indicated genotypes over time in seconds (s). (**C**) Survival of age matched adult flies of the indicated genotypes over time in days. At least three biological replicated were tested for each genotype. Significance values are indicated .

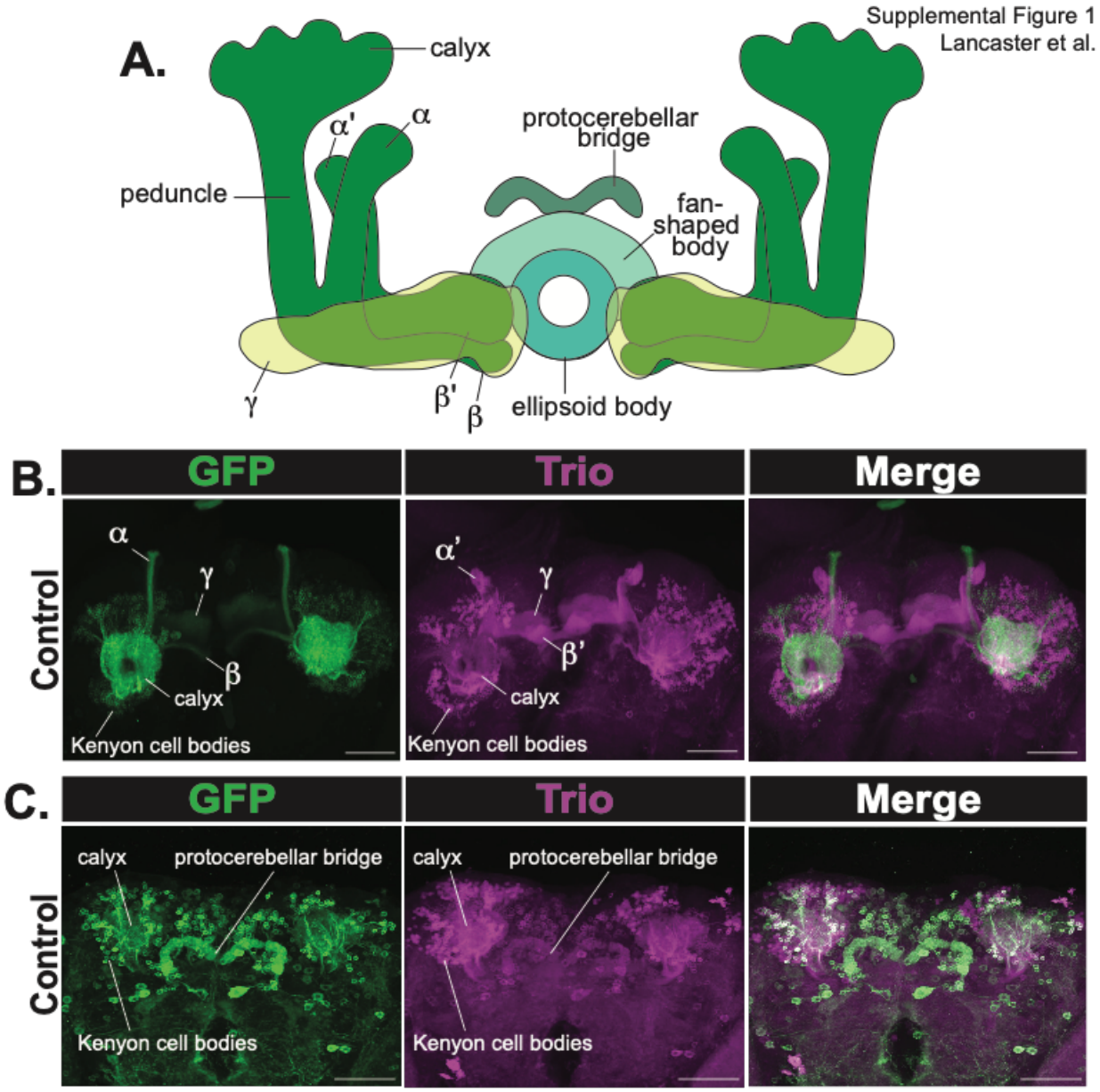

Supplemental Figure 3-1. Trio is present in *Drosophila* Kenyon cell bodies and Caylx. (**A**) Diagram of the adult *Drosophila* mushroom body depicting the Caylx, peduncle, protocerebellar bridge, fan-shaped body, ellipsoid body, and axons of the vertically projecting alpha (α) and alpha prime (α') neurons, the medially projecting gamma (γ), beta (β), and beta prime (β') neurons. (**B**) Immunofluorescence images of Control (*w-;UAS-mcd8::GFP/201Y-Gal4;;*) mushroom bodies driving *UAS-mcd8::GFP* under the α, β, γ lobe-specific mushroom body *201Y-Gal4* driver. (**C**) Immunofluorescence images of Control (*w-;UAS-mcd8::GFP/C305a-Gal4;;*) mushroom bodies driving *UAS-mcd8::GFP* under the α' and β' lobe-specific mushroom body *C305a-Gal4* driver. False colored panels show fluorescence corresponding to α-GFP (green, mcd8::GFP), α-trio (purple), and merges of the channels. At least 25 brains were analyzed for this analysis. Scale bar = 50 μm.

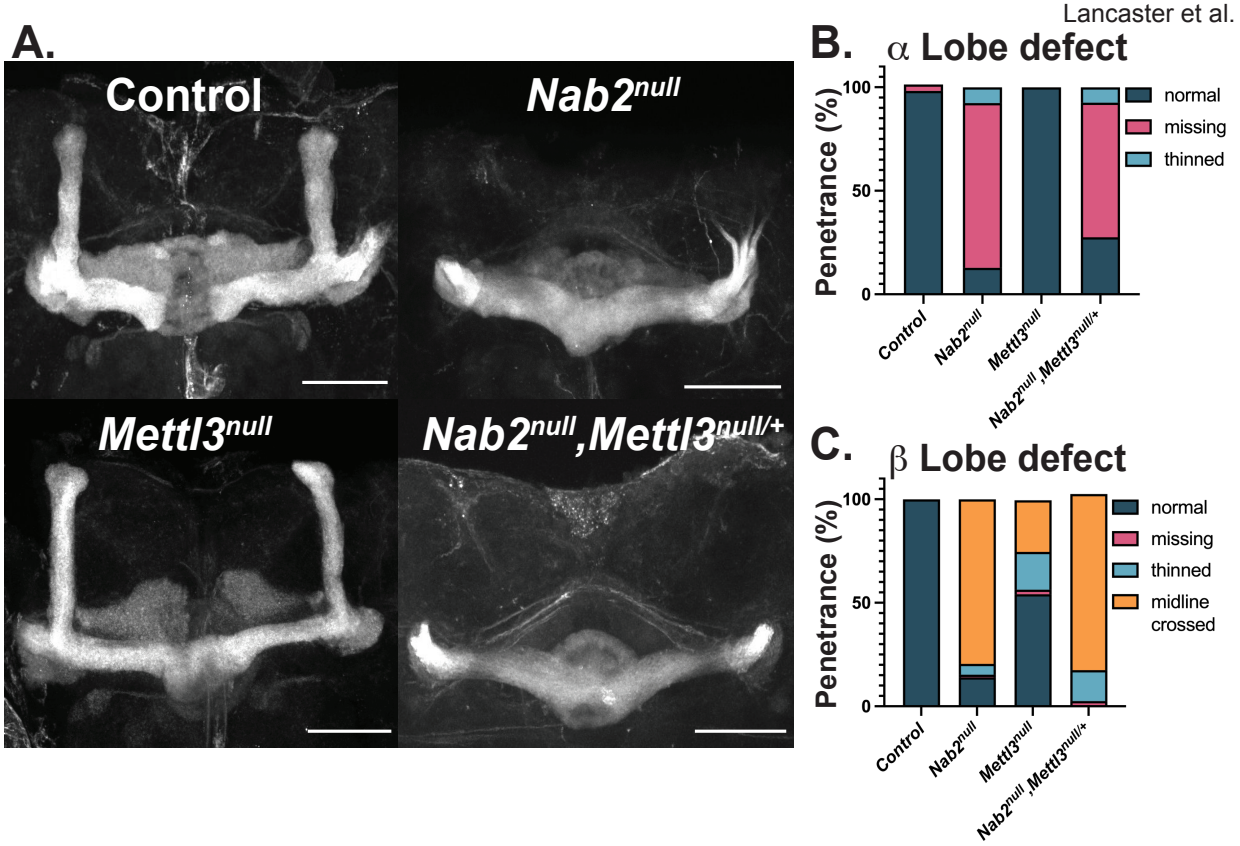

Supplemental Figure 3-2. Heterozygosity for Mettl3 does not dominantly rescue *Nab2*^{null} mushroom body phenotypes. (**A**) Representative max projections of mushroom bodies of indicated genotypes stained by α-FasII. (**B**) Quantification of frequency of α lobe defects in each indicated genotype. (**C**) Quantification of frequency of β lobe defects in indicated genotypes. Morphology of at least 25 brains was assessed for each genotype. Scale bar = 50 μm.

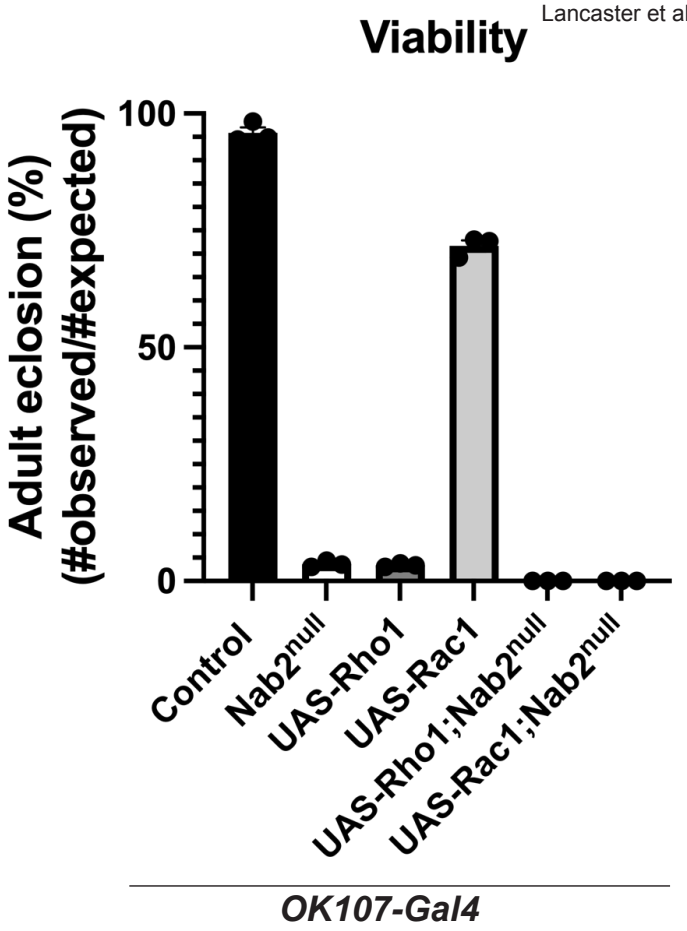

Supplemental Figure 3-3. Expression of Rac1 or Rho1/A in the mushroom body of *Nab2*^{null} flies is lethal. (**A**) Percent of Control, *Nab2*^{null}, *UAS-Rho1, UAS-Rac1, UAS-Rho1;Nab2*^{null} and *UAS-Rac1;Nab2*^{null} flies that eclose as viable adults (calculated as #observed/#expected) using the *OK107-Gal4* mushroom body driver. The viability of at least 100 larvae were analyzed for each genotype and biological replicate. Biological triplicates were performed for each genotype.

CHAPTER 4: EXPANDED DATA

Outcrossing the *Nab2^{ex3}* allele to improve *Nab2^{ex3}* adult viability

The *Nab2^{ex3}* stock experiences periods of unexplained loss of viability, ultimately reaching viability frequencies close to 0% of the expected eclosion rates. As a result of this near-lethal status, experiments requiring *Nab2^{ex3}* adult flies become extremely difficult or even impossible to perform within normal timelines, and productivity rates reach low points. In response to this challenge, the previous graduate student, Dr. J. Christopher Rounds, found that outcrossing the *Nab2^{ex3}* allele to a control stock can return the stock to its original viability at 3-5% (the viability is still very low) making collecting flies for experiments slightly less daunting and time-consuming. During my tenure as a graduate student, the *Nab2^{ex3}* stock once again fell lethal, and I therefore performed outcrossing and recovery of the *Nab2^{ex3}* allele for improved viability.

The *Drosophila* outcrossing scheme for *Nab2^{ex3}* outcrossing and recovery is detailed in **Figure 4-1A**. This outcross was performed using the control *W^{1118}* fly line. In hindsight, I probably should have performed this by outcrossing *Nab2^{ex3}* to isogenic control flies (*iso-1*). However, at the time I was new to the lab, the iso-1 stock had died during the COVID-19 pandemic, and I did not have the experience or knowledge under my belt to know the difference between *iso-1* and *W^{1118}* (I figured a control fly was a control fly). This mistake does not change much, other than the fact that the new *Nab2^{ex3}* allele may have a genetic background more similar to *W^{1118}* than *iso-1.*

The outcrossing scheme begins by crossing virgin *W^{1118}* females to *Nab2^{ex3}/TM6B,w+* males. F1 progeny that inherit the *Nab2^{ex3}* allele (and not the recombination-suppressing *TM6B,w+* balancer chromosome) are mated to one another.

In F2 progeny, any homozygous *Nab2*^{ex3} flies are removed (wings held out, kinked bristles), and a sibling cross is performed in bulk. Another bulk sibling cross is performed for F3 progeny, and once again, *Nab2*^{ex3} homozygotes are removed. In the F4 generation a single virgin female *Nab2*^{ex3} homozygote was recovered (Honestly, I should dedicate this thesis to this individual virgin) and crossed to four males of the *w-;;TM3/TM6B,w+* balancer line. Critically, this cross was performed on Pen-Strep food to prevent fungal and bacterial colonization of the vial which could have killed the flies and/or resulting progeny. Finally, virgin *Nab2*^{ex3}/TM6B,w+ females were crossed to *Nab2*^{ex3}/TM6B,w+ males of this progeny to establish the "new" *Nab2*^{ex3} stock. Confirmation of the genotype is performed via RT-PCR analysis and Sanger sequencing using primers flanking the *Nab2*^{null} P-element excision (*EY08422*).

The viability of these flies increased from almost 0% to approximately 18% (**Figure 4-1B**). Moreover, the new, outcrossed *Nab2*^{ex3} allele dramatically reduced the female: male sex skew observed in the previous stocks[215,274]. Unfortunately, I did not perform any calculations of the sex-skew improvement, so these data are anecdotal. However, when Dr. J. Christopher Rounds performed this outcross before me, he noted that the original stock had a sex skew of 5.7:1, reflecting an unknown male-specific reduction in viability. After Dr. Rounds outcrossed this stock, he noted a reduction in the sex-skew to 1.6:1, indicating that the outcross substantially suppresses this sex-specific viability defect. Thus, the reduced sex-skew I observed may have been similar to the results obtained by Dr. Rounds.

In summary, outcrossing the *Nab2*^{ex3} allele significantly suppresses *Nab2*^{ex3} viability and sex-skewing defects that worsen over time. Thus, in the outcrossed stock,

the effects of genomic Nab2 loss have likely been separated from the effects of a genetic background or epigenetic modifier in the previous *Nab2*^{ex3} stock, thereby improving viability and sex-skewing ratios. Moreover, the ability to outcross this stock greatly improves experimental feasibility by making *Nab2*^{ex3} adults easier to collect and therefore work with.

Preliminary evidence suggests Sxl regulates mushroom body morphology in the female brain

Drosophila melanogaster like most other creatures in the animal kingdom display highly stereotyped, sexually dimorphic physical characteristics and behaviors[451]. As discussed briefly in **Chapter 1.6.b** and **Chapter 2** there are genetic pathways that translate chromosomal sex (XX or XY) into sexually dimorphic behaviors and phenotypes. Intriguingly, recent studies suggest there are anatomical and functional differences between *Drosophila* male and female central nervous systems[452,453]. To date, few gross structural dimorphisms have been found and those that have been uncovered are relatively small[454,455]. For example, the *Drosophila fruitless* (*fru*) gene has been postulated to be a neural sex determination factor that directs development of the CNS, thereby producing male-typical courtship behavior[456,457]. Male-specific Fru (FruM) is expressed in small groups of neurons throughout the male CNS, indicating that FruM may 'masculinize' certain neurons to establish male-specific behaviors[458].

Fru is downstream of *tra* the sex-determination splicing cascade discussed in **Chapter 1.6.b**. Indeed, in XX animals expressing Sxl protein, Tra forms a heterodimer with Tra-2, which modulates the splicing of both *dsx* and *fru* (not pictured in **Figure 1-15**) generating sex-specific splicing products that encode a nonfunctional female-specific

FruF protein and the DsxF protein[459]. DsxF goes on to control the expression of genes necessary for female sex differentiation and behavior. In XY animals, no Sxl protein is produced and consequently, no functional Tra is made. Thus, *fru* and *dsx* undergo male-specific splicing to produce male-specific FruM and DsxM proteins which control the expression of target genes necessary for male-specific sex differentiation[459]. Despite our understanding of the molecular mechanisms underlying *Drosophila* sex-determination, we have a very limited understanding of differences in sexual development in the *Drosophila* brain.

As discussed, throughout this thesis, the Nab2 RNA binding protein has well established roles as a regulator of nervous system development. Specifically, Nab2 plays a critical role in the regulation of mushroom body morphology (introduced in **Chapter 1.4.b** and discussed in **Chapter 3**) within the *Drosophila* CNS. A requested experimental revision by a reviewer of **Chapter 2** of this thesis was to determine whether masculinized splicing and loss of Sxl protein levels in the female $Nab2^{null}$ brain contributed to the mushroom body morphology defects observed in *Nab2* mutant flies. To being to address this question, we started by testing whether Sxl, a female-specific RNA binding protein, regulates mushroom body morphology in the female brain. A transgene encoding *Sxl* RNAi (*UAS-SxlRNAi*) was expressed in all mushroom body lobes using the *OK107-Gal4* driver, which would deplete the Sxl protein.

As shown in **Figure 4-2, A-C**, *OK107/+* (control) and males overexpressing *Sxl-RNAi* within the mushroom body (*UAS-SxlRNAi;OK107)* have no gross morphological defects in mushroom body structure. Shockingly, females overexpressing *Sxl-RNAi* within the mushroom body exhibit severe morphological defects in the α lobe (missing or thinned) and β lobe (missing, thinned, or midline crossed) structures as detected by α-FasII staining, which specifically

recognizes the α, β and weakly the γ lobes (**Figure 4-2, A-C**). These results imply a role for the female-specific Sxl RBP in regulating mushroom body morphology within the female and suggest sex-specific mechanisms for regulating gross anatomical structures within the female *Drosophila* brain.

Despite the interesting nature of these results, further studies are required to validate a role for Sxl in regulation of mushroom body morphology. Indeed, validation with another *UAS-Sxl-RNAi* line would be the first step in verifying these results. Secondly, determining the localization of Sxl in the female brain by co-staining with α-Sxl antibody and an α-FasII antibody would reveal whether Sxl is enriched within the *Drosophila* mushroom body. Finally, recombining the *UAS-SxlRNAi* allele with the *Nab2*^{null} allele would reveal whether further loss of Sxl levels in the *Nab2*^{null} female brain exacerbates established *Nab2*^{null} mushroom body defects.

In truth, these results bring up far more questions than answers, which is why these results were omitted from the published version of **Chapter 2** of this thesis. For instance, why would a sex-specific protein govern axon guidance of an anatomical structure shared by both male and female flies? If Sxl indeed plays a role in patterning these axons, are some of these axons 'feminized'? If so, are mushroom body axons in males without Sxl expression 'masculinized'? Evidence suggests that the *Drosophila* mushroom body is not required for courtship behavior in flies[460]. If this is the case, what is the biological purpose of sexually dimorphic axon guidance mechanisms in the *Drosophila* mushroom body? What are the mechanisms underlying this phenotype? Are there other CNS or PNS structures that are regulated in a sexually dimorphic manner? All these questions and many more will have to wait until more data emerge about a role (or lack thereof) for Sxl in patterning CNS axon development. This experiment is truly the basis for an entirely different thesis project that has nothing to do with Nab2, which is why we left this alone. My hope is that one day someone will follow up on these interesting data and begin to answer some of the questions that have been swimming around my brain.

Preliminary evidence suggests Nab2 causes ectopic methylation of the *trio M* transcript

To more precisely define how loss of Nab2 alters the relative abundance and/or location of m^{6}A deposition along the *trio M* transcript, we utilized *in vitro* DART-Sanger sequencing (Deamination adjacent to RNA modification Targets followed by Sanger sequencing) [372,373] (**Figure 4-3**). This method overcomes several limitations of traditional antibody-based methods including limited sensitivity and selectivity, and struggle to distinguish m^{6}A from other RNA modifications (i.e., m^{6}Am) [372]. Briefly, *in vitro* DART-Sanger sequencing involves incubating RNA with a chimeric fusion protein consisting of the deaminating enzyme APOBEC1 fused to the m^{6}A-binding YTH domain of m^{6}A 'reader' proteins. As m^{6}A-modified adenosine (A) residues are followed by a cytosine (C) residue in the most common consensus sequence [126,372,374], the APOBEC-YTH fusion recognizes m^{6}A-modified A and deaminates the neighboring C, creating a uracil (U) base which is read as a thymine (T) during Sanger sequencing. Therefore, C-to-U transitions and the frequency at which they occur permit mapping of m^{6}A location and relative abundance. Thus, this method enables us to define the m^{6}A modification status of the *trio M* transcript comparing Control to *Nab2^{null}* heads. For this experiment, we treated RNA extracted from Control or *Nab2^{null}* heads with APOBEC1-YTH, and subsequently performed RT-PCR with primers that amplify *trio M* exon 1- intron 1- exon 2 boundaries. Sanger sequencing and subsequent analysis of C-to-U transitions revealed the presence of three m^{6}A within the exon 1- intron 1- exon 2 region of *trio M* in Control heads (green lollipops; **Figure 4-3**). Interestingly, these sites do not fall within or adjacent to sites mapped in a previous

study of *Drosophila* head RNAs, unlike our DART-Sanger seq analysis of *Sxl* [147]. Shockingly, this n=1 analysis mapped 16 ectopic m^{6}A sites along the *trio M* on 1- intron 1- exon 2 boundaries in *Nab2^{null}* heads (red lollipops; **Figure 4-3** top and three examples on sites 5, 8, and 12 on bottom of Figure). These results are consistent with a role for Nab2 in inhibiting ectopic m^{6}A methylation on the *trio M* pre-mRNA transcript and suggest that modulation of m^{6}A levels may link Nab2 to other RNA targets within the *Drosophila* head transcriptome.

Further analysis is required to validate these n=1 results. DART-Sanger sequencing of the *trio M* transcript was challenging for several reasons, and I was only able to capture these results one time. For instance, intron 1 of the *trio M* transcript is very long (approximately ~4kb in length), meaning that removal of this intron likely requires a sophisticated molecular mechanism. For example, it is possible that intron 1 is spliced recursively (in a multi-step slicing reaction). However, our RNA sequencing reads from *Drosophila* heads were produced from short-read sequencing of mRNAs (**Chapter 2**), meaning that information about the precise structure of individual RNAs is lost. Thus, the precise structure of this region of the *trio M* transcript is not known. This makes designing primers to properly amplify a transient pre-mRNA species in enough abundance for sanger sequencing uniquely challenging. In the future, direct RNA sequencing of mRNAs from *Drosophila* heads will be performed to validate whether loss of Nab2 causes ectopic m6A methylation and this approach will also provide long-read sequencing information to detail the structure of the exon 1- intron 1- exon 2 regions of the *trio M* transcript.

Nanopore direct sequencing of poly(A)+ RNA to map m^6A modifications within the *Drosophila* head transcriptome

To date, transcriptome-wide detection of m^6A modifications relies primarily on methods utilizing next generation sequencing (NGS) platforms. There are currently five NGS-based strategies for mapping m^6A modifications: (1) me-RIP-seq and (2) miCLIP which both depend on the use of an anti-m^6A antibody, (3) m^6A-REF-seq/MATZER, and (4) DART-seq, which are both antibody- independent methods. Both me-RIP-seq and miCLIP-seq suffer from high false-positive rates due to non-specific binding of the m6A antibody and the ability of the antibody to recognize other modifications including m^6Am. On the other hand, m^6A-REF-seq/MAZTER seq utilizes an endonuclease that cleaves unmethylated ACA motifs to quantify methylation rates. However, ACA motifs only cover ~16-25% of m^6A sites within the transcriptome. Finally, DART-seq utilizes the APOBEC-YTH fusion protein to induce C-to-U deamination at sites adjacent to m^6A modifications (discussed in detail in **Chapter 2**). However, in my personal experience, I found this method to be experimentally challenging given the abundance of RNA needed to recover to precisely map m^6A modifications within transient pre-mRNA species. Fortunately, Oxford Nanopore Technologies has developed an exciting alternative method for mapping RNA. This sequencing platform directly sequences RNA (thus there is no need for a PCR amplification step) based on the principle of monitoring shifts in electric current as an RNA molecule passes through a nanopore embedded within a synthetic polymer membrane. Modified bases effect the flow of the current through the pore in a manner distinct from their unmodified counterpart, allowing detection of modifications at a single-nucleotide level (**Figure 4-4A**).

To determine how loss of Nab2 effects the levels and location of m6A modifications on mRNA within *Drosophila* nervous tissue, we piloted an Oxford Nanopore direct RNA sequencing approach. By mapping m^6A modifications in Control, *Nab2*^{null}, and *Mettl3*^{null} (negative control) heads we will be able to more clearly define how Nab2 regulates levels of m6A on target mRNAs. We piloted this experiment with the help and expertise of the Emory Integrated Genomics Core (EIGC). Because this a direct-RNA sequencing approach, and there is no library amplification step, a large concentration of input RNA is required to yield quality results. The EGIC requested 10μg of total RNA for the experiment, and figuring conservatively, I collected and extracted RNA from approximately 500 female *Drosophila* heads from each genotype. We chose to only perform the pilot experiment on female heads because of the known effect of Nab2 on the regulation of Sxl splicing and protein levels (see **Chapter 2**). To isolate mRNA species from the total RNA sample, poly(A) enrichment was performed followed by annealing and ligation of a reverse transcription adapter. Next, the RNA goes through reverse transcription to generate a complimentary cDNA strand followed by attachment of primers for sequencing that contain a motor protein which facilitates threading of the mRNA through the nanopore (Figure **4-4B**). The sequencing of our RNA samples was performed in early June of 2024, and hopefully with the help of the EIGC we will get some exciting new data to help us better understand how Nab2 regulates the *Drosophila* head epitranscriptome.

Figure 4-1

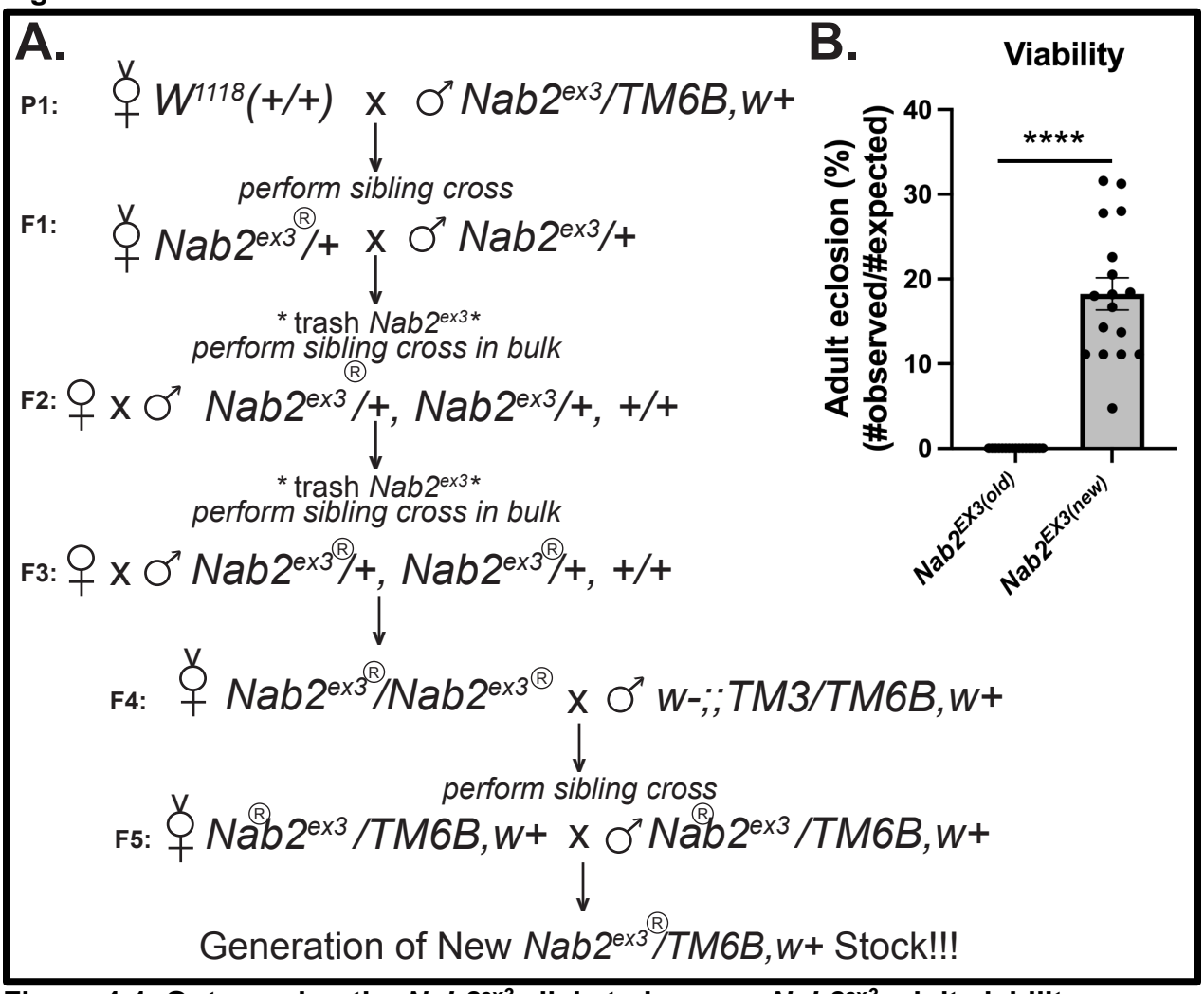

Figure 4-1. Outcrossing the *Nab2^{ex3}* allele to improve *Nab2^{ex3}* adult viability
(**A**)The outcrossing and allele recovery scheme for the *Nab2^{ex3}* allele. The circled "R" indicates a recombined chromosome. (**B**) The new, outcrossed *Nab2^{ex3}* allele exhibits increased adult viability compared to the old *Nab2^{ex3}* allele. Significance values indicated (****p≤0.0001).

Figure 4-2

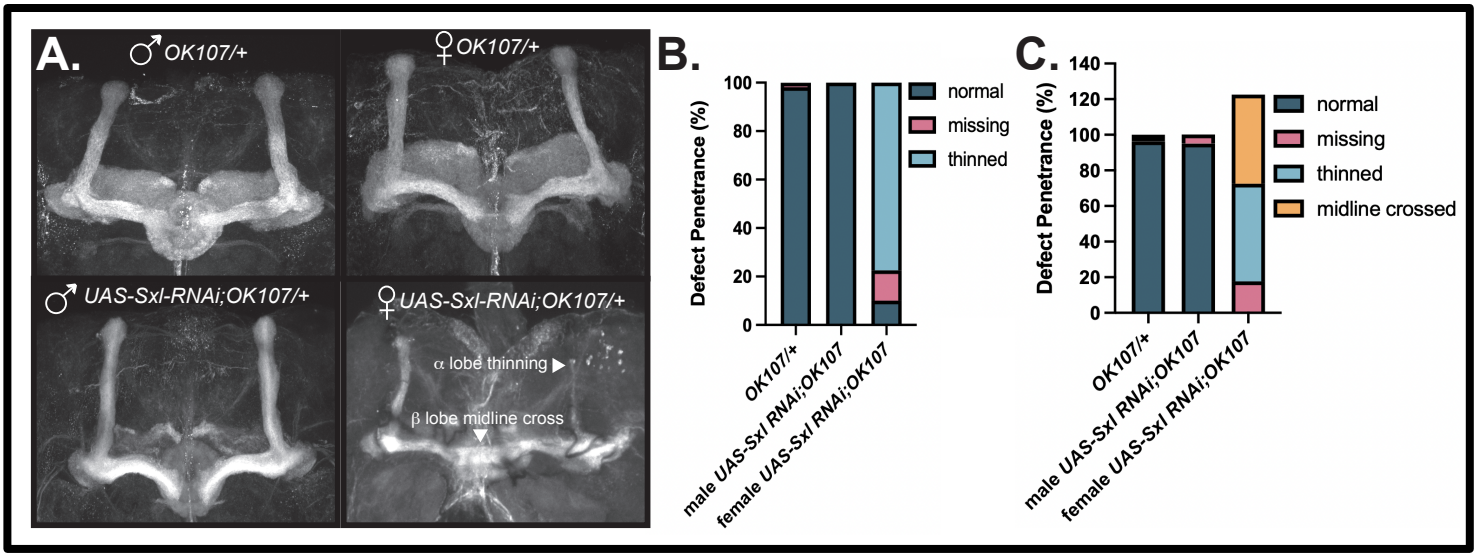

Figure 4-2. Preliminary evidence suggests Sxl regulates mushroom body development in the female brain. (**A**) Representative max projections of mushroom bodies of indicated genotypes stained by α-FasII. (**B**) Quantification of frequency of α lobe defects in each indicated genotype. (**C**) Quantification of frequency of β lobe defects in indicated genotypes.

Figure 4-3

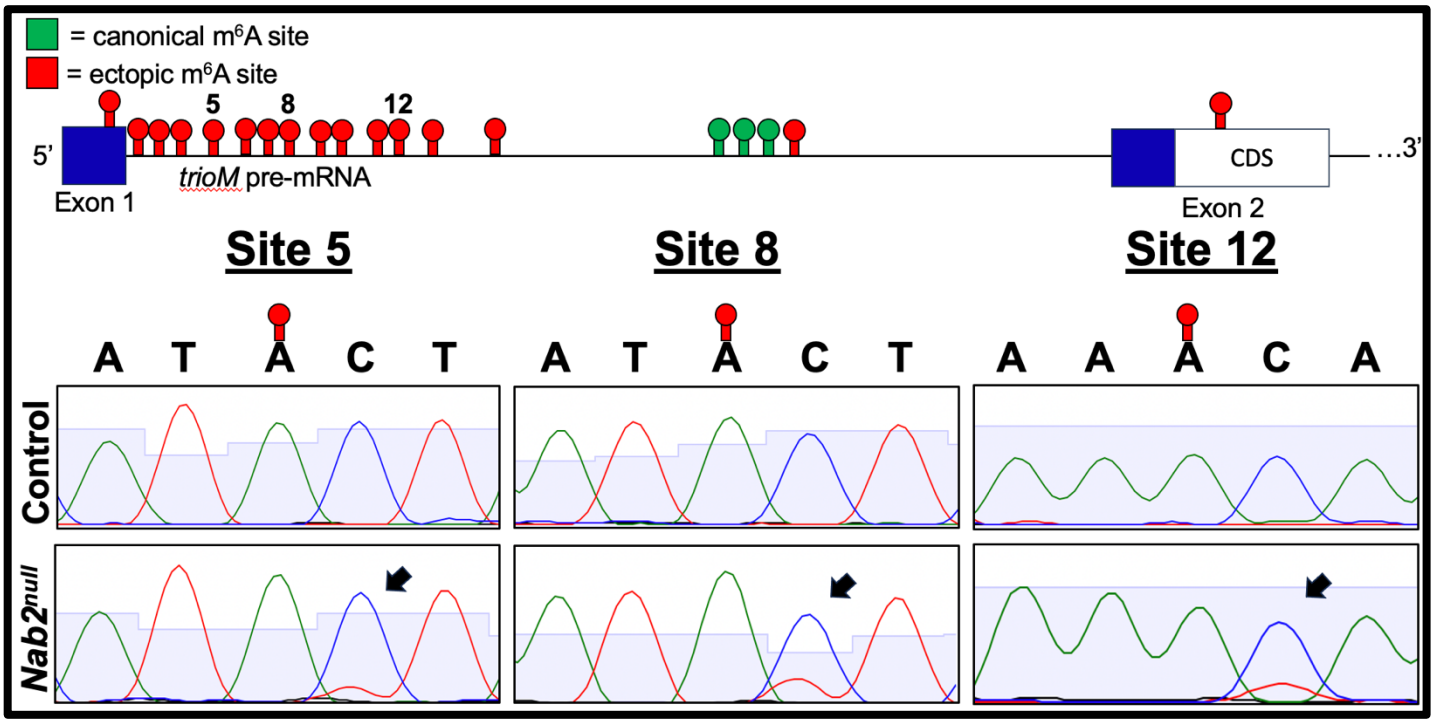

Figure 4-3 Preliminary evidence suggests that loss of Nab2 causes ectopic methylation of the Exon 1-Intron 1- Exon 2 boundary of the *trio M* transcript. (Top) Schematic of the *trio M* exon 1- intron 1 – exon 2 boundaries with mapped m6A sites (lollipops) by DART sanger sequencing (green lollipops= canonical m^{6}A sites); red lollipops= ectopic m^{6}A sites. (Bottom) Example of Sanger sequencing reads from sites 5, 8, and 12, showing C-to-T transitions in *Nab2^{null}* ectopic m^{6}A sites (black arrows) that are not present in Control.

Figure 4-4

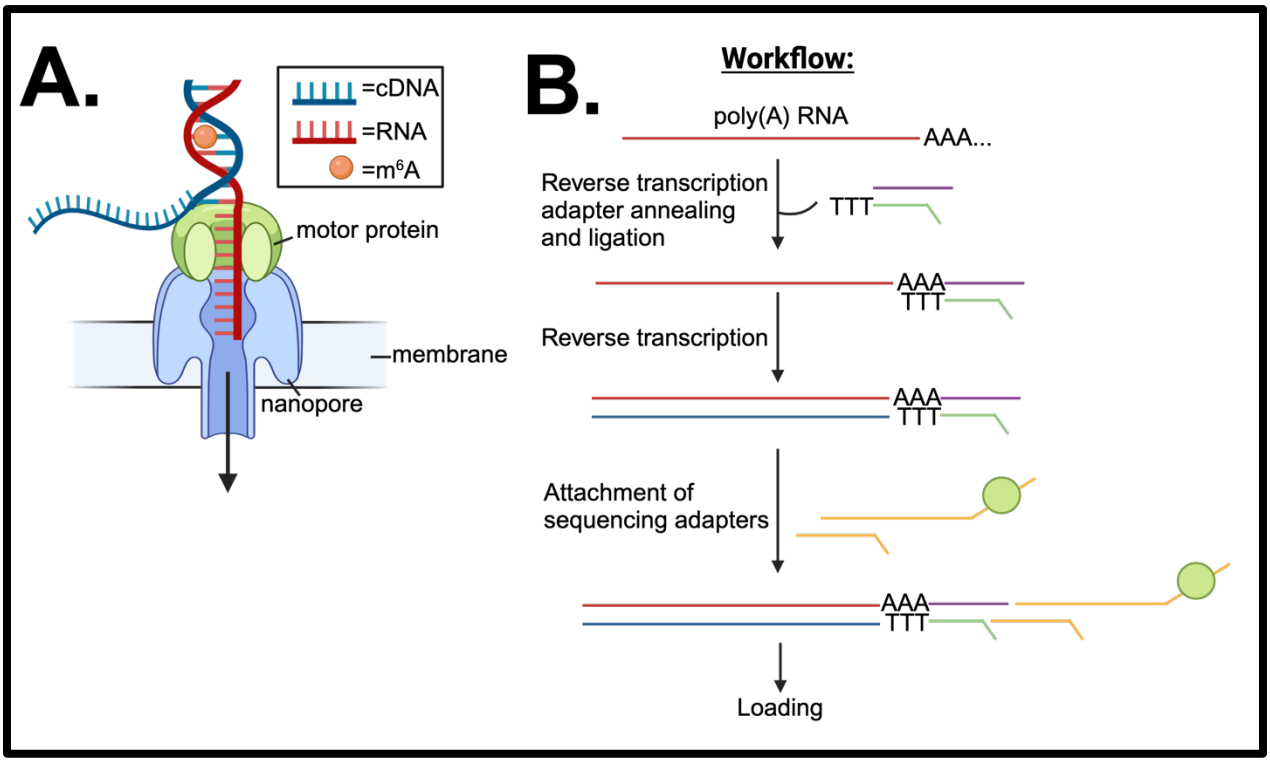

Figure 4-4 Nanopore direct RNA sequencing. (**A**) Schematic of RNA (red) being threaded through a nanopore (blue). (**B**) Library prep workflow for nanopore direct sequencing of RNA. First, reverse transcription adapters are annealed and ligated to the poly(A) RNA. Next reverse transcription is performed to generate a complementary cDNA strand from the poly(A) RNA molecule. Finally, sequencing adapters with the motor protein are attached and the library can be loaded onto a flow cell.

CHAPTER 5: DISCUSSION AND CONCLUSION

This chapter has been written by Carly L. Lancaster specifically for inclusion in this thesis dissertation.

DISCUSSION

Chapter-by-chapter discussion of research performed, and questions answered herein

Here, we identify a role for the *Drosophila* Nab2 RBP and Mettl3 m^6A methyltransferase in regulating the *Sxl* and *trio* mRNAs. The data presented here provide strong evidence that the *Sxl* and *trio* transcripts are key downstream targets of Nab2 in nervous tissue based on both m^6A- and Nab2-dependent splicing events and identifies the specific effects of these transcripts on *Drosophila* organismal phenotypes and neurodevelopment in flies lacking Nab2. The results of this study support a model in which Nab2 regulates transcripts that encode key regulators of neurodevelopment. In the broader context, the phenotypic consequences of loss of an RBP result from the collective changes to numerous target transcripts, and defining the mechanistic basis of these phenotypes requires systematic analysis of how individual targets, such as *Sxl* and *trio*, are impacted. In the case of Nab2, evidence now supports both m^6A-dependent and independent roles in *Sxl* and *trio* mRNA splicing as well as potential effects on downstream processing such as cytoplasmic metabolism of these transcripts. Taken together, these findings support a model where RBPs such as Nab2/ZC3H14 regulate a collection of target transcripts, potentially through multiple mechanisms, that all contribute to downstream phenotypes.

In this thesis, we present extensive experimental evidence addressing gaps in our understanding of Nab2/ZC3H14 function and further define how loss of this critical RBP causes a form of severe intellectual disability. Utilizing *Drosophila melanogaster* as a model, we answer critical questions pertaining to fundamental Nab2 functions in pre-

mRNA processing and neurodevelopment. In **Chapter 2**, we present indirect evidence of Nab2 specificity illustrating a role for Nab2 in the regulation of splicing and steady state levels of select neuronally enriched transcripts within the fly head. Specifically, we demonstrate that loss of Nab2 alters splicing and m^6A levels on the *Sxl* transcript, providing evidence that Nab2 plays a role in regulation of m^6A levels on other transcripts within the brain. In **Chapter 3**, we focus specifically on the Nab2-regulated *trio* transcript encoding a RhoGEF critical for neurodevelopment. We illustrate a critical role for Nab2 and Mettl3 in the regulation of splicing and protein levels of *trio M* and demonstrate that loss of Trio M GEF2-function in *Nab2^{null} Drosophila* contributes to the morphological and phenotypical defects observed in these flies. Finally, in **Chapter 4**, we present the technique by which researchers can clean-up the *Nab2^{null}* stock (originally performed by Dr. J. Christopher Rounds) which exhibits waning viability over time. We further demonstrate that the female Sxl RBP may play a critical role in patterning *Drosophila* mushroom body neurons during development, and finally show that loss of Nab2 may cause ectopic m^6A deposition on the *trio M* transcript, which could contribute to the intron-retention defects observed in *Nab2^{null}* heads. Taken together, these findings expand upon our knowledge of ZC3H14/Nab2 function while also opening up new questions that can be examined in future studies.

In **Chapter 2** of this thesis, RNA-sequencing analysis of *Nab2^{null}* male and female heads provides high-resolution detail of changes to steady-state RNA structure and abundance, defining a critical role for Nab2 in the regulation of splicing and steady-state transcript levels of many neuronally-enriched mRNAs. Unlike the pervasive function of Nab2 in *S. cerevisiae*[8,64,337,461], this experiment provides evidence that *Drosophila* Nab2

only regulates a select subset of mRNAs within head tissue. Intriguingly, many RNAs exhibit statistically significant changes in steady-state abundance upon loss of Nab2, but only a relatively specific set of 453 and 305 transcripts (representing 3.7% and 2.2% of all statistically testable transcripts, respectively) change in abundance by more than 2-fold in females and males, respectively. These results illustrate that Nab2 exerts very specific effects on the *Drosophila* transcriptome. Of these transcripts, an even more specific subset of transcripts exhibit altered splicing patterns based on comparison of exon usage patterns between control and $Nab2^{null}$. These results showed that 151 and 114 transcripts show defects in splicing patterns in females and males, respectively. These data aid significantly in our understanding of how loss of Nab2 alters the brain transcriptome and unveil specific roles for Nab2 in pre-mRNA processing in-line with a very specific role for this RBP in neurodevelopment. However, whether Nab2 regulates each of these transcripts directly, or indirectly via regulation of third-party RBPs remains unclear. In the best example, we demonstrate here that Nab2 regulates splicing and protein levels of the RBP Sxl. Thus, it stands to reason that a subset of transcripts identified in our RNA-seq of female heads may by directly regulated by Sxl, and thereby indirectly regulated by Nab2. Moreover, these data raise questions about the mechanism by which Nab2 regulates splicing and/or levels of each of these transcripts. Indeed, it is possible that Nab2 regulates the abundance of some transcripts via a mechanism independent of its regulation of the abundance of other transcripts. In the same line of thought, the data presented in both Chapter 2 and Chapter 3 of this thesis would argue that Nab2 regulates mRNA structure of some transcripts in an m^6A-dependet manner, and other transcripts in an m^6A-independent manner. Overall, the transcriptomic data

presented here support a model where Nab2 acts via a multitude of distinct mechanisms to regulate the transcriptome. Furthermore these data highlight gaps in our understanding of Nab2 function.

Chapter 2 of this thesis further demonstrates that loss of Nab2 causes missplicing and loss of Sxl protein. As another RBP, Sxl is also a critical regulator of alternative splicing. This prompted analysis of RBP motifs enriched in Nab2-regulated splicing events. Unsurprisingly, Sxl binding sites were highly enriched within Nab2-regulated splicing events in females followed by the hnRNPL homolog *smooth* [*sm*], RNA binding protein 9 [*Rbp9*], the U1-SNRNPA homolog *sans fille* [*snf*], and the U2-SNRNP [*U2AF50*] (**Figure 2-3**). The enrichment for Sxl binding sites among Nab2-regulated splicing events raises the possibility that Nab2 indirectly regulates splicing of some transcripts identified in our RNA sequencing analysis via a Sxl-regulated splicing program. To determine which Nab2-target transcripts are regulated by Sxl, RNA sequencing of Sxl-mutant *Drosophila* heads should be performed allowing comparison between the two datasets. This analysis would allow us to better identify which Nab2-regulated transcripts are directly regulated by Nab2, and which ones are potentially indirectly regulated by Nab2 via Sxl. Moreover, the analysis of RBP motifs enriched in Nab2 regulated splicing events raises the possibility that Nab2 acts in concert with these other RBPs to guide splicing events within the *Drosophila* brain. Future studies should be designed to test genetic and physical interactions between Nab2 and other RBPs such as Sm, Snf, and Rbp9 to further elucidate the mechanism by which Nab2 governs splicing of neuronal transcripts.

The data presented in **Chapters 2**, **3**, and **4** also raise several key questions about the relationship between Nab2 and the Methyltransferase complex: (1) How does Nab2

regulate m^{6}A levels on target mRNAs; and (2) Does Nab2 physically associate with the methyltransferase complex? Each of these questions have been partially answered by the data presented in this thesis as well as in preliminary data in the lab, however, future studies are necessary to thoroughly define the relationship between Nab2 and m^{6}A. To address question (1), there are several mechanisms by which Nab2 could regulate m^{6}A levels on target transcripts. As an RBP that associates with A-rich regions of RNAs[259,264,462], one possibility is that Nab2 could physically bind A-rich regions and occlude access to these sequences by the methyltransferase machinery. Supporting this model, loss of Nab2 causes an increase in levels of m^{6}A on canonical sites of the *Sxl* transcript, particularly on a site directly adjacent to the putative Nab2-binding site ($AC(A)_{13}$; **Figure 2-6**) within Intron 3 (**Figure 2-6**), and preliminary evidence suggests loss of Nab2 causes ectopic methylation on non-canonical sites of the *trio M* transcript (**Figure 4-3**). On the other hand, Nab2 could recruit the m^{6}A machinery to specific sites on a given transcript which is also supported by the preliminary evidence that loss of Nab2 causes ectopic methylation on the *trio M* transcript (**Figure 4-3**)**.** Another (almost heinous) possibility is that Nab2 could recruit an unidentified *Drosophila* m^{6}A eraser protein to target transcripts to regulate m^{6}A methylation states. This mechanism could explain why loss of Nab2 results in an increase in m^{6}A levels on the *Sxl* transcript (**Figure 2-6**). To date, no m^{6}A eraser has been identified in *Drosophila*, and while our data do not support a role for Nab2 as a recruiter of an m^{6}A eraser, this model remains within the realm of possibility as a potential molecular mechanism by which Nab2 could govern m^{6}A levels. Moreover, Nab2 could regulate m^{6}A through a mechanism requiring physical association with the methyltransferase machinery. Preliminary experiments performed by Dr. Sara

Leung in the Corbett lab provide evidence that ZC3H14 interacts with Mettl3, the catalytic subunit of the methyltransferase complex, in human cell culture lysates. However, these results remain preliminary, and a co-IP from *Drosophila* head lysates has yet to be performed. Taken together, future experiments will further define the mechanism by which Nab2 regulates m^{6}A levels and locations on target transcripts.

To gain a better understanding of the relationship between Nab2 and m^{6}A, future studies in our lab are underway to analyze changes in m^{6}A upon loss of Nab2 utilizing a transcriptome-wide approach. Recently Oxford Nanopore released a one-of-a-kind method for site-specific detection of RNA modifications via direct sequencing of RNA[463]. In brief, a helicase motor protein guides native RNA movement through a protein nanopore. As the RNA is driven through the nanopore by an applied voltage, monovalent ionic current varies depending on the identification of the nucleotide, as well as modifications present on a nucleotide within the pore[463]. This ionic current signature can be converted into a sequence for individual strands by a neural network trained on a variety of RNA samples, providing a comprehensive understanding of the structure of individual RNA molecules within a cell. Utilizing this technology will allow transcriptome wide identification of changes to m6A profiles in *Nab2^{null}* heads compared to Control and will also provide long-read transcript information allowing our labs to further define how Nab2 alters RNA structure and regulates m^{6}A levels on target transcripts.

Previous studies in our labs illustrate that Nab2 physically and genetically interacts with the fly orthologue of Fragile X mental retardation protein (FMRP), Fmr1, to control select Fmr1-bound neuronal mRNAs (e.g. *CaMKII*) and regulate *Drosophila* neurodevelopment[278]. Intriguingly, recent studies have identified vertebrate FMRP as a

novel m^{6}A reader protein that promotes nuclear export of methylated RNAs during neuronal differentiation[464,465]. Given that ZC3H14/Nab2 also has established roles in nuclear export and regulation of m^{6}A[257,266,380], is it possible that Nab2 and Fmr1 co-regulate m^{6}A on target mRNAs to govern downstream pre-mRNA metabolism? To date, there is no evidence to support a role for Nab2 and FMRP-co regulation of neuronal transcripts in an m^{6}A-dependent manner, however, recent studies set a precedent for future investigations into the relationship between Nab2, Fmr1, and m^{6}A, and highlight a potential mechanism by which Nab2 regulates methylation of target transcripts.

In **Chapter 3** of this thesis, we detail genetic interactions between *nab2* and *trio* and highlight a role for Nab2 in the regulation of *trio* processing and downstream neurodevelopment. However, this study did not uncover whether Nab2 physically associates with the *trio M* or *trio L* transcripts. Analysis of these transcripts reveals that there are several A-rich tracts within the introns serving as possible motifs where Nab2 could bind to regulate splicing and m^{6}A methylation. RNA immunoprecipitation of FLAG-tagged Nab2 overexpressed in neurons (*UAS-Nab2-FLAG;;elav-Gal4*) followed by RT-qPCR analysis for the *trio M* and *trio L* transcripts is necessary to determine whether Nab2 could mediate splicing and methylation via direct physical interaction with these transcripts.

The data presented within **Chapters 2**, **3**, and **4** highlight the possibility that other unidentified neuronally enriched transcripts may also be co-regulated by Nab2 and m^{6}A to govern proper neurodevelopmental programs within the *Drosophila* nervous system. Determining the identity of these transcripts is crucial to understanding the function of Nab2 in neurons and unraveling how loss of this conserved and ubiquitously expressed

RNA binding protein causes non-syndromic intellectual disability. Several candidates can be selected by cross referencing our RNA seq dataset with the me-RIP seq dataset published by Eric Lai's lab[147]. However, oxford nanopore direct RNA-seq analysis from *Control, Mettl3*^{null} and *Nab2*^{null} heads will provide a more in-depth analysis of splicing events that are regulated by both Nab2 and m^{6}A. Dissecting the functions of these transcripts in the regulation of neurodevelopment is key to rounding out our understanding of critical neuronal and molecular functions for this RBP.

CONCLUSION

In summary, the research we present in this dissertation represents a series of valuable contributions to our understanding of the function of Nab2/ZC3H14. These results advance our understanding of Nab2/ZC3H14 function and how loss of function of a conserved RBP contributes to intellectual disability and neurodevelopmental disease. Our results answer many questions about Nab2 function and define the first mRNA targets regulated by Nab2 to govern organismal phenotypes and neurodevelopment (**Figure 1-18**). Moreover, thesis studies guide questions for future studies of ZC3H14/Nab2 molecular and developmental roles. The research presented in this dissertation expands our understanding of *Drosophila* Nab2 function, and thereby its mammalian ZC3H14 orthologue, revealing roles for Nab2 in the regulation of m^{6}A methylation and further defines the function of ZC3H14/Nab2 in neurodevelopment. Ultimately, this research provides better clarity and enables future studies of ZC3H14/Nab2, bringing us one step closer to elucidating how a ubiquitously expressed polyadenosine RNA binding protein contributes to human neurodevelopment and neurodevelopmental disease.

APPENDIX: How to Select a Graduate School for a Ph.D. in Biomedical Science

Carly L. Lancaster[1,2,3], Lauryn Higginson[4,5], Brandon Chen[6], Lucas Encarnacion-Rivera[7,8], Derrick J. Morton[3] and Anita H. Corbett[1,*]

[1]Department of Biology, Emory University, [2]Department of Cell Biology, Emory University, and [3]Graduate Program in Biochemistry, Cell, and Developmental Biology, Emory University, Atlanta, GA, USA; [4]Department of Biological Sciences, University of Southern California, Los Angeles, CA 90089, USA ; [5]Graduate Program in Molecular and Computational Biology, University of Southern California, Los Angeles, CA 90089, USA [6]Department of Molecular and Integrative Physiology, University of Michigan, Ann Arbor, MI, USA;[7]Department of Bioengineering and [8]Department of Biology, Stanford University, Stanford, CA 94305, USA

This appendix has been excerpted from a manuscript published in *Current Protocols*:
Lancaster CL, Higginson L, Chen B, Encarnacion-Rivera L, Morton DJ, Corbett AH. How to Select a Graduate School Program for a PhD in Biomedical Science. Curr Protoc. 2022 Jun;2(6):e450. doi: 10.1002/cpz1.450.

*Correspondence:

Anita H. Corbett, Ph.D.
Department of Biology
Emory University
Atlanta, GA 30322

Tel: 404-421-9061
E-mail: acorbe2@emory.edu

Abstract

The goal of this article is to provide guidance for those who have made the decision to apply to graduate school with the plan to obtain a PhD in a STEM field. Choosing an appropriate graduate school and program can seem like a daunting choice. There are numerous graduate training programs that offer excellent training with multiple specific program choices at any given institution. Thus, the goal of identifying a program that provides an optimal training environment, which aligns with the applicant's training and career goals, can be daunting. There is no single training program that is ideal for all applicants and, fortunately, there is no sole perfect place for any individual applicant to obtain a PhD. This article presents points to consider at multiple phases of this process as collected from the authors who include a senior faculty member, a junior faculty member, and four current graduate students who all made different choices for their graduate training. In Phase 1 of the process, the vast number of choices must be culled to a reasonable number of schools/programs for the initial application. This is one of the most challenging steps because the number of training programs is very large, and most applicants will rely primarily on information readily available on the internet. Phase 2 is the exciting stage of visiting the program for an interview where you can ask questions and get a feel for the place. Finally, Phase 3 suggests information to collect following the interview when comparing choices and making a final decision. While the process may feel long and can be stressful, the good news is that making informed decisions along the way should result in multiple options that can support excellent training and career development.

Key Words: graduate school, graduate program, PhD, STEM, decisions, considerations

Author Biographies

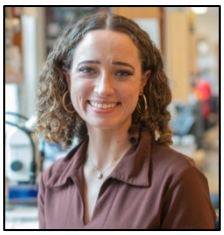

Carly Lancaster is a third-year Ph.D. candidate in the Biochemistry, Cell and Developmental Biology Program at Emory University co-mentored by Drs. Anita H. Corbett and Kenneth H. Moberg. Presently, Carly is working on characterizing the role of a conserved RNA binding protein in the regulation of RNAs critical for neurodevelopment. After graduating, she plans to complete her postdoctoral studies and pursue a career in biotechnology.

Lauryn Higginson is a first-year Ph.D. student in the Molecular and Computational Biology Program in the Department of Biological Sciences at the University of Southern California. Lauryn recently joined her thesis lab and will be utilizing the *Drosophila* model to investigate how defects in subunits of a ubiquitous and critical RNA processing complex cause tissue-specific disease. Following graduate school, she plans to become a postdoctoral researcher and ultimately pursue a faculty position in biological sciences.

Brandon Chen is a third-year Ph.D. candidate in the Cellular and Molecular Biology Program at University of Michigan co-mentored by Dr. Yatrik Shah and Dr. Costas Lyssiotis. Brandon's research focuses on understanding how endoplasmic reticulum (ER)-mitochondria contact sites contribute to tumor metabolic rewiring. His long-term career goal is to pursue an academic position and eventually become a primary investigator.

Lucas Encarnacion-Riviera is a second-year Ph.D. candidate in the Neurosciences Program at Stanford University co-advised by Drs. Karl Deisseroth and Liqun Luo. Lucas is studying how the brain generates internal states and how motivated drives transform into behavior. After graduate school, Lucas wishes to become a professor of neuroscience and lead his own lab.

Derrick Morton, PhD is an Assistant Professor in the Molecular and Computational Biology section of the Department of Biological Sciences at the University of Southern California. His research interest ranges from defining tissue-specific roles of RNA processing, surveillance, and decay machinery to how defects in essential and ubiquitous RNA processing factors cause human disease. He attended Clark Atlanta University (CAU), a Historically Black University, for graduate school. The supportive training environment he experienced at CAU played a major role in him pursuing postdoctoral fellowship and ultimately an independent career in science.

Anita Corbett, PhD is Samuel C. Dobbs Professor of Biology at Emory University. She plays numerous roles in graduate program leadership and has a strong commitment to building an inclusive STEM community. When she applied to graduate school, the internet did not exist, and her resource was a dusty file cabinet drawer in the chemistry department conference room; however, even under these archaic conditions, she chose a graduate school, obtained a PhD, and proceeded to an academic career.

Introduction

So, you decided you want to go to graduate school to pursue a PhD in a STEM field? Now is the time to take the next step– choosing the graduate school you would like to attend. Graduate school can be a very fulfilling and stimulating experience, particularly for those who choose graduate programs best suited for their unique needs and aspirations. However, choosing the right school is not like choosing between regular or decaf, paper or plastic, or wake-up or snooze. A PhD is a major time investment and a significant career decision that requires in-depth analysis of all your options. Beyond selecting a specific school, the proliferation of different graduate programs means that even within a single school, there could be a dizzying array of program options, often with confusing and interrelated names. Thus, choosing both a school and a program that align with your personal and professional goals is paramount. There are many wonderful PhD programs and several important factors you should consider when selecting the program best tailored to your learning style, training goals, and future career aspirations.

Choosing a graduate school is an intimidating task when you do not know what you are looking for. Moreover, there are many significant considerations to be made at each step of the selection process. Here we break down the selection process into three key phases: Phase I: Research for Applications; Phase II: The Interview; and Phase III: Follow-Up Research (**Figure 1**). Within each of these Phases, there are multiple factors that require careful examination to determine the graduate program(s) that will provide you with the best training aligned with your needs and ambitions (**Figure 1**). We hope that by defining these key considerations, one can more easily determine what to look for in a prospective PhD program.

A key consideration for graduate training is that most of your training will take place within the context of your research laboratory. This constitutes a substantial shift from the undergraduate mentality where classes are the main venue for training. While the curriculum in graduate school can be important and should be considered, most STEM graduate programs limit coursework to

the first one or two years of training. Thus, prioritizing research options and secondarily considering the curriculum and course structure is recommended.

The purpose of this article is to help those seeking a PhD in STEM-related fields select a graduate school that will provide them with an excellent training experience by narrowing down key factors one should consider throughout the selection process. Although comprehensive, this article does not encompass all considerable factors of the graduate school selection process which will vary from student to student. Thus, we advise prospective students to take these, and other personal considerations into account when choosing the right graduate school. We will solely focus on the key factors one should consider at each phase of the graduate school selection process.

Ph.D. or Master's?

While the advice offered here is directed to those who have made the decision to pursue a PhD in STEM, there are other options for graduate school. Those who are uncertain about whether they are willing to commit to a PhD may consider enrolling in a Master's program. However, there is large variation in the value of a Master's degree across STEM fields. For example, in many biomedical sciences, a Master's degree brings the same value as two years of experience, such as working in a research laboratory. To be clear, for a Master's degree program, the tuition is likely to be substantial with no stipend provided, which contrasts with many PhD programs that provide a full tuition waiver and a stipend. Master's programs are typically revenue generating, requiring tuition commiserate with other professional degrees and significant scholarships to offset the cost of tuition are rare. Some Master's programs are gateways to university PhD programs and this may be appropriate for an individual who is not yet ready to commit to a PhD, but the cost of the Master's phase of training may be substantial to ultimately end up in a PhD program where one could have been fully funded from the start. While a Master's

program may be an option for some, it is important to carefully consider the cost/benefit of such a program in your specific field. For example, in basic biomedical sciences, an investment in a Master's degree is often not the most cost efficient choice.

An alternative to Master's program for some students are post-baccalaureate training programs. These programs typically provide some graduate coursework together with a focused research experience. They can be ideal for the student who is still exploring their interest in a research career. While some of these are revenue-generating and as costly as Master's programs, those supported by the National Institutes of Health termed Postbaccalaureate Research Education Programs or PREP can be excellent choices Schwartz et al. [466].The goal of PREP is to support educational activities that enhance the diversity of the biomedical research workforce. Unlike Master's programs, PREP programs are designed for students who plan to pursue a PhD or a combined degree such as an MD/PhD. These programs can be an excellent alternative for students who are uncertain if they want to pursue a PhD and do not want to accumulate burdensome debt while they make their decision. However, this does not mean that Master's degrees are not worth the time and money for all STEM students. Thus, we encourage students who are considering enrolling in Master's programs to carefully consider whether a Master's degree in their respective STEM field in necessary and beneficial for their future endeavors.

Phase I: Research for Applications

Choosing where to apply to graduate school can be an overwhelming and burdensome task. With over 1,000 graduate schools with PhD-track programs in the United States alone [467,468], selecting the schools you want to apply to may seem daunting.

Moreover, the average cost of a graduate school application ranges between $50-$100 USD [468-470] and each application takes approximately 10 hours to complete and submit [471]. Given the pricey and time-consuming nature of graduate school applications, you owe it to yourself to make an informed and carefully thought-out decision when choosing where to apply. General industry advice is to apply to between *three and eight* graduate schools [472], but how do you narrow down your search when you have over 1,000 options? Here we present six key considerations to help you narrow down the list of graduate schools to apply to.

Location, Location, Location

Studies show that nearly 87% of students choose to relocate to attend graduate school [473]. The location of your graduate school may not seem like a top priority on your list of things to consider, however, you are not just picking a school– you are picking a location where you will spend the next 5-7 years of your life. Although picking schools based on location may seem superficial, enjoying the place you live makes enduring the stresses of graduate school much easier. There are many reasons why students choose to live in specific geographical regions including proximity to family and friends, climate, as well as career opportunities. Whatever your reasons may be, it is important to ensure that the location of your graduate school is a good fit for you.

While most students choose to relocate to different cities for graduate school, over half of students who relocate choose to remain in the same geographical region (e.g. Southeast, Northeast, Midwest) [473]. This is generally because students want to remain near family and friends. If proximity to family and friends is something important to you,

consider how far is “too far” away for you. For instance, if a plane is required to make the trip home in a days’ time, you may consider schools that are within reasonable driving distance to your family and friends. Many students seek the emotional and financial support that living close to home has to offer and therefore, may only consider schools within a 100-mile radius of home. On the other hand, many students choose to push themselves outside of their comfort zone and experience graduate school far away from the familiarity of their hometown. These students may instead decide to apply to schools located on opposite sides of the country and spend a several years exploring a new city. Regardless, understanding where you want to live in proximity to your current location will largely influence the graduate schools you choose to apply to.

Another factor to consider when thinking about the location of your graduate studies is the seasonal and social climate within the region. For example, if harsh, cold winters are not your style, you may decide to apply to schools located in warmer climates. If you abhor big cities and heavy traffic you may want to avoid applying to the plethora of schools located in urban metropolitan areas. If you want to avoid driving and the overall cost of car maintenance during your PhD, you may consider locations with superior public transportation. Moreover, each city you consider will have its own cultural values and unique atmospheres. Thus, ensuring that you select a city favorable to both work and play will go a long way toward helping you guarantee happiness and perform your best.

Finally, you may consider applying to graduate schools in geographical regions in which you want to pursue your future career. For instance, students interested in careers in biotechnology may choose to apply to graduate schools in Boston, California, or in the Research Triangle Park area of North Carolina as these schools are near a diverse range

of biotechnology companies. Selecting schools close to careers of interest may allow for enhanced networking and thus may aid in achieving professional goals.

Taken together, the location of prospective graduate schools is a significant determinant of those that you may want to apply to. Whether you pick locations based upon distance from home, climate, or proximity to potential careers, determining the geographical location in which you would like to attend graduate school can really help narrow down the list of schools to apply to.

Research

A PhD program typically takes 5-7 years, including 1-2 years of coursework and several years of intensive independent research. Thus, it is critical that applicants consider their research interests when deciding which graduate schools and subsequent programs to apply to. The specific research area and research opportunities available should impact not only your choice of graduate school but also your choice of graduate program within a school. Faculty at a given graduate school can be members of one or more graduate programs within that school, meaning that they teach and mentor graduate students within the programs that they have appointments. As you delve into your research, you might consider whether schools allow you to work with faculty only specifically within a certain program or whether there is more flexibility. For instance, some schools only allow students to join the labs of faculty members with appointments in that students' graduate program, and others allow students to explore labs across program lines. Prospective students who have yet to decide what area of research they want to pursue may consider applying to schools with umbrella programs which allow new

students to rotate with faculty among a diverse array of programs within the graduate school. These umbrella programs are designed to allow students to explore multiple different types of research opportunities before deciding what lab they want to join.

When considering your research interests, a key point is to ensure that multiple scientists within a graduate school or program work in that area. Common and astute advice is to never select a school or program because of a single faculty member performing your dream research [474] That faculty member may not be taking students, or you may not work well with that individual. Thus, a recommendation is to ensure that there are at least three professors studying an array of topics you can see yourself working on. Moreover, if you are particularly interested in certain professors, you may try reaching out to these professors prior to the application deadline. This will allow you to get your foot in the door and talk to someone that can tell you more about the program, the learning environment, and provide details about their willingness to accept new graduate trainees [474]. This will also allow you to get a better sense of whether you are still interested in these labs and could see yourself working for the advisor long-term. Another suggestion is to simply keep an open mind. Many students enter graduate school with limited research experience, so considering areas beyond their current expertise may be the best approach. Finally, research dynamically evolves with time as new global threats and cutting-edge technologies emerge, so the topics that were of interest during the application process could easily change as new opportunities arise.

Another point to consider is that graduate school is about research *training*. An ideally suited graduate program should arm you with key skills you need to develop into the best scientist you can be, including experimental design, hypothesis generation, data

analysis, and the many other transferable skills such as scientific writing and communication, teaching, mentoring, and project management [475]. While you need to select a research topic that engages you, this topic is unlikely to be the focus of your career. You may be passionate and driven to tackle a specific research area, but you do not need to work on that specific topic in graduate school. Instead, try to focus on identifying a program where you can acquire the skills needed to develop into a scientist who is best equipped to pursue that research question at a future stage in your career.

When and if you decide to attend a specific PhD program, most schools require that students take time (approximately six months to one year) to perform laboratory rotations. Rotations are designed with the students' best interest in mind. These rotations allow students to explore different research topics and environments. Moreover, rotations are an invaluable opportunity for students to decide whether a specific advisor and laboratory environment is a good fit for their individual needs, goals, and learning styles, without the pressure of scientific productivity. Although somewhat uncommon, there are schools that will allow you to join a lab directly upon admission to the program. The challenges of graduate necessitate that students make a thoughtful and informed decision when picking a lab that they will spend the next 5-7 years of their life in, and lab rotations are an important part of this process. Unless a student has steadfast confidence that a specific lab and mentor is the best choice for them, we highly recommend that students do lab rotations to ensure that their graduate school experience is a pleasant one.

Reputation

School choice is often driven by reputation. While there are many published rankings of graduate schools, the key thing to recall is that the rankings are typically for the school overall and not the specific programs that you may be considering. Thus, while all students are likely to take reputation into consideration, this should not be a primary driving force. Some schools are better known nationally or internationally because they have excellent athletic teams, but the national ranking of the football team is unlikely to impact your STEM PhD to any significant extent. Determining the reputation of a specific graduate program or research area is more challenging than determining the reputation of a school. For this reason, reputation is an area that should be considered most extensively later in the decision tree when the choice is between a specific set of options.

Although many prestigious schools presumably have excellent graduate programs in your field of interest, it is not necessarily true that these programs are superior to the those at schools without the big name. In fact, you will find stellar graduate programs at schools that US News and World Report has ranked third tier [476], and potentially weak graduate programs in otherwise highly ranked schools. Moreover, a PhD from a highly ranked school does not necessarily ensure a better job or a higher starting salary after graduation. Companies and hiring committees tend not to focus on the school a candidate graduated from, but instead look for the relevance and quality of a candidates research and how well this research fits with the needs of the company or department [477]. Thus, it is critical that prospective PhD students look for graduate schools and programs that foster supportive and innovative research environments that allow their students to thrive.

In sum, if you want to find a program that will make you a skilled and competitive job applicant, your priority should be finding a graduate program that places emphasis on

graduate student training. But how do you decipher between schools that emphasize training and those that do not? Graduate programs that place importance on graduate student training and development will often provide students with opportunities to take courses in grant writing, public speaking and communications, and expose students to a diverse array of research throughout their graduate career. Moreover, these programs will cultivate student collaborations and often have access to a multitude of core facilities that aid students in effectively using the latest technologies to support their individual research. By keeping in mind that the quality of your schools' training environment is more important than the schools ranking or reputation, your final list of schools will guarantee that you make the right choice when it comes time to enroll in a specific program.

Stipend

Fortunately, most STEM PhD students in the US, particularly those enrolled in biomedical science programs, are typically paid a living stipend for the duration of their graduate career with a complete tuition waiver. As many programs offer such a stipend, take care in considering any program that does not guarantee a stipend. Moreover, the ways in which this stipend may be provided can differ. For instance, some programs require a significant amount of teaching in the form of teaching assistantships (as discussed in the Teaching section) to cover a large portion of their stipend, while other programs fully support their students' stipends and require minimal teaching as a part of the required curriculum. Thus, prospective students should consider their desire to teach as well as their research priorities before applying to programs that require significant amounts of teaching to cover their stipend.

Despite offering a living stipend, this stipend typically just enough to keep food on the table, bills paid, and gas in your car, leaving very little room for extra expenses. Thus, it is vital that prospective graduate students consider the stipend and assess their financial responsibilities. More importantly, do not get distracted by schools that offer more money than others. It is not uncommon for schools that offer bigger stipends to be located in areas with a higher-than-average cost of living. Wherever you apply, you need to ensure that the stipend matches the cost of living and will be enough to keep your 'head above water' throughout graduate school. A PhD can be very long with lots of stressful ups and downs, and financial insecurity is the last thing you want to worry about.

At the time this article was written, the average graduate student makes a yearly stipend of approximately $32,000 [478]. If you are going to graduate school right out of your undergraduate studies, this may be the most money you have ever made. On the other hand, if you are leaving a job to go to graduate school, this may be a significant pay decrease. It is not impossible to live on a graduate student stipend and most schools provide yearly cost-of-living increases to student stipends. So, when deciding between graduate schools, make sure that the stipend is livable given the cost-of living in that area. You may consider utilizing MIT's living wage calculator (found at https://livingwage.mit.edu/) [479], which can help you determine the cost-of-living in different areas around the United States to help you make an informed decision when choosing what schools you want to apply to.

Curriculum

PhD curriculum varies widely between graduate schools and even between different PhD programs within a given school. Although you certainly cannot avoid taking difficult classes during your PhD, it is worth understanding what courses you will have to take, when you will have to take them, and how these courses are structured to ensure you are getting the most out of your educational experience. However, it is also important to recall that graduate training primarily takes place within the context of your research project, so curriculum and coursework are not the driving force to consider in the same way that choices are made for an undergraduate school.

When analyzing your graduate school and program options, you want to ensure that the program you are interested in offers excellent training for enrolled PhD students. But what should this training venue look like? You should consider the broader context of the training, including curriculum as well as other professional development opportunities. Most programs require that first and second-year students take foundational courses to both deepen and broaden the students' knowledge of the field in which they are pursuing a PhD [480]. Depending on the school and program, these courses may take place in lecture hall settings with a large group of graduate students, or in small, intimate classroom settings with a smaller number of students. Here, it is important to consider how you learn best. Do you know whether you have a more favorable learning experience in passive learning environments with large groups of students, or in smaller groups where you are free to engage and ask questions during class? This consideration is unique to the individual applicant but can be an impactful consideration when determining the learning environment that is best suited for you. Many students applying to graduate school may only have experiences in large-seminar type courses rather than small, intimate learning

settings and therefore may not understand the benefits of small class sizes. Thus, we encourage students to keep an open mind when considering their graduate learning environment. Moreover, many graduate schools require that students take other courses including courses in statistics (depending on which STEM program you are applying to), writing, ethics, and seminar [480]. These courses are designed to enhance the students critical thinking skills as well as written and verbal communication skills [480]. These courses are all taken while students simultaneously focus on their respective dissertation research. It is important to get a good sense of what courses you are expected to take and when you are expected to take them to ensure that you can sufficiently meet the requirements of both your program and your advisor without overextending yourself.

Graduate Records Exam (GRE)

If you are thinking about going to graduate school, you have probably heard about the Graduate Records Examination (GRE). The GRE is a standardized test created and administered by the Educational Testing Service (ETS), which is designed to test a student's overall preparedness for graduate-level studies [481]. The GRE is like the SAT college entrance exam and seeks to assess general competence in areas such as analytical writing, mathematics, and verbal reasoning [482]. Recently, however, the utility of the GRE as a predictor of graduate student success has been intensely debated. A 2014 study published in *Nature* illustrated that women and individuals from underrepresented groups often score lower on the GRE than their white male counterparts (Miller & Stassun, 2014). Moreover, the exam cost approximately $205 which is prohibitively expensive for many low-income students, further impeding promising students from entering graduate

school [483,484]. Interestingly, these studies show that GRE scores are very poor predictors of a graduate students' scientific productivity [484,485]. Fortunately, many leading STEM graduate programs have begun to recognize that the GRE is a weak predictor of PhD student success and have dropped the GRE as an admissions requirement [486]. Therefore, students can easily apply to a slate of top biomedical graduate programs without taking the GRE. For information about the many programs that no longer require the GRE, see Dr. Joshua Hall's public spreadsheet (BioGRE.info), which lists many of the biomedical PhD programs that have dropped the GRE admissions requirement[485]. To be crystal clear, most of these programs no longer accept or consider the GRE in admissions decisions, so taking the GRE brings no value for such applications. Moreover, there are no graduate fellowships or grant opportunities that require the GRE. However, there are some specific areas of graduate education that continue to rely more heavily on the GRE than others, so whether the GRE is required for applications may depend on your specific area of study. Regardless of whether you choose to take the GRE before applying to graduate school, it is important to know that your performance on this standardized exam does not directly correlate with your readiness for the hands-on intensity of a PhD program.

Phase II: The Interview

Congratulations! You have been invited to interview at some of the schools you applied to. Many applicants consider this to be the most stressful part of the application process but fail to realize that while the school is interviewing you, *you are also interviewing the school*. This is your chance to get an up-close and personal look at the

life of a typical graduate student in each of these programs. Here you can ask the nitty-gritty questions your late-night google searches left unanswered. There are also many questions you may not know you should ask! Thus, we have provided a chart of key questions prospective students may consider asking faculty and current students during their interview weekend (**Box 1**). Importantly, you also have the chance to have candid talks with the current students and get a feel for their overall satisfaction with the program. Moreover, you may get a chance to speak with faculty members whose labs you are interested in joining.

All in all, the interview process is one of the most important steps to deciding what graduate school would be the best for your training and career development. Here, we have outlined things to consider finding out when you embark on your interviews.

Funding mechanism(s)

During Phase I of the process, you should have narrowed your choices to schools that provide a tuition waiver and offer a living stipend. At this stage, you should gather more information about the mechanisms to fund your stipend. In the ideal situation, your stipend is guaranteed if you are making satisfactory progress. You should seek options that clearly state this to be the case. Typically, such a situation means that the university has some resources to support your stipend early in training (1-2 years) and then your research mentor has grant funding to support your stipend and any associated fees. This model can differ from program to program, but you should seek clarity during the interview about the source of funding. There are also some options that may offer additional training or opportunities.

Some schools or programs will require you to commit to serving as a teaching assistant. While teaching experience can be valuable, be sure you understand the commitment. Will you be responsible for teaching a whole section of a course or are you acting as a teaching assistant? Even if you enjoy teaching, the need to teach each semester while trying to balance your research progress can be daunting. Ensure you understand the commitment and speak to more senior students to gather more information about the time required.

Many programs have some form of training grant support. These training grants can be provided from various sources, including federal agencies such as the National Institutes of Health (NIH) T32 training grants or the National Science Foundation (NSF). These training grants can support student stipend at specific training stages and offer some additional perks such as funds for travel or supplies. As such training grants require a clear plan for training, schools or programs that have such a support mechanism may offer additional training that is mandated by such funding mechanisms. The NIH National Institute of General Medical Science (NIGMS) funds many such training mechanisms and this institute has led the way in requiring training to produce well rounded ethical scientists that are prepared to function within the biomedical research community. These funding mechanisms must be renewed every five years, so this is essentially a required regular refresh of the training offered. Checking whether the school or program you are interested in has such funding mechanisms can provide you with information about how the school of program values graduate training because such funding mechanisms also require significant institutional support.

Some schools will offer support for students to apply for their own independent research funding [487]. There are several mechanisms for this support where the graduate student is the principal investigator (PI) for the grant. Some schools also offer an increase in the stipend to those students who secure their own extramural research funding. Like a training grant, these individual pre-doctoral fellowships often have some funds available to support travel and purchase supplies. The experience of crafting a persuasive proposal to see your research to those who make funding decisions can be a very valuable part of graduate training.

In summary, learning the details of the funding, including the sources available should be a key part of your investigation during the interview process. You should ask questions on this important topic of both program leadership and current students to paint the full picture. A goal should be to select a school or program that aligns with your goals and offers you stable funding that aligns with your needs.

Teaching Requirements

Most graduate students are required to teach at some point during their graduate career. However, at some universities teaching is necessary to make up a significant portion of your stipend, while other universities ask students to teach for only a semester or two as a part of the standard curriculum. While teaching can be a fun and enriching experience, for students who do not necessarily need in-depth teaching skills for their future career, having multiple semesters of required teaching can become distracting and burdensome when trying to focus on thesis work. Thus, it is important to understand the teaching requirements at the different programs you interview with.

Teaching assistantships are designed to help postgraduate students develop invaluable teaching and assessment skills. After meeting curricular requirements, some students choose to continue teaching to earn extra money and/or gain valuable teaching experiences (a skill that can easily be applied in your future career and added to your CV). The responsibilities of graduate student teaching assistants (TAs) include leading undergraduate classes, grading papers, as well as providing laboratory supervision and demonstration [488]. Teaching as a graduate student is an excellent opportunity to expand your horizons, gain invaluable scientific communication skills, and put your knowledge to the test. Whether you teach for one semester, or you decide to teach throughout your graduate career, try to take pride in the fact that you will be teaching and engaging undergraduates in your academic discipline.

Career Exploration

Career Exploration, sometimes referred to as professionalization, is an important aspect of your graduate career. After completing your PhD, you will need to enter the job market with transferrable skills– skills that can be applied in your future career. Although some graduate students remain in academia after completing their PhD, over 50% of STEM PhD graduates do not work in academia or even perform research as their primary job [489]. Instead, many talented graduate students pursue careers in industry, government, or even medical writing. Moreover, it is very common for graduate students change their career goals during the duration of their graduate studies [490]Therefore, we recommend that applicants consider attending graduate programs that adequately prepare students for a diverse set of careers after graduating.

But what professionalization and career exploration opportunities should you look for in a graduate program? Lautz et al. recommend that graduate programs invested in student professionalization and career exploration hold a student-led foundational seminar course to address career needs. These seminars should provide students with early exposure to multiple career pathways to develop a sense of community as well as a professional network [489]. Moreover, graduate programs should encourage and support students seeking professional training specialization and internships in academic and non-academic sectors[489]. By showing STEM graduate students multiple career options, graduate programs can adequately meet the needs of today's PhD students and prepare them for life beyond graduate school.

Support Network

Every successful graduate student has a support network [491]. This support network typically includes faculty and staff, other graduate students, postdoctoral students, technicians, friends, and even family. Graduate school is a long and challenging process. Therefore, having a network of people to support you and help you along the way is essential to your success.

Although prospective students are not yet ready to build their support network, it is important that they get a feeling for the current support networks within prospective schools. When interviewing, ask the current students about their support networks. Are these support networks made up of diverse group of people at different stages in their career? You may also consider asking if these students feel supported by the programs' faculty and staff or whether the program has built-in student support systems. Many graduate schools also have graduate student unions (GSUs). These unions serve to

protect graduate students' rights and advocate for support from multiple branches of the university. Moreover, many schools have graduate student associations (GSA) comprised of graduate students from many different departments [491]. Attending GSU- and GSA-like events can be a great way to get to know people outside of your program and will help you build a support network that will last even after graduation.

Community, Diversity, and Inclusion

Building a community of supportive colleagues and mentors as you transition to graduate-level research training will be instrumental to your overall success as a scientist. Commonly, ambivalence and/or feelings of doubt about one's abilities almost always accompany any major transition, the decision to kick-off your professional academic career by enrolling into graduate school will be no different [492]. It is important to note that you are not alone, and the community you build will play a pivotal role in helping you steer the ins and outs of graduate school. These supportive connections are very important for several reasons: First, your network of colleagues and mentors can act as a team of advocates, providing support and guidance as you develop personally, academically, and professionally. Second, this network often becomes your "family away from home" – helping you to not only navigate deeply personal issues that inevitably arise during graduate school, but also making themselves available to grab ice cream after a long day in the laboratory. Ultimately, the community you build will play an essential role in you living a healthy, balanced, and fulfilling life while in graduate school.

As noted above, the decision to apply to graduate school, interview, and ultimately weigh the multitude of factors that inform where you will spend the next 5-7 years of your

life is a very challenging, but rewarding process—for everyone. However, often, individuals from groups that are historically excluded and underrepresented in STEM fields face unique challenges that many of their graduate school peers do not have to consider when deciding what graduate school program best suits them. For example, many of these students face the challenge of finding a program that includes faculty that reflect the diversity of the broader population. In fact, only 10% of STEM faculty members in the US are from underrepresented groups, according to a recent NSF-funded report (Bennett, 2020). Therefore, in the eyes of interviewees from underrepresented groups, this reality emphasizes the sentiment of a familiar quote by Marian Wright Edelman, “You can’t be what you can’t see”, which in turn intensifies doubts about the likelihood of success. In addition to finding mentors with similar backgrounds, many of these students often have the additional pressure of trusting that diversity, equity, and inclusion (DEI) values espoused by programs are not just lip-service, but closely held beliefs of the faculty, staff, and students. Thus, students must have a great deal of faith that graduate programs will invest the time and resources to support stated DEI values. Taken together, the process of choosing a graduate school presents unique challenges for all students, but particularly for students from underrepresented groups that span the application phase through matriculation.

While there has been a long-standing push to diversify and create a sense of belonging in STEM, universities in the US and by extension graduate programs still trail behind in establishing an inclusive community for its faculty, students, and staff. Historically, US institutions of higher learning have supported hierarchies of race and other forms of difference since their founding, and remnants of this very ideology persist

in the academy broadly including graduate education. However, the recent rise of social justice movements has led to a renewed sense of urgency to break social barriers and pave the way for the realization of true DEI in all US institutions. As in many sectors of life in the US, graduate schools still have a long way to go before achieving their goals specific to DEI. These efforts will need to address all aspects of student differences, including many that have not been the focus of efforts such as ableism [493]. Recent support for social, gender, and racial equity by leaders in higher education are an important first step and provide hope to many graduate students who are from groups historically excluded and underrepresented in STEM fields. As you navigate graduate school, build and leverage your community to be a force for social change. Thus, leaving behind a more inclusive and equitable environment for junior trainees. Importantly, DEI in STEM is a continuous effort that does not have a finish line and will require action from the entire scientific community to keep improving. While navigating through the interview process, it is critical that you begin to identify efforts made by the program to establish an equitable and inclusive environment. For example, as you converse with current students and faculty, ask about initiatives for diversification and inclusion, such as student-led empowerment organizations, community outreach, and DEI committees.

Program Responsibilities

Graduate school, like a ‘real job’, occurs in a matrixed environment where students are a part of multiple chains of accountability and therefore have responsibilities not only to their thesis advisors, but also to their program [494]. Thus, it is necessary to determine what your responsibilities outside of the lab will entail and if these responsibilities change

as you progress through your degree. For example, many students are required to help with recruitment of new students, organize program-related events, and attend program seminars. These responsibilities, while important, may serve as a distraction from your thesis work. Thus, it is critical that you determine what your program responsibilities are within each graduate program. These answers are likely not found on the internet but can be readily discussed with current graduate students and faculty members at your interview.

Phase III: Follow-Up Research

The interviews are finally over, and you have solidified acceptances from several schools. Take a deep breath and pat yourself on the back! The bulk of the work is over, but now comes the hard part- deciding which graduate school and program you would like to attend. You may be able to see yourself at multiple different schools/programs making the decision burdensome and potentially anxiety-inducing. At this point, reminding yourself that there is no single “right choice” may relieve some stress. However, there is some follow-up research which may not have been provided during the interviews that can be beneficial as you consider your options and make your final choice.

Student Fees

Unfortunately, student fees do not disappear in graduate school. Despite the fact that the average graduate student stipend is $32,000 a year [478], most schools still require that graduate students pay fees each semester. While most of the price of the fees is covered by the graduate school, the burden of the remainder of the fees falls on the student. The

average graduate student pays some amount in student fees per semester. These fees typically include technology fees, health and wellness fees, athletic fees, and even activity fees. However, the types of fees and the semesterly rates vary greatly between schools and programs. Thus, we recommend that applicants research student fee rates for each of the schools they are interested in. Unfortunately, these data may be hard to find with a simple google search and a scroll through the university website. Applicants may instead consider reaching out to current graduate students to get an idea of the cost of student fees as well as how these students feel about the fees. You may consider asking current students if they are able to easily pay the fees with their current stipend, or if they feel that the fees are fair. Regardless of where you attend, you will probably have to pay some amount of student fees, but it's a good idea to know how much and how often you will have to pay as a graduate student.

Health Benefits

Health benefits can be a stressful topic for many incoming graduate students, especially for students previously covered under their parents' health insurance plan. Typically, student health insurance plans are offered by the institution, however these plans can vary greatly in cost and coverage. Unforeseen medical expenses, such as those related to treating a cold or a simple rash can cost hundreds of dollars, and you do not want to be blindsided by a medical situation in which you do not have adequate financial coverage. This can cause students financial hardship and lead to added stress. Therefore, as you contemplate your graduate school options, it is important to compare the health benefits each school has to offer.

What should you look for in an acceptable student health insurance plan? According to U.S. News, students should expect that plans offer a minimum coverage per year with an annual deductible [495]. Moreover, plans should provide coverage for both inpatient and outpatient services anywhere in the U.S. as well as coverage for mental health services, prescription drugs, and physical therapy [495] . Applicants should also determine when their coverage starts and lapses as well as whether they are required to use specific doctors, hospitals, or clinics to be covered.

Gut Feelings

When you know, you know. We cannot emphasize enough the importance of trusting your 'gut feelings' when considering if a graduate school and program is the right one for you. This refers to relying on inclination that you cannot readily explain. Although you should not disregard objective facts, balancing an objective outlook with your subconscious intuition is ideal when deciding what program suits you best. The American Psychological Association reports that decisions recruiting gut feelings are often a reflection of one's true self [496], and when picking a graduate school which you will attend for the next 5-7 years, it is best to make a decision that is an authentic reflection of your goals.

Concluding Remarks

Seeking out a stimulating and supportive environment where you can gain the skills needed for the next stage of your career is a daunting, but exciting task. We have presented many different factors applicants should take into consideration when selecting a graduate training program. However, each decision is unique to the individual and there

is no single “right” choice, especially when presented with many excellent options. Selecting a graduate school and subsequent program is a major life decision, thus, considering your individual values and aspirations is critical to ensure your success and happiness throughout your graduate career. PhD training can potentially be a consuming and strenuous process; therefore, we advise students to seek training environments that encourage a healthy work-life balance and offer a breadth of training opportunities to support your values and future goals. Although deciding where you want to carry out your graduate studies is a challenging task, we hope that the information presented here will arm you with the knowledge necessary to select a graduate training program that will allow you to thrive personally and professionally. We wish you the best of luck in your graduate school-hunting and future endeavors!

Acknowledgements

The authors acknowledge funding from the National Institutes of Health to A.H.C (R25GM125598,R01NS125768) and C.L.L (F31NS127545) as well as fellowships from NSF (L.E.-R.) and the Department of Defense (B.C.). We would like to acknowledge Dr. TJ Murphy for his insight and intellectual contribution to the creation and ideas presented within this article. We would also like to acknowledge Dr. Raven Peterson who has contributed insightful commentary on topics included here. The authors declare no conflict of interest.

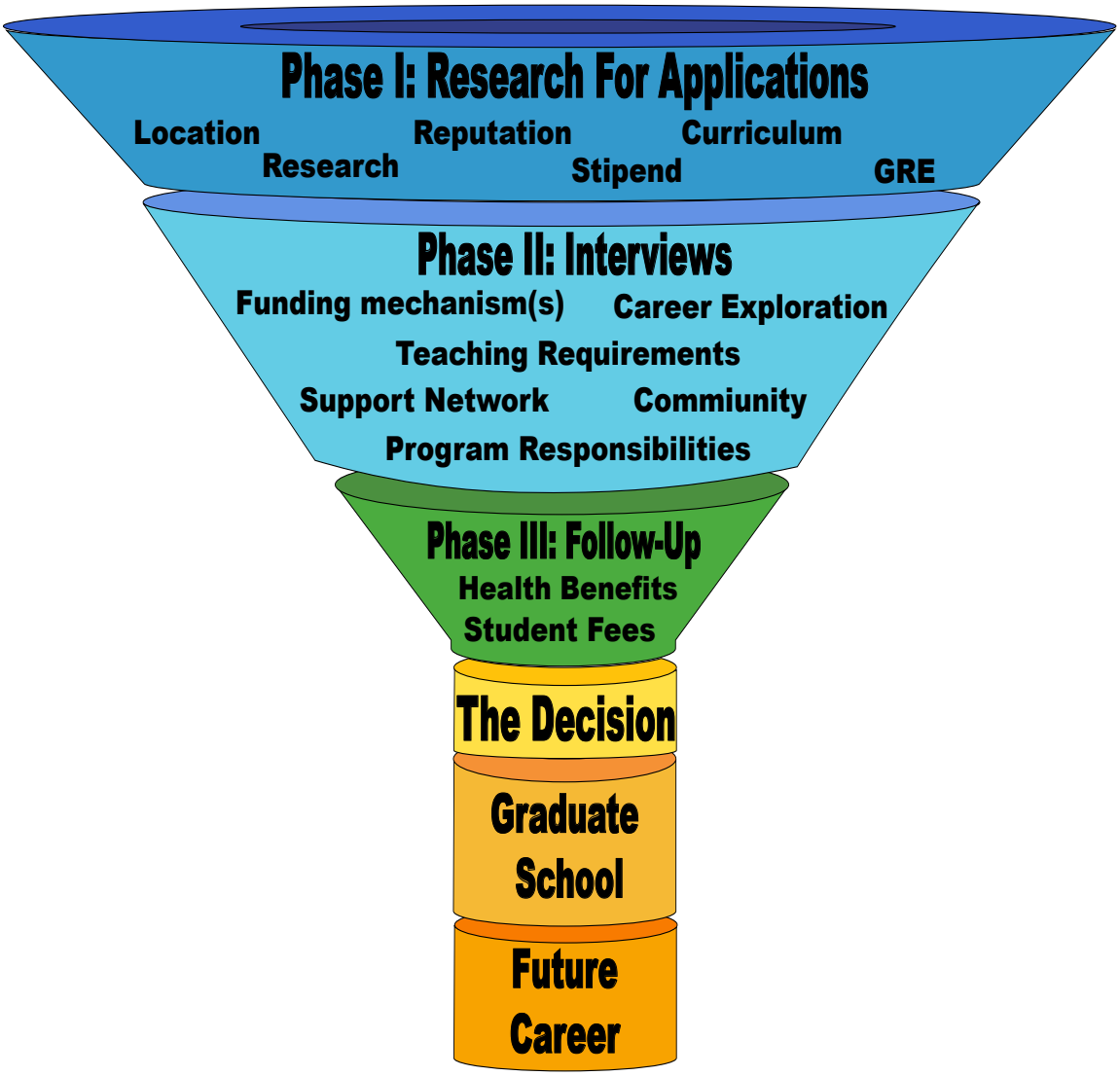

Figure A-1. The Considerations Funnel. Selecting a graduate school and/or graduate program can be a daunting task when students do not know exactly what they are looking for. Here we have illustrated the selection process which can be broken down into three main phases (Phase I, Phase II, and Phase II), including key factors to consider at each stage of the selection process. Each of these factors is discussed in more detail in the text.

REFERENCES

1. Crick, F. (1970). Central dogma of molecular biology. Nature *227*, 561-563. 10.1038/227561a0.
2. Costa, V., Angelini, C., De Feis, I., and Ciccodicola, A. (2010). Uncovering the complexity of transcriptomes with RNA-Seq. J Biomed Biotechnol *2010*, 853916. 10.1155/2010/853916.
3. Costa, V., Aprile, M., Esposito, R., and Ciccodicola, A. (2013). RNA-Seq and human complex diseases: recent accomplishments and future perspectives. Eur J Hum Genet *21*, 134-142. 10.1038/ejhg.2012.129.
4. Carninci, P., and Hayashizaki, Y. (2007). Noncoding RNA transcription beyond annotated genes. Curr Opin Genet Dev *17*, 139-144. 10.1016/j.gde.2007.02.008.
5. Schieweck, R., Ninkovic, J., and Kiebler, M.A. (2021). RNA-binding proteins balance brain function in health and disease. Physiol Rev *101*, 1309-1370. 10.1152/physrev.00047.2019.
6. Corbett, A.H. (2018). Post-transcriptional regulation of gene expression and human disease. Curr Opin Cell Biol *52*, 96-104. 10.1016/j.ceb.2018.02.011.
7. Gilbert, W.V., and Nachtergaele, S. (2023). mRNA Regulation by RNA Modifications. Annu Rev Biochem *92*, 175-198. 10.1146/annurev-biochem-052521-035949.
8. Moore, M.J. (2005). From birth to death: the complex lives of eukaryotic mRNAs. Science *309*, 1514-1518. 10.1126/science.1111443.
9. Kuehner, J.N., Pearson, E.L., and Moore, C. (2011). Unravelling the means to an end: RNA polymerase II transcription termination. Nat Rev Mol Cell Biol *12*, 283-294. 10.1038/nrm3098.
10. Lodish, H., Berk, A., Matsudaira, P., Kaiser, C.A., Krieger, M., Scott, M.P., et al. (2013). Molecular Cell Biology.
11. Moteki, S., and Price, D. (2002). Functional coupling of capping and transcription of mRNA. Mol Cell *10*, 599-609. 10.1016/s1097-2765(02)00660-3.
12. Shatkin, A.J., and Manley, J.L. (2000). The ends of the affair: capping and polyadenylation. Nat Struct Biol *7*, 838-842. 10.1038/79583.
13. Wei, C.M., Gershowitz, A., and Moss, B. (1975). Methylated nucleotides block 5' terminus of HeLa cell messenger RNA. Cell *4*, 379-386. 10.1016/0092-8674(75)90158-0.
14. Jiao, X., Chang, J.H., Kilic, T., Tong, L., and Kiledjian, M. (2013). A mammalian pre-mRNA 5' end capping quality control mechanism and an unexpected link of capping to pre-mRNA processing. Mol Cell *50*, 104-115. 10.1016/j.molcel.2013.02.017.
15. Konarska, M.M., Padgett, R.A., and Sharp, P.A. (1984). Recognition of cap structure in splicing in vitro of mRNA precursors. Cell *38*, 731-736. 10.1016/0092-8674(84)90268-x.
16. Fresco, L.D., and Buratowski, S. (1996). Conditional mutants of the yeast mRNA capping enzyme show that the cap enhances, but is not required for, mRNA splicing. RNA *2*, 584-596.

17. Inoue, K., Ohno, M., Sakamoto, H., and Shimura, Y. (1989). Effect of the cap structure on pre-mRNA splicing in Xenopus oocyte nuclei. Genes Dev *3*, 1472-1479. 10.1101/gad.3.9.1472.
18. Izaurralde, E., and Adam, S. (1998). Transport of macromolecules between the nucleus and the cytoplasm. RNA *4*, 351-364.
19. Ohno, M., Sakamoto, H., and Shimura, Y. (1987). Preferential excision of the 5' proximal intron from mRNA precursors with two introns as mediated by the cap structure. Proc Natl Acad Sci U S A *84*, 5187-5191. 10.1073/pnas.84.15.5187.
20. Losh, J.S., and van Hoof, A. (2015). Gateway Arch to the RNA Exosome. Cell *162*, 940-941. 10.1016/j.cell.2015.08.013.
21. Meyer, S., Temme, C., and Wahle, E. (2004). Messenger RNA turnover in eukaryotes: pathways and enzymes. Crit Rev Biochem Mol Biol *39*, 197-216. 10.1080/10409230490513991.
22. Cvitkovic, I., and Jurica, M.S. (2013). Spliceosome database: a tool for tracking components of the spliceosome. Nucleic Acids Res *41*, D132-141. 10.1093/nar/gks999.
23. Schmidt, C., Gronborg, M., Deckert, J., Bessonov, S., Conrad, T., Luhrmann, R., and Urlaub, H. (2014). Mass spectrometry-based relative quantification of proteins in precatalytic and catalytically active spliceosomes by metabolic labeling (SILAC), chemical labeling (iTRAQ), and label-free spectral count. RNA *20*, 406-420. 10.1261/rna.041244.113.
24. Wilkinson, M.E., Charenton, C., and Nagai, K. (2020). RNA Splicing by the Spliceosome. Annu Rev Biochem *89*, 359-388. 10.1146/annurev-biochem-091719-064225.
25. Black, D.L. (2003). Mechanisms of alternative pre-messenger RNA splicing. Annu Rev Biochem *72*, 291-336. 10.1146/annurev.biochem.72.121801.161720.
26. Collins, C.A., and Guthrie, C. (2000). The question remains: is the spliceosome a ribozyme? Nat Struct Biol *7*, 850-854. 10.1038/79598.
27. Hrdlickova, R., Toloue, M., and Tian, B. (2017). RNA-Seq methods for transcriptome analysis. Wiley Interdiscip Rev RNA *8*. 10.1002/wrna.1364.
28. Stark, R., Grzelak, M., and Hadfield, J. (2019). RNA sequencing: the teenage years. Nat Rev Genet *20*, 631-656. 10.1038/s41576-019-0150-2.
29. Gehring, N.H., and Roignant, J.Y. (2021). Anything but Ordinary - Emerging Splicing Mechanisms in Eukaryotic Gene Regulation. Trends Genet *37*, 355-372. 10.1016/j.tig.2020.10.008.
30. Burnette, J.M., Miyamoto-Sato, E., Schaub, M.A., Conklin, J., and Lopez, A.J. (2005). Subdivision of large introns in Drosophila by recursive splicing at nonexonic elements. Genetics *170*, 661-674. 10.1534/genetics.104.039701.
31. Hatton, A.R., Subramaniam, V., and Lopez, A.J. (1998). Generation of alternative Ultrabithorax isoforms and stepwise removal of a large intron by resplicing at exon-exon junctions. Mol Cell *2*, 787-796. 10.1016/s1097-2765(00)80293-2.
32. Shepard, S., McCreary, M., and Fedorov, A. (2009). The peculiarities of large intron splicing in animals. PLoS One *4*, e7853. 10.1371/journal.pone.0007853.
33. Duff, M.O., Olson, S., Wei, X., Garrett, S.C., Osman, A., Bolisetty, M., Plocik, A., Celniker, S.E., and Graveley, B.R. (2015). Genome-wide identification of zero nucleotide recursive splicing in Drosophila. Nature *521*, 376-379. 10.1038/nature14475.

34. Sibley, C.R., Emmett, W., Blazquez, L., Faro, A., Haberman, N., Briese, M., Trabzuni, D., Ryten, M., Weale, M.E., Hardy, J., et al. (2015). Recursive splicing in long vertebrate genes. Nature *521*, 371-375. 10.1038/nature14466.
35. Starke, S., Jost, I., Rossbach, O., Schneider, T., Schreiner, S., Hung, L.H., and Bindereif, A. (2015). Exon circularization requires canonical splice signals. Cell Rep *10*, 103-111. 10.1016/j.celrep.2014.12.002.
36. Ragan, C., Goodall, G.J., Shirokikh, N.E., and Preiss, T. (2019). Insights into the biogenesis and potential functions of exonic circular RNA. Sci Rep *9*, 2048. 10.1038/s41598-018-37037-0.
37. Hansen, T.B., Jensen, T.I., Clausen, B.H., Bramsen, J.B., Finsen, B., Damgaard, C.K., and Kjems, J. (2013). Natural RNA circles function as efficient microRNA sponges. Nature *495*, 384-388. 10.1038/nature11993.
38. Memczak, S., Jens, M., Elefsinioti, A., Torti, F., Krueger, J., Rybak, A., Maier, L., Mackowiak, S.D., Gregersen, L.H., Munschauer, M., et al. (2013). Circular RNAs are a large class of animal RNAs with regulatory potency. Nature *495*, 333-338. 10.1038/nature11928.
39. Ustianenko, D., Weyn-Vanhentenryck, S.M., and Zhang, C. (2017). Microexons: discovery, regulation, and function. Wiley Interdiscip Rev RNA *8*. 10.1002/wrna.1418.
40. Raj, B., O'Hanlon, D., Vessey, J.P., Pan, Q., Ray, D., Buckley, N.J., Miller, F.D., and Blencowe, B.J. (2011). Cross-regulation between an alternative splicing activator and a transcription repressor controls neurogenesis. Mol Cell *43*, 843-850. 10.1016/j.molcel.2011.08.014.
41. Blijlevens, M., Li, J., and van Beusechem, V.W. (2021). Biology of the mRNA Splicing Machinery and Its Dysregulation in Cancer Providing Therapeutic Opportunities. Int J Mol Sci *22*. 10.3390/ijms22105110.
42. Poulos, M.G., Batra, R., Charizanis, K., and Swanson, M.S. (2011). Developments in RNA splicing and disease. Cold Spring Harb Perspect Biol *3*, a000778. 10.1101/cshperspect.a000778.
43. Lee, Y., and Rio, D.C. (2015). Mechanisms and Regulation of Alternative Pre-mRNA Splicing. Annu Rev Biochem *84*, 291-323. 10.1146/annurev-biochem-060614-034316.
44. Schwerk, C., and Schulze-Osthoff, K. (2005). Regulation of apoptosis by alternative pre-mRNA splicing. Mol Cell *19*, 1-13. 10.1016/j.molcel.2005.05.026.
45. Pan, Q., Shai, O., Lee, L.J., Frey, B.J., and Blencowe, B.J. (2008). Deep surveying of alternative splicing complexity in the human transcriptome by high-throughput sequencing. Nat Genet *40*, 1413-1415. 10.1038/ng.259.
46. Sultan, M., Schulz, M.H., Richard, H., Magen, A., Klingenhoff, A., Scherf, M., Seifert, M., Borodina, T., Soldatov, A., Parkhomchuk, D., et al. (2008). A global view of gene activity and alternative splicing by deep sequencing of the human transcriptome. Science *321*, 956-960. 10.1126/science.1160342.
47. Wang, E.T., Sandberg, R., Luo, S., Khrebtukova, I., Zhang, L., Mayr, C., Kingsmore, S.F., Schroth, G.P., and Burge, C.B. (2008). Alternative isoform regulation in human tissue transcriptomes. Nature *456*, 470-476. 10.1038/nature07509.
48. Fu, X.D., and Ares, M., Jr. (2014). Context-dependent control of alternative splicing by RNA-binding proteins. Nat Rev Genet *15*, 689-701. 10.1038/nrg3778.

49. Proudfoot, N.J. (2011). Ending the message: poly(A) signals then and now. Genes Dev *25*, 1770-1782. 10.1101/gad.17268411.
50. Tian, B., and Graber, J.H. (2012). Signals for pre-mRNA cleavage and polyadenylation. Wiley Interdiscip Rev RNA *3*, 385-396. 10.1002/wrna.116.
51. Nicholson, A.L., and Pasquinelli, A.E. (2019). Tales of Detailed Poly(A) Tails. Trends Cell Biol *29*, 191-200. 10.1016/j.tcb.2018.11.002.
52. Meyer, S., Urbanke, C., and Wahle, E. (2002). Equilibrium studies on the association of the nuclear poly(A) binding protein with poly(A) of different lengths. Biochemistry *41*, 6082-6089. 10.1021/bi0160866.
53. Sheiness, D., and Darnell, J.E. (1973). Polyadenylic acid segment in mRNA becomes shorter with age. Nat New Biol *241*, 265-268. 10.1038/newbio241265a0.
54. Brawerman, G. (1981). The Role of the poly(A) sequence in mammalian messenger RNA. CRC Crit Rev Biochem *10*, 1-38. 10.3109/10409238109114634.
55. Gallie, D.R. (1991). The cap and poly(A) tail function synergistically to regulate mRNA translational efficiency. Genes Dev *5*, 2108-2116. 10.1101/gad.5.11.2108.
56. Passmore, L.A., and Coller, J. (2022). Roles of mRNA poly(A) tails in regulation of eukaryotic gene expression. Nat Rev Mol Cell Biol *23*, 93-106. 10.1038/s41580-021-00417-y.
57. Beck, M., and Hurt, E. (2017). The nuclear pore complex: understanding its function through structural insight. Nat Rev Mol Cell Biol *18*, 73-89. 10.1038/nrm.2016.147.
58. Tran, E.J., and Wente, S.R. (2006). Dynamic nuclear pore complexes: life on the edge. Cell *125*, 1041-1053. 10.1016/j.cell.2006.05.027.
59. Terry, L.J., and Wente, S.R. (2007). Nuclear mRNA export requires specific FG nucleoporins for translocation through the nuclear pore complex. J Cell Biol *178*, 1121-1132. 10.1083/jcb.200704174.
60. Alber, F., Dokudovskaya, S., Veenhoff, L.M., Zhang, W., Kipper, J., Devos, D., Suprapto, A., Karni-Schmidt, O., Williams, R., Chait, B.T., et al. (2007). The molecular architecture of the nuclear pore complex. Nature *450*, 695-701. 10.1038/nature06405.
61. Madrid, A.S., and Weis, K. (2006). Nuclear transport is becoming crystal clear. Chromosoma *115*, 98-109. 10.1007/s00412-005-0043-3.
62. Quimby, B.B., and Corbett, A.H. (2001). Nuclear transport mechanisms. Cell Mol Life Sci *58*, 1766-1773. 10.1007/PL00000816.
63. Ding, B., and Sepehrimanesh, M. (2021). Nucleocytoplasmic Transport: Regulatory Mechanisms and the Implications in Neurodegeneration. Int J Mol Sci *22*. 10.3390/ijms22084165.
64. Stewart, M. (2007). Ratcheting mRNA out of the nucleus. Mol Cell *25*, 327-330. 10.1016/j.molcel.2007.01.016.
65. Aibara, S., Katahira, J., Valkov, E., and Stewart, M. (2015). The principal mRNA nuclear export factor NXF1:NXT1 forms a symmetric binding platform that facilitates export of retroviral CTE-RNA. Nucleic Acids Res *43*, 1883-1893. 10.1093/nar/gkv032.
66. Forler, D., Rabut, G., Ciccarelli, F.D., Herold, A., Kocher, T., Niggeweg, R., Bork, P., Ellenberg, J., and Izaurralde, E. (2004). RanBP2/Nup358 provides a major binding site for NXF1-p15 dimers at the nuclear pore complex and functions in nuclear mRNA export. Mol Cell Biol *24*, 1155-1167. 10.1128/MCB.24.3.1155-1167.2004.

67. Mor-Shaked, H., and Eiges, R. (2016). Modeling Fragile X Syndrome Using Human Pluripotent Stem Cells. Genes (Basel) *7*. 10.3390/genes7100077.
68. Schuster, S.L., and Hsieh, A.C. (2019). The Untranslated Regions of mRNAs in Cancer. Trends Cancer *5*, 245-262. 10.1016/j.trecan.2019.02.011.
69. Boivin, M., Deng, J., Pfister, V., Grandgirard, E., Oulad-Abdelghani, M., Morlet, B., Ruffenach, F., Negroni, L., Koebel, P., Jacob, H., et al. (2021). Translation of GGC repeat expansions into a toxic polyglycine protein in NIID defines a novel class of human genetic disorders: The polyG diseases. Neuron *109*, 1825-1835 e1825. 10.1016/j.neuron.2021.03.038.
70. Mayr, C. (2019). What Are 3' UTRs Doing? Cold Spring Harb Perspect Biol *11*. 10.1101/cshperspect.a034728.
71. Davis, B.M., McCurrach, M.E., Taneja, K.L., Singer, R.H., and Housman, D.E. (1997). Expansion of a CUG trinucleotide repeat in the 3' untranslated region of myotonic dystrophy protein kinase transcripts results in nuclear retention of transcripts. Proc Natl Acad Sci U S A *94*, 7388-7393. 10.1073/pnas.94.14.7388.
72. Richter, J.D. (1999). Cytoplasmic polyadenylation in development and beyond. Microbiol Mol Biol Rev *63*, 446-456. 10.1128/MMBR.63.2.446-456.1999.
73. Gao, F.B. (1998). Messenger RNAs in dendrites: localization, stability, and implications for neuronal function. Bioessays *20*, 70-78. 10.1002/(SICI)1521-1878(199801)20:1<70::AID-BIES10>3.0.CO;2-5.
74. Chen, C.Y., and Shyu, A.B. (1995). AU-rich elements: characterization and importance in mRNA degradation. Trends Biochem Sci *20*, 465-470. 10.1016/s0968-0004(00)89102-1.
75. Wang, X., Kiledjian, M., Weiss, I.M., and Liebhaber, S.A. (1995). Detection and characterization of a 3' untranslated region ribonucleoprotein complex associated with human alpha-globin mRNA stability. Mol Cell Biol *15*, 1769-1777. 10.1128/MCB.15.3.1769.
76. Morales, J., Russell, J.E., and Liebhaber, S.A. (1997). Destabilization of human alpha-globin mRNA by translation anti-termination is controlled during erythroid differentiation and is paralleled by phased shortening of the poly(A) tail. J Biol Chem *272*, 6607-6613. 10.1074/jbc.272.10.6607.
77. Boucher, C.A., King, S.K., Carey, N., Krahe, R., Winchester, C.L., Rahman, S., Creavin, T., Meghji, P., Bailey, M.E., Chartier, F.L., and et al. (1995). A novel homeodomain-encoding gene is associated with a large CpG island interrupted by the myotonic dystrophy unstable (CTG)n repeat. Hum Mol Genet *4*, 1919-1925. 10.1093/hmg/4.10.1919.
78. Kontoyiannis, D., Pasparakis, M., Pizarro, T.T., Cominelli, F., and Kollias, G. (1999). Impaired on/off regulation of TNF biosynthesis in mice lacking TNF AU-rich elements: implications for joint and gut-associated immunopathologies. Immunity *10*, 387-398. 10.1016/s1074-7613(00)80038-2.
79. Rimokh, R., Berger, F., Bastard, C., Klein, B., French, M., Archimbaud, E., Rouault, J.P., Santa Lucia, B., Duret, L., Vuillaume, M., and et al. (1994). Rearrangement of CCND1 (BCL1/PRAD1) 3' untranslated region in mantle-cell lymphomas and t(11q13)-associated leukemias. Blood *83*, 3689-3696.

80. Chagnovich, D., Fayos, B.E., and Cohn, S.L. (1996). Differential activity of ELAV-like RNA-binding proteins in human neuroblastoma. J Biol Chem *271*, 33587-33591. 10.1074/jbc.271.52.33587.
81. Stern-Ginossar, N., Thompson, S.R., Mathews, M.B., and Mohr, I. (2019). Translational Control in Virus-Infected Cells. Cold Spring Harb Perspect Biol *11*. 10.1101/cshperspect.a033001.
82. Wek, R.C. (2018). Role of eIF2alpha Kinases in Translational Control and Adaptation to Cellular Stress. Cold Spring Harb Perspect Biol *10*. 10.1101/cshperspect.a032870.
83. Yang, Y., and Wang, Z. (2019). IRES-mediated cap-independent translation, a path leading to hidden proteome. J Mol Cell Biol *11*, 911-919. 10.1093/jmcb/mjz091.
84. Leppek, K., Das, R., and Barna, M. (2018). Functional 5' UTR mRNA structures in eukaryotic translation regulation and how to find them. Nat Rev Mol Cell Biol *19*, 158-174. 10.1038/nrm.2017.103.
85. Rodnina, M.V., Korniy, N., Klimova, M., Karki, P., Peng, B.Z., Senyushkina, T., Belardinelli, R., Maracci, C., Wohlgemuth, I., Samatova, E., and Peske, F. (2020). Translational recoding: canonical translation mechanisms reinterpreted. Nucleic Acids Res *48*, 1056-1067. 10.1093/nar/gkz783.
86. Morley, S.J., and Coldwell, M.J. (2008). An alternative mechanism of eukaryotic translation initiation. Sci Signal *1*, 32. 10.1126/scisignal.125pe32.
87. Jan, E., Kinzy, T.G., and Sarnow, P. (2003). Divergent tRNA-like element supports initiation, elongation, and termination of protein biosynthesis. Proc Natl Acad Sci U S A *100*, 15410-15415. 10.1073/pnas.2535183100.
88. Avanzino, B.C., Fuchs, G., and Fraser, C.S. (2017). Cellular cap-binding protein, eIF4E, promotes picornavirus genome restructuring and translation. Proc Natl Acad Sci U S A *114*, 9611-9616. 10.1073/pnas.1704390114.
89. Rodnina, M.V. (2018). Translation in Prokaryotes. Cold Spring Harb Perspect Biol *10*. 10.1101/cshperspect.a032664.
90. Hellen, C.U.T. (2018). Translation Termination and Ribosome Recycling in Eukaryotes. Cold Spring Harb Perspect Biol *10*. 10.1101/cshperspect.a032656.
91. Dever, T.E., Dinman, J.D., and Green, R. (2018). Translation Elongation and Recoding in Eukaryotes. Cold Spring Harb Perspect Biol *10*. 10.1101/cshperspect.a032649.
92. Martin, K.C., and Ephrussi, A. (2009). mRNA localization: gene expression in the spatial dimension. Cell *136*, 719-730. 10.1016/j.cell.2009.01.044.
93. Johnstone, O., and Lasko, P. (2001). Translational regulation and RNA localization in Drosophila oocytes and embryos. Annu Rev Genet *35*, 365-406. 10.1146/annurev.genet.35.102401.090756.
94. Paquin, N., and Chartrand, P. (2008). Local regulation of mRNA translation: new insights from the bud. Trends Cell Biol *18*, 105-111. 10.1016/j.tcb.2007.12.004.
95. Ciolli Mattioli, C., Rom, A., Franke, V., Imami, K., Arrey, G., Terne, M., Woehler, A., Akalin, A., Ulitsky, I., and Chekulaeva, M. (2019). Alternative 3' UTRs direct localization of functionally diverse protein isoforms in neuronal compartments. Nucleic Acids Res *47*, 2560-2573. 10.1093/nar/gky1270.
96. Wong, H.H., Lin, J.Q., Strohl, F., Roque, C.G., Cioni, J.M., Cagnetta, R., Turner-Bridger, B., Laine, R.F., Harris, W.A., Kaminski, C.F., and Holt, C.E. (2017). RNA Docking and Local

Translation Regulate Site-Specific Axon Remodeling In Vivo. Neuron *95*, 852-868 e858. 10.1016/j.neuron.2017.07.016.

97. Yoon, Y.J., Wu, B., Buxbaum, A.R., Das, S., Tsai, A., English, B.P., Grimm, J.B., Lavis, L.D., and Singer, R.H. (2016). Glutamate-induced RNA localization and translation in neurons. Proc Natl Acad Sci U S A *113*, E6877-E6886. 10.1073/pnas.1614267113.

98. Miller, S., Yasuda, M., Coats, J.K., Jones, Y., Martone, M.E., and Mayford, M. (2002). Disruption of dendritic translation of CaMKIIalpha impairs stabilization of synaptic plasticity and memory consolidation. Neuron *36*, 507-519. 10.1016/s0896-6273(02)00978-9.

99. Donlin-Asp, P.G., Polisseni, C., Klimek, R., Heckel, A., and Schuman, E.M. (2021). Differential regulation of local mRNA dynamics and translation following long-term potentiation and depression. Proc Natl Acad Sci U S A *118*. 10.1073/pnas.2017578118.

100. Doyle, M., and Kiebler, M.A. (2011). Mechanisms of dendritic mRNA transport and its role in synaptic tagging. EMBO J *30*, 3540-3552. 10.1038/emboj.2011.278.

101. Vogel, C., and Marcotte, E.M. (2012). Insights into the regulation of protein abundance from proteomic and transcriptomic analyses. Nat Rev Genet *13*, 227-232. 10.1038/nrg3185.

102. Houseley, J., and Tollervey, D. (2009). The many pathways of RNA degradation. Cell *136*, 763-776. 10.1016/j.cell.2009.01.019.

103. Chen, C.Y., Ezzeddine, N., and Shyu, A.B. (2008). Messenger RNA half-life measurements in mammalian cells. Methods Enzymol *448*, 335-357. 10.1016/S0076-6879(08)02617-7.

104. Yang, E., van Nimwegen, E., Zavolan, M., Rajewsky, N., Schroeder, M., Magnasco, M., and Darnell, J.E., Jr. (2003). Decay rates of human mRNAs: correlation with functional characteristics and sequence attributes. Genome Res *13*, 1863-1872. 10.1101/gr.1272403.

105. Garneau, N.L., Wilusz, J., and Wilusz, C.J. (2007). The highways and byways of mRNA decay. Nat Rev Mol Cell Biol *8*, 113-126. 10.1038/nrm2104.

106. Labno, A., Tomecki, R., and Dziembowski, A. (2016). Cytoplasmic RNA decay pathways - Enzymes and mechanisms. Biochim Biophys Acta *1863*, 3125-3147. 10.1016/j.bbamcr.2016.09.023.

107. Wahle, E., and Winkler, G.S. (2013). RNA decay machines: deadenylation by the Ccr4-not and Pan2-Pan3 complexes. Biochim Biophys Acta *1829*, 561-570. 10.1016/j.bbagrm.2013.01.003.

108. Cooke, A., Prigge, A., and Wickens, M. (2010). Translational repression by deadenylases. J Biol Chem *285*, 28506-28513. 10.1074/jbc.M110.150763.

109. Tharun, S. (2009). Lsm1-7-Pat1 complex: a link between 3' and 5'-ends in mRNA decay? RNA Biol *6*, 228-232. 10.4161/rna.6.3.8282.

110. Nishimura, T., Padamsi, Z., Fakim, H., Milette, S., Dunham, W.H., Gingras, A.C., and Fabian, M.R. (2015). The eIF4E-Binding Protein 4E-T Is a Component of the mRNA Decay Machinery that Bridges the 5' and 3' Termini of Target mRNAs. Cell Rep *11*, 1425-1436. 10.1016/j.celrep.2015.04.065.

111. Jinek, M., Coyle, S.M., and Doudna, J.A. (2011). Coupled 5' nucleotide recognition and processivity in Xrn1-mediated mRNA decay. Mol Cell *41*, 600-608. 10.1016/j.molcel.2011.02.004.

112. Muhlrad, D., Decker, C.J., and Parker, R. (1994). Deadenylation of the unstable mRNA encoded by the yeast MFA2 gene leads to decapping followed by 5'-->3' digestion of the transcript. Genes Dev *8*, 855-866. 10.1101/gad.8.7.855.
113. Schaeffer, D., Tsanova, B., Barbas, A., Reis, F.P., Dastidar, E.G., Sanchez-Rotunno, M., Arraiano, C.M., and van Hoof, A. (2009). The exosome contains domains with specific endoribonuclease, exoribonuclease and cytoplasmic mRNA decay activities. Nat Struct Mol Biol *16*, 56-62. 10.1038/nsmb.1528.
114. Schneider, C., Anderson, J.T., and Tollervey, D. (2007). The exosome subunit Rrp44 plays a direct role in RNA substrate recognition. Mol Cell *27*, 324-331. 10.1016/j.molcel.2007.06.006.
115. Tomecki, R., and Dziembowski, A. (2010). Novel endoribonucleases as central players in various pathways of eukaryotic RNA metabolism. RNA *16*, 1692-1724. 10.1261/rna.2237610.
116. Arzumanian, V.A., Dolgalev, G.V., Kurbatov, I.Y., Kiseleva, O.I., and Poverennaya, E.V. (2022). Epitranscriptome: Review of Top 25 Most-Studied RNA Modifications. Int J Mol Sci *23*. 10.3390/ijms232213851.
117. Zhao, L.Y., Song, J., Liu, Y., Song, C.X., and Yi, C. (2020). Mapping the epigenetic modifications of DNA and RNA. Protein Cell *11*, 792-808. 10.1007/s13238-020-00733-7.
118. Yang, Y., Hsu, P.J., Chen, Y.S., and Yang, Y.G. (2018). Dynamic transcriptomic m(6)A decoration: writers, erasers, readers and functions in RNA metabolism. Cell Res *28*, 616-624. 10.1038/s41422-018-0040-8.
119. Ma, C., Chang, M., Lv, H., Zhang, Z.W., Zhang, W., He, X., Wu, G., Zhao, S., Zhang, Y., Wang, D., et al. (2018). RNA m(6)A methylation participates in regulation of postnatal development of the mouse cerebellum. Genome Biol *19*, 68. 10.1186/s13059-018-1435-z.
120. Desrosiers, R., Friderici, K., and Rottman, F. (1974). Identification of methylated nucleosides in messenger RNA from Novikoff hepatoma cells. Proc Natl Acad Sci U S A *71*, 3971-3975. 10.1073/pnas.71.10.3971.
121. Luo, S., and Tong, L. (2014). Molecular basis for the recognition of methylated adenines in RNA by the eukaryotic YTH domain. Proc Natl Acad Sci U S A *111*, 13834-13839. 10.1073/pnas.1412742111.
122. Theler, D., Dominguez, C., Blatter, M., Boudet, J., and Allain, F.H. (2014). Solution structure of the YTH domain in complex with N6-methyladenosine RNA: a reader of methylated RNA. Nucleic Acids Res *42*, 13911-13919. 10.1093/nar/gku1116.
123. Xu, C., Wang, X., Liu, K., Roundtree, I.A., Tempel, W., Li, Y., Lu, Z., He, C., and Min, J. (2014). Structural basis for selective binding of m6A RNA by the YTHDC1 YTH domain. Nat Chem Biol *10*, 927-929. 10.1038/nchembio.1654.
124. Dominissini, D., Moshitch-Moshkovitz, S., Schwartz, S., Salmon-Divon, M., Ungar, L., Osenberg, S., Cesarkas, K., Jacob-Hirsch, J., Amariglio, N., Kupiec, M., et al. (2012). Topology of the human and mouse m6A RNA methylomes revealed by m6A-seq. Nature *485*, 201-206. 10.1038/nature11112.
125. Ke, S., Alemu, E.A., Mertens, C., Gantman, E.C., Fak, J.J., Mele, A., Haripal, B., Zucker-Scharff, I., Moore, M.J., Park, C.Y., et al. (2015). A majority of m6A residues are in the last

exons, allowing the potential for 3' UTR regulation. Genes Dev *29*, 2037-2053. 10.1101/gad.269415.115.

126. Meyer, K.D., Saletore, Y., Zumbo, P., Elemento, O., Mason, C.E., and Jaffrey, S.R. (2012). Comprehensive analysis of mRNA methylation reveals enrichment in 3' UTRs and near stop codons. Cell *149*, 1635-1646. 10.1016/j.cell.2012.05.003.

127. Xiao, W., Adhikari, S., Dahal, U., Chen, Y.S., Hao, Y.J., Sun, B.F., Sun, H.Y., Li, A., Ping, X.L., Lai, W.Y., et al. (2016). Nuclear m(6)A Reader YTHDC1 Regulates mRNA Splicing. Mol Cell *61*, 507-519. 10.1016/j.molcel.2016.01.012.

128. Haussmann, I.U., Bodi, Z., Sanchez-Moran, E., Mongan, N.P., Archer, N., Fray, R.G., and Soller, M. (2016). m(6)A potentiates Sxl alternative pre-mRNA splicing for robust Drosophila sex determination. Nature *540*, 301-304. 10.1038/nature20577.

129. Lence, T., Akhtar, J., Bayer, M., Schmid, K., Spindler, L., Ho, C.H., Kreim, N., Andrade-Navarro, M.A., Poeck, B., Helm, M., and Roignant, J.Y. (2016). m(6)A modulates neuronal functions and sex determination in Drosophila. Nature *540*, 242-247. 10.1038/nature20568.

130. Roundtree, I.A., Luo, G.Z., Zhang, Z., Wang, X., Zhou, T., Cui, Y., Sha, J., Huang, X., Guerrero, L., Xie, P., et al. (2017). YTHDC1 mediates nuclear export of N(6)-methyladenosine methylated mRNAs. Elife *6*. 10.7554/eLife.31311.

131. Meyer, K.D., Patil, D.P., Zhou, J., Zinoviev, A., Skabkin, M.A., Elemento, O., Pestova, T.V., Qian, S.B., and Jaffrey, S.R. (2015). 5' UTR m(6)A Promotes Cap-Independent Translation. Cell *163*, 999-1010. 10.1016/j.cell.2015.10.012.

132. Wang, X., Zhao, B.S., Roundtree, I.A., Lu, Z., Han, D., Ma, H., Weng, X., Chen, K., Shi, H., and He, C. (2015). N(6)-methyladenosine Modulates Messenger RNA Translation Efficiency. Cell *161*, 1388-1399. 10.1016/j.cell.2015.05.014.

133. Wang, X., Lu, Z., Gomez, A., Hon, G.C., Yue, Y., Han, D., Fu, Y., Parisien, M., Dai, Q., Jia, G., et al. (2014). N6-methyladenosine-dependent regulation of messenger RNA stability. Nature *505*, 117-120. 10.1038/nature12730.

134. Uzonyi, A., Dierks, D., Nir, R., Kwon, O.S., Toth, U., Barbosa, I., Burel, C., Brandis, A., Rossmanith, W., Le Hir, H., et al. (2023). Exclusion of m6A from splice-site proximal regions by the exon junction complex dictates m6A topologies and mRNA stability. Mol Cell *83*, 237-251 e237. 10.1016/j.molcel.2022.12.026.

135. Zaccara, S., and Jaffrey, S.R. (2020). A Unified Model for the Function of YTHDF Proteins in Regulating m(6)A-Modified mRNA. Cell *181*, 1582-1595 e1518. 10.1016/j.cell.2020.05.012.

136. Meyer, K.D., and Jaffrey, S.R. (2017). Rethinking m(6)A Readers, Writers, and Erasers. Annu Rev Cell Dev Biol *33*, 319-342. 10.1146/annurev-cellbio-100616-060758.

137. Bokar, J.A., Shambaugh, M.E., Polayes, D., Matera, A.G., and Rottman, F.M. (1997). Purification and cDNA cloning of the AdoMet-binding subunit of the human mRNA (N6-adenosine)-methyltransferase. RNA *3*, 1233-1247.

138. McGraw, S., Vigneault, C., and Sirard, M.A. (2007). Temporal expression of factors involved in chromatin remodeling and in gene regulation during early bovine in vitro embryo development. Reproduction *133*, 597-608. 10.1530/REP-06-0251.

139. Liu, J., Yue, Y., Han, D., Wang, X., Fu, Y., Zhang, L., Jia, G., Yu, M., Lu, Z., Deng, X., et al. (2014). A METTL3-METTL14 complex mediates mammalian nuclear RNA N6-adenosine methylation. Nat Chem Biol *10*, 93-95. 10.1038/nchembio.1432.
140. Ping, X.L., Sun, B.F., Wang, L., Xiao, W., Yang, X., Wang, W.J., Adhikari, S., Shi, Y., Lv, Y., Chen, Y.S., et al. (2014). Mammalian WTAP is a regulatory subunit of the RNA N6-methyladenosine methyltransferase. Cell Res *24*, 177-189. 10.1038/cr.2014.3.
141. Yue, Y., Liu, J., Cui, X., Cao, J., Luo, G., Zhang, Z., Cheng, T., Gao, M., Shu, X., Ma, H., et al. (2018). VIRMA mediates preferential m(6)A mRNA methylation in 3'UTR and near stop codon and associates with alternative polyadenylation. Cell Discov *4*, 10. 10.1038/s41421-018-0019-0.
142. Patil, D.P., Chen, C.K., Pickering, B.F., Chow, A., Jackson, C., Guttman, M., and Jaffrey, S.R. (2016). m(6)A RNA methylation promotes XIST-mediated transcriptional repression. Nature *537*, 369-373. 10.1038/nature19342.
143. Lin, S., Liu, J., Jiang, W., Wang, P., Sun, C., Wang, X., Chen, Y., and Wang, H. (2019). METTL3 Promotes the Proliferation and Mobility of Gastric Cancer Cells. Open Med (Wars) *14*, 25-31. 10.1515/med-2019-0005.
144. Agarwala, S.D., Blitzblau, H.G., Hochwagen, A., and Fink, G.R. (2012). RNA methylation by the MIS complex regulates a cell fate decision in yeast. PLoS Genet *8*, e1002732. 10.1371/journal.pgen.1002732.
145. Geula, S., Moshitch-Moshkovitz, S., Dominissini, D., Mansour, A.A., Kol, N., Salmon-Divon, M., Hershkovitz, V., Peer, E., Mor, N., Manor, Y.S., et al. (2015). Stem cells. m6A mRNA methylation facilitates resolution of naive pluripotency toward differentiation. Science *347*, 1002-1006. 10.1126/science.1261417.
146. Zhong, S., Li, H., Bodi, Z., Button, J., Vespa, L., Herzog, M., and Fray, R.G. (2008). MTA is an Arabidopsis messenger RNA adenosine methylase and interacts with a homolog of a sex-specific splicing factor. Plant Cell *20*, 1278-1288. 10.1105/tpc.108.058883.
147. Kan, L., Ott, S., Joseph, B., Park, E.S., Dai, W., Kleiner, R.E., Claridge-Chang, A., and Lai, E.C. (2021). A neural m(6)A/Ythdf pathway is required for learning and memory in Drosophila. Nat Commun *12*, 1458. 10.1038/s41467-021-21537-1.
148. Wu, B., Li, L., Huang, Y., Ma, J., and Min, J. (2017). Readers, writers and erasers of N(6)-methylated adenosine modification. Curr Opin Struct Biol *47*, 67-76. 10.1016/j.sbi.2017.05.011.
149. Batista, P.J., Molinie, B., Wang, J., Qu, K., Zhang, J., Li, L., Bouley, D.M., Lujan, E., Haddad, B., Daneshvar, K., et al. (2014). m(6)A RNA modification controls cell fate transition in mammalian embryonic stem cells. Cell Stem Cell *15*, 707-719. 10.1016/j.stem.2014.09.019.
150. Jia, G., Fu, Y., Zhao, X., Dai, Q., Zheng, G., Yang, Y., Yi, C., Lindahl, T., Pan, T., Yang, Y.G., and He, C. (2011). N6-methyladenosine in nuclear RNA is a major substrate of the obesity-associated FTO. Nat Chem Biol *7*, 885-887. 10.1038/nchembio.687.
151. Zheng, G., Dahl, J.A., Niu, Y., Fedorcsak, P., Huang, C.M., Li, C.J., Vagbo, C.B., Shi, Y., Wang, W.L., Song, S.H., et al. (2013). ALKBH5 is a mammalian RNA demethylase that impacts RNA metabolism and mouse fertility. Mol Cell *49*, 18-29. 10.1016/j.molcel.2012.10.015.

152. Mauer, J., Luo, X., Blanjoie, A., Jiao, X., Grozhik, A.V., Patil, D.P., Linder, B., Pickering, B.F., Vasseur, J.J., Chen, Q., et al. (2017). Reversible methylation of m(6)A(m) in the 5' cap controls mRNA stability. Nature *541*, 371-375. 10.1038/nature21022.
153. Hess, M.E., Hess, S., Meyer, K.D., Verhagen, L.A., Koch, L., Bronneke, H.S., Dietrich, M.O., Jordan, S.D., Saletore, Y., Elemento, O., et al. (2013). The fat mass and obesity associated gene (Fto) regulates activity of the dopaminergic midbrain circuitry. Nat Neurosci *16*, 1042-1048. 10.1038/nn.3449.
154. Lunde, B.M., Moore, C., and Varani, G. (2007). RNA-binding proteins: modular design for efficient function. Nat Rev Mol Cell Biol *8*, 479-490. 10.1038/nrm2178.
155. Finn, R.D., Mistry, J., Schuster-Bockler, B., Griffiths-Jones, S., Hollich, V., Lassmann, T., Moxon, S., Marshall, M., Khanna, A., Durbin, R., et al. (2006). Pfam: clans, web tools and services. Nucleic Acids Res *34*, D247-251. 10.1093/nar/gkj149.
156. Carballo, E., Lai, W.S., and Blackshear, P.J. (1998). Feedback inhibition of macrophage tumor necrosis factor-alpha production by tristetraprolin. Science *281*, 1001-1005. 10.1126/science.281.5379.1001.
157. Picard, B., and Wegnez, M. (1979). Isolation of a 7S particle from Xenopus laevis oocytes: a 5S RNA-protein complex. Proc Natl Acad Sci U S A *76*, 241-245. 10.1073/pnas.76.1.241.
158. Lee, B.M., Xu, J., Clarkson, B.K., Martinez-Yamout, M.A., Dyson, H.J., Case, D.A., Gottesfeld, J.M., and Wright, P.E. (2006). Induced fit and "lock and key" recognition of 5S RNA by zinc fingers of transcription factor IIIA. J Mol Biol *357*, 275-291. 10.1016/j.jmb.2005.12.010.
159. Hudson, B.P., Martinez-Yamout, M.A., Dyson, H.J., and Wright, P.E. (2004). Recognition of the mRNA AU-rich element by the zinc finger domain of TIS11d. Nat Struct Mol Biol *11*, 257-264. 10.1038/nsmb738.
160. Lu, D., Searles, M.A., and Klug, A. (2003). Crystal structure of a zinc-finger-RNA complex reveals two modes of molecular recognition. Nature *426*, 96-100. 10.1038/nature02088.
161. Valverde, R., Edwards, L., and Regan, L. (2008). Structure and function of KH domains. FEBS J *275*, 2712-2726. 10.1111/j.1742-4658.2008.06411.x.
162. Thandapani, P., O'Connor, T.R., Bailey, T.L., and Richard, S. (2013). Defining the RGG/RG motif. Mol Cell *50*, 613-623. 10.1016/j.molcel.2013.05.021.
163. Cooper, T.A., Wan, L., and Dreyfuss, G. (2009). RNA and disease. Cell *136*, 777-793. 10.1016/j.cell.2009.02.011.
164. Lukong, K.E., Chang, K.W., Khandjian, E.W., and Richard, S. (2008). RNA-binding proteins in human genetic disease. Trends Genet *24*, 416-425. 10.1016/j.tig.2008.05.004.
165. Darnell, R.B. (2010). RNA regulation in neurologic disease and cancer. Cancer Res Treat *42*, 125-129. 10.4143/crt.2010.42.3.125.
166. Brinegar, A.E., and Cooper, T.A. (2016). Roles for RNA-binding proteins in development and disease. Brain research *1647*, 1-8. 10.1016/j.brainres.2016.02.050.
167. Gebauer, F., Schwarzl, T., Valcarcel, J., and Hentze, M.W. (2021). RNA-binding proteins in human genetic disease. Nat Rev Genet *22*, 185-198. 10.1038/s41576-020-00302-y.
168. Pique, M., Lopez, J.M., Foissac, S., Guigo, R., and Mendez, R. (2008). A combinatorial code for CPE-mediated translational control. Cell *132*, 434-448. 10.1016/j.cell.2007.12.038.

169. Iadevaia, V., and Gerber, A.P. (2015). Combinatorial Control of mRNA Fates by RNA-Binding Proteins and Non-Coding RNAs. Biomolecules *5*, 2207-2222. 10.3390/biom5042207.
170. Achsel, T., and Bagni, C. (2016). Cooperativity in RNA-protein interactions: the complex is more than the sum of its partners. Curr Opin Neurobiol *39*, 146-151. 10.1016/j.conb.2016.06.007.
171. Beckmann, B.M., Castello, A., and Medenbach, J. (2016). The expanding universe of ribonucleoproteins: of novel RNA-binding proteins and unconventional interactions. Pflugers Arch *468*, 1029-1040. 10.1007/s00424-016-1819-4.
172. Parra, A.S., and Johnston, C.A. (2022). Emerging Roles of RNA-Binding Proteins in Neurodevelopment. J Dev Biol *10*. 10.3390/jdb10020023.
173. Prashad, S., and Gopal, P.P. (2021). RNA-binding proteins in neurological development and disease. RNA Biol *18*, 972-987. 10.1080/15476286.2020.1809186.
174. Banerjee, A., Apponi, L.H., Pavlath, G.K., and Corbett, A.H. (2013). PABPN1: molecular function and muscle disease. FEBS J *280*, 4230-4250. 10.1111/febs.12294.
175. Abu-Baker, A., and Rouleau, G.A. (2007). Oculopharyngeal muscular dystrophy: recent advances in the understanding of the molecular pathogenic mechanisms and treatment strategies. Biochim Biophys Acta *1772*, 173-185. 10.1016/j.bbadis.2006.10.003.
176. Wang, S., Sun, Z., Lei, Z., and Zhang, H.T. (2022). RNA-binding proteins and cancer metastasis. Semin Cancer Biol *86*, 748-768. 10.1016/j.semcancer.2022.03.018.
177. Sonenberg, N., and Hinnebusch, A.G. (2007). New modes of translational control in development, behavior, and disease. Mol Cell *28*, 721-729. 10.1016/j.molcel.2007.11.018.
178. Wendel, H.G., Silva, R.L., Malina, A., Mills, J.R., Zhu, H., Ueda, T., Watanabe-Fukunaga, R., Fukunaga, R., Teruya-Feldstein, J., Pelletier, J., and Lowe, S.W. (2007). Dissecting eIF4E action in tumorigenesis. Genes Dev *21*, 3232-3237. 10.1101/gad.1604407.
179. Raj, T., Li, Y.I., Wong, G., Humphrey, J., Wang, M., Ramdhani, S., Wang, Y.C., Ng, B., Gupta, I., Haroutunian, V., et al. (2018). Integrative transcriptome analyses of the aging brain implicate altered splicing in Alzheimer's disease susceptibility. Nat Genet *50*, 1584-1592. 10.1038/s41588-018-0238-1.
180. Voineagu, I., Wang, X., Johnston, P., Lowe, J.K., Tian, Y., Horvath, S., Mill, J., Cantor, R.M., Blencowe, B.J., and Geschwind, D.H. (2011). Transcriptomic analysis of autistic brain reveals convergent molecular pathology. Nature *474*, 380-384. 10.1038/nature10110.
181. Irimia, M., Weatheritt, R.J., Ellis, J.D., Parikshak, N.N., Gonatopoulos-Pournatzis, T., Babor, M., Quesnel-Vallieres, M., Tapial, J., Raj, B., O'Hanlon, D., et al. (2014). A highly conserved program of neuronal microexons is misregulated in autistic brains. Cell *159*, 1511-1523. 10.1016/j.cell.2014.11.035.
182. Tollervey, J.R., Curk, T., Rogelj, B., Briese, M., Cereda, M., Kayikci, M., Konig, J., Hortobagyi, T., Nishimura, A.L., Zupunski, V., et al. (2011). Characterizing the RNA targets and position-dependent splicing regulation by TDP-43. Nat Neurosci *14*, 452-458. 10.1038/nn.2778.
183. Gupta, N. (2023). Deciphering Intellectual Disability. Indian J Pediatr *90*, 160-167. 10.1007/s12098-022-04345-3.

184. Curry, C.J., Stevenson, R.E., Aughton, D., Byrne, J., Carey, J.C., Cassidy, S., Cunniff, C., Graham, J.M., Jr., Jones, M.C., Kaback, M.M., et al. (1997). Evaluation of mental retardation: recommendations of a Consensus Conference: American College of Medical Genetics. Am J Med Genet *72*, 468-477. 10.1002/(sici)1096-8628(19971112)72:4<468::aid-ajmg18>3.0.co;2-p.
185. Chelly, J., Khelfaoui, M., Francis, F., Cherif, B., and Bienvenu, T. (2006). Genetics and pathophysiology of mental retardation. Eur J Hum Genet *14*, 701-713. 10.1038/sj.ejhg.5201595.
186. Najmabadi, H., Hu, H., Garshasbi, M., Zemojtel, T., Abedini, S.S., Chen, W., Hosseini, M., Behjati, F., Haas, S., Jamali, P., et al. (2011). Deep sequencing reveals 50 novel genes for recessive cognitive disorders. Nature *478*, 57-63. 10.1038/nature10423.
187. van Bokhoven, H. (2011). Genetic and epigenetic networks in intellectual disabilities. Annu Rev Genet *45*, 81-104. 10.1146/annurev-genet-110410-132512.
188. Agha, Z., Iqbal, Z., Azam, M., Ayub, H., Vissers, L.E., Gilissen, C., Ali, S.H., Riaz, M., Veltman, J.A., Pfundt, R., et al. (2014). Exome sequencing identifies three novel candidate genes implicated in intellectual disability. PLoS One *9*, e112687. 10.1371/journal.pone.0112687.
189. Verma, V., Paul, A., Amrapali Vishwanath, A., Vaidya, B., and Clement, J.P. (2019). Understanding intellectual disability and autism spectrum disorders from common mouse models: synapses to behaviour. Open Biol *9*, 180265. 10.1098/rsob.180265.
190. Hagerman, R.J., Berry-Kravis, E., Hazlett, H.C., Bailey, D.B., Jr., Moine, H., Kooy, R.F., Tassone, F., Gantois, I., Sonenberg, N., Mandel, J.L., and Hagerman, P.J. (2017). Fragile X syndrome. Nat Rev Dis Primers *3*, 17065. 10.1038/nrdp.2017.65.
191. Choi, L., and An, J.Y. (2021). Genetic architecture of autism spectrum disorder: Lessons from large-scale genomic studies. Neurosci Biobehav Rev *128*, 244-257. 10.1016/j.neubiorev.2021.06.028.
192. Sutcliffe, J.S., Nelson, D.L., Zhang, F., Pieretti, M., Caskey, C.T., Saxe, D., and Warren, S.T. (1992). DNA methylation represses FMR-1 transcription in fragile X syndrome. Hum Mol Genet *1*, 397-400. 10.1093/hmg/1.6.397.
193. Oberle, I., Rousseau, F., Heitz, D., Kretz, C., Devys, D., Hanauer, A., Boue, J., Bertheas, M.F., and Mandel, J.L. (1991). Instability of a 550-base pair DNA segment and abnormal methylation in fragile X syndrome. Science *252*, 1097-1102. 10.1126/science.252.5009.1097.
194. Hornstra, I.K., Nelson, D.L., Warren, S.T., and Yang, T.P. (1993). High resolution methylation analysis of the FMR1 gene trinucleotide repeat region in fragile X syndrome. Hum Mol Genet *2*, 1659-1665. 10.1093/hmg/2.10.1659.
195. Kumari, D., Lokanga, R., Yudkin, D., Zhao, X.N., and Usdin, K. (2012). Chromatin changes in the development and pathology of the Fragile X-associated disorders and Friedreich ataxia. Biochim Biophys Acta *1819*, 802-810. 10.1016/j.bbagrm.2011.12.009.
196. Coffee, B., Zhang, F., Warren, S.T., and Reines, D. (1999). Acetylated histones are associated with FMR1 in normal but not fragile X-syndrome cells. Nat Genet *22*, 98-101. 10.1038/8807.

197. Hinds, H.L., Ashley, C.T., Sutcliffe, J.S., Nelson, D.L., Warren, S.T., Housman, D.E., and Schalling, M. (1993). Tissue specific expression of FMR-1 provides evidence for a functional role in fragile X syndrome. Nat Genet *3*, 36-43. 10.1038/ng0193-36.
198. Ashley, C.T., Jr., Wilkinson, K.D., Reines, D., and Warren, S.T. (1993). FMR1 protein: conserved RNP family domains and selective RNA binding. Science *262*, 563-566. 10.1126/science.7692601.
199. Siomi, H., Choi, M., Siomi, M.C., Nussbaum, R.L., and Dreyfuss, G. (1994). Essential role for KH domains in RNA binding: impaired RNA binding by a mutation in the KH domain of FMR1 that causes fragile X syndrome. Cell *77*, 33-39. 10.1016/0092-8674(94)90232-1.
200. Darnell, J.C., Van Driesche, S.J., Zhang, C., Hung, K.Y., Mele, A., Fraser, C.E., Stone, E.F., Chen, C., Fak, J.J., Chi, S.W., et al. (2011). FMRP stalls ribosomal translocation on mRNAs linked to synaptic function and autism. Cell *146*, 247-261. 10.1016/j.cell.2011.06.013.
201. Dictenberg, J.B., Swanger, S.A., Antar, L.N., Singer, R.H., and Bassell, G.J. (2008). A direct role for FMRP in activity-dependent dendritic mRNA transport links filopodial-spine morphogenesis to fragile X syndrome. Dev Cell *14*, 926-939. 10.1016/j.devcel.2008.04.003.
202. Kanai, Y., Dohmae, N., and Hirokawa, N. (2004). Kinesin transports RNA: isolation and characterization of an RNA-transporting granule. Neuron *43*, 513-525. 10.1016/j.neuron.2004.07.022.
203. Davidovic, L., Jaglin, X.H., Lepagnol-Bestel, A.M., Tremblay, S., Simonneau, M., Bardoni, B., and Khandjian, E.W. (2007). The fragile X mental retardation protein is a molecular adaptor between the neurospecific KIF3C kinesin and dendritic RNA granules. Hum Mol Genet *16*, 3047-3058. 10.1093/hmg/ddm263.
204. Richter, J.D., Bassell, G.J., and Klann, E. (2015). Dysregulation and restoration of translational homeostasis in fragile X syndrome. Nat Rev Neurosci *16*, 595-605. 10.1038/nrn4001.
205. Antar, L.N., Afroz, R., Dictenberg, J.B., Carroll, R.C., and Bassell, G.J. (2004). Metabotropic glutamate receptor activation regulates fragile x mental retardation protein and FMR1 mRNA localization differentially in dendrites and at synapses. J Neurosci *24*, 2648-2655. 10.1523/JNEUROSCI.0099-04.2004.
206. Kao, D.I., Aldridge, G.M., Weiler, I.J., and Greenough, W.T. (2010). Altered mRNA transport, docking, and protein translation in neurons lacking fragile X mental retardation protein. Proc Natl Acad Sci U S A *107*, 15601-15606. 10.1073/pnas.1010564107.
207. Irwin, S.A., Galvez, R., and Greenough, W.T. (2000). Dendritic spine structural anomalies in fragile-X mental retardation syndrome. Cereb Cortex *10*, 1038-1044. 10.1093/cercor/10.10.1038.
208. Ilyas, M., Mir, A., Efthymiou, S., and Houlden, H. (2020). The genetics of intellectual disability: advancing technology and gene editing. F1000Res *9*. 10.12688/f1000research.16315.1.
209. Bier, E. (2005). Drosophila, the golden bug, emerges as a tool for human genetics. Nat Rev Genet *6*, 9-23. 10.1038/nrg1503.
210. Oortveld, M.A., Keerthikumar, S., Oti, M., Nijhof, B., Fernandes, A.C., Kochinke, K., Castells-Nobau, A., van Engelen, E., Ellenkamp, T., Eshuis, L., et al. (2013). Human

intellectual disability genes form conserved functional modules in Drosophila. PLoS Genet *9*, e1003911. 10.1371/journal.pgen.1003911.

211. Bellen, H.J., Tong, C., and Tsuda, H. (2010). 100 years of Drosophila research and its impact on vertebrate neuroscience: a history lesson for the future. Nat Rev Neurosci *11*, 514-522. 10.1038/nrn2839.

212. Potter, C.J., Turenchalk, G.S., and Xu, T. (2000). Drosophila in cancer research. An expanding role. Trends Genet *16*, 33-39. 10.1016/s0168-9525(99)01878-8.

213. Xiao, G. (2021). Methods to Assay the Behavior of Drosophila melanogaster for Toxicity Study. Methods Mol Biol *2326*, 47-54. 10.1007/978-1-0716-1514-0_4.

214. Nichols, C.D., Becnel, J., and Pandey, U.B. (2012). Methods to assay Drosophila behavior. J Vis Exp. 10.3791/3795.

215. Pak, C., Garshasbi, M., Kahrizi, K., Gross, C., Apponi, L.H., Noto, J.J., Kelly, S.M., Leung, S.W., Tzschach, A., Behjati, F., et al. (2011). Mutation of the conserved polyadenosine RNA binding protein, ZC3H14/dNab2, impairs neural function in Drosophila and humans. Proc Natl Acad Sci U S A *108*, 12390-12395. 10.1073/pnas.1107103108.

216. Ruiz-Canada, C., and Budnik, V. (2006). Introduction on the use of the Drosophila embryonic/larval neuromuscular junction as a model system to study synapse development and function, and a brief summary of pathfinding and target recognition. Int Rev Neurobiol *75*, 1-31. 10.1016/S0074-7742(06)75001-2.

217. Quach, T.T., Stratton, H.J., Khanna, R., Kolattukudy, P.E., Honnorat, J., Meyer, K., and Duchemin, A.M. (2021). Intellectual disability: dendritic anomalies and emerging genetic perspectives. Acta Neuropathol *141*, 139-158. 10.1007/s00401-020-02244-5.

218. Spindler, S.R., and Hartenstein, V. (2010). The Drosophila neural lineages: a model system to study brain development and circuitry. Dev Genes Evol *220*, 1-10. 10.1007/s00427-010-0323-7.

219. Scheffer, L.K., and Meinertzhagen, I.A. (2019). The Fly Brain Atlas. Annu Rev Cell Dev Biol *35*, 637-653. 10.1146/annurev-cellbio-100818-125444.

220. Stahl, A., and Tomchik, S.M. (2024). Modeling neurodegenerative and neurodevelopmental disorders in the Drosophila mushroom body. Learn Mem *31*. 10.1101/lm.053816.123.

221. Joiner, W.J., Crocker, A., White, B.H., and Sehgal, A. (2006). Sleep in Drosophila is regulated by adult mushroom bodies. Nature *441*, 757-760. 10.1038/nature04811.

222. Krashes, M.J., DasGupta, S., Vreede, A., White, B., Armstrong, J.D., and Waddell, S. (2009). A neural circuit mechanism integrating motivational state with memory expression in Drosophila. Cell *139*, 416-427. 10.1016/j.cell.2009.08.035.

223. Pitman, J.L., McGill, J.J., Keegan, K.P., and Allada, R. (2006). A dynamic role for the mushroom bodies in promoting sleep in Drosophila. Nature *441*, 753-756. 10.1038/nature04739.

224. Keleman, K., Vrontou, E., Kruttner, S., Yu, J.Y., Kurtovic-Kozaric, A., and Dickson, B.J. (2012). Dopamine neurons modulate pheromone responses in Drosophila courtship learning. Nature *489*, 145-149. 10.1038/nature11345.

225. Adel, M., and Griffith, L.C. (2021). The Role of Dopamine in Associative Learning in Drosophila: An Updated Unified Model. Neurosci Bull *37*, 831-852. 10.1007/s12264-021-00665-0.

226. Aso, Y., Hattori, D., Yu, Y., Johnston, R.M., Iyer, N.A., Ngo, T.T., Dionne, H., Abbott, L.F., Axel, R., Tanimoto, H., and Rubin, G.M. (2014). The neuronal architecture of the mushroom body provides a logic for associative learning. Elife *3*, e04577. 10.7554/eLife.04577.
227. Lim, J., Fernandez, A.I., Hinojos, S.J., Aranda, G.P., James, J., Seong, C.S., and Han, K.A. (2018). The mushroom body D1 dopamine receptor controls innate courtship drive. Genes Brain Behav *17*, 158-167. 10.1111/gbb.12425.
228. Owald, D., and Waddell, S. (2015). Olfactory learning skews mushroom body output pathways to steer behavioral choice in Drosophila. Curr Opin Neurobiol *35*, 178-184. 10.1016/j.conb.2015.10.002.
229. Sayin, S., De Backer, J.F., Siju, K.P., Wosniack, M.E., Lewis, L.P., Frisch, L.M., Gansen, B., Schlegel, P., Edmondson-Stait, A., Sharifi, N., et al. (2019). A Neural Circuit Arbitrates between Persistence and Withdrawal in Hungry Drosophila. Neuron *104*, 544-558 e546. 10.1016/j.neuron.2019.07.028.
230. Senapati, B., Tsao, C.H., Juan, Y.A., Chiu, T.H., Wu, C.L., Waddell, S., and Lin, S. (2019). A neural mechanism for deprivation state-specific expression of relevant memories in Drosophila. Nat Neurosci *22*, 2029-2039. 10.1038/s41593-019-0515-z.
231. Tsao, C.H., Chen, C.C., Lin, C.H., Yang, H.Y., and Lin, S. (2018). Drosophila mushroom bodies integrate hunger and satiety signals to control innate food-seeking behavior. Elife *7*. 10.7554/eLife.35264.
232. Armstrong, J.D., de Belle, J.S., Wang, Z., and Kaiser, K. (1998). Metamorphosis of the mushroom bodies; large-scale rearrangements of the neural substrates for associative learning and memory in Drosophila. Learn Mem *5*, 102-114.
233. Ito, K., and Hotta, Y. (1992). Proliferation pattern of postembryonic neuroblasts in the brain of Drosophila melanogaster. Dev Biol *149*, 134-148. 10.1016/0012-1606(92)90270-q.
234. Lee, T., Lee, A., and Luo, L. (1999). Development of the Drosophila mushroom bodies: sequential generation of three distinct types of neurons from a neuroblast. Development *126*, 4065-4076. 10.1242/dev.126.18.4065.
235. Li, F., Lindsey, J.W., Marin, E.C., Otto, N., Dreher, M., Dempsey, G., Stark, I., Bates, A.S., Pleijzier, M.W., Schlegel, P., et al. (2020). The connectome of the adult Drosophila mushroom body provides insights into function. Elife *9*. 10.7554/eLife.62576.
236. Tanaka, N.K., Tanimoto, H., and Ito, K. (2008). Neuronal assemblies of the Drosophila mushroom body. J Comp Neurol *508*, 711-755. 10.1002/cne.21692.
237. Cohn, R., Morantte, I., and Ruta, V. (2015). Coordinated and Compartmentalized Neuromodulation Shapes Sensory Processing in Drosophila. Cell *163*, 1742-1755. 10.1016/j.cell.2015.11.019.
238. Gao, F.B., and Bogert, B.A. (2003). Genetic control of dendritic morphogenesis in Drosophila. Trends Neurosci *26*, 262-268. 10.1016/S0166-2236(03)00078-X.
239. Scott, E.K., and Luo, L. (2001). How do dendrites take their shape? Nat Neurosci *4*, 359-365. 10.1038/86006.
240. Brown, H.E., Desai, T., Murphy, A.J., Pancholi, H., Schmidt, Z.W., Swahn, H., and Liebl, E.C. (2017). The function of Drosophila larval class IV dendritic arborization sensory neurons

in the larval-pupal transition is separable from their function in mechanical nociception responses. PLoS One *12*, e0184950. 10.1371/journal.pone.0184950.

241. Yang, W.K., and Chien, C.T. (2019). Beyond being innervated: the epidermis actively shapes sensory dendritic patterning. Open Biol *9*, 180257. 10.1098/rsob.180257.

242. Grueber, W.B., Jan, L.Y., and Jan, Y.N. (2002). Tiling of the Drosophila epidermis by multidendritic sensory neurons. Development *129*, 2867-2878. 10.1242/dev.129.12.2867.

243. Zhong, L., Hwang, R.Y., and Tracey, W.D. (2010). Pickpocket is a DEG/ENaC protein required for mechanical nociception in Drosophila larvae. Curr Biol *20*, 429-434. 10.1016/j.cub.2009.12.057.

244. Bardoni, B., Abekhoukh, S., Zongaro, S., and Melko, M. (2012). Intellectual disabilities, neuronal posttranscriptional RNA metabolism, and RNA-binding proteins: three actors for a complex scenario. Prog Brain Res *197*, 29-51. 10.1016/B978-0-444-54299-1.00003-0.

245. Leung, S.W., Apponi, L.H., Cornejo, O.E., Kitchen, C.M., Valentini, S.R., Pavlath, G.K., Dunham, C.M., and Corbett, A.H. (2009). Splice variants of the human ZC3H14 gene generate multiple isoforms of a zinc finger polyadenosine RNA binding protein. Gene *439*, 71-78. 10.1016/j.gene.2009.02.022.

246. Fasken, M.B., and Corbett, A.H. (2016). Links between mRNA splicing, mRNA quality control, and intellectual disability. RNA Dis *3*.

247. Al-Nabhani, M., Al-Rashdi, S., Al-Murshedi, F., Al-Kindi, A., Al-Thihli, K., Al-Saegh, A., Al-Futaisi, A., Al-Mamari, W., Zadjali, F., and Al-Maawali, A. (2018). Reanalysis of exome sequencing data of intellectual disability samples: Yields and benefits. Clin Genet *94*, 495-501. 10.1111/cge.13438.

248. Kuss, A.W., Garshasbi, M., Kahrizi, K., Tzschach, A., Behjati, F., Darvish, H., Abbasi-Moheb, L., Puettmann, L., Zecha, A., Weissmann, R., et al. (2011). Autosomal recessive mental retardation: homozygosity mapping identifies 27 single linkage intervals, at least 14 novel loci and several mutation hotspots. Hum Genet *129*, 141-148. 10.1007/s00439-010-0907-3.

249. Wigington, C.P., Morris, K.J., Newman, L.E., and Corbett, A.H. (2016). The Polyadenosine RNA-binding Protein, Zinc Finger Cys3His Protein 14 (ZC3H14), Regulates the Pre-mRNA Processing of a Key ATP Synthase Subunit mRNA. J Biol Chem *291*, 22442-22459. 10.1074/jbc.M116.754069.

250. Kraemer, B.C., Zhang, B., Leverenz, J.B., Thomas, J.H., Trojanowski, J.Q., and Schellenberg, G.D. (2003). Neurodegeneration and defective neurotransmission in a Caenorhabditis elegans model of tauopathy. Proc Natl Acad Sci U S A *100*, 9980-9985. 10.1073/pnas.1533448100.

251. Guthrie, C.R., Greenup, L., Leverenz, J.B., and Kraemer, B.C. (2011). MSUT2 is a determinant of susceptibility to tau neurotoxicity. Hum Mol Genet *20*, 1989-1999. 10.1093/hmg/ddr079.

252. Guthrie, C.R., Schellenberg, G.D., and Kraemer, B.C. (2009). SUT-2 potentiates tau-induced neurotoxicity in Caenorhabditis elegans. Hum Mol Genet *18*, 1825-1838. 10.1093/hmg/ddp099.

253. Lee, V.M., Goedert, M., and Trojanowski, J.Q. (2001). Neurodegenerative tauopathies. Annu Rev Neurosci *24*, 1121-1159. 10.1146/annurev.neuro.24.1.1121.
254. Baker, J.D., Uhrich, R.L., Strovas, T.J., Saxton, A.D., and Kraemer, B.C. (2020). Targeting Pathological Tau by Small Molecule Inhibition of the Poly(A):MSUT2 RNA-Protein Interaction. ACS Chem Neurosci *11*, 2277-2285. 10.1021/acschemneuro.0c00214.
255. Anderson, J.T., Wilson, S.M., Datar, K.V., and Swanson, M.S. (1993). NAB2: a yeast nuclear polyadenylated RNA-binding protein essential for cell viability. Mol Cell Biol *13*, 2730-2741. 10.1128/mcb.13.5.2730-2741.1993.
256. Marfatia, K.A., Crafton, E.B., Green, D.M., and Corbett, A.H. (2003). Domain analysis of the Saccharomyces cerevisiae heterogeneous nuclear ribonucleoprotein, Nab2p. Dissecting the requirements for Nab2p-facilitated poly(A) RNA export. J Biol Chem *278*, 6731-6740. 10.1074/jbc.M207571200.
257. Green, D.M., Marfatia, K.A., Crafton, E.B., Zhang, X., Cheng, X., and Corbett, A.H. (2002). Nab2p is required for poly(A) RNA export in Saccharomyces cerevisiae and is regulated by arginine methylation via Hmt1p. J Biol Chem *277*, 7752-7760. 10.1074/jbc.M110053200.
258. Hector, R.E., Nykamp, K.R., Dheur, S., Anderson, J.T., Non, P.J., Urbinati, C.R., Wilson, S.M., Minvielle-Sebastia, L., and Swanson, M.S. (2002). Dual requirement for yeast hnRNP Nab2p in mRNA poly(A) tail length control and nuclear export. EMBO J *21*, 1800-1810. 10.1093/emboj/21.7.1800.
259. Kelly, S.M., Pabit, S.A., Kitchen, C.M., Guo, P., Marfatia, K.A., Murphy, T.J., Corbett, A.H., and Berland, K.M. (2007). Recognition of polyadenosine RNA by zinc finger proteins. Proc Natl Acad Sci U S A *104*, 12306-12311. 10.1073/pnas.0701244104.
260. Grant, R.P., Marshall, N.J., Yang, J.C., Fasken, M.B., Kelly, S.M., Harreman, M.T., Neuhaus, D., Corbett, A.H., and Stewart, M. (2008). Structure of the N-terminal Mlp1-binding domain of the Saccharomyces cerevisiae mRNA-binding protein, Nab2. J Mol Biol *376*, 1048-1059. 10.1016/j.jmb.2007.11.087.
261. Aitchison, J.D., Blobel, G., and Rout, M.P. (1996). Kap104p: a karyopherin involved in the nuclear transport of messenger RNA binding proteins. Science *274*, 624-627. 10.1126/science.274.5287.624.
262. Lee, D.C., and Aitchison, J.D. (1999). Kap104p-mediated nuclear import. Nuclear localization signals in mRNA-binding proteins and the role of Ran and Rna. J Biol Chem *274*, 29031-29037. 10.1074/jbc.274.41.29031.
263. Truant, R., Fridell, R.A., Benson, R.E., Bogerd, H., and Cullen, B.R. (1998). Identification and functional characterization of a novel nuclear localization signal present in the yeast Nab2 poly(A)+ RNA binding protein. Mol Cell Biol *18*, 1449-1458. 10.1128/MCB.18.3.1449.
264. Kelly, S.M., Leung, S.W., Apponi, L.H., Bramley, A.M., Tran, E.J., Chekanova, J.A., Wente, S.R., and Corbett, A.H. (2010). Recognition of polyadenosine RNA by the zinc finger domain of nuclear poly(A) RNA-binding protein 2 (Nab2) is required for correct mRNA 3'-end formation. J Biol Chem *285*, 26022-26032. 10.1074/jbc.M110.141127.
265. Green, D.M., Johnson, C.P., Hagan, H., and Corbett, A.H. (2003). The C-terminal domain of myosin-like protein 1 (Mlp1p) is a docking site for heterogeneous nuclear

ribonucleoproteins that are required for mRNA export. Proc Natl Acad Sci U S A *100*, 1010-1015. 10.1073/pnas.0336594100.

266. Fasken, M.B., Stewart, M., and Corbett, A.H. (2008). Functional significance of the interaction between the mRNA-binding protein, Nab2, and the nuclear pore-associated protein, Mlp1, in mRNA export. J Biol Chem *283*, 27130-27143. 10.1074/jbc.M803649200.

267. Zheng, C., Fasken, M.B., Marshall, N.J., Brockmann, C., Rubinson, M.E., Wente, S.R., Corbett, A.H., and Stewart, M. (2010). Structural basis for the function of the Saccharomyces cerevisiae Gfd1 protein in mRNA nuclear export. J Biol Chem *285*, 20704-20715. 10.1074/jbc.M110.107276.

268. Galy, V., Gadal, O., Fromont-Racine, M., Romano, A., Jacquier, A., and Nehrbass, U. (2004). Nuclear retention of unspliced mRNAs in yeast is mediated by perinuclear Mlp1. Cell *116*, 63-73. 10.1016/s0092-8674(03)01026-2.

269. Strambio-de-Castillia, C., Blobel, G., and Rout, M.P. (1999). Proteins connecting the nuclear pore complex with the nuclear interior. J Cell Biol *144*, 839-855. 10.1083/jcb.144.5.839.

270. Kolling, R., Nguyen, T., Chen, E.Y., and Botstein, D. (1993). A new yeast gene with a myosin-like heptad repeat structure. Mol Gen Genet *237*, 359-369. 10.1007/BF00279439.

271. Suntharalingam, M., Alcazar-Roman, A.R., and Wente, S.R. (2004). Nuclear export of the yeast mRNA-binding protein Nab2 is linked to a direct interaction with Gfd1 and to Gle1 function. J Biol Chem *279*, 35384-35391. 10.1074/jbc.M402044200.

272. Hodge, C.A., Colot, H.V., Stafford, P., and Cole, C.N. (1999). Rat8p/Dbp5p is a shuttling transport factor that interacts with Rat7p/Nup159p and Gle1p and suppresses the mRNA export defect of xpo1-1 cells. EMBO J *18*, 5778-5788. 10.1093/emboj/18.20.5778.

273. Soucek, S., Zeng, Y., Bellur, D.L., Bergkessel, M., Morris, K.J., Deng, Q., Duong, D., Seyfried, N.T., Guthrie, C., Staley, J.P., et al. (2016). The Evolutionarily-conserved Polyadenosine RNA Binding Protein, Nab2, Cooperates with Splicing Machinery to Regulate the Fate of pre-mRNA. Mol Cell Biol *36*, 2697-2714. 10.1128/MCB.00402-16.

274. Jalloh, B., Lancaster, C.L., Rounds, J.C., Brown, B.E., Leung, S.W., Banerjee, A., Morton, D.J., Bienkowski, R.S., Fasken, M.B., Kremsky, I.J., et al. (2023). The Drosophila Nab2 RNA binding protein inhibits m(6)A methylation and male-specific splicing of Sex lethal transcript in female neuronal tissue. Elife *12*. 10.7554/eLife.64904.

275. Wan, L., Dockendorff, T.C., Jongens, T.A., and Dreyfuss, G. (2000). Characterization of dFMR1, a Drosophila melanogaster homolog of the fragile X mental retardation protein. Mol Cell Biol *20*, 8536-8547. 10.1128/MCB.20.22.8536-8547.2000.

276. Moore, M.C., and Taylor, D.T. (2023). Effects of valproate on seizure-like activity in Drosophila melanogaster with a knockdown of Ube3a in different neuronal populations as a model of Angelman Syndrome. Epilepsy Behav Rep *24*, 100622. 10.1016/j.ebr.2023.100622.

277. Wu, Y., Bolduc, F.V., Bell, K., Tully, T., Fang, Y., Sehgal, A., and Fischer, J.A. (2008). A Drosophila model for Angelman syndrome. Proc Natl Acad Sci U S A *105*, 12399-12404. 10.1073/pnas.0805291105.

278. Bienkowski, R.S., Banerjee, A., Rounds, J.C., Rha, J., Omotade, O.F., Gross, C., Morris, K.J., Leung, S.W., Pak, C., Jones, S.K., et al. (2017). The Conserved, Disease-Associated RNA Binding Protein dNab2 Interacts with the Fragile X Protein Ortholog in Drosophila Neurons. Cell Rep *20*, 1372-1384. 10.1016/j.celrep.2017.07.038.
279. Kelly, S.M., Leung, S.W., Pak, C., Banerjee, A., Moberg, K.H., and Corbett, A.H. (2014). A conserved role for the zinc finger polyadenosine RNA binding protein, ZC3H14, in control of poly(A) tail length. RNA *20*, 681-688. 10.1261/rna.043984.113.
280. Corgiat, E.B., List, S.M., Rounds, J.C., Corbett, A.H., and Moberg, K.H. (2021). The RNA-binding protein Nab2 regulates the proteome of the developing Drosophila brain. J Biol Chem *297*, 100877. 10.1016/j.jbc.2021.100877.
281. Corgiat, E.B., List, S.M., Rounds, J.C., Yu, D., Chen, P., Corbett, A.H., and Moberg, K.H. (2022). The Nab2 RNA-binding protein patterns dendritic and axonal projections through a planar cell polarity-sensitive mechanism. G3 (Bethesda) *12*. 10.1093/g3journal/jkac100.
282. Rounds, J.C., Corgiat, E.B., Ye, C., Behnke, J.A., Kelly, S.M., Corbett, A.H., and Moberg, K.H. (2022). The disease-associated proteins Drosophila Nab2 and Ataxin-2 interact with shared RNAs and coregulate neuronal morphology. Genetics *220*. 10.1093/genetics/iyab175.
283. Bellen, H.J., Levis, R.W., Liao, G., He, Y., Carlson, J.W., Tsang, G., Evans-Holm, M., Hiesinger, P.R., Schulze, K.L., Rubin, G.M., et al. (2004). The BDGP gene disruption project: single transposon insertions associated with 40% of Drosophila genes. Genetics *167*, 761-781. 10.1534/genetics.104.026427.
284. Kelly, S.M., Bienkowski, R., Banerjee, A., Melicharek, D.J., Brewer, Z.A., Marenda, D.R., Corbett, A.H., and Moberg, K.H. (2016). The Drosophila ortholog of the Zc3h14 RNA binding protein acts within neurons to pattern axon projection in the developing brain. Dev Neurobiol *76*, 93-106. 10.1002/dneu.22301.
285. Grmai, L., Pozmanter, C., and Van Doren, M. (2022). The Regulation of Germline Sex Determination in Drosophila by Sex lethal. Sex Dev *16*, 323-328. 10.1159/000521235.
286. Salz, H.K., and Erickson, J.W. (2010). Sex determination in Drosophila: The view from the top. Fly (Austin) *4*, 60-70. 10.4161/fly.4.1.11277.
287. Gebauer, F., Merendino, L., Hentze, M.W., and Valcarcel, J. (1998). The Drosophila splicing regulator sex-lethal directly inhibits translation of male-specific-lethal 2 mRNA. RNA *4*, 142-150.
288. Kan, L., Grozhik, A.V., Vedanayagam, J., Patil, D.P., Pang, N., Lim, K.S., Huang, Y.C., Joseph, B., Lin, C.J., Despic, V., et al. (2017). The m(6)A pathway facilitates sex determination in Drosophila. Nat Commun *8*, 15737. 10.1038/ncomms15737.
289. Wang, Y., Zhang, L., Ren, H., Ma, L., Guo, J., Mao, D., Lu, Z., Lu, L., and Yan, D. (2021). Role of Hakai in m(6)A modification pathway in Drosophila. Nat Commun *12*, 2159. 10.1038/s41467-021-22424-5.
290. Diaz, A.V., Matheny, T., Stephenson, D., Nemkov, T., D'Alessandro, A., and Reis, T. (2023). Spenito-dependent metabolic sexual dimorphism intrinsic to fat storage cells. bioRxiv. 10.1101/2023.02.17.528952.
291. Jaffe, A.B., and Hall, A. (2005). Rho GTPases: biochemistry and biology. Annu Rev Cell Dev Biol *21*, 247-269. 10.1146/annurev.cellbio.21.020604.150721.

292. Cherfils, J., and Zeghouf, M. (2013). Regulation of small GTPases by GEFs, GAPs, and GDIs. Physiol Rev *93*, 269-309. 10.1152/physrev.00003.2012.
293. Bloch-Gallego, E., and Anderson, D.I. (2023). Key role of Rho GTPases in motor disorders associated with neurodevelopmental pathologies. Mol Psychiatry *28*, 118-126. 10.1038/s41380-022-01702-8.
294. Ellenbroek, S.I., and Collard, J.G. (2007). Rho GTPases: functions and association with cancer. Clin Exp Metastasis *24*, 657-672. 10.1007/s10585-007-9119-1.
295. Kempers, L., Driessen, A.J.M., van Rijssel, J., Nolte, M.A., and van Buul, J.D. (2021). The RhoGEF Trio: A Protein with a Wide Range of Functions in the Vascular Endothelium. Int J Mol Sci *22*. 10.3390/ijms221810168.
296. Dufies, O., and Boyer, L. (2021). RhoGTPases and inflammasomes: Guardians of effector-triggered immunity. PLoS Pathog *17*, e1009504. 10.1371/journal.ppat.1009504.
297. Kjoller, L., and Hall, A. (1999). Signaling to Rho GTPases. Exp Cell Res *253*, 166-179. 10.1006/excr.1999.4674.
298. Rossman, K.L., Der, C.J., and Sondek, J. (2005). GEF means go: turning on RHO GTPases with guanine nucleotide-exchange factors. Nat Rev Mol Cell Biol *6*, 167-180. 10.1038/nrm1587.
299. Cote, J.F., and Vuori, K. (2002). Identification of an evolutionarily conserved superfamily of DOCK180-related proteins with guanine nucleotide exchange activity. J Cell Sci *115*, 4901-4913. 10.1242/jcs.00219.
300. Schmidt, A., and Hall, A. (2002). Guanine nucleotide exchange factors for Rho GTPases: turning on the switch. Genes Dev *16*, 1587-1609. 10.1101/gad.1003302.
301. Cook, D.R., Rossman, K.L., and Der, C.J. (2014). Rho guanine nucleotide exchange factors: regulators of Rho GTPase activity in development and disease. Oncogene *33*, 4021-4035. 10.1038/onc.2013.362.
302. Cote, J.F., and Vuori, K. (2006). In vitro guanine nucleotide exchange activity of DHR-2/DOCKER/CZH2 domains. Methods Enzymol *406*, 41-57. 10.1016/S0076-6879(06)06004-6.
303. Schmidt, S., and Debant, A. (2014). Function and regulation of the Rho guanine nucleotide exchange factor Trio. Small GTPases *5*, e29769. 10.4161/sgtp.29769.
304. Portales-Casamar, E., Briancon-Marjollet, A., Fromont, S., Triboulet, R., and Debant, A. (2006). Identification of novel neuronal isoforms of the Rho-GEF Trio. Biol Cell *98*, 183-193. 10.1042/BC20050009.
305. Ba, W., Yan, Y., Reijnders, M.R., Schuurs-Hoeijmakers, J.H., Feenstra, I., Bongers, E.M., Bosch, D.G., De Leeuw, N., Pfundt, R., Gilissen, C., et al. (2016). TRIO loss of function is associated with mild intellectual disability and affects dendritic branching and synapse function. Hum Mol Genet *25*, 892-902. 10.1093/hmg/ddv618.
306. Katrancha, S.M., Shaw, J.E., Zhao, A.Y., Myers, S.A., Cocco, A.R., Jeng, A.T., Zhu, M., Pittenger, C., Greer, C.A., Carr, S.A., et al. (2019). Trio Haploinsufficiency Causes Neurodevelopmental Disease-Associated Deficits. Cell Rep *26*, 2805-2817 e2809. 10.1016/j.celrep.2019.02.022.
307. Paskus, J.D., Herring, B.E., and Roche, K.W. (2020). Kalirin and Trio: RhoGEFs in Synaptic Transmission, Plasticity, and Complex Brain Disorders. Trends Neurosci *43*, 505-518. 10.1016/j.tins.2020.05.002.

308. Pengelly, R.J., Greville-Heygate, S., Schmidt, S., Seaby, E.G., Jabalameli, M.R., Mehta, S.G., Parker, M.J., Goudie, D., Fagotto-Kaufmann, C., Mercer, C., et al. (2016). Mutations specific to the Rac-GEF domain of TRIO cause intellectual disability and microcephaly. J Med Genet *53*, 735-742. 10.1136/jmedgenet-2016-103942.
309. Debant, A., Serra-Pages, C., Seipel, K., O'Brien, S., Tang, M., Park, S.H., and Streuli, M. (1996). The multidomain protein Trio binds the LAR transmembrane tyrosine phosphatase, contains a protein kinase domain, and has separate rac-specific and rho-specific guanine nucleotide exchange factor domains. Proc Natl Acad Sci U S A *93*, 5466-5471. 10.1073/pnas.93.11.5466.
310. Grubisha, M.J., DeGiosio, R.A., Wills, Z.P., and Sweet, R.A. (2022). Trio and Kalirin as unique enactors of Rho/Rac spatiotemporal precision. Cell Signal *98*, 110416. 10.1016/j.cellsig.2022.110416.
311. Sun, Y.J., Nishikawa, K., Yuda, H., Wang, Y.L., Osaka, H., Fukazawa, N., Naito, A., Kudo, Y., Wada, K., and Aoki, S. (2006). Solo/Trio8, a membrane-associated short isoform of Trio, modulates endosome dynamics and neurite elongation. Mol Cell Biol *26*, 6923-6935. 10.1128/MCB.02474-05.
312. Yoshizuka, N., Moriuchi, R., Mori, T., Yamada, K., Hasegawa, S., Maeda, T., Shimada, T., Yamada, Y., Kamihira, S., Tomonaga, M., and Katamine, S. (2004). An alternative transcript derived from the trio locus encodes a guanosine nucleotide exchange factor with mouse cell-transforming potential. J Biol Chem *279*, 43998-44004. 10.1074/jbc.M406082200.
313. Awasaki, T., Saito, M., Sone, M., Suzuki, E., Sakai, R., Ito, K., and Hama, C. (2000). The Drosophila trio plays an essential role in patterning of axons by regulating their directional extension. Neuron *26*, 119-131. 10.1016/s0896-6273(00)81143-5.
314. Bircher, J.E., and Koleske, A.J. (2021). Trio family proteins as regulators of cell migration and morphogenesis in development and disease - mechanisms and cellular contexts. J Cell Sci *134*. 10.1242/jcs.248393.
315. Kannan, R., Song, J.K., Karpova, T., Clarke, A., Shivalkar, M., Wang, B., Kotlyanskaya, L., Kuzina, I., Gu, Q., and Giniger, E. (2017). The Abl pathway bifurcates to balance Enabled and Rac signaling in axon patterning in Drosophila. Development *144*, 487-498. 10.1242/dev.143776.
316. Newsome, T.P., Schmidt, S., Dietzl, G., Keleman, K., Asling, B., Debant, A., and Dickson, B.J. (2000). Trio combines with dock to regulate Pak activity during photoreceptor axon pathfinding in Drosophila. Cell *101*, 283-294. 10.1016/s0092-8674(00)80838-7.
317. Ng, J., and Luo, L. (2004). Rho GTPases regulate axon growth through convergent and divergent signaling pathways. Neuron *44*, 779-793. 10.1016/j.neuron.2004.11.014.
318. Ni, J.-Q., Liu, L.-P., Binari, R., Hardy, R., Shim, H.-S., Cavallaro, A., Booker, M., Pfeiffer, B.D., Markstein, M., Wang, H., et al. (2009). A Drosophila Resource of Transgenic RNAi Lines for Neurogenetics. Genetics *182*, 1089-1100. 10.1534/genetics.109.103630.
319. Leeuwen, F.N., Kain, H.E., Kammen, R.A., Michiels, F., Kranenburg, O.W., and Collard, J.G. (1997). The guanine nucleotide exchange factor Tiam1 affects neuronal morphology; opposing roles for the small GTPases Rac and Rho. J Cell Biol *139*, 797-807. 10.1083/jcb.139.3.797.

320. Iyer, S.C., Wang, D., Iyer, E.P., Trunnell, S.A., Meduri, R., Shinwari, R., Sulkowski, M.J., and Cox, D.N. (2012). The RhoGEF trio functions in sculpting class specific dendrite morphogenesis in Drosophila sensory neurons. PLoS One *7*, e33634. 10.1371/journal.pone.0033634.
321. Nakahata, Y., and Yasuda, R. (2018). Plasticity of Spine Structure: Local Signaling, Translation and Cytoskeletal Reorganization. Front Synaptic Neurosci *10*, 29. 10.3389/fnsyn.2018.00029.
322. Wills, Z.P., Mandel-Brehm, C., Mardinly, A.R., McCord, A.E., Giger, R.J., and Greenberg, M.E. (2012). The nogo receptor family restricts synapse number in the developing hippocampus. Neuron *73*, 466-481. 10.1016/j.neuron.2011.11.029.
323. Chen, L., Liao, G., Waclaw, R.R., Burns, K.A., Linquist, D., Campbell, K., Zheng, Y., and Kuan, C.Y. (2007). Rac1 controls the formation of midline commissures and the competency of tangential migration in ventral telencephalic neurons. J Neurosci *27*, 3884-3893. 10.1523/JNEUROSCI.3509-06.2007.
324. Dupraz, S., Hilton, B.J., Husch, A., Santos, T.E., Coles, C.H., Stern, S., Brakebusch, C., and Bradke, F. (2019). RhoA Controls Axon Extension Independent of Specification in the Developing Brain. Curr Biol *29*, 3874-3886 e3879. 10.1016/j.cub.2019.09.040.
325. Pegtel, D.M., Ellenbroek, S.I., Mertens, A.E., van der Kammen, R.A., de Rooij, J., and Collard, J.G. (2007). The Par-Tiam1 complex controls persistent migration by stabilizing microtubule-dependent front-rear polarity. Curr Biol *17*, 1623-1634. 10.1016/j.cub.2007.08.035.
326. Ahnert-Hilger, G., Holtje, M., Grosse, G., Pickert, G., Mucke, C., Nixdorf-Bergweiler, B., Boquet, P., Hofmann, F., and Just, I. (2004). Differential effects of Rho GTPases on axonal and dendritic development in hippocampal neurones. J Neurochem *90*, 9-18. 10.1111/j.1471-4159.2004.02475.x.
327. Lee, T., Winter, C., Marticke, S.S., Lee, A., and Luo, L. (2000). Essential roles of Drosophila RhoA in the regulation of neuroblast proliferation and dendritic but not axonal morphogenesis. Neuron *25*, 307-316. 10.1016/s0896-6273(00)80896-x.
328. Nakayama, A.Y., Harms, M.B., and Luo, L. (2000). Small GTPases Rac and Rho in the maintenance of dendritic spines and branches in hippocampal pyramidal neurons. J Neurosci *20*, 5329-5338. 10.1523/JNEUROSCI.20-14-05329.2000.
329. Pilpel, Y., and Segal, M. (2004). Activation of PKC induces rapid morphological plasticity in dendrites of hippocampal neurons via Rac and Rho-dependent mechanisms. Eur J Neurosci *19*, 3151-3164. 10.1111/j.0953-816X.2004.03380.x.
330. Bateman, J., Shu, H., and Van Vactor, D. (2000). The guanine nucleotide exchange factor trio mediates axonal development in the Drosophila embryo. Neuron *26*, 93-106. 10.1016/s0896-6273(00)81141-1.
331. Bateman, J., and Van Vactor, D. (2001). The Trio family of guanine-nucleotide-exchange factors: regulators of axon guidance. J Cell Sci *114*, 1973-1980. 10.1242/jcs.114.11.1973.
332. Kelly, S., Pak, C., Garshasbi, M., Kuss, A., Corbett, A.H., and Moberg, K. (2012). New kid on the ID block: neural functions of the Nab2/ZC3H14 class of Cys(3)His tandem zinc-finger polyadenosine RNA binding proteins. RNA Biol *9*, 555-562. 10.4161/rna.20187.
333. Gerstberger, S., Hafner, M., and Tuschl, T. (2014). A census of human RNA-binding proteins. Nature Reviews Genetics *15*, 829-845. 10.1038/nrg3813.

334. Conlon, E.G., and Manley, J.L. (2017). RNA-binding proteins in neurodegeneration: mechanisms in aggregate. Genes Dev *31*, 1509-1528. 10.1101/gad.304055.117.
335. Darnell, J.C., and Richter, J.D. (2012). Cytoplasmic RNA-binding proteins and the control of complex brain function. Cold Spring Harb Perspect Biol *4*, a012344. 10.1101/cshperspect.a012344.
336. Smith, R.W., Blee, T.K., and Gray, N.K. (2014). Poly(A)-binding proteins are required for diverse biological processes in metazoans. Biochem Soc Trans *42*, 1229-1237. 10.1042/BST20140111.
337. Fasken, M.B., Corbett, A.H., and Stewart, M. (2019). Structure-function relationships in the Nab2 polyadenosine-RNA binding Zn finger protein family. Protein Sci *28*, 513-523. 10.1002/pro.3565.
338. Rha, J., Jones, S.K., Fidler, J., Banerjee, A., Leung, S.W., Morris, K.J., Wong, J.C., Inglis, G.A.S., Shapiro, L., Deng, Q., et al. (2017). The RNA-binding Protein, ZC3H14, is Required for Proper Poly(A) Tail Length Control, Expression of Synaptic Proteins, and Brain Function in Mice. Hum Mol Genet. 10.1093/hmg/ddx248.
339. Heisenberg, M. (2003). Mushroom body memoir: from maps to models. Nat Rev Neurosci *4*, 266-275. 10.1038/nrn1074.
340. Förch, P., and Valcárcel, J. (2003). Splicing regulation in Drosophila sex determination. Prog Mol Subcell Biol *31*, 127-151. 10.1007/978-3-662-09728-1_5.
341. Haussmann, I.U., Bodi, Z., Sanchez-Moran, E., Mongan, N.P., Archer, N., Fray, R.G., and Soller, M. (2016). m(6)A potentiates Sxl alternative pre-mRNA splicing for robust Drosophila sex determination. Nature. 10.1038/nature20577.
342. Dobin, A., Davis, C.A., Schlesinger, F., Drenkow, J., Zaleski, C., Jha, S., Batut, P., Chaisson, M., and Gingeras, T.R. (2013). STAR: ultrafast universal RNA-seq aligner. Bioinformatics *29*, 15-21. 10.1093/bioinformatics/bts635.
343. Liao, Y., Smyth, G.K., and Shi, W. (2014). featureCounts: an efficient general purpose program for assigning sequence reads to genomic features. Bioinformatics *30*, 923-930. 10.1093/bioinformatics/btt656.
344. Love, M.I., Huber, W., and Anders, S. (2014). Moderated estimation of fold change and dispersion for RNA-seq data with DESeq2. Genome Biology *15*, 550-550. 10.1186/s13059-014-0550-8.
345. Mootha, V.K., Lindgren, C.M., Eriksson, K.F., Subramanian, A., Sihag, S., Lehar, J., Puigserver, P., Carlsson, E., Ridderstråle, M., Laurila, E., et al. (2003). PGC-1α-responsive genes involved in oxidative phosphorylation are coordinately downregulated in human diabetes. Nature Genetics *34*, 267-273. 10.1038/ng1180.
346. Subramanian, A., Tamayo, P., Mootha, V.K., Mukherjee, S., Ebert, B.L., Gillette, M.A., Paulovich, A., Pomeroy, S.L., Golub, T.R., Lander, E.S., and Mesirov, J.P. (2005). Gene set enrichment analysis: a knowledge-based approach for interpreting genome-wide expression profiles. Proc Natl Acad Sci U S A *102*, 15545-15550. 10.1073/pnas.0506580102.
347. Ashburner, M., Ball, C.A., Blake, J.A., Botstein, D., Butler, H., Cherry, J.M., Davis, A.P., Dolinski, K., Dwight, S.S., Eppig, J.T., et al. (2000). Gene ontology: Tool for the unification of biology. NIH Public Access.

348. The Gene Ontology Consortium (2019). The Gene Ontology Resource: 20 years and still GOing strong. Nucleic Acids Research *47*, D330-D338. 10.1093/nar/gky1055.
349. Katz, Y., Wang, E.T., Airoldi, E.M., and Burge, C.B. (2010). Analysis and design of RNA sequencing experiments for identifying isoform regulation. Nat Methods *7*, 1009-1015. 10.1038/nmeth.1528.
350. Anders, S., Reyes, A., and Huber, W. (2012). Detecting differential usage of exons from RNA-seq data. Genome Res *22*, 2008-2017. 10.1101/gr.133744.111.
351. Harrison, D.A. (2007). Sex determination: controlling the master. Curr Biol *17*, R328-330. 10.1016/j.cub.2007.03.012.
352. Penalva, L.O., and Sanchez, L. (2003). RNA binding protein sex-lethal (Sxl) and control of Drosophila sex determination and dosage compensation. Microbiol Mol Biol Rev *67*, 343-359, table of contents. 10.1128/mmbr.67.3.343-359.2003.
353. Gawande, B., Robida, M.D., Rahn, A., and Singh, R. (2006). Drosophila Sex-lethal protein mediates polyadenylation switching in the female germline. EMBO J *25*, 1263-1272. 10.1038/sj.emboj.7601022.
354. Sakamoto, H., Inoue, K., Higuchi, I., Ono, Y., and Shimura, Y. (1992). Control of Drosophila Sex-lethal pre-mRNA splicing by its own female-specific product. Nucleic Acids Res *20*, 5533-5540. 10.1093/nar/20.21.5533.
355. Bell, L.R., Maine, E.M., Schedl, P., and Cline, T.W. (1988). Sex-lethal, a Drosophila sex determination switch gene, exhibits sex-specific RNA splicing and sequence similarity to RNA binding proteins. Cell *55*, 1037-1046. 10.1016/0092-8674(88)90248-6.
356. Robinson, J.T., Thorvaldsdottir, H., Wenger, A.M., Zehir, A., and Mesirov, J.P. (2017). Variant Review with the Integrative Genomics Viewer. Cancer Res *77*, e31-e34. 10.1158/0008-5472.CAN-17-0337.
357. Sanchez, L., Gorfinkiel, N., and Guerrero, I. (2001). Sex determination genes control the development of the Drosophila genital disc, modulating the response to Hedgehog, Wingless and Decapentaplegic signals. Development *128*, 1033-1043.
358. Horabin, J.I., and Schedl, P. (1993). Regulated splicing of the Drosophila sex-lethal male exon involves a blockage mechanism. Mol Cell Biol *13*, 1408-1414. 10.1128/mcb.13.3.1408.
359. Barbash, D.A., and Cline, T.W. (1995). Genetic and molecular analysis of the autosomal component of the primary sex determination signal of Drosophila melanogaster. Genetics *141*, 1451-1471.
360. Lucchesi, J.C., and Kuroda, M.I. (2015). Dosage compensation in Drosophila. Cold Spring Harb Perspect Biol *7*. 10.1101/cshperspect.a019398.
361. Keller, C.I., and Akhtar, A. (2015). The MSL complex: juggling RNA-protein interactions for dosage compensation and beyond. Curr Opin Genet Dev *31*, 1-11. 10.1016/j.gde.2015.03.007.
362. Amrein, H., and Axel, R. (1997). Genes expressed in neurons of adult male Drosophila. Cell *88*, 459-469. 10.1016/s0092-8674(00)81886-3.
363. Bevan, C., Roote, J., Russell, S., Ashburner, M. (1993). On the allelism of killer-of-male and male-specific lethal mutations. Drosophila Information Service *72*, 125.
364. Zhou, S., Yang, Y., Scott, M.J., Pannuti, A., Fehr, K.C., Eisen, A., Koonin, E.V., Fouts, D.L., Wrightsman, R., Manning, J.E., and et al. (1995). Male-specific lethal 2, a dosage

compensation gene of Drosophila, undergoes sex-specific regulation and encodes a protein with a RING finger and a metallothionein-like cysteine cluster. Embo j *14*, 2884-2895. 10.1002/j.1460-2075.1995.tb07288.x.

365. Meller, V.H., Wu, K.H., Roman, G., Kuroda, M.I., and Davis, R.L. (1997). roX1 RNA paints the X chromosome of male Drosophila and is regulated by the dosage compensation system. Cell *88*, 445-457. 10.1016/s0092-8674(00)81885-1.
366. Kelley, R.L., Solovyeva, I., Lyman, L.M., Richman, R., Solovyev, V., and Kuroda, M.I. (1995). Expression of msl-2 causes assembly of dosage compensation regulators on the X chromosomes and female lethality in Drosophila. Cell *81*, 867-877. 10.1016/0092-8674(95)90007-1.
367. Rounds, J.C., Corgiat, E.B., Ye, C., Behnke, J.A., Kelly, S.M., Corbett, A.H., and Moberg, K.H. (2021). The Disease-Associated Proteins Drosophila Nab2 and Ataxin-2 Interact with Shared RNAs and Coregulate Neuronal Morphology. bioRxiv, 2021.2003.2001.433469. 10.1101/2021.03.01.433469.
368. Lin, D.M., and Goodman, C.S. (1994). Ectopic and increased expression of Fasciclin II alters motoneuron growth cone guidance. Neuron *13*, 507-523. 10.1016/0896-6273(94)90022-1.
369. Granadino, B., Campuzano, S., and Sanchez, L. (1990). The Drosophila melanogaster fl(2)d gene is needed for the female-specific splicing of Sex-lethal RNA. EMBO J *9*, 2597-2602. 10.1002/j.1460-2075.1990.tb07441.x.
370. Hilfiker, A., Amrein, H., Dubendorfer, A., Schneiter, R., and Nothiger, R. (1995). The gene virilizer is required for female-specific splicing controlled by Sxl, the master gene for sexual development in Drosophila. Development *121*, 4017-4026.
371. Niessen, M., Schneiter, R., and Nothiger, R. (2001). Molecular identification of virilizer, a gene required for the expression of the sex-determining gene Sex-lethal in Drosophila melanogaster. Genetics *157*, 679-688.
372. Meyer, K.D. (2019). DART-seq: an antibody-free method for global m(6)A detection. Nat Methods *16*, 1275-1280. 10.1038/s41592-019-0570-0.
373. Tegowski, M., Zhu, H., and Meyer, K.D. (2022). Detecting m(6)A with In Vitro DART-Seq. Methods Mol Biol *2404*, 363-374. 10.1007/978-1-0716-1851-6_20.
374. Linder, B., Grozhik, A.V., Olarerin-George, A.O., Meydan, C., Mason, C.E., and Jaffrey, S.R. (2015). Single-nucleotide-resolution mapping of m6A and m6Am throughout the transcriptome. Nat Methods *12*, 767-772. 10.1038/nmeth.3453.
375. Moschall, R., Gaik, M., and Medenbach, J. (2017). Promiscuity in post-transcriptional control of gene expression: Drosophila sex-lethal and its regulatory partnerships. FEBS Lett *591*, 1471-1488. 10.1002/1873-3468.12652.
376. Bashaw, G.J., and Baker, B.S. (1995). The msl-2 dosage compensation gene of Drosophila encodes a putative DNA-binding protein whose expression is sex specifically regulated by Sex-lethal. Development *121*, 3245-3258.
377. Bashaw, G.J., and Baker, B.S. (1997). The regulation of the Drosophila msl-2 gene reveals a function for Sex-lethal in translational control. Cell *89*, 789-798. 10.1016/s0092-8674(00)80262-7.

378. Primus, S., Pozmanter, C., Baxter, K., and Van Doren, M. (2019). Tudor-domain containing protein 5-like promotes male sexual identity in the Drosophila germline and is repressed in females by Sex lethal. PLoS Genet *15*, e1007617. 10.1371/journal.pgen.1007617.
379. Ota, R., Morita, S., Sato, M., Shigenobu, S., Hayashi, M., and Kobayashi, S. (2017). Transcripts immunoprecipitated with Sxl protein in primordial germ cells of Drosophila embryos. Dev Growth Differ *59*, 713-723. 10.1111/dgd.12408.
380. Morris, K.J., and Corbett, A.H. (2018). The polyadenosine RNA-binding protein ZC3H14 interacts with the THO complex and coordinately regulates the processing of neuronal transcripts. Nucleic Acids Res *46*, 6561-6575. 10.1093/nar/gky446.
381. Obrdlik, A., Lin, G., Haberman, N., Ule, J., and Ephrussi, A. (2019). The Transcriptome-wide Landscape and Modalities of EJC Binding in Adult Drosophila. Cell Rep *28*, 1219-1236 e1211. 10.1016/j.celrep.2019.06.088.
382. Singh, G., Kucukural, A., Cenik, C., Leszyk, J.D., Shaffer, S.A., Weng, Z., and Moore, M.J. (2012). The Cellular EJC Interactome Reveals Higher-Order mRNP Structure and an EJC-SR Protein Nexus. Cell *151*, 915-916. 10.1016/j.cell.2012.10.032.
383. He, P.C., Wei, J., Dou, X., Harada, B.T., Zhang, Z., Ge, R., Liu, C., Zhang, L.S., Yu, X., Wang, S., et al. (2023). Exon architecture controls mRNA m(6)A suppression and gene expression. Science *379*, 677-682. 10.1126/science.abj9090.
384. Yang, X., Triboulet, R., Liu, Q., Sendinc, E., and Gregory, R.I. (2022). Exon junction complex shapes the m(6)A epitranscriptome. Nat Commun *13*, 7904. 10.1038/s41467-022-35643-1.
385. Serin, H.M., Simsek, E., Isik, E., and Gokben, S. (2018). WWOX-associated encephalopathies: identification of the phenotypic spectrum and the resulting genotype-phenotype correlation. Neurol Sci *39*, 1977-1980. 10.1007/s10072-018-3528-6.
386. Mallaret, M., Synofzik, M., Lee, J., Sagum, C.A., Mahajnah, M., Sharkia, R., Drouot, N., Renaud, M., Klein, F.A., Anheim, M., et al. (2014). The tumour suppressor gene WWOX is mutated in autosomal recessive cerebellar ataxia with epilepsy and mental retardation. Brain *137*, 411-419. 10.1093/brain/awt338.
387. Afgan, E., Baker, D., Batut, B., van den Beek, M., Bouvier, D., Cech, M., Chilton, J., Clements, D., Coraor, N., Gruning, B.A., et al. (2018). The Galaxy platform for accessible, reproducible and collaborative biomedical analyses: 2018 update. Nucleic Acids Res *46*, W537-W544. 10.1093/nar/gky379.
388. dos Santos, G., Schroeder, A.J., Goodman, J.L., Strelets, V.B., Crosby, M.A., Thurmond, J., Emmert, D.B., Gelbart, W.M., and FlyBase, C. (2015). FlyBase: introduction of the Drosophila melanogaster Release 6 reference genome assembly and large-scale migration of genome annotations. Nucleic Acids Res *43*, D690-697. 10.1093/nar/gku1099.
389. Yates, A.D., Achuthan, P., Akanni, W., Allen, J., Allen, J., Alvarez-Jarreta, J., Amode, M.R., Armean, I.M., Azov, A.G., Bennett, R., et al. (2020). Ensembl 2020. Nucleic Acids Res *48*, D682-D688. 10.1093/nar/gkz966.
390. Wickham, H. (2016). ggplot2 : Elegant Graphics for Data Analysis. Use R!,. 2nd ed. Springer International Publishing : Imprint: Springer,.

391. Slowikowski, K. (2019). ggrepel: Automatically Position Non-Overlapping Text Labels with 'ggplot2'.
392. Team, R.S. (2018). RStudio: Integrated Development Environment for R. RStudio, Inc.
393. Thurmond, J., Goodman, J.L., Strelets, V.B., Attrill, H., Gramates, L.S., Marygold, S.J., Matthews, B.B., Millburn, G., Antonazzo, G., Trovisco, V., et al. (2019). FlyBase 2.0: the next generation. Nucleic Acids Res *47*, D759-D765. 10.1093/nar/gky1003.
394. Powell, J.A. (2014). GO2MSIG, an automated GO based multi-species gene set generator for gene set enrichment analysis. BMC Bioinformatics *15*, 146. 10.1186/1471-2105-15-146.
395. Carbon, S., Ireland, A., Mungall, C.J., Shu, S., Marshall, B., Lewis, S., Ami, G.O.H., and Web Presence Working, G. (2009). AmiGO: online access to ontology and annotation data. Bioinformatics *25*, 288-289. 10.1093/bioinformatics/btn615.
396. Quinlan, A.R., and Hall, I.M. (2010). BEDTools: a flexible suite of utilities for comparing genomic features. Bioinformatics *26*, 841-842. 10.1093/bioinformatics/btq033.
397. Grant, C.E., Bailey, T.L., and Noble, W.S. (2011). FIMO: scanning for occurrences of a given motif. Bioinformatics *27*, 1017-1018. 10.1093/bioinformatics/btr064.
398. Morton, D.J., Jalloh, B., Kim, L., Kremsky, I., Nair, R.J., Nguyen, K.B., Rounds, J.C., Sterrett, M.C., Brown, B., Le, T., et al. (2020). A Drosophila model of Pontocerebellar Hypoplasia reveals a critical role for the RNA exosome in neurons. PLoS Genet *16*, e1008901. 10.1371/journal.pgen.1008901.
399. Kluesner, M.G., Nedveck, D.A., Lahr, W.S., Garbe, J.R., Abrahante, J.E., Webber, B.R., and Moriarity, B.S. (2018). EditR: A Method to Quantify Base Editing from Sanger Sequencing. CRISPR J *1*, 239-250. 10.1089/crispr.2018.0014.
400. Corley, M., Burns, M.C., and Yeo, G.W. (2020). How RNA-Binding Proteins Interact with RNA: Molecules and Mechanisms. Mol Cell *78*, 9-29. 10.1016/j.molcel.2020.03.011.
401. Maniatis, T., and Reed, R. (2002). An extensive network of coupling among gene expression machines. Nature *416*, 499-506. 10.1038/416499a.
402. McKee, A.E., and Silver, P.A. (2007). Systems perspectives on mRNA processing. Cell Res *17*, 581-590. 10.1038/cr.2007.54.
403. Santoro, M.R., Bray, S.M., and Warren, S.T. (2012). Molecular mechanisms of fragile X syndrome: a twenty-year perspective. Annu Rev Pathol *7*, 219-245. 10.1146/annurev-pathol-011811-132457.
404. Thelen, M.P., and Kye, M.J. (2019). The Role of RNA Binding Proteins for Local mRNA Translation: Implications in Neurological Disorders. Front Mol Biosci *6*, 161. 10.3389/fmolb.2019.00161.
405. Agrawal, S., Kuo, P.H., Chu, L.Y., Golzarroshan, B., Jain, M., and Yuan, H.S. (2019). RNA recognition motifs of disease-linked RNA-binding proteins contribute to amyloid formation. Sci Rep *9*, 6171. 10.1038/s41598-019-42367-8.
406. Edens, B.M., Ajroud-Driss, S., Ma, L., and Ma, Y.C. (2015). Molecular mechanisms and animal models of spinal muscular atrophy. Biochim Biophys Acta *1852*, 685-692. 10.1016/j.bbadis.2014.07.024.
407. Gross, C., Berry-Kravis, E.M., and Bassell, G.J. (2012). Therapeutic strategies in fragile X syndrome: dysregulated mGluR signaling and beyond. Neuropsychopharmacology *37*, 178-195. 10.1038/npp.2011.137.

408. Barbe, B., Franke, P., Maier, W., and Leboyer, M. (1996). Fragile X syndrome. I. An overview on its genetic mechanism. Eur Psychiatry *11*, 227-232. 10.1016/0924-9338(96)82328-5.
409. Brais, B. (2003). Oculopharyngeal muscular dystrophy: a late-onset polyalanine disease. Cytogenet Genome Res *100*, 252-260. 10.1159/000072861.
410. Franke, P., Barbe, B., Leboyer, M., and Maier, W. (1996). Fragile X syndrome. II. Cognitive and behavioral correlates of mutations of the FMR-1 gene. Eur Psychiatry *11*, 233-243. 10.1016/0924-9338(96)82329-7.
411. Kolb, S.J., and Kissel, J.T. (2011). Spinal muscular atrophy: a timely review. Arch Neurol *68*, 979-984. 10.1001/archneurol.2011.74.
412. Lage, K., Hansen, N.T., Karlberg, E.O., Eklund, A.C., Roque, F.S., Donahoe, P.K., Szallasi, Z., Jensen, T.S., and Brunak, S. (2008). A large-scale analysis of tissue-specific pathology and gene expression of human disease genes and complexes. Proc Natl Acad Sci U S A *105*, 20870-20875. 10.1073/pnas.0810772105.
413. Pirozzi, F., Tabolacci, E., and Neri, G. (2011). The FRAXopathies: definition, overview, and update. Am J Med Genet A *155A*, 1803-1816. 10.1002/ajmg.a.34113.
414. Goss, D.J., and Kleiman, F.E. (2013). Poly(A) binding proteins: are they all created equal? Wiley Interdiscip Rev RNA *4*, 167-179. 10.1002/wrna.1151.
415. Wigington, C.P., Williams, K.R., Meers, M.P., Bassell, G.J., and Corbett, A.H. (2014). Poly(A) RNA-binding proteins and polyadenosine RNA: new members and novel functions. Wiley Interdiscip Rev RNA *5*, 601-622. 10.1002/wrna.1233.
416. Wheeler, J.M., McMillan, P., Strovas, T.J., Liachko, N.F., Amlie-Wolf, A., Kow, R.L., Klein, R.L., Szot, P., Robinson, L., Guthrie, C., et al. (2019). Activity of the poly(A) binding protein MSUT2 determines susceptibility to pathological tau in the mammalian brain. Sci Transl Med *11*. 10.1126/scitranslmed.aao6545.
417. Schmid, M., Olszewski, P., Pelechano, V., Gupta, I., Steinmetz, L.M., and Jensen, T.H. (2015). The Nuclear PolyA-Binding Protein Nab2p Is Essential for mRNA Production. Cell Rep *12*, 128-139. 10.1016/j.celrep.2015.06.008.
418. Grenier St-Sauveur, V., Soucek, S., Corbett, A.H., and Bachand, F. (2013). Poly(A) tail-mediated gene regulation by opposing roles of Nab2 and Pab2 nuclear poly(A)-binding proteins in pre-mRNA decay. Mol Cell Biol *33*, 4718-4731. 10.1128/MCB.00887-13.
419. Lee, W.H., Corgiat, E., Rounds, J.C., Shepherd, Z., Corbett, A.H., and Moberg, K.H. (2020). A Genetic Screen Links the Disease-Associated Nab2 RNA-Binding Protein to the Planar Cell Polarity Pathway in Drosophila melanogaster. G3 (Bethesda) *10*, 3575-3583. 10.1534/g3.120.401637.
420. Jones, S.K., Rha, J., Kim, S., Morris, K.J., Omotade, O.F., Moberg, K.H., Myers, K.R., and Corbett, A.H. (2020). The Polyadenosine RNA Binding Protein ZC3H14 is Required in Mice for Proper Dendritic Spine Density. bioRxiv, 2020.2010.2008.331827. 10.1101/2020.10.08.331827.
421. Rha, J., Jones, S.K., Fidler, J., Banerjee, A., Leung, S.W., Morris, K.J., Wong, J.C., Inglis, G.A.S., Shapiro, L., Deng, Q., et al. (2017). The RNA-binding protein, ZC3H14, is required for proper poly(A) tail length control, expression of synaptic proteins, and brain function in mice. Hum Mol Genet *26*, 3663-3681. 10.1093/hmg/ddx248.

422. Currey, H.N., Kraemer, B.C., and Liachko, N.F. (2023). sut-2 loss of function mutants protect against tau-driven shortened lifespan and hyperactive pharyngeal pumping in a C. elegans model of tau toxicity. MicroPubl Biol *2023*. 10.17912/micropub.biology.000844.
423. McMillan, P.J., Strovas, T.J., Baum, M., Mitchell, B.K., Eck, R.J., Hendricks, N., Wheeler, J.M., Latimer, C.S., Keene, C.D., and Kraemer, B.C. (2021). Pathological tau drives ectopic nuclear speckle scaffold protein SRRM2 accumulation in neuron cytoplasm in Alzheimer's disease. Acta Neuropathol Commun *9*, 117. 10.1186/s40478-021-01219-1.
424. Alpert, T., Straube, K., Oesterreich, F.C., Herzel, L., and Neugebauer, K.M. (2020). Widespread Transcriptional Readthrough Caused by Nab2 Depletion Leads to Chimeric Transcripts with Retained Introns. Cell Rep *33*, 108496. 10.1016/j.celrep.2020.108496.
425. Batisse, J., Batisse, C., Budd, A., Bottcher, B., and Hurt, E. (2009). Purification of nuclear poly(A)-binding protein Nab2 reveals association with the yeast transcriptome and a messenger ribonucleoprotein core structure. J Biol Chem *284*, 34911-34917. 10.1074/jbc.M109.062034.
426. Kahsai, L., and Zars, T. (2011). Learning and memory in Drosophila: behavior, genetics, and neural systems. Int Rev Neurobiol *99*, 139-167. 10.1016/B978-0-12-387003-2.00006-9.
427. Takemura, S.Y., Aso, Y., Hige, T., Wong, A., Lu, Z., Xu, C.S., Rivlin, P.K., Hess, H., Zhao, T., Parag, T., et al. (2017). A connectome of a learning and memory center in the adult Drosophila brain. Elife *6*. 10.7554/eLife.26975.
428. Yagi, R., Mabuchi, Y., Mizunami, M., and Tanaka, N.K. (2016). Convergence of multimodal sensory pathways to the mushroom body calyx in Drosophila melanogaster. Sci Rep *6*, 29481. 10.1038/srep29481.
429. Backer, S., Lokmane, L., Landragin, C., Deck, M., Garel, S., and Bloch-Gallego, E. (2018). Trio GEF mediates RhoA activation downstream of Slit2 and coordinates telencephalic wiring. Development *145*. 10.1242/dev.153692.
430. Briancon-Marjollet, A., Ghogha, A., Nawabi, H., Triki, I., Auziol, C., Fromont, S., Piche, C., Enslen, H., Chebli, K., Cloutier, J.F., et al. (2008). Trio mediates netrin-1-induced Rac1 activation in axon outgrowth and guidance. Mol Cell Biol *28*, 2314-2323. 10.1128/MCB.00998-07.
431. Katrancha, S.M., Wu, Y., Zhu, M., Eipper, B.A., Koleske, A.J., and Mains, R.E. (2017). Neurodevelopmental disease-associated de novo mutations and rare sequence variants affect TRIO GDP/GTP exchange factor activity. Hum Mol Genet *26*, 4728-4740. 10.1093/hmg/ddx355.
432. Bellanger, J.M., Zugasti, O., Lazaro, J.B., Diriong, S., Lamb, N., Sardet, C., and Debant, A. (1998). [Role of the multifunctional Trio protein in the control of the Rac1 and RhoA gtpase signaling pathways]. C R Seances Soc Biol Fil *192*, 367-374.
433. DeGeer, J., Kaplan, A., Mattar, P., Morabito, M., Stochaj, U., Kennedy, T.E., Debant, A., Cayouette, M., Fournier, A.E., and Lamarche-Vane, N. (2015). Hsc70 chaperone activity underlies Trio GEF function in axon growth and guidance induced by netrin-1. J Cell Biol *210*, 817-832. 10.1083/jcb.201505084.
434. Shivalkar, M., and Giniger, E. (2012). Control of dendritic morphogenesis by Trio in Drosophila melanogaster. PLoS One *7*, e33737. 10.1371/journal.pone.0033737.

435. Bellanger, J.M., Lazaro, J.B., Diriong, S., Fernandez, A., Lamb, N., and Debant, A. (1998). The two guanine nucleotide exchange factor domains of Trio link the Rac1 and the RhoA pathways in vivo. Oncogene *16*, 147-152. 10.1038/sj.onc.1201532.
436. Song, J.K., and Giniger, E. (2011). Noncanonical Notch function in motor axon guidance is mediated by Rac GTPase and the GEF1 domain of Trio. Dev Dyn *240*, 324-332. 10.1002/dvdy.22525.
437. Peng, Y.J., He, W.Q., Tang, J., Tao, T., Chen, C., Gao, Y.Q., Zhang, W.C., He, X.Y., Dai, Y.Y., Zhu, N.C., et al. (2010). Trio is a key guanine nucleotide exchange factor coordinating regulation of the migration and morphogenesis of granule cells in the developing cerebellum. J Biol Chem *285*, 24834-24844. 10.1074/jbc.M109.096537.
438. Patil, D.P., Pickering, B.F., and Jaffrey, S.R. (2018). Reading m(6)A in the Transcriptome: m(6)A-Binding Proteins. Trends Cell Biol *28*, 113-127. 10.1016/j.tcb.2017.10.001.
439. Xu, C., Liu, K., Ahmed, H., Loppnau, P., Schapira, M., and Min, J. (2015). Structural Basis for the Discriminative Recognition of N6-Methyladenosine RNA by the Human YT521-B Homology Domain Family of Proteins. J Biol Chem *290*, 24902-24913. 10.1074/jbc.M115.680389.
440. Worpenberg, L., Paolantoni, C., Longhi, S., Mulorz, M.M., Lence, T., Wessels, H.H., Dassi, E., Aiello, G., Sutandy, F.X.R., Scheibe, M., et al. (2021). Ythdf is a N6-methyladenosine reader that modulates Fmr1 target mRNA selection and restricts axonal growth in Drosophila. EMBO J *40*, e104975. 10.15252/embj.2020104975.
441. Heisenberg, M. (1998). What do the mushroom bodies do for the insect brain? an introduction. Learn Mem *5*, 1-10.
442. Roman, G., and Davis, R.L. (2001). Molecular biology and anatomy of Drosophila olfactory associative learning. Bioessays *23*, 571-581. 10.1002/bies.1083.
443. Crittenden, J.R., Skoulakis, E.M., Han, K.A., Kalderon, D., and Davis, R.L. (1998). Tripartite mushroom body architecture revealed by antigenic markers. Learn Mem *5*, 38-51.
444. Fushima, K., and Tsujimura, H. (2007). Precise control of fasciclin II expression is required for adult mushroom body development in Drosophila. Dev Growth Differ *49*, 215-227. 10.1111/j.1440-169X.2007.00922.x.
445. Rueden, C.T., Schindelin, J., Hiner, M.C., DeZonia, B.E., Walter, A.E., Arena, E.T., and Eliceiri, K.W. (2017). ImageJ2: ImageJ for the next generation of scientific image data. BMC Bioinformatics *18*, 529. 10.1186/s12859-017-1934-z.
446. Schindelin, J., Arganda-Carreras, I., Frise, E., Kaynig, V., Longair, M., Pietzsch, T., Preibisch, S., Rueden, C., Saalfeld, S., Schmid, B., et al. (2012). Fiji: an open-source platform for biological-image analysis. Nat Methods *9*, 676-682. 10.1038/nmeth.2019.
447. Robinson, J.T., Thorvaldsdottir, H., Winckler, W., Guttman, M., Lander, E.S., Getz, G., and Mesirov, J.P. (2011). Integrative genomics viewer. Nat Biotechnol *29*, 24-26. 10.1038/nbt.1754.
448. Arshadi, C., Gunther, U., Eddison, M., Harrington, K.I.S., and Ferreira, T.A. (2021). SNT: a unifying toolbox for quantification of neuronal anatomy. Nat Methods *18*, 374-377. 10.1038/s41592-021-01105-7.
449. Ferreira, T.A., Blackman, A.V., Oyrer, J., Jayabal, S., Chung, A.J., Watt, A.J., Sjostrom, P.J., and van Meyel, D.J. (2014). Neuronal morphometry directly from bitmap images. Nat Methods *11*, 982-984. 10.1038/nmeth.3125.

450. Lottes, E.N., Ciger, F.H., Bhattacharjee, S., Timmins-Wilde, E.A., Tete, B., Tran, T., Matta, J., Patel, A.A., and Cox, D.N. (2023). CCT and Cullin1 regulate the TORC1 pathway to promote dendritic arborization in health and disease. bioRxiv. 10.1101/2023.07.31.551324.
451. Hall, J.C. (1994). The mating of a fly. Science *264*, 1702-1714. 10.1126/science.8209251.
452. Jiao, W., Spreemann, G., Ruchti, E., Banerjee, S., Vernon, S., Shi, Y., Stowers, R.S., Hess, K., and McCabe, B.D. (2022). Intact Drosophila central nervous system cellular quantitation reveals sexual dimorphism. Elife *11*. 10.7554/eLife.74968.
453. Hotta, Y., and Benzer, S. (1972). Mapping of behaviour in Drosophila mosaics. Nature *240*, 527-535. 10.1038/240527a0.
454. Rein, K., Zockler, M., Mader, M.T., Grubel, C., and Heisenberg, M. (2002). The Drosophila standard brain. Curr Biol *12*, 227-231. 10.1016/s0960-9822(02)00656-5.
455. Jefferis, G.S., Potter, C.J., Chan, A.M., Marin, E.C., Rohlfing, T., Maurer, C.R., Jr., and Luo, L. (2007). Comprehensive maps of Drosophila higher olfactory centers: spatially segregated fruit and pheromone representation. Cell *128*, 1187-1203. 10.1016/j.cell.2007.01.040.
456. Gailey, D.A., and Hall, J.C. (1989). Behavior and cytogenetics of fruitless in Drosophila melanogaster: different courtship defects caused by separate, closely linked lesions. Genetics *121*, 773-785. 10.1093/genetics/121.4.773.
457. Billeter, J.C., Rideout, E.J., Dornan, A.J., and Goodwin, S.F. (2006). Control of male sexual behavior in Drosophila by the sex determination pathway. Curr Biol *16*, R766-776. 10.1016/j.cub.2006.08.025.
458. Kimura, K., Ote, M., Tazawa, T., and Yamamoto, D. (2005). Fruitless specifies sexually dimorphic neural circuitry in the Drosophila brain. Nature *438*, 229-233. 10.1038/nature04229.
459. Cachero, S., Ostrovsky, A.D., Yu, J.Y., Dickson, B.J., and Jefferis, G.S. (2010). Sexual dimorphism in the fly brain. Curr Biol *20*, 1589-1601. 10.1016/j.cub.2010.07.045.
460. Kido, A., and Ito, K. (2002). Mushroom bodies are not required for courtship behavior by normal and sexually mosaic Drosophila. J Neurobiol *52*, 302-311. 10.1002/neu.10100.
461. Tuck, A.C., and Tollervey, D. (2013). A transcriptome-wide atlas of RNP composition reveals diverse classes of mRNAs and lncRNAs. Cell *154*, 996-1009. 10.1016/j.cell.2013.07.047.
462. Brockmann, C., Soucek, S., Kuhlmann, S.I., Mills-Lujan, K., Kelly, S.M., Yang, J.C., Iglesias, N., Stutz, F., Corbett, A.H., Neuhaus, D., and Stewart, M. (2012). Structural basis for polyadenosine-RNA binding by Nab2 Zn fingers and its function in mRNA nuclear export. Structure *20*, 1007-1018. 10.1016/j.str.2012.03.011.
463. Jain, M., Abu-Shumays, R., Olsen, H.E., and Akeson, M. (2022). Advances in nanopore direct RNA sequencing. Nat Methods *19*, 1160-1164. 10.1038/s41592-022-01633-w.
464. Hsu, P.J., Shi, H., Zhu, A.C., Lu, Z., Miller, N., Edens, B.M., Ma, Y.C., and He, C. (2019). The RNA-binding protein FMRP facilitates the nuclear export of N(6)-methyladenosine-containing mRNAs. J Biol Chem *294*, 19889-19895. 10.1074/jbc.AC119.010078.
465. Edens, B.M., Vissers, C., Su, J., Arumugam, S., Xu, Z., Shi, H., Miller, N., Rojas Ringeling, F., Ming, G.L., He, C., et al. (2019). FMRP Modulates Neural Differentiation through m(6)A-

Dependent mRNA Nuclear Export. Cell Rep *28*, 845-854 e845. 10.1016/j.celrep.2019.06.072.

466. Schwartz, N.B., Risner, L.E., Domowicz, M., and Freedman, V.H. (2020). Comparisons and Approaches of PREP Programs at Different Stages of Maturity: Challenges, Best Practices and Benefits. Ethn Dis *30*, 55-64. 10.18865/ed.30.1.55.

467. State, U.S.D.o. (n.d.). Step 1: Research Your Options Graduate. https://educationusa.state.gov/your-5-steps-us-study/research-your-options/graduate.

468. Bennett, M. (2022). PhD Study in the USA-A Guide for 2022. https://www.findaphd.com/study-abroad/america/phd-study-in-usa.aspx.

469. Roberts, E. (2017). The Full Cost of Applying to PhD Programs. http://pfforphds.com/full-cost-applying-phd-programs/.

470. GradSchoolMatch (2021). Choosing Your Final Programs to Apply To. https://www.gradschoolmatch.com/resources/articles/choose-final-program-list.html.

471. Minnesota, U.o. (2022). Keeping your graduate school applications on track.

472. GradSchoolMatch (2021). How Many Graduate Schools Should You Apply To? https://www.gradschoolmatch.com/resources/articles/how-many-apply-to.html.

473. GradSchoolMatch (2016). Students Relocate To Attend Graduate School. https://blog.gradschoolmatch.com/students-relocate-attend-graduate-school/.

474. Baghdassarian, H. (2021). How to Apply to STEM PhD Programs (U.S.).

475. Melanie Sinche, R.L.L., Patrick D. Brandt,Anna B. O'Connell,Joshua D. Hall,Ashalla M. Freeman,Jessica R. Harrell,Jeanette Gowen Cook ,Patrick J. Brennwald (2017). An evidence-based evaluation of transferrable skills and job satisfaction for science PhDs. PLos One *12*.

476. Report, U.N.a.W. (2018). Best Science Schools. https://www.usnews.com/best-graduate-schools/top-science-schools.

477. Barr, P. (2020). PhD Program Selection: Does School Ranking Matter? https://blog.accepted.com/phd-program-selection-does-school-ranking-matter/.

478. Glassdoor (2022). How much does a PhD Student make? https://www.glassdoor.com/Salaries/phd-student-salary-SRCH_KO0,11.htm.

479. Glasmeier, A.K. (2022). Living Wage calculator. https://livingwage.mit.edu/.

480. National Academies of Sciences, E., and Medicine, Policy and Global Affairs,Board on Higher Education and Workforce, Committee on Revitalizing Graduate STEM Education for the 21st Century. (2018). Graduate STEM Education for the 21st Century (The National Academies Press). https://doi.org/10.17226/25038.

481. Kowarski, I. (2021). What the GRE Test Is and How to Prepare. https://www.usnews.com/education/best-graduate-schools/articles/what-the-gre-test-is-and-how-to-prepare.

482. PrinstonReview (2022). GRE Sections. https://www.princetonreview.com/grad/gre-sections#:~:text=The%20GRE%20is%20a%203,Section%20and%20a%20Verbal%20Section.

483. Blanco, A.T. (2021). To Diversify STEM Graduate Programs, Eliminate the GRE. http://mjpa.umich.edu/2021/01/19/to-diversify-stem-graduate-programs-eliminate-the-gre/#:~:text=Recently%2C%20however%2C%20graduate%20programs%E2%80%93,GRE%20as%20an%20admissions%20requirement.

484. Miller, C., and Stassun, K. (2014). A test that fails. Nature *510*, 303-304. 10.1038/nj7504-303a.
485. Hall, J.D., O'Connell, A.B., and Cook, J.G. (2017). Predictors of Student Productivity in Biomedical Graduate School Applications. PLoS One *12*, e0169121. 10.1371/journal.pone.0169121.
486. Moneta-Koehler, L., Brown, A.M., Petrie, K.A., Evans, B.J., and Chalkley, R. (2017). The Limitations of the GRE in Predicting Success in Biomedical Graduate School. PLoS One *12*, e0166742. 10.1371/journal.pone.0166742.
487. Kahn, R.A., Conn, G.L., Pavlath, G.K., and Corbett, A.H. (2016). Use of a Grant Writing Class in Training PhD Students. Traffic *17*, 803-814. https://doi.org/10.1111/tra.12398.
488. Taylor, B. (2022). Teaching as a PD Student. https://www.findaphd.com/advice/doing/teaching-as-a-phd-student.aspx.
489. Lautz, L.K., McCay, D. H.,Driscoll, C. T.,Glas, R. L.,Gutchess, K. M.,Johnson, A. J., and Millard, G. D. (2018). Preparing graduate students for STEM careers outside academia. Eos *99*.
490. Cornell, B. (2020). PhD students and their careers. Higher Education Policy Institute.
491. Studies, U.o.N.-L.O.o.G. (2020). Building a Support Network. https://www.unl.edu/gradstudies/connections/building-support-network.
492. Joseph, R.L., Harris Alexes Y. (2022). The Imposter Syndrome. https://grad.uw.edu/for-students-and-post-docs/core-programs/mentoring/mentor-memos/the-imposter-syndrome/.
493. Peterson, R.J. (2021). We need to address ableism in science. Mol Biol Cell *32*, 507-510. 10.1091/mbc.E20-09-0616.
494. Peterson, R. (2021). A Letter to My Younger Self. Behind the Microscope: Science Behind the Scenes.
495. Martin, D. (2013). Explore Health Insurance Options for Grad Students. https://www.usnews.com/education/blogs/graduate-school-road-map/2013/05/10/explore-health-insurance-options-for-grad-students.
496. Association, A.P. (2018). In gut we trust when it comes to choices:Decisions recruiting gut feelings seen as reflection of true self, more assuredly held, study says. www.sciencedaily.com/releases/2018/09/180910093528.htm.